UNIVERSIDADE ESTADUAL PAULISTA "JÚLIO DE MESQUITA FILHO"- UNESP

INSTITUTO DE QUÍMICA DE ARARAQUARA

PROGRAMA DE PÓS-GRADUAÇÃO EM BIOTECNOLOGIA

Stela Virgilio

Regulation of reserve carbohydrates metabolism in *Neurospora crassa*: responses to pH, calcium and carbon source stresses and to the biological clock

ARARAQUARA

2016

STELA VIRGILIO

Regulation of reserve carbohydrates metabolism in *Neurospora crassa*: responses to pH, calcium and carbon source stresses and to the biological clock

Thesis submitted to Instituto de Química, Universidade Estadual Paulista, Programa de Pós-Graduação em Biotecnologia, for fulfillment of the requirements for the degree of Doctor in Biotechnology

Advisor: Prof. Dr. Maria Célia Bertolini

ARARAQUARA
2016

FICHA CATALOGRÁFICA

Virgilio, Stela
V816r Regulation of reserve carbohydrates metabolism in *Neurospora crassa:* responses to pH, calcium and carbon source stresses and to the biological clock = Regulação do metabolismo de carboidratos de reserva em *Neurospora crassa:* respostas a estresses de pH, cálcio e fonte de carbono e ao relógio biológico / Stela Virgilio. – Araraquara: [s.n.], 2016
221 f.: il.

Tese (doutorado) – Universidade Estadual Paulista, Instituto de Química
Orientador: Maria Célia Bertolini

1. Biologia molecular. 2. Glicogênio. 3. Trealose. 4. DNA. 5. Expressão gênica. I. Título

Elaboração: Seção Técnica de Tratamento da Informação
Biblioteca do Instituto de Química, Unesp, câmpus de Araraquara

STELA VIRGILIO

Regulação do metabolismo de carboidratos de reserva em *Neurospora crassa*: respostas a estresses de pH, cálcio e fonte de carbono e ao relógio biológico

Tese apresentada ao Instituto de Química, Universidade Estadual Paulista, Programa de Pós-Graduação em Biotecnologia, como parte dos requisitos para obtenção do título de Doutor em Biotecnologia

Orientadora: Profª. Dr. Maria Célia Bertolini

ARARAQUARA

2016

STELA VIRGILIO

Tese apresentada ao Instituto de Química, Universidade Estadual Paulista, como parte dos requisitos para obtenção do título de Doutora em Biotecnologia.

Araraquara, 20 de setembro de 2016.

BANCA EXAMINADORA

Profª Drª Maria Célia Bertolini (Orientadora)
Instituto de Química / UNESP / Araraquara - SP

Profª Drª Nilce Maria Martinez Rossi
Faculdade de Medicina / USP / Ribeirão Preto - SP

Prof. Dr. Rafael Silva Rocha
Faculdade de Medicina / USP / Ribeirão Preto - SP

Prof. Dr. Carlos Takeshi Hotta
Instituto de Química / USP / São Paulo - SP

Prof. Dr. Iran Malavazi
Centro de Ciências Biológicas e da Saúde / UFSCar / São Carlos - SP

CURRICULUM VITAE

Stela Virgilio

1. Personal Information

Filiation: Celso José Virgilio and Rita de Cássia Rampani Virgilio
Birth: January 5, 1988 - Araraquara - São Paulo, Brazil
Personal Address: Avenida Marzio Munhoz Garcia Perez, 53 - Vila Xavier
CEP: 14810-152 - Araraquara - São Paulo
Professional Address: Instituto de Química de Araraquara - UNESP
Departamento de Bioquímica e Tecnologia Química
Rua Prof. Francisco Degni, 55 - Jardim Quitandinha
CEP: 14800-060 - Araraquara - São Paulo
Profession: Bachelor in Biotechnology

2. Education

2012-2016: PhD in Biotechnology, Programa de Pós-Graduação em Biotecnologia. Title: Regulation of reserve carbohydrates metabolism in *Neurospora crassa*: responses to pH, calcium and carbon source stresses and to the biological clock. Supervisor: Dr. Maria Célia Bertolini, Instituto de Química de Araraquara, Universidade Estadual Paulista - UNESP, Araraquara, São Paulo, Brazil

2010-2012: Master in Biotechnology, Programa de Pós-Graduação em Biotecnologia. Title: Metabolismo de glicogênio e relógio biológico em *Neurospora crassa*. Fatores e cofatores de transcrição envolvidos nos processos. Supervisor: Dr. Maria Célia Bertolini, Instituto de Química de Araraquara, Universidade Estadual Paulista - UNESP, Araraquara, São Paulo, Brazil

2006-2010: Undergraduate course in Biotecnology, Universidade Federal de São Carlos - UFSCar, Araras, São Paulo, Brazil

3. Publications

VIRGILIO, S.; CUPERTINO, F. B.; BERNARDES, N. E.; FREITAS, F. Z.; TAKEDA, A. A. S.; FONTES, M. R. M.; BERTOLINI, M. C. Molecular components of the *Neurospora crassa* pH signaling pathway and their regulation by pH and the PAC-3 transcription factor. PLoS ONE, v. 11, n. 8, 2016. doi:10.1371/journal.pone.0161659

FREITAS, F. Z.; VIRGILIO, S.; CUPERTINO, F. B.; KOWBEL, D. J.; FIORAMONTE, M.; GOZZO, F. C.; GLASS, N. L.; BERTOLINI, M. C. The SEB-1 transcription factor binds to the STRE motif in *Neurospora crassa* and regulates a variety of cellular processes including the stress response and reserve carbohydrate metabolism. G3: Genes, Genomes, Genetics (Bethesda), v. 6, p. 1327-1343, 2016.

CUPERTINO, F. B.; VIRGILIO, S.; FREITAS, F. Z.; CANDIDO, T. S.; BERTOLINI, M. C. Regulation of glycogen metabolism by the CRE-1, RCO-1 and RCM-1 proteins in *Neurospora crassa*. The role of CRE-1 as the central transcriptional regulator. Fungal Genetics and Biology, v. 77, p. 82-94, 2015.

4. Abstracts presented in Conferences

4.1 International Conferences

VIRGILIO, S.; CUPERTINO, F. B.; BERNARDES, N. E.; FREITAS, F. Z.; TAKEDA, A. A. S.; FONTES, M. R. M.; BERTOLINI, M. C. Molecular components of the *Neurospora crassa* pH-signaling pathway and their regulation by pH and by the PAC-3 transcription factor. In: 13th European Conference on Fungal Genetics - ECFG13. Abtract Book. Paris, p. 292, 2016.

BAEK, M.; VIRGILIO, S,; DOVZHENOK, A.; IBARRA, O.; LIM, S.; BELL-PEDERSEN, D.; BERTOLINI, M. C.; HONG, C. Interdisciplinary approaches for identification of circadian-controlled glycogen metabolism in *Neurospora crassa*. In: Society for Research on Biological Rhythms 2016, Palm Harbor, FL. SRBR 2016 Conference Program, p. 182, 2016.

VIRGILIO, S.; CUPERTINO, F. B.; BERTOLINI, M. C. Reserve carbohydrate metabolism is controlled by pH signaling pathway in *Neurospora crassa*. In: 28th Fungal Genetics Conference, Pacific Grove, CA. Fungal Genetics Reports 60 (Suppl): Abstract # 58, p. 143, 2015.

VIRGILIO, S.; IBARRA, O.; BELL-PEDERSEN, D.; BERTOLINI, M. C. The transcription factor VOS-1 connects the circadian clock to rhythmic glycogen metabolism in *Neurospora crassa*. In: 23rd Congress of the International Union of Biochemistry and Molecular Biology (IUBMB) and 44th Annual Meeting of the

Brazilian Society for Biochemistry and Molecular Biology (SBBq), Foz do Iguaçu, PR. Abstracts Book, p. 294, 2015.

MATEOS, P. A.; FREITAS, F. Z.; IMAMURA, K. B.; CANDIDO, T. S.; VIRGILIO, S.; BERTOLINI, M. C. The RUV-1/2 proteins have a functional role in heat shock response in *Neurospora crassa*. In: 23rd Congress of the International Union of Biochemistry and Molecular Biology (IUBMB) and 44th Annual Meeting of the Brazilian Society for Biochemistry and Molecular Biology (SBBq), Foz do Iguaçu, PR. Abstracts Book, p. 304, 2015 **(award)**.

VIRGILIO, S.; IBARRA, O.; BONI, A. C.; BELL-PEDERSEN, D.; BERTOLINI, M. C. Connection between glycogen metabolism regulation, light and the circadian clock in *Neurospora crassa*. In: Neurospora meeting, Pacific Grove, CA. Neurospora 2014 Program and Abstracts, p. 37, 2014.

VIRGILIO, S.; CUPERTINO, F. B.; BERTOLINI, M. C. *pal* genes regulation in *Neurospora crassa*: connection between pH signaling pathway and glycogen metabolism. In: International Symposium on Fungal Stress, São José dos Campos. Book of Abstracts, p. 18-19, 2014 **(award)**.

VIRGILIO, S.; CANDIDO, T. S.; BERTOLINI, M. C. Glycogen metabolism is regulated by the circadian clock in *Neurospora crassa*. In: 27th Fungal Genetics Conference, 2013, Pacific Grove. Fungal Genetics Reports 60(Suppl), p. 215, 2013.

CUPERTINO, F. B.; VIRGILIO, S.; FREITAS, F. Z.; CANDIDO, T. S.; BERTOLINI, M. C. The transcriptional repressor CRE-1 regulates glycogen metabolism in *Neurospora crassa*. In: 27th Fungal Genetics Conference, Pacific Grove, CA. Fungal Genetics Reports 60(Suppl), p. 223-224, 2013.

4.2 Nacional Conferences

VIRGILIO, S. A conexão entre relógio biológico e o rítmo do metabolismo de glicogênio no fungo *Neurospora crassa*. Abordagens biológicas e modelagens matemáticas. In: VII Simpósio de Microbiologia, São José do Rio Preto, SP. VII Simpósio de Microbiologia - Microbiologia Industrial e Aplicada, 2015.

VIRGILIO, S.; CUPERTINO, F. B.; BERTOLINI, M. C. pH signaling pathway in *Neurospora crassa*: *pal* genes regulation and PAC-3 processing. In: 61º Congresso Brasileiro de Genética, Águas de Lindóia, SP. Resumos do 61º Congresso Brasileiro de Genética, p. 36, 2015.

ARAUJO, A. V. C.; VIRGILIO, S.; BERTOLINI, M. C. Avaliação do fitness da linhagem mutante no fator de transcrição VOS-1 do fungo *Neurospora crassa* em diferentes condições de estresse. In: V Congresso Farmacêutico da UNESP, 2015,

Araraquara, SP. Revista de Ciências Farmacêuticas Básica e Aplicada: Supl.1 CB 04, v. 36, 2015.

VIRGILIO, S.; BELL-PEDERSEN, D.; BERTOLINI, M. C. Circadian clock control of glycogen accumulation and the role of the transcription factor VOS-1 in *Neurospora crassa*. In: 60º Congresso Brasileiro de Genética, Guarujá. SP. Resumos do 60º Congresso Brasileiro de Genética, p. 26, 2014.

5. Oral Presentation

VIRGILIO, S. Correlação entre relógio biológico e metabolismo nos diferentes organismos. Instituto de Química, UNESP, Araraquara, SP, 2015.

VIRGILIO, S.; IBARRA, O.; BELL-PEDERSEN, D.; BERTOLINI, M. C. Correlação entre relógio biológico e o metabolismo de glicogênio no fungo *Neurospora crassa*: da modelagem matemática aos experimentos biológicos. In: V Congresso Farmacêutico da UNESP, Araraquara, SP. Revista de Ciências Farmacêuticas Básica e Aplicada: Supl.1 BB 10, v. 36, 2015 **(award)**.

VIRGILIO, S.; IBARRA, O.; BONI, A. C.; BELL-PEDERSEN, D.; BERTOLINI, M. C. Connection between glycogen metabolism regulation, light and the circadian clock in *Neurospora crassa*. In: Neurospora meeting, Pacific Grove, CA. Neurospora 2014 Program and Abstracts, p. 37, 2014.

6. Academic Experiences

6.1 Scientific Supervisor

2015-2016: Amanda Ventura Campos Araujo. Caracterização do fator de transcrição VOS-1 em resposta a diferentes condições de estresse e sua relação com o acúmulo de glicogênio em *Neurospora crassa*. Undergraduate student, FAPESP fellowship - Instituto de Química, UNESP, Araraquara.

6.2 Graduate Teaching Assistant

2015: Molecular Biology (75 h)

2015: Biochemistry (60 h)

6.3 Academic Service Committees

2015-2016: Graduated Representation in the Comissão Permanente de Pesquisa

2015-2016: Graduated Representation in the Comissão de Biblioteca

2014-2016: Graduated Representation in the Conselho de Pós-Graduação em Biotecnologia

7. Awards

2015: Honor mention for 3rd position in PósMicro Scientific Text Competition, Graduation and Researcher Category, with text "A microbiologia no avanço biotecnológico", Instituto de Biociências, Letras e Ciências Exatas - IBILCE/UNESP.

2015: Award "Profª Dra Márcia da Silva" for 1st oral scientific work position in V Congresso Farmacêutico da UNESP and I Jornada de Engenharia de Bioprocessos e Biotecnologia, Faculdade de Ciências Farmacêuticas - UNESP Araraquara.

2015: SBBq Award for the best poster presented by authors Mateos, P. A.; Freitas, F. Z.; Imamura, K. B.; Candido, T. S.; Virgilio, S.; Bertolini, M. C., in SBBq and IUBMB.

2014: Elsevier Microbiology Gold Poster Award for Virgilio, S.; Cupertino, F. B.; Bertolini, M. C., in 2014 ISFUS International Symposium on Fungal Stress, Elsevier and ISFUS.

I dedicate this thesis to God,
to my parentes Celso e Rita,
my sister Letícia and
my boyfriend Alisson,
people that I love so much!

ACKNOWLEDGEMENTS

At the end of this stage, I have the immense joy to remember many special people and moments that occurred in my life. During my undergraduate degree in Biotechnology in UFSCar, I started my scientific career and those teachings would be fundamental to my academic life. I did my Master Degree and now I completed the Doctoral Degree. Everything happened so fast that seems I did my choices yesterday. There were many happy days, others not so good, but with perseverance, I reached my goals. I could not forget to thank everyone who shared these moments with me and had influence on making this thesis possible.

First, I thank God, for gracing me with health, faith and wisdom.

I want to thank my advisor Dr. Maria Célia Bertolini for giving me the opportunity to work in your lab, to learn and discover new things about the orange fungi *Neurospora crassa*. I am also thankful for the ideas that excited me to looking for new approaches and conferences. In special I grateful to Antonio Tarcisio Delfino for technical assistance and for the wonderful barbecue meetings.

Additional energy and hopeful for this research was to meet many good friends that became a part of my life. I would like to thank my lab collegues Fernanda Cupertino, Fernanda Zanolli, Kely, Thiago, Pablo, Amanda, Carol, Carla, André, Dani, Flávia, Eliane, Ana Paula, Susi, Rodrigo, Jonatas, Henrique, Rhayanne and Allan, for the friendship, cooperation, suggestions and help me to ground to a fine powder in a pre-chilled mortar as a competition to see who finished first. Moreover, of course, I could not forget the lots of laughs eating “pão de queijo” (Brazilian cheese bread). Thanks to my collegue in the Department that help me a lot.

I had a great opportunity to develop part of my Doctorate in Center of Biological Clocks Research, in Texas A&M University (TAMU), College Station, Texas, USA, under Dr. Deborah Bell-Pedersen supervision. I express my deepest gratitude to Dr. Bell-Pedersen for providing me constant encouragement, suggestions in the experiments, and during lab meetings and oral presentations. I extend my special thanks for all friends and collegues in Bell-Pedersen Lab: Oneida, Teresa, Nikita, Nirmala, Rigzin, Stephen and the technician Johnny Fazzino.

I would like to thank the Instituto de Química Library employees, professors of Programa de Pós-Graduação em Biotecnologia, members of Conselho de Pós-

graduação em Biotecnologia, Comissão Permanente de Pesquisa and Comissão de Biblioteca. I would immensely like to thank the Seção de Pós-Graduação: Wennia, Paula, Cintia, Brenda, Célia, and Sandra.

Thanks to Departamento de Bioquímica e Tecnologia Química and Programa de Pós-Graduação em Biotecnologia, Instituto de Química, UNESP Araraquara for the opportunity to accomplish my Doctorate.

My sincere thanks to Dr. Carlos Takeshi Hotta (USP) and Dr. Karen Martinez de Moraes (UNESP) for the Exame Geral de Qualificação participation and great suggestions.

I extend my appreciation to Dr. Nilce Maria Martinez-Rossi (USP), Dr. Rafael Silva Rocha (USP), Dr. Carlos Takeshi Hotta (USP) and Dr. Iran Malavazi (UFSCar) for the Defense participation and suggestions.

My Doctorate has been greatly supported by my beloved Family. I would like to thank my boyfriend Alisson, my father and my mother Celso and Rita, my sister Letícia and my brother in law Adriano for constant support and motivation. I extend my thanks to all my relatives: Marli, Sérgio, Alex, André, Thais; Raquel, Laerte, Lara; Renata, Rogério, Michele, Duda and Arthur. To my friends Maria Nieves, Rafaela, Giovana, Lívia, Diego, Heitor, Paula, Sarah, Ricardo, Laura, and Lígia. In addition, I could not forget to thank my second Family, the Alisson's family: Bete, Paulo, Maurício, Talita and the grandmothers. Thanks for all love received, prayers and encouragement unconditional support.

Finally, I would like to thank Fundação de Amparo à Pesquisa do Estado de São Paulo (FAPESP) for financial support all these years: Doctorate and Doctorate BEPE Research Fellowships, besides the technical reserve. Thank you very much!

“If you want different results, do not do the same things” (Albert Einstein)

“The important thing is to not stop questioning. Curiosity has its own reason for existing. One cannot help but be in awe when he contemplates the mysteries of eternity; of life; of the marvelous structure of reality…”
(Albert Einstein)

ABSTRACT

The fungus *Neurospora crassa*, a model organism in studies of gene expression, metabolism, photobiology and circadian rhythm, is able to respond and adapt to different environmental stresses, such as heat shock, pH changes, nutrient limitation, osmotic stress, and others. Besides that, *N. crassa* has the genome sequenced and collections of knocked-out strains are avalaible to the scientific community. A systematic screening analysis performed with mutant strains in genes encoding transcription factors led to identify proteins involved in the glycogen metabolism regulation in this fungus. Glycogen and trehalose are storage carbohydrates that functions as a carbon and energy reserve. Trehalose can also protect membranes and proteins, increasing the tolerance to adverse conditions. In this work, some transcription factors were functionally characterized regarding their role in glycogen and trehalose metabolism regulation. The first condition investigated was the influence of the circadian clock in the glycogen metabolism. We observed that the glycogen accumulation and the expression of genes encoding glycogen synthase (*gsn*) and glycogen phosphorylase (*gpn*) are rhythmic in a wild-type strain and dependent on the FREQUENCY (FRQ) oscillator, the core component of the *N. crassa* circadian clock. The VOS-1 transcription factor, that is controlled by clock and can act in the connection between clock and glycogen metabolism, binds to *gsn* and *gpn* promoters rhythmically. However, the expression of *gsn* and *gpn* and the glycogen accumulation are still rhythmic in Δ*vos-1* strain, suggesting that not only VOS-1 but additional transcription factors could contribute to glycogen accumulation rhythmicity. Under pH and calcium stress, the PAC-3 transcription factor was investigated. First, we characterized the protein components of the pH signaling pathway, using the Δ*pal* and Δ*pac-3* mutant strains. The mutants present high melanin production and inability to grow under alkaline pH. PAC-3 undergoes only one proteolytic cleavage, binds to *pal* promoters and regulates the expression of some *pal* genes under alkaline pH. PAC-3 is predominantly nuclear under alkaline condition and is able to bind to importin-α *in vitro*. Moreover, the components of pH signaling showed high glycogen and trehalose accumulation under normal and alkaline pH when compared to the wild-type. PAC-3 binds to some glycogenic and trehalose genes, and regulates their expression. Under calcium stress, *pac-3* was induced and the carbohydrates metabolism was differently regulated. Finally, the CRE-1 transcription factor and the RCO-1 and RCM-1 cofactors, orthologs of the Mig1-Tup1-Ssn6 yeast complex, respectively, were investigated regarding their regulation of the glycogen metabolism under different carbon sources. CRE-1 is involved in catabolic repression and plays a role as repressor in glycogen regulation. CRE-1 binds *in vivo* and *in vitro* to *gsn* and *gpn* promoters, regulating their expression. This transcription factor is present in nucleus and cytoplasm in derepressed and starved conditions. RCO-1 and RCM-1 also regulated the glycogen accumulation, the glycogen synthase activity and the expression of some glycogenic genes, but do not play a major role in glycogen metabolism, while CRE-1 is the central regulator.

Keywords: glycogen, trehalose, transcription factor, circadian clock, gene expression

RESUMO

O fungo *Neurospora crassa*, um organismo modelo em estudos de expressão gênica, metabolismo, fotobiologia e ritmo circadiano, é capaz de responder e se adaptar a diferentes condições de estresse, tais como choque térmico, alterações de pH, limitação de nutrientes, estresse osmótico, entre outras. Além disso, *N. crassa* tem seu genoma sequenciado e coleções de linhagens mutantes estão disponíveis para a comunidade científica. Uma análise sistemática utilizando linhagens mutantes em genes que codificam fatores de transcrição permitiu a identificação de proteínas envolvidas na regulação do metabolismo do glicogênio neste fungo. Glicogênio, juntamente com trealose, são carboidratos de reserva que funcionam como fonte de carbono e energia. A trealose também pode proteger membranas e proteínas, aumentando a tolerância a condições adversas. Neste trabalho, alguns fatores de transcrição foram funcionalmente caracterizados em relação as suas participações na regulação do metabolismo de glicogênio e trealose. A primeira condição investigada foi a influência do relógio circadiano sob o metabolismo de glicogênio. Observamos que o acúmulo de glicogênio e a expressão dos genes codificadores das enzimas glicogênio sintase (*gsn*) e glicogênio fosforilase (*gpn*) foram rítmicos em uma linhagem selvagem do fungo, e dependentes do oscilador FREQUENCY (FRQ), principal componente do relógio de *N. crassa*. O fator de transcrição VOS-1, o qual é controlado pelo relógio e pode atuar na conexão do relógio ao metabolismo de glicogênio, se liga aos promotores *gsn* e *gpn* ritmicamente. Entretanto a expressão dos genes *gsn* e *gpn* e o acúmulo de glicogênio se mantiveram rítmicos na linhagem Δ*vos-1*, sugerindo que além de VOS-1 outros fatores de transcrição poderiam contribuir para a ritmicidade do acúmulo de glicogênio. Sob condições de estresse de pH e cálcio, o fator de transcrição PAC-3 foi investigado. Primeiro, foram caracterizadas as proteínas envolvidas na via de sinalização de pH, usando as linhagens mutantes nos genes *pal* e *pac-3*. Os mutantes apresentam alta produção de melanina e incapacidade de crescer em pH alcalino. PAC-3 sofre uma única clivagem proteolítica, se liga aos promotores dos genes *pal* e regula a expressão de alguns destes genes em meio alcalino. PAC-3 é predominantemente nuclear sob condições alcalinas e é capaz de se ligar à importina-α *in vitro*. Além disso, os componentes de sinalização de pH mostraram acumular mais glicogênio e trealose sob pH normal e alcalino quando comparado à linhagem selvagem. PAC-3 se liga a alguns genes do metabolismo de glicogênio e trealose, regulando-os. Sob estresse de cálcio, a expressão de *pac-3* foi induzida e o metabolismo de carboidratos diferentemente regulado. Finalmente, o fator de transcrição CRE-1 e os cofatores RCO-1 e RCM-1, ortólogos ao complexo Mig1-Tup1-Ssn6 de levedura, respectivamente, foram investigados na regulação do glicogênio sob diferentes fontes de carbono. CRE-1 está envolvido na repressão catabólica e atua como repressor na regulação do glicogênio. CRE-1 se liga *in vivo* e *in vitro* aos promotors *gsn* e *gpn*, regulando suas expressões. Este fator de transcrição está presente no núcleo e no citoplasma em condições de derepressão e baixa fonte de carbono. RCO-1 e RCM-1 também regulam o acúmulo de glicogênio, a atividade glicogênio sintase e alguns genes do glicogênio, mas não desempenham um papel primordial, enquanto CRE-1 mostrou ser um regulador central.

Palavras-chave: glicogênio, trealose, fator de transcrição, relógio circadiano, expressão gênica

RESUMO EXPANDIDO

Neurospora crassa é um fungo filamentoso que se destaca como um excelente organismo modelo em estudos de expressão gênica, desenvolvimento e diferenciação celular, defesa do genoma, ritmo circadiano, bem como outros aspectos da biologia de eucariotos (PERKINS; DAVIS, 2000). O genoma desse fungo está organizado em sete cromossomos que variam entre 4 a 10 Mb de tamanho (SCHUTLE et al., 2002) e foi sequenciado por Galagan et al. (2003) revelando ser constituído por cerca de 40 Mb, muito maior se comparado com outros fungos com genomas já conhecidos como *Saccharomyces cerevisiae* e *Schizosaccharomyces pombe*.

N. crassa vem sendo utilizado para o estudo de mecanismos celulares básicos como os mecanismos moleculares envolvidos na regulação do metabolismo de glicogênio e trealose. O glicogênio é um polímero ramificado de glicose encontrado em diferentes organismos com a função de armazenamento de energia para as células. Seus resíduos de glicose estão unidos covalentemente por ligações glicosídicas α-1,4 lineares e ligações α-1,6. A síntese e degradação deste polímero são processos conservados e envolvem as enzimas regulatórias glicogênio sintase, que catalisa a formação das ligações glicosídicas α-1,4, via transferência de resíduos glicosil a partir de UDP-glicose (LELOIR, 1971) e a enzima glicogênio fosforilase, que catalisa a liberação dos resíduos de glicose-1-P a partir das extremidades da cadeia polissacarídica. As enzimas regulatórias glicogênio sintase e glicogênio fosforilase estão sujeitas ao controle pós-traducional, via fosforilação multi-sítios através da ação de proteínas quinases e também modulação alostérica (FRANÇOIS; VILLANUEVA; HERS, 1988). Trealose é um dissacarídeo composto por ligações de glicose α-1,1, catalizado pelo complexo trealose sintase, composto pela trealose fosfato sintase e pela trealose fosfato fosfatase e degradado por duas trealases: trealase neutra e ácida (BELL et al., 1998; FRANÇOIS; PARROU, 2001).

O término do sequenciamento do genoma de *N. crassa*, aliado aos avanços das metodologias disponíveis envolvidas na inativação de genes específicos (NINOMIYA et al., 2004), deram início às análises da genômica funcional do fungo. Linhagens contendo genes individualmente inativados começaram a se tornar disponíveis para a comunidade científica pelo *Fungal Genetics Stock Center*. Assim, linhagens mutantes do fungo *N. crassa* contendo genes que codificam fatores de

transcrição individualmente nocauteados foram utilizadas na busca de fatores de transcrição que participam, diretamente ou indiretamente, da regulação do metabolismo de glicogênio. Muitos fatores de transcrição foram identificados como reguladores do conteúdo de glicogênio em diversas situações distintas, tais como choque térmico (SEB-1), resposta a mudança de pH (PAC-3), alteração de fontes de carbono (CRE-1), crescimento vegetativo (VOS-1), dentre outros (GONÇALVES et al., 2011; CUPERTINO et al., 2012; BONI, 2014; FREITAS et al., 2016).

Alguns fatores de transcrição identificados foram descritos participar de vias de sinalização reguladas por luz e/ou relógio biológico, levando-nos a especular sobre a existência de uma possível conexão entre relógio biológico e metabolismo de glicogênio em *N. crassa*. Em mamíferos, muitos genes associados com o metabolismo de glicose no fígado exibiram uma regulação circadiana robusta (PANDA et al., 2002; UEDA et al., 2002; MILLER et al., 2007), sugerindo que o relógio circadiano desempenha um papel significativo no metabolismo da glicose hepática. O conteúdo de glicogênio hepático apresentou ritmo circadiano com pico durante a transição noite-dia em roedores noturnos (ISHIKAWA; SHIMAZU, 1976).

Em *N. crassa*, o relógio circadiano é menos complexo que nos mamíferos e consiste nos fatores de transcrição WHITE-COLLAR-1 (WC-1) e WHITE-COLLAR-2 (WC-2), que formam o Complexo White-Collar (WCC) e seu regulador negativo FRQ (FREQUENCY). WC-1 é um receptor de luz azul que sincroniza o relógio endógeno com o exógeno em um ciclo de aproximadamente 24 horas dia/noite (SCHAFMEIER; DIERNFELLNER, 2011). Na presença de luz, o WCC transientemente se liga à promotores de genes rapidamente responsivos à luz, ativando a expressão de *frq*, de genes controlados pelo relógio e de genes que codificam alguns fatores de transcrição (SMITH et al., 2010). Evidências do ensaio de ChIP-seq (*Neurospora Program Project*, EUA) mostraram que vários fatores de transcrição se ligam aos promotores das enzimas do glicogênio durante experimentos de luz (dados não publicados), e VOS-1 se ligaria aos promotores glicogênio sintase (*gsn*) e glicogênio fosforilase (*gpn*). Portanto, avaliamos o controle da regulação do metabolismo de glicogênio pelo relógio biológico do fungo. Nossos resultados mostraram que o acúmulo de glicogênio foi rítmico na linhagem selvagem, com picos no *subjective night*, e esta ritmicidade foi dependente de FRQ, oscilador negativo do relógio. A expressão dos genes *gsn* e *gpn*, envolvidos na síntese e degradação do carboidrato, respectivamente, também foram rítmicos e dependentes de FRQ. O fator de

transcrição VOS-1, controlado pelo relógio, ritmicamente se ligou *in vivo* às regiões promotoras de *gsn* e *gpn*. Entretanto, o acúmulo de glicogênio e a expressão dos genes do glicogênio se mantiveram rítmicos na ausência de VOS-1, embora as amplitutes tenham diminuído. Sugerimos que o relógio circadiano regula o metabolismo de glicogênio através de fatores de transcrição múltiplos, e que VOS-1 seria um dos fatores de transcrição que regularia a expressão dos genes *gsn* e *gpn* nestas condições, atuando provavelmente como ativador.

Além do fator de transcrição VOS-1, também estudamos outro fator de transcrição envolvido com o metabolismo de glicogênio e na regulação de genes em resposta a pH alcalino, a proteína PAC-3. PacC, ortólogo a PAC-3 de *N. crassa*, foi primeiramente descrito em *Aspergillus nidulans*, sendo ativado depois de duas etapas proteolíticas: a primeira, sinalizada por seis produtos dos genes da via *pal*, no qual a proteína PacC de 72 kDa é processada para 53 kDa (PEÑALVA; ARST, 2004), e a segunda, por uma protease pH-independente (HERVÁZ-AGUILAR et al., 2007), quando o pH do meio é alterado de ácido para alcalino. A forma ativa da PacC (27 kDa) contém apenas a região N-terminal da proteína, onde está localizado o domínio de ligação ao DNA formado por três C_2H_2 *zinc fingers*. Desta forma, $PacC^{27}$ ativa a transcrição de genes regulados em pH alcalino e reprime aqueles em pH ácido (TILBURN et al., 1995; ESPESO et al., 1997).

A proteína PacC é ortóloga a proteína Rim101 de *S. cerevisiae*, a qual foi primeiramente descrita como um regulador transcricional positivo no processo de meiose. A linhagem de levedura mutante no gene *rim101* é sensível a íons Na^+ ou Li^+ e tem o crescimento afetado quando crescida em baixas temperaturas (SU; MITCHELL, 1993). Assim, a proteína Rim101 parece estar envolvida em outros processos celulares além da resposta a pH alcalino. O fator de transcrição Rim101 de *S. cerevisiae* difere em alguns aspectos da proteína PacC de *A. nidulans*: sofre apenas um único processamento proteolítico para se tornar ativo e está associado à repressão de genes induzidos por alcalinidade (LAMB; MITCHELL, 2003; LI; MITCHELL, 1997).

Os fatores de transcrição PacC/Rim101 tem sido largamente estudados em fungos e leveduras. Alguns estudos mostraram o envolvimento de PacC na regulação de genes de diferentes processos celulares e na patogenicidade de fungos (ROLLINS; DICKMAN, 2001; ZOU et al., 2010), na regulação da expressão de enzimas extracelulares (MACCABE et al., 1998), permeases (VANKUYK et al.,

2004) e transportadoras (CARACUEL et al., 2003; EISENDLE et al., 2004). Em *N. crassa*, um elemento *cis* específico para a ligação da proteína PAC-3 na região promotora do gene *gsn* foi encontrado (GONÇALVES et al., 2011). A linhagem mutante no fator de transcrição PAC-3 apresentou alterações no acúmulo de glicogênio, tanto antes quanto depois do choque térmico e experimentos mostraram claramente que o gene *gsn* foi regulado negativamente em pH alcalino (CUPERTINO et al., 2012). Recentemente o *motif* consenso 5'-BGCCVAGV-3' (B=C/G/T; V=A/C/G) (WEIRAUCH et al., 2014) da proteína PAC-3 de *N. crassa* foi identificado apresentando grande similaridade ao apresentado para *A. nidulans*.

Algumas diferenças entre as vias nos dois fungos filamentosos *A. nidulans* e *N. crassa* foram apresentadas e algumas questões permaneciam ainda não esclarecidas em relação à cascata de sinalização envolvendo o fator de transcrição PAC-3 em *N. crassa.* Por este motivo, realizamos a caracterização das proteínas que participam da via de sinalização de pH, uma vez que *N. crassa* possui os seis genes *pal*, ortólogos aos genes de *A. nidulans*. Além disso, o *motif* consenso para PAC-3 de *N. crassa* foi encontrado nos promotores dos genes da via de sinalização de pH (via das proteínas PAL).

Primeiramente observamos que quase todas as linhagens mutantes apresentam alta produção de melanina e incapacidade de crescer em pH alcalino, com exceção da linhagem Δ*pal-9*, em comparação à linhagem selvagem. O gene tirosinase, que codifica para uma enzima limitante da produção de melanina, foi superexpresso nas linhagens mutantes Δ*pal* e regulado por pH alcalino. A expressão dos genes *pac-3*, *pal-1*, *pal-2*, *pal-6*, e *pal-9* também foi regulada pelo fator de transcrição PAC-3 e por pH 7,8. PAC-3 sofre um único processamento proteolítico, que pode ser independente do pH, e se liga *in vivo* aos promotores dos gene *pal*. PAC-3 apresentou uma forte afinidade à importina-α de *N. crassa* e está predominantemente no núcleo em pH alcalino. Sugerimos que PAC-3 requer importina-α para sua translocação ao núcleo, a qual deve ocorrer pela via clássica de importação nuclear. Nossos resultados mostraram que os genes *pal* de *N. crassa* participam da via de sinalização por pH, conduzindo a ativação de PAC-3, sendo que esta regula sua própria cascata e a biossíntese de melanina.

Além disso, os componentes da via de sinalização de pH, principalmente o fator de transcrição PAC-3, poderiam participar de outros processos biológicos como descrito em *S. cerevisiae*, podendo ser estes dependentes ou não da regulação por

pH. É conhecido que os carboidratos de reserva são regulados em situações de estresse, tal como pH e choque térmico (CUPERTINO et al., 2012), e que a via de calcineurina ativa a expressão de um grande número de genes através da desfosforilação do fator de transcrição Crz1. Em *S. cerevisiae*, pH elevado provoca um aumento transiente no cálcio citoplasmático resultando na ativação da calcineurina e indução de genes através de Crz1. Além disso, houve redução da expressão do gene *ENA1*, que codifica para uma Na^+-ATPase, nos mutantes *crz1* e *rim101*, demonstrando que a resposta transcricional a pH alcalino envolve diferentes mecanismos de sinalização, e que a sinalização por cálcio é relevante nesta resposta (SERRANO et al., 2002). Todos estes dados mostraram uma provável integração entre as vias de transdução de sinal por pH e cálcio. Portanto, avaliamos o acúmulo de glicogênio e trealose e a expressão de alguns genes em resposta a pH e a estresse por cálcio, tentando inferir uma interconexão entre as vias.

Observamos um alto acúmulo de glicogênio e trealose em todas as linhagens mutantes, exceto Δ*pal-9*, em pH normal (pH 5,8). Entretanto, glicogênio manteve seus níveis altos até 4 horas após transferência para pH alcalino, enquanto trealose apresentou o mesmo conteúdo nas linhagens mutantes e selvagem após 1 hora de transferência para pH alcalino. A expressão dos genes do glicogênio e trealose foram influenciados por pH e regulados por PAC-3, uma vez que houve ligação *in vivo* aos promotores destes genes. A linhagem mutante Δ*pac-3* apresentou maior crescimento em presença de cálcio, quando comparado a linhagem selvagem, e houve inibição do crescimento na presença de ciclosporina, um inibidor da via de calcineurina. A expressão de *pac-3* foi altamente induzida na presença de cálcio. O acúmulo de glicogênio e trealose foi diferentemente influenciado por cálcio a 10 mM e 300 mM, assim como alguns genes do metabolismo de glicogênio e trealose. Estes resultados indicam que a via de sinalização por pH regula glicogênio e trealose em diferentes pHs e em estresse por cálcio, sugerindo uma provável conexão entre as vias de sinalização com a regulação do metabolismo de carboidrato.

Finalmente, avaliamos o papel regulatório do fator de transcrição CRE-1, juntamente com os cofatores RCO-1 e RCM-1 no metabolismo do glicogênio em *N. crassa*. O fator de transcrição CRE-1 de *N. crassa*, ortólogo as proteínas CreA de *A. nidulans* e Mig1 de *S. cerevisiae*, reconhece a sequência consenso 5'-SYGGRG-3' (S= G/C, Y= T/C, R= A/G) e se liga a regiões promotoras de genes alvos envolvidos

em vias celulolíticas, em vias de utilização de fontes de carbono e em genes transportadores de açúcar (SUN; GLASS, 2011). CRE-1 pode atuar reprimindo genes que codificam para enzimas que metabolizam carbono e pode desenvolver suas funções juntamente com os cofatores de transcrição RCO-1 e RCM-1. Observamos que as proteínas CRE-1, RCO-1 e RCM-1 regulam o metabolismo de glicogênio em *N. crassa*, pois o acúmulo de glicogênio, a atividade glicogênio sintase e a expressão de genes que codificam para enzimas do metabolismo de glicogênio estão alterados nas linhagens mutantes. A proteína CRE-1 parece ter um papel central, uma vez que a expressão gênica de todos os genes que codificam enzimas do metabolismo do glicogênio está desregulada no mutante Δ*cre-1*. Ensaios com diferentes fontes de carbonos, fontes repressoras (glicose) e não repressoras (xilose e glicerol), mostraram que CRE-1 atua como repressor do metabolismo de glicogênio. Além disso, um grande número de *motifs* foi encontrado nos promotores de genes que codificam enzimas do metabolismo de glicogênio. A proteína recombinante GST::CRE-1 reconheceu e se ligou especificamente aos promotores de *gsn* e *gpn* e análises de ChIP-qPCR confirmaram que CRE-1 foi capaz de se ligar *in vivo* a todos os promotores de genes do glicogênio. Concluímos que RCO-1 e RCM-1 parecem não ter um papel regulatório no metabolismo de glicogênio em condições repressoras e não repressoras, entretanto CRE-1 apresenta um papel central como repressor deste processo.

O uso de linhagens mutantes tem sido importante em todas as abordagens, principalmente no estudo de conexões metabólicas. Vários fatores de transcrição parecem atuar na regulação do metabolismo de glicogênio e/ou trealose sob diferentes condições, como alteração de pH, estresse de cálcio, meio de cultivo com fonte de carbono repressora e não-repressora, choque térmico e durante o relógio biológico, atuando diretamente na regulação dos genes que codificam para as enzimas limitantes dos processos. Outros fatores de transcrição estão sendo investigados e, conjuntamente com os resultados aqui apresentados, fornecerão dados para compor um grande *network*, interconectando carboidrato de reserva e múltiplos processos celulares em *N. crassa*.

SUMMARY

INTRODUCTION **23**

1. *Neurospora crassa*: a model fungus 24

2. The sequencing of the *N. crassa* genome and its consequences 27

3. The biological clock in *N. crassa* 30

4. Reserve carbohydrates metabolism: glycogen and trehalose 34

5. Regulation of glycogen and trehalose metabolism 37

5.1 Environmental conditions regulating reserve carbohydrate accumulation and metabolism 38

5.2 Transcription factors regulating carbohydrate accumulation in *N. crassa* 40

5.2.1 VOS-1 transcription factor 42

5.2.2 PAC-3 transcription factor 42

5.2.3 CRE-1 transcription factor and RCO-1 and RCM-1 corepressors 43

OBJECTIVES **45**

CHAPTER 1 **47**

Abstract 50

Introduction 50

Materials and Methods 52

Results 58

Discussion 62

Acknowledgments 65

References 65

CHAPTER 2 **81**

Abstract 84

Introduction 84

Materials and Methods 86

Results 92

Discussion 98

Acknowledgments 102

Author Contributions 102

References 102

CHAPTER 3 **118**

Introduction 121
Materials and Methods 123
Results 126
Acknowledgments 132
References 132
CHAPTER 4 **147**
Abstract 150
Introduction 150
Materials and methods 153
Results 158
Discussion 164
Acknowledgments 167
References 168
DISCUSSION AND CONCLUSION **180**
REFERENCES **188**
ATTACHMENT **201**
APPENDIX **219**

Introduction

1. *Neurospora crassa*: a model fungus

Scientists have long adopted a group of microorganism as models for detailed morphologies, genetics and evolutionaries analyses. Approximately 10% of all know living organisms are fungi, with only 70,000 different species described until now (BLACKWELL, 2011). However, it is estimated that there are around 1.5 million species of fungi (HAWKSWORTH, 2001), and the more recent prediction based on molecular approaches calculates a total of 5.1 million of fungi species (O'BRIEN et al., 2005; TAYLOR et al., 2010). Fungi are found in all niches, some in symbiotic association with plants and algae, many causing diseases, and most others playing a beneficial role in the environment. Some fungi are used for food or fermentation (reviewed in RAJU, 2009). Because fungi constitute the Kingdom most closely related to Animalia, and are exceptionally accessible experimentally, fungi are universally used as model organisms for understanding all aspects of basic cellular regulation (DUNLAP et al., 2007).

The filamentous fungus *Neurospora crassa* has been used as genetic model system since 1930 (SHEAR; DODGE, 1927; LINDEGREN; BEANFIELD; BARBER, 1939), and possesses numerous characteristics that make it a suitable model: simple nutritional requirements; fast vegetative growth; two distinct mating types; haploid vegetative phase; production of ascospores and growth on defined media (DAVIS; PERKINS, 2002). In 1941, Beadle and Tatum demonstrated the relationship between genes and proteins using *N. crassa*; they formulated what became known as the 'one gene, one enzyme' hypothesis. These findings allowed *N. crassa* became a popular experimental model for genome defense mechanisms, metabolism, circadian rhythms, gene expression, regulation of meiotic recombination, signal transduction, responses to light, post-transcriptional gene silencing and biochemistry, genetic and molecular studies (PERKINS, 1992; DAVIS, 2000; DAVIS; PERKINS, 2002; DUNLAP et al., 2007).

Neurospora can grow with only carbon source, mineral salts and one vitamin, biotin, which is absolutely required. The Vogel's salts contain Na_3 citrate, KNO_3, $(NH_4)H_2PO_4$, KH_2PO_4, $MgSO_4$, $CaCl_2$ and trace element. Many carbon sources can be used such as glucose, mannose, fructose, xylose, sucrose, maltose, cellobiose, and trehalose (METZENBERG, 1979). Its optimal growth is around pH 5.4-5.8, but is quite tolerant and can grow in a pH varying from 4.0 to 9.0 (THEDEI JUNIOR;

DOUBOWETZ; ROSSI, 1994), with growth being poor at either extreme. Vegetative growth is optimal at about 30ºC to 35ºC, although it can grow at temperatures as high as 42ºC and as low as 5ºC. Neurospora is an absolute aerobe and is considered completely nonpathogenic to humans, animals, and plants (METZENBERG, 1979).

The first record of *N. crassa* was in 1843, when an orange mould infestation in French bakeries was investigated (PAYEN, 1843; PERKINS, 1991). In nature, *N. crassa* is often found on scorched vegetation after wildfires or agricultural burns (RAJU, 2009). In Brazil, Neurospora was described as an orange fungus growing on burned vegetation (MÖLLER, 1901). The combination of Neurospora and heat is known for a long time. The ascospores are tolerant to high temperatures and remain dormant until they are exposed to heat. Activation of ascospores explains the occurrence of the fungus in bakeries or after wildfires (PERKINS, 1992).

N. crassa is haploid during the vegetative growth, when it is possible to see assexual strutures called macroconidia, or simply conidia, and microconidia, and diploid during a short time in the sexual phase, when it is possible to verify the formation of a fruiting body. As *N. crassa* is heterothallic, it exists in two mating types, designated A and a, and no mating can occur unless both are present. The two mating types are phenotypically indistinguishable. If mating type A was inoculated onto the medium first and the growth allowed for several days, it will be the female. The later arrival will function as male (METZENBERG, 1979). Both asexual development and sexual differentiation are highly influenced by environmental factors including nutrient, light, and temperature (DUNLAP et al., 2007). The *N. crassa* life cycle is shown in the Figure 1.

In the asexual cycle phase, the mycelium is composed of haploid hyphae and the reproduction occurs by conidia produced by two pathways: the macroconidiation and microconidiation (Figure 1). Both pathways require water-air interface and are suppressed in submerged cultures. The multinucleate macroconidia is promoted by apical structures called conidiophores (ADAMS; WIESER; YU, 1998; SPRINGER, 1993; BORKOVICH et al., 2004). The macroconidiation can be induced by environmental signals such as heat shock, desiccation and nutritional limitation (TURIAN; BIANCHI, 1972), and is regulated by the endogenous biological clock in *N. crassa* (LOROS; DUNLAP, 2001). In microconidiation, the microconidia are formed within the basal hypha and expelled from the wall when the maturation process is completed (PERKINS; TURNER; BARRY, 1976) or by microconidiophores

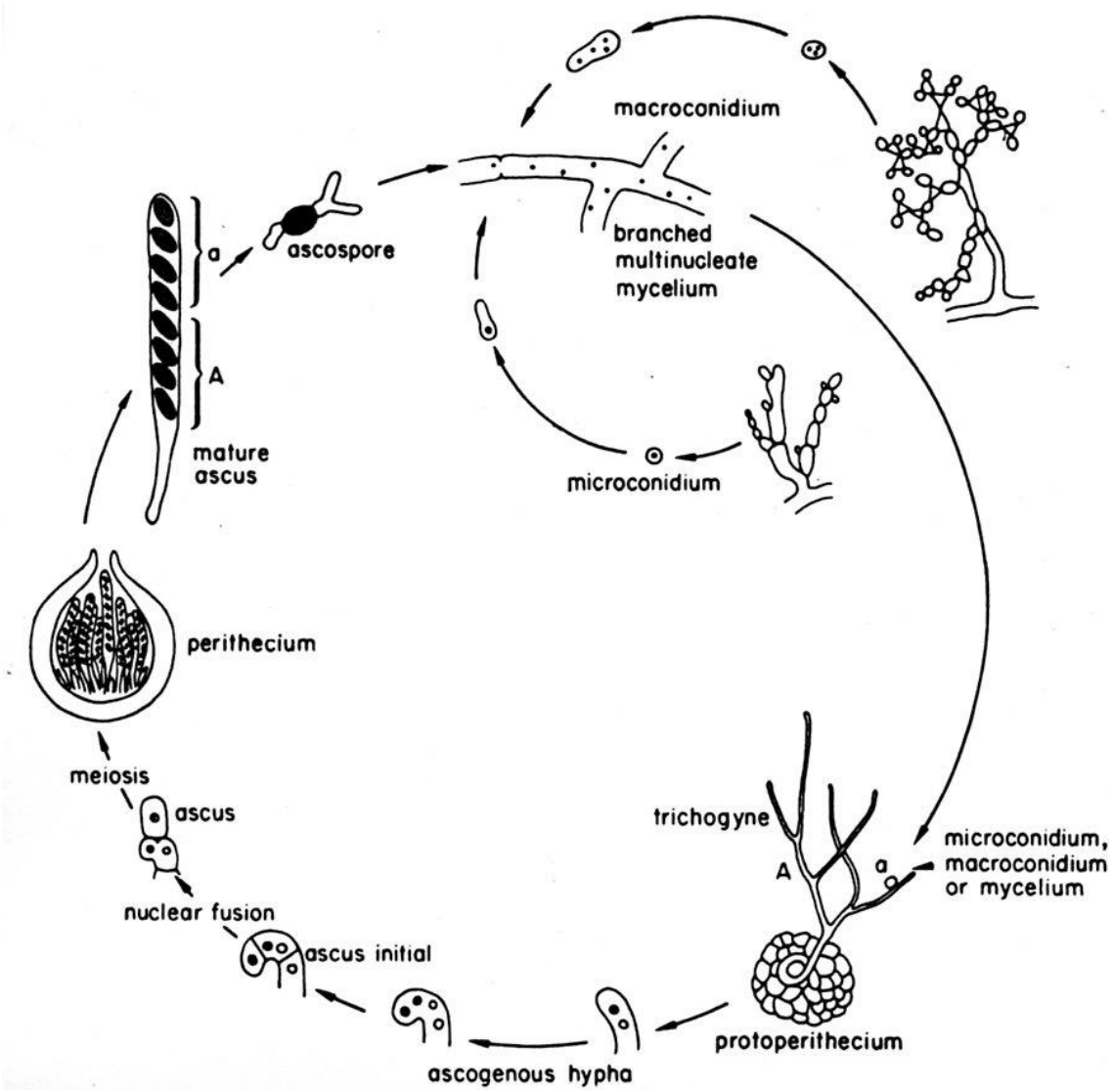

Figure 1- The life cycle of *Neurospora crassa* showing some of the many life stages and cell types in the sexual and asexual cycles (DUNLAP et al., 2007).

(SPRINGER; YANOFSKY, 1989; MAHESHWARI, 1999; BISTIS; PERKINS; READ, 2003). The microconidia are uninucleate and smaller than macroconidia. They are generally produced only in relatively small numbers (METZENBERG, 1979). Another form of asexual propagation is through arthroconidia that are multinucleate hyphae fragments produced by segmentation of pre-existing fungal hyphae (MAHESHWARI, 1999).

The complex sexual reproductive pathway occurs when any structure (A or a) is submitted by nitrogen limitation. In this case, some of the hyphae curl up into a specialized form, the ascogonium, where occurs the formation of a fruiting body called protoperithecium (female structure). The end of a specialized ascogonial hypha is differentiated into a trichogyne. When a conidium, microconidium, or even a piece of mycelium of the opposite mating type lands on the trichogyne, a donor nucleus (male) is conducted into the ascogonium, where it meets the resident nucleus (female). In this phase, the cover mycelium involving the ascogonium begins to develop a wall resulting in a structure called perithecium. When the nuclei of the two mating types fuse, meiosis proceeds promptly. The four meiotic products undergo a mitotic division to give eight sister nuclei (four for each mating type) that will result in ascospores or sexual spores. The maturing black ascospores (or spores) are contained in a sack, the ascus (Figure 1). The spores will germinate and produce hyphae resulting in colonies exactly like those produced by asexual spores (METZENBERG, 1979).

2. The sequencing of the *N. crassa* genome and its consequences

The sequencing of the *N. crassa* genome was reported by Galagan et al. (2003), which has about 40 Mb, much higher when compared to other fungi with known genomes, such as *Saccharomyces cerevisiae* and *Schizosaccharomyces pombe*. A total of 10,082 protein-coding genes has been predicted with, on average, one gene per 3.7 kilobases and an average of 1.7 short introns (134 bp on average) per gene (HYNES, 2003). Its genome is organized in seven chromosomes ranging from 4 to 10 Mb (SCHULTE et al*.,* 2002) and 44% of genome are represented by genes encoding proteins. When the genome was sequenced, it was reported that only 13% of the genes encoded known proteins, 46% represented ORFs encoding hyphotetical proteins and 41% represented ORFs encoding predicted proteins that

have no significant matches to known proteins. In addition, of 1,421 *N. crassa* genes with highest matches to either plant or animal proteins, a significant number (584) have no high-scoring protein matches in either *S. cerevisiae* or *S. pombe*. Many of these proteins may be involved in determining hyphal growth and multicellular developmental structures in Neurospora, as these characteristics are not found in yeasts, suggesting good relation between filamentous fungi and upper eukaryotes, compared with yeasts and lower eukaryotes (GALAGAN et al., 2003; HYNES, 2003).

New computational analysis of the *N. crassa* genome demonstrated that 40% of genes encode proteins functionally annotated in databases and estimated 27.588 protein-protein interactions among 3,006 proteins, showing that probably each protein has, on average, 18.4 partners (WANG et al., 2011). After the genome sequencing of *N. crassa*, an overall effort was proposed by the scientific community to develop the functional genomic of Neurospora. Four projects were proposed: the generation of knockout constructs (Project 1); the annotation of genes (Project 2); the knockouts analysis by microarrays (Project 3); and cDNA libraries and SNP (Single Nucleotide Polymorphism) MAP generation (Project 4) (DUNLAP et al., 2007).

After the proposed projects, new methodologies were developed to inactivate specific genes (NINOMIYA et al., 2004) and create knockout strains (DUNLAP et al., 2007). However, there are more genes in filamentous fungi as compared to yeasts and different ways in which gene function can be eliminated in Neurospora (DUNLAP et al., 2007). One is RIP (Repeat Induced Point mutation), that utilizes a Neurospora-specific phenomenon in which duplicated sequences, when passed through meiosis, undergo frequent C to T transitions, resulting in loss of total or partial function (ROUNTREE; SELKER, 1997). Based on the natural process of *N. crassa*, inactivation of genes to construct mutant strains by RIP is based on introducing an extra copy of the target gene in the fungus. Transformants containing an additional copy of the gene introduce point mutations in the genome sequence when subjected to cross followed by meiosis (SELKER, 1990). This technique is an effective method, but requires a long time to be developed, and today is used for the partial inactivation of essential genes.

Other process for inactivate genes and generate knockout mutant strains is by replacement through standard homologous recombination. In eukaryotes, there are two mechanisms of genetic recombination: homologous recombination involves interaction between homologous sequences, whereas non-homologous

recombination involves integration of exogenous DNA into any region of the genome, independent of homology. The homologous recombination é predominant in *S. cerevisiae*, but in *N. crassa* the frequency of homologous recombination rarely approaches 100% but lies instead between a few percent and 30% depending on the gene and the length of the homologous DNA flanking the gene in the construct (DUNLAP et al., 2007).

The non-homologous recombination mechanism is evolutionarily conserved, being the predominant mechanism for upper eukaryotes such as humans, plants and insects. Among the proteins involved in this mechanism, Ku70 and Ku80 proteins form a heterodimer that binds to the DNA ends (WALKER; CORPINA; GOLDBERG, 2001). In *N. crassa, mus-51* and *mus-52* are the orthologs genes of human *KU70* and *KU80*, respectively, and a procedure based on PCR was developed to inactivate these genes and, thus, to construct strains in which non-homologous recombination process is ineffective, promoting homologous recombination (NINOMIYA et al., 2004).

The knockout approach allowed the construction of strains containing individual inactivated genes that are available to the scientific community by the Fungal Genetics Stock Center (FGSC, Kansas City, Missouri, USA). In addition, the disruption groups of genes that can form the basis of research projects are available and included, for instance, genes encoding transcription factors, genes encoding protein kinases and phosphatases, and chromatin-remodeling enzymes. In 2006, Colot et al. published the first results relating to mutant strains in genes encoding transcription factors, showing that some transcription factors highly conserved could play different roles in various fungi and 43% of the deletion mutants revealed phenotypes, with more than half of these strains possessing multiple defects.

In 2011, Park et al. published a global morphology analysis using the colletion of mutant strains in genes enconding protein kinases, showing that 71% of the serine-threonine (S/T) kinases mutated were either essential or necessary for normal growth, development, or chemical resistance underscores the central importance of S/T protein kinases to Neurospora biology. The results also revealed important differences between S/T kinases and transcription factors in the regulation of growth and development. A greater number of kinase mutants were defective in at least one phenotype compared to transcription factor mutants and, significantly, more kinase genes (40%) are involved in the regulation of two or more functions, compared to

transcription factors (18%). Thus, the data demonstrate that the impacts of kinases on fungal growth and differentiation are more dramatic than that on transcription factors, likely due to less functional redundancy in the kinases.

The annotation of the *N. crassa* genome and gene sequences has been done by association with the scientific community (Project 2), and gene expression data generated by microarray technology (Project 3) and analysis of EST sequences and SNP maps are going on, and interesting results are being published (DUNLAP et al., 2007). The use of mutant strains has become an interesting material for the early studies on the regulatory mechanism of many biological processes in *N. crassa* by the absent of a unique protein in the specific mutant strain.

3. The biological clock in *N. crassa*

The ability to sense and respond to light is critical for the survival of most organisms. *N. crassa* has been widely used as a model organism for the study of diverse biological processes ranging from metabolism to circadian rhythms and photobiology (BORKOVICH et al., 2004). This fungus is a good model system to further elucidate the connection between the clock and light to metabolism because the main components of the oscillator and input pathways of the clock have been identified and the metabolic process is less complex than in the mammals. The light activates a variety of physiological processes in Neurospora, including the biosynthesis of carotenoid pigment (HARDING; TURNER, 1981), conidiation (KLEMM; NINNEMANN, 1978; LAUTER, 1996), protoperithecium development (DEGLI-INNOCENTI; POHL; RUSSO, 1983) and the resetting of the circadian clock (CHEN; LOROS, 2009). More than 5% of *N. crassa* genes responded to the light stimulus by increasing transcript levels (CHEN et al., 2009). Genes involved in the synthesis of pigments, vitamins, cofactors, secondary metabolism, DNA processing and cellular signaling were found enriched in the early light response (high peak levels after 15-30 min light exposure). In contrast, genes involved in carbohydrate metabolism and oxidation of fatty acid were found enriched in the late light response (high peak levels after 1-2 h light exposure) (CHEN; LOROS, 2009).

The light responses in *N. crassa* are near UV/blue light, suggesting the presence of a photoreceptor dedicated to blue light sensing and signal transduction (CHEN; LOROS, 2009). It was isolated only two fully blind mutants, *wc-1* and *wc-2*,

both GATA family zinc finger transcription fator, that directly regulate the gene activation under light sensing (LINDEN; RODRIGUEZ-FRANCO; MACINO, 1997; COLLETT et al., 2002; LEE; DUNLAP; LOROS, 2003). WC-1 (White Collar-1) has a PAS domain to protein-protein interation (BALLARIO et al., 1996) and a LOV domain to FAD binding, allowing WC-1 to act as blue light photoreceptor (FROEHLICH et al., 2002). The WC-2 protein (White Collar-2) has a PAS domain (LINDEN; MACINO, 1997), and forms an obligate complex with WC-1 resulting in the White Collar Complex (WCC) that binds to specific DNA sequences (FROEHLICH; LOROS; DUNLAP, 2003). After the WCC, VIVID (VVD) is other photoreceptor intensely studied in the fungus, acting as repressor for most of all light-induced gene expression controlled by the WCC (SHRODE et al., 2001; SCHWERDTFEGER; LINDEN, 2003; CHEN et al., 2009). VVD is a small 21 kDa PAS photoreceptor consisting of a LOV domain (ZOLTOWSKI; CRANE, 2008). The activation of gene expression by light is transient and stops after a long exposure to light, when occurs the interation between VVD and WCC (Figure 2) (LAUTER; YANOFSKY, 1993; ARPAIA et al., 1999; HEINTZEN; LOROS; DUNLAP, 2001; SCHAFMEIER; DIERNFELLNER, 2011).

Light is important to synchronize the biological clock with the day-night cycle environmental (SCHAFMEIER; DIERNFELLNER, 2011). The circadian clock is an intrinsic time-tracking system, present in almost all organisms from bacteria to mammals, that provides a mechanism to predict and prepare for changes that occur in the environment, providing an adaptive advantage (DUNLAP; LOROS; DECOURSEY, 2004). The daily rhythms are generated by the biological clock and are manifested by the cyclic expression of genes or the products encoded by genes. Circadian rhythms are coordinated according to exogenous environmental cycles, allowing the species organize the metabolism and behavior appropriately (EDMUNDS, 1987). In *N. crassa*, the circadian clock consists of the WCC, the negative regulator FRQ (FREQUENCY) and FRQ-interacting RNA helicase (FRH) (HEINTZEN; LIU, 2007).

The White-Collar Complex binds to the *frq* promoter and activates gene transcription leading to FRQ accumulation. FRQ interacts with FRH forming the FRQ/FRH complex (FFC), inhibits WCC activities and, therefore, decreases the *frq* transcription (DUNLAP, 1999). Function, activity, turnover, and subcellular localization of clock proteins are tightly post-translationally regulated, and

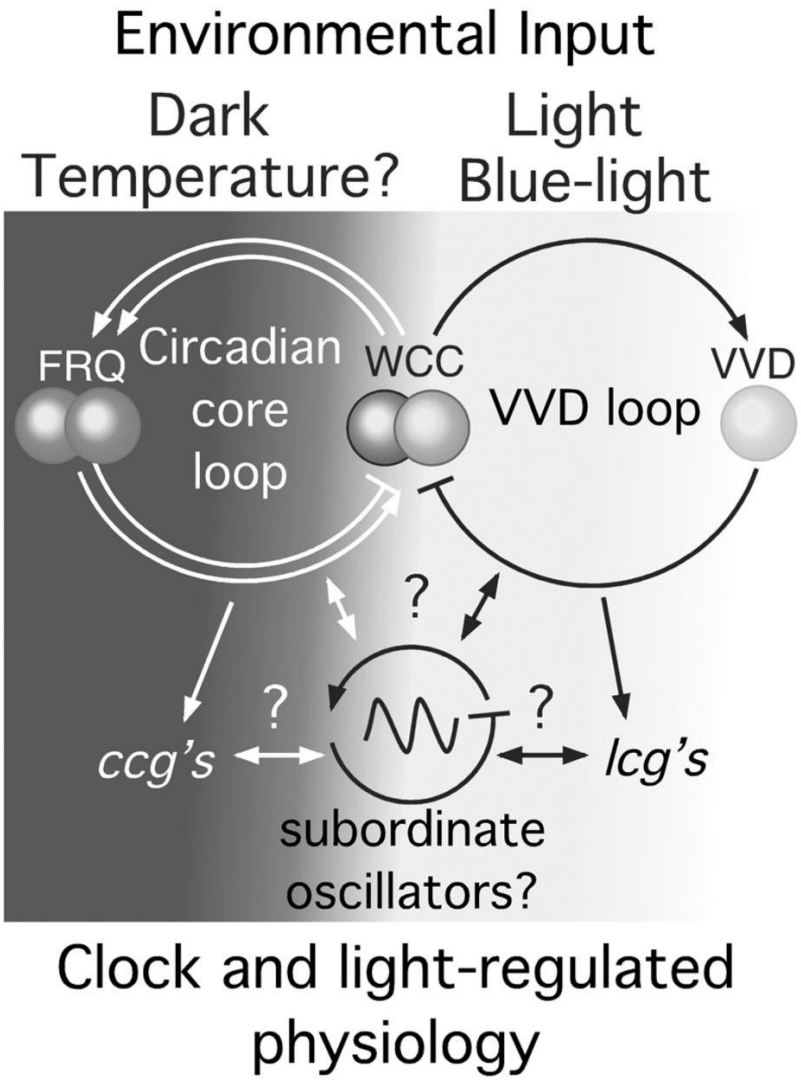

Figure 2- Interactions of the Neurospora light and circadian clock pathways. Simplified model of the Neurospora circadian system: the *frq*, *wc-1* and *wc-2* genes and their encoded proteins interact via a transcription/translation-based feedback loop that is essential for circadian rhythmicity. Light input, via WCC, induces *frq* transcription thus facilitating light-resetting and entrainment of the clock. VVD interferes with light signal-transduction pathways by repressing the WCC activity. Downstream pathways, clock- and light-controlled genes can be regulated. Dark shading indicates pathways that operate in darkness and light shading indicates pathways that are activated in the light (PRICE-LLOYD; ELVIN; HEINTZEN, 2005).

phosphorylation is crucial for clock function (REISCHL; KRAMER, 2011). Over the course of a circadian cycle, FRQ is progressively phosphorylated and then degraded via ubiquitin proteasome pathway (QUERFURTH et al., 2011). As the levels of FRQ decrease, dephosphorylation of WCC by protein phosphatase reactivates the transcription factor, thereby initiating a new circadian cycle (DUNLAP, 1999). Downstream of the clock oscillator and light-input pathways, clock- and light-controlled genes (*ccg* and *lcg*) ultimately control circadian behaviour and light-responses. Additional, subordinate feedback loops may regulate subsets of clock-controlled processes (Figure 2).

Insight into circadian clocks and metabolism started from the discovery that biological rhythms are sustained by a genetically encoded transcription network that functions as a molecular oscillator in most cell types, maintaining phase alignment in a range of behavioral, physiological, and biochemical processes with the environmental light cycle (MARCHEVA et al., 2013). In humans, the clock impacts many aspects of our lives, ranging from the regulation of our sleep/wake cycle, to cell division, and rhythms in gene expression. Therefore, defects in the clock are associated with a wide range of diseases, such as mental disorders and metabolic syndrome (ECKEL-MAHAN; SASSONE-CORSI, 2013; ASHER; SASSONE-CORSI, 2015; ZARRINPAR; CHAIX; PANDA, 2016).

Experiments performed in the last decade have highlighted the importance of connection between the circadian clock and metabolism. In mammals, many genes associated with glucose metabolism in the liver exhibit robust circadian regulation (PANDA et al., 2002; UEDA et al., 2002; MILLER et al., 2007), suggesting that the circadian clock plays a significant role in hepatic glucose metabolism. Hepatic glycogen content, which is important for glucose homeostasis, exhibits circadian rhythm that peaks during the dark-light transition in nocturnal rodents (ISHIKAWA; SHIMAZU, 1976). The activities of glycogen synthase and glycogen phosphorylase also show circadian variation, and the balance between them forms the basis for circadian variation in the hepatic glycogen content (ISHIKAWA; SHIMAZU, 1976). It was shown that CLOCK mouse transcription factor regulates the circadian variation of hepatic glycogen synthesis through the direct transcriptional activation of *Gys2*, the gene encoding the rate-limiting enzyme in glycogenesis (DOI; OISHI; ISHIDA, 2010). Another study has demonstrated the connection between biological clock and diabetes, since the mutants in clock components showed a decrease in rhythmic

oscillation of genes involved in insulin signaling and glucose detection (MARCHEVA et al., 2010).

In *N. crassa*, *ccg-9*, one of the genes controlled by the clock, encoding trehalose synthase that participates in the synthesis of the trehalose, is required for rhythmic conidiation under dark conditions (SHINOHARA et al., 2002). Correa et al. (2003) demonstrated the first correlation between clock and glycogen metabolism. They showed, according to microarray analysis, that several genes encoding enzymes involved in carbon and nitrogen metabolism showed circadian rhythms in mRNA accumulation, with peaks occurring in the late night to early morning. The glycogen phosphorylase and branching enzyme genes was circadianly regulated. Moreover, recently, many genes involved in metabolism have been shown to be clock-controlled (HURLEY et al., 2014). However, there is still much to learn about the connection between the clock and metabolism, particularly in the details of how the oscillator directs metabolic rhythms. Furthermore, the transcriptional network regulating light and clock metabolism response is increasingly being explored, putting *N. crassa* at the forefront of understanding genome wide regulation and the output from the clock.

4. Reserve carbohydrates metabolism: glycogen and trehalose

We have been investigating how *N. crassa* controls the metabolism of glycogen and trehalose, storage carbohydrates that function as a carbon and energy reserve. Glycogen is a branched polymer of glucose found in cells of different organisms (HARRIS, 1997; NELSON; COX, 2008). The glycogen is a uniform molecule characterized by glucose units linked by α-1,4 linear glycosidic bounds and α-1,6 linked glucose at the branching points, that occurs each four glycose units and are responsible to the ramification of the molecule (NELSON; COX, 2008). The synthesis and degradation of this polymer are processes conserved in eukaryotes, and three steps are involved in the synthesis, which are: initiation, elongation, and branching, and requires the activities of glycogenin, glycogen synthase, and the branching enzyme, respectively. The glycogenin is a self-glucosylate protein that uses UDP-glucose (UDPG) as the glucan donor and acts as an initiator molecule for glycogen initiation (FARKAS et al., 1991; CHENG et al., 1995). The glycogen synthase catalyzes the formation of α-1,4 glycosidic bounds, using UDPG as the

donor of the glucose residues and promotes the chain extension (LELOIR, 1971; ALONSO et al., 1995). Finally, the branching enzyme catalyzes the formation of α-1,6 glycosidic bounds, transferring approximately seven glucose residues from the nascent chain to the glucose C6 in an adjacent chain, creating a ramification point (NELSON; COX, 2008).

Degradation of glycogen requires the activities of glycogen phosphorylase, that releases glucose-1-phosphate (G1P) from a terminal α-1,4 glycosidc bond, and the activity of debranching enzyme, that carries out two distinct enzymatic functions: 1) glucosyltransferase, that transfers of three glucose residues from one branch to another, and 2) glucosidase, that breaks α-1,6 glycosidic bounds (NELSON; COX, 2008).

The trehalose, another reserve carbohydrate, is a non-reducing disaccharide composed of two linked glucose by α-1,1 glycosidic bounds and can be synthesized by bacteria, fungi, plants, and invertebrate animals. In fungi, trehalose is present mainly in spores to be further used as carbon and energy source for conidia germination (HANKS; SUSSMAN, 1969; FILLINGER et al., 2001). Trehalose biosynthesis is catalyzed by a large trehalose synthase complex consisting of trehalose-phosphate synthase and trehalose-phosphate phosphatase subunits (BELL et al., 1998). The degradation occurs by two trehalases: neutral trehalase with an optimum activity at pH 6.8-7.0 (also referred to as regulatory trehalase) and acid trehalase with an optimum activity at pH 4.5-5.0 (also referred to as nonregulatory trehalase). It is also considered that the neutral trehalase enzyme is cytosolic, while the acidic trehalose is vacuolar (cited by FRANÇOIS; PARROU, 2001). The synthesis and breakdown processes of glycogen and trehalose in *S. cerevisiae* can be seen in Figure 3.

In overall, the glucose enters the cell via passive transport, mediated by specialized proteins (OLSON; PESSIN, 1996; THORENS, 1996) and converted to glucose-6-phosphate (G6P) in a reaction catalyzed by hexokinase. G6P is first converted to glucose-1-phosphate (G1P) by the enzyme phosphoglucomutase, which serve as substrate for the production of UDPG by the action of UDP-glucose pyrophosphorylase. The UDPG molecules are direct glucose donor residues for the synthesis of glycogen and trehalose (ROACH, 2002; NELSON; COX, 2008). For glycogen synthase extend the molecule is necessary the presence of an oligosaccharide containing at least eight glucose residues, which is provided by the

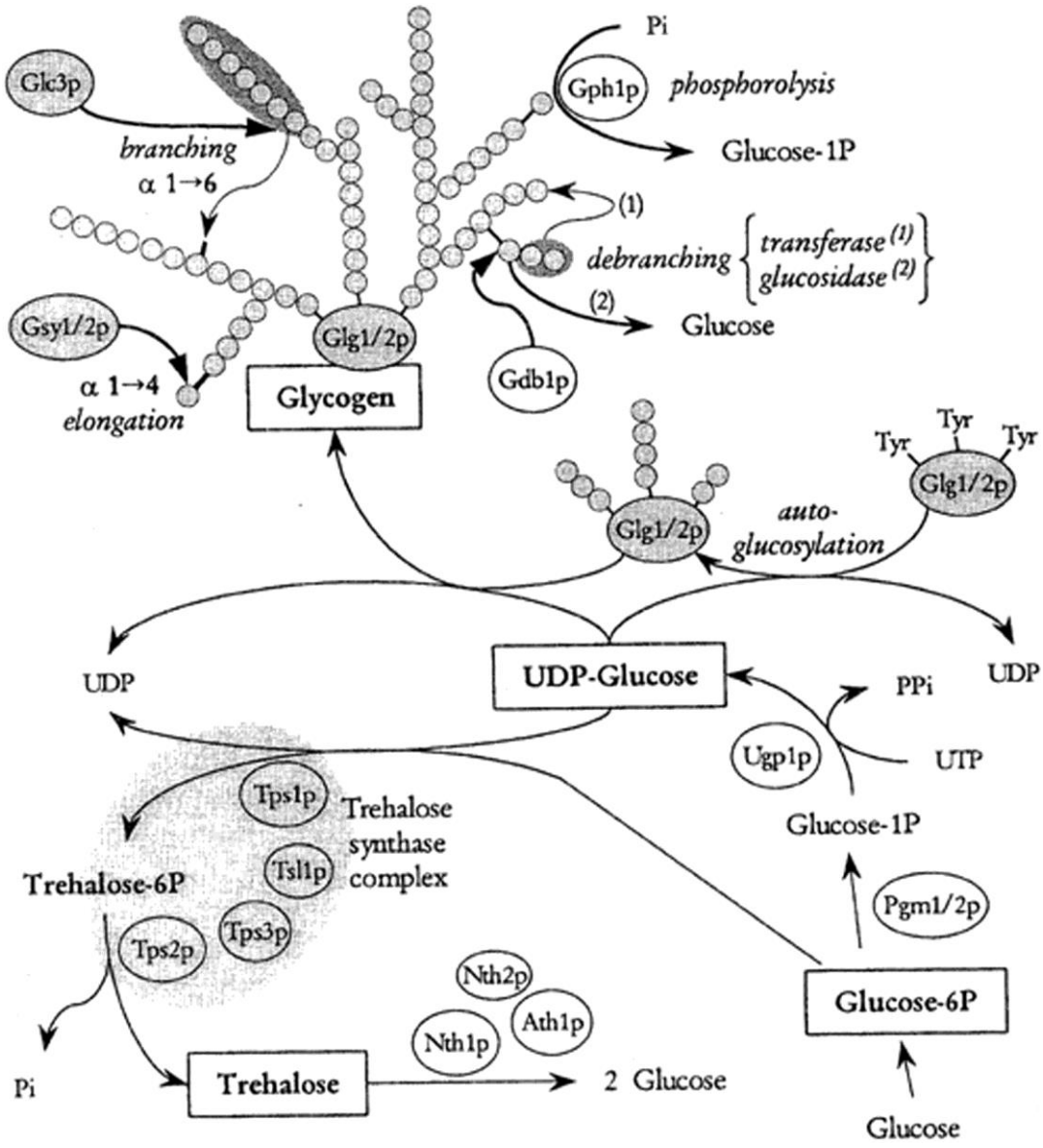

Figure 3- Schematic representation of glycogen and trehalose metabolic pathways in the *S. cerevisiae*. In glycogen process, glucose enters the cell and is converted to glucose-6P (G6P) and thus to glucose-1P (G1P) by phosphoglucomutase (Pgm1/2p). G1P is converted into UDP-glucose (UDPG), the donor molecule of glucose, by UDPG pyrophosphorylase (Ugp1p). Glycogen synthesis is initiated by glycogenin (Glg1/2p), that self-glucosylated, produces a short α (1,4)-glucosyl chain that is elongated by glycogen synthase (Gsy1/2p), through the formation of α-1,4 glycosidic bonds. The chains are ramified by the branching enzyme (Glc3p) which transfers a block of 6-8 residues from the end of a linear chain to an internal glucosyl unit and creates an α (1,6)-linkage. Glycogen degradation occurs by the combined action of glycogen phosphorylase (Gph1p) which releases glucose-1-P, and a debranching enzyme (Gdb1p) which transfers a maltosyl unit to the end of an adjacent linear α (1,4)-chain and releases glucose by cleaving the remaining α (1,6)-linkage. Trehalose biosynthesis is catalyzed by the trehalose synthase complex composed of four subunits. The trehalose-6-phosphate synthase (Tps1p) produces trehalose-6P from UDPG and G6P, which is dephosphorylated in trehalose by the trehalose-6-phosphate phosphatase (Tps2p). Tps3p and Tsl1p are two regulatory subunits that stabilize the complex. Trehalose is degraded by neutral (Nth1p) or acid (Ath1p) trehalase (FRANÇOIS; PARROU, 2001).

self-glucosylated glycogenin in their tyrosine residues. The synthesis is completed by the action of the branching enzyme, which transfers a fragment of six to seven glucose residues to the branch points (ROACH, 2002). For breakdrown of glycogen, the glycogen phosphorylase enzyme catalyzes the phosphorolysis of glycogen yielding G1P and shortened glycogen as product. The debranching enzyme transfers three glucose residues to the end of an adjacent linear chain and releases glucose by cleaving the remaining α (1,6)-linkage (Figure 3). For trehalose biosynthesis, the G6P and UDPG are used to produce trehalose-6-P by the trehalose-6-phosphate synthase. The trehalose-6-P is dephosphorylated to trehalose by the trehalose-6-phosphate phosphatase. In degradation, the disaccharide is hydrolyzed into two molecules of glucose by either the neutral or acid trehalase enzymes (Figure 3).

5. Regulation of glycogen and trehalose metabolism

Glycogen synthase and phophorylase are the rate-limiting enzymes and are subjected to different types of regulation: allosteric modulation and post-translational control by the action of protein kinases and protein phosphatases (FRANÇOIS; VILLANUEVA; HERS, 1988). The two enzymes are regulated by allosterism, where glucose-6-phophate and AMP are the allosteric effectors of glycogen synthase and glycogen phosphorylase, respectively. Glucose-6-phophate reverses the glycogen synthase inactivation by phosphorylation and AMP is the allosteric activator for the dephosphorylated glycogen phosphorylase (TÉLLEZ-IÑÓN; TORRES, 1970; MADSEN, 1986; FRANÇOIS; VILLANUEVA; HERS, 1988; JOHNSON; BARFORD, 1990; JOHNSON, 1992). In addition, they are also regulated by reversible covalent modification, in which phosphorylation activates glycogen phosphorylase and inhibits glycogen synthase. Multiple phosphorylation sites were identified in glycogen synthases, which are phosphorylated by different protein kinases, depending on the organism, whereas glycogen phosphorylase is phosphorylated in a single residue, which is modified by the phosphorylase kinase protein (HARDY; ROACH, 1993; NELSON; COX, 2008, cited in BERTOLINI et al., 2012).

In contrast to glycogen metabolism, the trehalose synthase complex is not subject to reversible phosphorylation. A peculiar property of this protein complex is its strong temperature activation, with an optimum at 42ºC to 45ºC in the presence of physiological concentrations of substrates and effectors. The trehalose synthesis can

be strongly influenced by changes in substrates concentration (G6P and UDPG), temperature and the steady-state levels of the protein. In the breakdown of trehalose, only the neutral trehalase from yeasts exhibits a N-terminal extension that contains the phosphorylation regulatory domain (NWAKA; HOLZER, 1998). Thus, this enzyme exists in two interconvertible forms by reversible phosphorylation. PKA is the only protein kinase known to directly phosphorylate and activate neutral trehalase isoform 1 (cited in FRANÇOIS; PARROU, 2001).

5.1 Environmental conditions regulating reserve carbohydrate accumulation and metabolism

Glycogen and trehalose are the two glucose stores of the cells, and the large variations in the cell content in these two compounds in response to different environmental changes indicate that their metabolism is controlled by complex regulatory systems. The amount of glycogen found in a particular situation results from the balance between glycogen synthase and glycogen phosphorylase activities. Besides reversible changes in their activities, glycogen levels are also correlated with physiological conditions through control of gene expression, and the activation of different signaling pathways affects glycogen storage (reviewed in ROACH et al., 2012).

Microorganisms and mammals synthesize and accumulate glycogen in periods of abundance of nutrients and degrade under periods of stress, such as nutritional shortage (HARRIS, 1997; LILLIE; PRINGLE, 1980). In mammalian cells, the liver and the skeletal muscle are the main depository of glycogen. In the yeast *S. cerevisiae*, the synthesis and degradation of glycogen vary with environmental conditions and stages of the life cycle (JOHNSTON; CARLSON, 1992). Cells acumulate glycogen when the culture begins the stationary phase during vegetative growth or when submitted to heat shock (NI; LAPORTE, 1995), or during the sporulation or germination induction of the spores (THEVELEIN, 1984; COLONNA; MAGEE, 1978; KANE; ROTH, 1974), or in nutrient limitation (LILLIE; PRINGLE, 1980). Such conditions induce the transcription of the *GSY2* gene (glycogen synthase isoform 2) (NI; LAPORTE, 1995). The *GSY2* encodes the predominant glycogen synthase since loss of its function resulted in a 90% reduction in both enzyme activity and glycogen levels in *S. cerevisiae* (FRANÇOIS; PARROU, 2001).

N. crassa accumulates glycogen late in the exponential phase of the vegetative growth (24 h), when the glycogen synthase activity and the expression of *gsn* (glycogen synthase) transcript are increased, and degrades it at the beginning of the stationary phase (NOVENTA-JORDÃO et al., 1996; DE PAULA et al., 2002). Besides that, glycogen levels were highly regulated on exposure of cultures to some stress conditions, such as heat shock (transfer from 30ºC to 45ºC) and carbon source limitation (sugar-free medium) (DE PAULA et al., 2002). In *N. crassa*, the glycogen is degraded under heat shock stress (NOVENTA-JORDÃO et al., 1996). The levels of *gsn* transcript, the glycogen content and the glycogen synthase activity were reduced when the mycelium was exposed to heat shock and carbon starvation, however were recovered when the cultures returned to normal growth conditions (30ºC and 2% of sugar) (DE PAULA et al., 2002; FREITAS; BERTOLINI, 2004). These results suggest that transcriptional regulation may account for the decrease in glycogen synthase activity and subsequent glycogen mobilization observed under these conditions. On the other hand, glycogen phosphorylase activity was activated under heat shock showing that reversible changes in the two regulatory enzymes were observed upon temperature shifting (NOVENTA-JORDÃO et al., 1996).

Trehalose is another reserve carbohydrate that can be mobilized under different growth conditions. Yeast cells submitted to heat shock accumulate trehalose (GRBA; OURA; SUOMALAINEN, 1975). In *N. crassa* conidia, trehalose corresponds to 10% of dry-weight, its levels decrease to a minimal value upon germination, remains at lower levels during all vegetative growth, and rises again at the end of the growth, accumulating into the conidia (HANKS; SUSSMAN, 1969). Under heat shock (from 30°C to 45°C), trehalose accumulates (DE PINHO et al., 2001; NEVES et al., 1991) and this effect may depend on trehalose-phosphate synthase enzymatic activities since it is the regulatory enzyme in trehalose metabolism (NOVENTA-JORDÃO et al., 1996). Under source carbon starvation, the levels of glycogen and trehalose content are reduced, but can be recovered after glucose additional in the medium (DE PINHO et al., 2001; NOVENTA-JORDÃO et al., 1996).

Studies of biochemistry and molecular characterization of proteins glycogenin (GNN) and glycogen synthase (GSN) were performed in *N. crassa* (DE PAULA et al., 2002, 2005a, 2005b). Only one isoform of GNN has been identified and gene inactivation by RIP completely abolished the glycogen accumulation (DE PAULA et al., 2005a). GNN has two glucosylation sites (Tyr196 and Tyr198) in the N-terminal

region, however each residue contributes differently to the self-glycosylation process, and the long C-terminal extension seems to be importante to enchance the interaction with the GSN (DE PAULA et al., 2005b). All glycogen synthases are conserved proteins among microbes and higher organisms and the differences are located mostly in the N- and C-termini of the protein, where the regulatory phosphorylation sites are located. The GSN enzyme of *N. crassa* shared much conservation with the Gsy1p and Gsy2p proteins of *S. cerevisiae* and with enzymes of mammals (rabbit muscle and human muscle) (DE PAULA et al., 2002). It was identified four putative phosphorylation sites in GSN enzyme based on a sequence alignment of different glycogen synthase and in *in vitro* phosphorylation reactions, all located at the C-terminus. However, *N. crassa* GSN seems to have an additional phosphorylation site (BARBOSA, 2007).

The decrease in glycogen content observed in *N. crassa* cells exposed to heat stress may result from down-regulation of the *gsn* gene mediated by the STRE (Stress Responsive Elements) motif within the promoter region. The *gsn* promoter has two STRE motifs and nuclear proteins activated by heat shock specifically bound DNA fragments containing both motifs (FREITAS; BERTOLINI, 2004). However, Msn2/4p homolog proteins, involved in yeast gene activation via STRE motifs, were not identified in the *N. crassa* database, suggesting the existence of a different mechanism to regulate the heat shock response (FREITAS et al., 2008) or different transcription factors acting in heat shock conditions.

5.2 Transcription factors regulating carbohydrate accumulation in *N. crassa*

The construction of a set of deletion strains, each carrying a deletion in a specific ORF, has allowed the screening for proteins linked to a particular phenotype. A transcription factor mutant strains collection available at FGSC was used to identify proteins that either directly or indirectly regulate glycogen metabolism in *N. crassa*. Transcription factors or regulatory protein modulate the activity of RNA polymerase II, by binding to gene regulatory sequences (COOPER, 2000), and are classified into general transcription factors or activators/repressors. The general transcription factors are constituents of the transcriptional machinery while the activators/repressors are specific transcriptional regulatory proteins that modulate the expression of certain genes (ALBERTS et al., 2002). The proteins, that are

transcriptional regulators but do not have the ability to bind to DNA itself, are called cofactors or transcriptional coregulators, and interact with transcription factors to activate or repress specific genes transcription (GLASS; ROSENFELD, 2000).

A systematic screening of a *N. crassa* deletion strains collection was performed to search for mutant strains having glycogen accumulation profiles different that in the wild-type strain under normal growth temperature (30ºC) and after heat shock stress (45ºC for 30 min). It was identified 17 transcription factors potentially involved in glycogen metabolism regulation. The identified proteins are classified in different families of transcription factors. Many of them are annotated as hypothetical proteins, however some of them were biochemically characterized either in *N crassa* or in other fungi, as PacC, XlnR, SUB-1, FlbC, RCO-1, CSP-1 and NIT-2 (GONÇALVES et al., 2011). Some mutant strains showed impairment in the regulation of *gsn* and *gpn* expression, suggesting a putative regulation of glycogenic genes by the transcription factors (GONÇALVES et al., 2011; BERTOLINI et al., 2012). Some transcription factors are involved in metabolism control, biological clock, and cell cycle progression, suggesting the existence of a link between glycogen metabolism and these processes. Recently, a screening of mutant strains in protein kinases revealed hyphotetical and identified kinases as controlling glycogen and trehalose storage in *N. crassa* under normal temperature and after heat shock stress *in N. crassa* (CANDIDO et al., 2014).

Many transcription factors are being investigated for their roles as regulators of many processes in *N. crassa* and other fungi. Among the transcription factors already characterized, it is noteworthy to describe NIT-2 in nitrogen metabolism regulation (FU; MARZLUF, 1990), XlnR in alternative carbon sources regulation (VAN PEIJ et al., 1998), SUB-1 in late light response gene regulation (CHEN; DUNLAP; LOROS, 2010), CSP-1 in ergosterol synthesis and fatty acid desaturases (SANCAR et al., 2011) and Seb1/SebA/SEB-1 in stress response (PETERBAUER; LITSCHER; KUBICEK, 2002; HAN; PRADE, 2002; DINAMARCO et al., 2012; FREITAS et al., 2016).

This study aims to elucidate the role of the VOS-1, PAC-3, CRE-1, RCO-1 and RCM-1 proteins in the regulation of the glycogen and/or trehalose metabolism under different environmental conditions: circadian clock, alkaline pH, calcium stress, repressing and non-repressing carbon sources.

5.2.1 VOS-1 transcription factor

The VOS-1 transcription factor is the *Aspergillus nidulans* VosA ortholog (viability of spores), which belongs to the velvet protein family and, together with VelB protein, is involved in the spore maturation. This protein controls trehalose biogenesis and cell wall completion (NI; YU, 2007; PARK et al., 2012) and is interconnected to the central regulatory genes in the conidiation cascade by a negative feedback regulation of *brlA* (NI; YU, 2007). In *N. crassa,* VOS-1 was identified as a WCC target showing that the *vos-1* expression was light induced and abolished in the Δ*wc-2* mutant strain (SMITH et al., 2010). Recent data showed that the *N. crassa* Δ*vos-1* mutant strain exhibits impairments in glycogen accumulation during vegetative growth when compared to wild-type cells (BONI, 2014), suggesting that VOS-1 may participate in the regulation of glycogen accumulation. In addition, data from Neurospora Program Project exploring genome wide ChIP-seq to define transcription binding sites have shown that several transcription factors bind to the promoters of glycogen enzymes, including VOS-1 (unpublished data). The consensus *A. nidulans* VosA DNA binding site (5'-CTGGCCAAGGC-3') (AHMED et al., 2013) was identified in the *gsn* and *gpn* promoters. This observation led us to start investigating the connection between light and circadian clock and glycogen metabolism.

5.2.2 PAC-3 transcription factor

The PAC-3 is ortholog of the *A. nidulans* PacC and *S. cerevisiae* and *Candida albicans* Rim101 transcription factors that play a central role in pH signaling pathway. In *A. nidulans*, PacC is activated by two successive proteolytic cleavage steps, leading to the active protein PacC (27 kDa) capable of binding to the promoters of pH-regulated genes (ARST; PEÑALVA, 2003), activating genes under alkaline pH and repressing under acidic pH (TILBURN et al., 1995; ESPESO et al., 1997). In *S. cerevisiae*, Rim 101 undergoes only one proteolytic cleavage and exerts its role as a repressor (LAMB; MITCHELL, 2003).

Some studies have shown the involvement of PacC in gene regulation of different cellular processes, such as the production of antibiotics, antifungal, and toxins (ESPESO; PEÑALVA, 1996; KELLER et al., 1997; MEYER; STAHL, 2002;

MORENO-MATEOS et al., 2007), extracellular enzymes (MACCABE et al., 1998), heat shock proteins (SQUINA et al., 2010), and others. PacC/Rim101 has been widely studied in model fungi and in human pathogens fungi, such as *C. albicans*, *A. fumigatus* and *Cryptococcus neoformans*, in which the pH signaling pathway is required for various functions associated to pathogenicity and virulence. Advances in the understanding of this pathway can lead potential results for therapeutic targets in antifungal strategies (CORNET; GAILLARDIN, 2014).

The *N. crassa* PAC-3 regulates the *gsn* gene under alkaline pH, leading to reduced glycogen accumulation. The *pac-3* mutant strain showed deficiencies in the development of the fungus, being unable to grow in alkaline pH. Furthermore, the mutant strain showed changes in glycogen accumulation before and after heat shock when compared to the wild-type cells, suggesting a role of the PAC-3 in glycogen regulation (CUPERTINO et al., 2012). Clear differences between *A. nidulans* and *N. crassa* regarding the role of PAC-3 were observed and some questions remain unclear in relation to the signaling cascade involving the PAC-3 transcription factor in *N. crass*a. Therefore, here we investigated the pH-signaling pathway, focusing on the characterization of the proteins components of this pathway, based on what is described in *A. nidulans*. In addition, the consensus *N. crassa* PAC-3 motif 5'-BGCCVAGV-3' (B=C/G/T; V=A/C/G) (WEIRAUCH et al., 2014) was identified in promoters of genes involved in glycogen and trehalose metabolism. There are evidences that the pH signaling pathway and calcium response pathway can act together. In yeasts, the transcriptional response to alkaline pH by Rim101 involves different signaling mechanisms, and the calcium signaling seems to have an important role in this response (SERRANO et al., 2002) and Rim101 acts in parallel to Crz1 transcription factor for adaptation to alkaline pH (KULLAS; MARTIN; DAVIS, 2007). Thus, we also investigated the glycogen and trehalose metabolism regulation under alkaline pH and calcium stress.

5.2.3 CRE-1 transcription factor and RCO-1 and RCM-1 corepressors

The *N. crassa* CRE-1 transcription factor is the ortholog of the *A. nidulans* CreA and the *S. cerevisiae* Mig1, the mediators of carbon catabolite repression (CCR), which represses the expression of a variety of genes through its interaction with protein partners. The Tup1-Ssn6 complex, orthologs to the *N. crassa* RCO-1-

RCM-1 proteins, acts together Mig1 in *S. cerevisiae* (NEHLIN; CARLBERG; RONNE, 1991). This complex represses various genes that encode proteins of alternative carbon sources utilization, such as galactose, maltose, xylose, arabinose, glycerol, etc, when glucose are present in the medium (RUIJTER; VISSER, 1997; ARO; PAKULA; PENTTILA, 2005). The Mig1 transcription factor has been reported to regulate a high number of genes by binding to the DNA motif 5'-SYGGRG-3' (S= G/C; Y=T/C; R= A/G) (STRAUSS et al., 1999). In *N. crassa*, deletion of the *cre-1* gene led to an increase in the production of hydrolytic enzymes involved in cellulose degradation (SUN; GLASS, 2011) and many Mig1 motifs were identified in glycogenic promoters.

The RCO-1 protein, the *rco-1* gene product (regulator of conidiation-1), has previously been described as involved in glycogen metabolism under normal and heat shock conditions (GONÇALVES et al., 2011), conidiation, development and cell differentiation (YAMASHIRO et al., 1996; ALDABBOUS et al., 2010) and is the downstream efector in circadian rhythms (BRODY et al., 2010). The RCM-1 protein, the *rcm-1* gene product (*regulation of conidiation and morphology*), is an essential protein and the *rcm-1*^{RIP} mutant strain showed serious defects in the vegetative and sexual development (OLMEDO et al., 2010). The RCO-1 and RCM-1 probably form a corepressor complex similar to Tup1-Ssn6 in yeast. Olmedo et al. (2010) showed that RCO-1 and RCM-1 participate in photoadaptation of genes regulated by light and Sancar et al. (2011) showed that CSP-1 transcription factor forms a transient complex with RCO-1 and RCM-1, acting as repressor for genes controlled by clock in *N. crassa*. The CRE-1, RCO-1 and RCM-1 complex has not been reported in *N. crassa*. We investigated here the regulatory role of CRE-1, RCO-1 and RCM-1 proteins in the regulation of glycogen metabolism in *N. crassa* under repressing and non-repressing carbon sources.

Objectives

The main objective of this work was to investigate the roles of transcription factors and cofactors in the regulation of the reserve carbohydrates glycogen and trehalose metabolism under different growth conditions and stress. The results will be presented in four chapters, according to the different transcription factors and conditions, as described below:

Chapter 1- The connection between circadian clock and glycogen metabolism. The role of the VOS-1 transcription factor in this process.

Chapter 2- Regulation by the PAC-3 transcription factor and the protein components of the *N. crassa* pH signaling pathway.

Chapter 3- Effects of alkaline pH and calcium concentration on glycogen and trehalose metabolism regulation by PAC-3.

Chapter 4- CRE-1 transcription factor and RCO-1 and RCM-1 corepressor proteins regulating glycogen metabolism.

Chapter 1

Chapter 1: The connection between circadian clock and glycogen metabolism. The role of the VOS-1 transcription factor in this process.

In this chapter, we investigated the connection between glycogen metabolism and clock in *N. crassa,* a eukaryotic model for light responses and biological rhythms. We found that glycogen is rhythmically accumulated in wild-type cells, peaking in the subjective night, and the rhythms were dependent on FRQ, a core component of the *N. crassa* clock. Furthermore, the *gsn* and *gpn* transcripts, encoding glycogen synthase and glycogen phosphorylase, respectively, are clock-controlled, peaking in the subjective morning. Using ChIP-PCR, we demonstrated rhythmic binding of VOS-1 to the promoters of these genes. However, glycogen content and the expression of *gsn* and *gpn* were maintained in *vos-1* deletion strain, suggesting that additional transcription factors or proteins may control the circadian accumulation of glycogen and the rhythmic expression of *gsn* and *gpn*. Therefore, glycogen accumulates during the night and is degraded during the day to supply the appropriate levels of energy to cells at the right time of the day, and this regulation is, in part, through the control of *gsn* and *gpn* expression by VOS-1.

Observation: According to “Alterações das Normas Internas para a defesa da Dissertação de Mestrado ou da Tese de Doutorado, aprovadas pelo Conselho de Pós-Graduação em Biotecnologia do Instituto de Química, UNESP, Araraquara, em nov/2010 e pela Congregração em reunião de dez/2010” (Appendix), the results are presented in chapter format similar to a manuscript.

VOS-1 is a transcription factor that connects the circadian clock to rhythmic glycogen metabolism in *Neurospora crassa*

Authors' names: Stela Virgilio[a], Mokryun Baek[b], Oneida Ibarra[c], Christian I. Hong[b], Maria Célia Bertolini[a,1], and Deborah Bell-Pedersen[c,1]

Address: [a]Departamento de Bioquímica e Tecnologia Química, Instituto de Química, UNESP, Araraquara, São Paulo, Brazil, 14800-060; [b]Department of Molecular and Cellular Physiology, University of Cincinnati, Cincinnati, OH 45267-0529, USA; [c]Department of Biology, Texas A&M University, College Station, TX 77843, USA.

Short title: Glycogen metabolism is clock-controlled in *Neurospora*

[1]Corresponding authors:
Maria Célia Bertolini, Instituto de Química, 14800-060, Araraquara, SP, Brazil, Phone: +55-16-3301-9675, e-mail: mcbertol@iq.unesp.br
Deborah Bell-Pedersen, Department of Biology, TAMU 3258, College Station, TX 77843, USA, Phone: 979-847-9237, e-mail: dpedersen@bio.tamu.edu

Keywords: glycogen, circadian clock, VOS-1, *Neurospora crassa*

ABSTRACT

Circadian clocks allow organisms to anticipate daily environmental cycles, and regulate physiology and behavior to optimize the timing of resource allocation for improved fitness. In humans, misregulation of the clock can lead to metabolic disorder, although details of the mechanism of clock control of metabolic homeostasis are not fully understood. We found that the regulation of glycogen metabolism is controlled by the circadian clock in *N. crassa*, and identified a transcription factor, VOS-1, connecting the clock to the downstream genes *gsn* and *gpn,* which encode the regulatory enzymes involved in glycogen synthesis and degradation, respectively. In wild-type cells, glycogen accumulation peaks at subjective night and the rhythms are dependent on the core clock component FRQ. VOS-1 binds rhythmically to the promoters of *gsn* and *gpn,* and leads to rhythmic mRNA accumulation of both genes, peaking in the subjective morning. Glycogen levels and accumulation rhythms were maintained in Δ*vos-1* cells; however, the amplitude of the rhythms of *gsn* and *gpn* mRNA was reduced as compared to wild-type cells. These data suggest the existence of additional transcription factors and/or proteins controlling the circadian accumulation of glycogen and the expression of *gsn* and *gpn*.

INTRODUCTION

The circadian clock is an evolutionarily conserved time-keeping mechanism that, through the regulation of rhythmic gene expression, coordinates the physiology of an organism with daily environmental cycles. Because virtually all aspects of human physiology and behavior are linked to the clock, abnormalities in the circadian system are associated with a wide range of diseases, including metabolic syndrome (Eckel-Mahan and Sassone-Corsi, 2013; Asher and Sassone-Corsi, 2015; Zarrinpar et al., 2016). The core oscillator consists of transcriptional/translational feedback loops, in which the positive acting heterodimeric transcription factors (TFs) drive rhythmic expression of clock genes. The clock genes encode proteins that feedback to inhibit the TFs and shut down their own synthesis. The clock TFs also bind to the promoters

of downstream target genes leading to overt rhythms in gene expression, behavior and physiology.

One of the first observations linking the clock to the physiological state of the organism was the observation that, in rats, the clock controlled the rhythms in hepatic glycogen content, and the activities of glycogen synthetase and glycogen phosphorylase, enzymes involved in glycogen synthesis and degradation, respectively (Ishikawa and Shimazu, 1976). Since this discovery, numerous studies have focused on how the circadian clock is mechanistically connected to metabolism. It was found that mice lacking the positive elements of the oscillator, CLOCK and BMAL1, show hypoinsulinaemia and diabetes (Rudic et al., 2004; Marcheva et al., 2010), and that a *Clock* gene mutation alters rhythms in hepatic glycogen levels and in the circadian expression of glycogen synthase 2, the rate-limiting enzyme for glycogen synthesis in the liver (Doi et al., 2010). Clock regulation of glycogen levels appears to be conserved in different organisms as rhythmic glycogen accumulation was reported in cyanobacteria (Pattanayak et al., 2014; Diamond et al., 2015). Furthermore, many genes associated with glucose metabolism exhibit circadian regulation in the liver (Panda et al., 2002; Miller et al., 2007).

The circadian clock in the fungus *Neurospora crassa* has been well studied. In the core oscillator, tow PAS-domain containing GATA-type zinc finger TFs White Collar-1 (WC-1) and WC-2 dimerize forming the White-Collar Complex (WCC) (Ballario et al., 1996; Denault et al., 2001; Cheng et al., 2002). WCC activates transcription of *frequency* (*frq*) (Froehlich et al., 2002; Lee et al., 2003). The negative component FRQ accumulates, enters the nucleus, and interacts with FRQ-interacting RNA helicase (FRH) (Cheng et al., 2005; Shi et al., 2010) and casein kinase I (Baker et al., 2009), and inhibits the activity of the WCC (He et al., 2005; Schafmeier et al., 2005 and 2008). Reduced *frq* mRNA levels, together with progressive phosphorylation of FRQ, relieves WCC inhibition, reinitiates the cycle and leads to proteasome-dependent degradation of FRQ (Liu et al., 2000; He et al., 2003; Larrondo et al., 2015).

The first link between the clock and metabolism in *N. crassa* was the demonstration that the clock controlled the levels of mRNA of genes involved in carbon and nitrogen metabolism (Correa et al., 2003). Among them, were the genes encoding glycogen phosphorylase and the glycogen branching enzyme, enzymes involved in glycogen metabolism. More recently, many genes involved in the

regulation of carbohydrate, fatty acid, and vitamin metabolism have been shown to be clock-controlled (Hurley et al., 2014). Thus, while clock control of metabolic genes is well described in *N. crassa* and other organisms (Diamond et al., 2015), how the clock regulates these genes is not known in any system.

A screen for TFs regulating glycogen metabolism in *N. crassa* revealed that some TFs identified as glycogen metabolism regulators (Gonçalves et al., 2011) were previously described as participating in light and/or circadian clock signaling networks (Chen et al., 2009; Smith et al., 2010; Olmedo et al., 2010; Sancar et al., 2011; Wu et al., 2014). Here, we investigated the role of the VOS-1 TF as a candidate protein connecting the circadian clock to glycogen metabolism control in *N. crassa.* We demonstrate that the glycogen accumulation and the expression of the genes encoding the regulatory enzymes glycogen synthase (*gsn*) and glycogen phosphorylase (*gpn*) are clock-controlled. The clock also regulates VOS-1 levels, and VOS-1 rhythmically binds to the *gsn* and *gpn* promoters. However, glycogen accumulation and *gsn* and *gpn* expression remained rhythmic in Δ*vos-1* cells, suggesting that the circadian clock likely controls glycogen accumulation through multiple transcription factors, and that VOS-1 could be a transcription factor controlling the robustness of the *gsn* and *gpn* rhythmic expression in *N. crassa*.

MATERIALS AND METHODS

Strains and culture conditions. The *N. crassa* wild-type strains 74OR23-1 (FGSC #2489*;* A) and ORS-SL6a (FGSC #4200*;* a), Δ*gsn* (FGSC #18933*;* A), Δ*gpn* (FGSC #20155*;* A; heterokaryon strain) and Δ*vos-1* (FGSC #13536*;* A) were obtained from the Fungal Genetics Stock Center (FGSC, University Missouri, Kansas City) (McCluskey et al., 2010). The mutant strains were constructed by replacing the gene coding region with the hygromycin resistance gene (*hph*) (Colot et al., 2006). The Δ*frq* (DBP 1228; A) and Δ*wc-1* (DBP 1224; A) strains were generated by replacing, in 74OR23-1 strain, the gene coding region with the *bar* gene, conferring resistance to Basta (glufosinate-ammonium, Bayer) (Pall, 1993). The VOS-1-V5-tagged, FRQ-LUCIFERASE (LUC) *ras-1*^{bd}, and a *vos*-1 promoter fusion to luciferase p*vos-1-luc* strains were a gift from Jay Dunlap's laboratory and the Neurospora Program Project Grant. Briefly, to generate VOS-1-V5, the V5 tag (14 amino acids GKPIPNPLLGLDST) was added at the C-terminus of the 447 amino acid VOS-1

protein, away from the NF-kB-like DNA binding domain within the velvet domain (Ahmed et al., 2013) at amino acids 15-180. The p*vos-1-luc* construction was generated using recombinational cloning in yeast as described (Colot et al., 2006) whereby 5' PCR fragments [5' of *csr*, promoter region of *vos-1*, codon optimized *luc* sequence (Gooch et al., 2008), 3' UTR of *vos-1*, and the 3' end of *csr-1*], were co-transformed with gapped plasmid (pRS426) digested with *Xho*I and *BamH*I into yeast strain FY2 (MATα, *ura3-52*). Following recombination in yeast, the full-length product was amplified and transformed into wild-type *N. crassa* cells and transformants that recombined at the *csr-1* locus and grew on 5 µg/ml cyclosporin were selected (Bardiya and Shiu, 2007). The Δ*gpn* homokaryon strain was generated by crossing the FGSC #20155, A strain with the ORS-SL6a, a wild-type strain. In order to assay transcriptional expression profiles of *gsn* and *gpn*, we constructed bioluminescence reporters, *gsn-luciferase* and *gpn-luciferase*, by fusing the promoter to codon-optimized luciferase followed by the *bar* gene for selection (Gooch et al., 2008). *gsn-luc ras-1*^{bd} and *gpn-luc ras-1*^{bd} strains were made by constructing the above cassettes targeting *csr-1* locus in the *ras-1*^{bd} strain as preciously described (Hong et al., 2014). These strains were crossed with Δ*vos-1* (FGSC#13536, A) to generate Δ*vos-1 gsn-luc ras-1*^{bd} and Δ*vos-1 gpn-luc ras-1*^{bd} strains.

All strains were maintained on solid Vogel minimal (VM) media (1x Vogel's salts, 2% glucose, 1.5% agar, pH 6.0) (Vogel, 1956) supplemented with the appropriate antibiotic as needed. Strains containing the *hph* cassette were maintained on VM media supplemented with 200 µg/mL hygromycin B. Strains containing the *bar* cassette were maintained on VM media lacking NH_4NO_3 and supplemented with 0.5% proline and 200 µg/mL Basta. Crossing was carried out on Westergaard and Mitchells's (1947) synthetic crossing medium containing 0.5% sucrose as carbon source. The Δ*gsn*, Δ*gpn* and Δ*vos-1* strains were crossed with the FRQ-LUC *ras-1*^{bd} (DBP 1985 *a*) strain to generate FRQ-LUC Δ*gsn* (DBP 2035, 2036, 2038, and 2040), FRQ-LUC Δ*gpn* (DBP 2033 and 2034), FRQ-LUC Δ*vos-1* (DBP 2037 and 2039) and FRQ-LUC WT (DBP 2029, 2031 and 2032) strains.

Light induction experiments. Conidia were inoculated in Petri dishes containing 25 mL of VM medium, 2% glucose, pH 6.0, and incubated under constant light at 30ºC for 24 h to prepare mycelia mats. Mycelial mats were cut in 4 mm discs, and individually transferred to Erlenmeyer flasks containing 65 mL of growth media and

incubated under light for 24 h at 30ºC with shaking (100 rpm). Subsequently, the flasks were transferred to dark for 24 h at 25ºC with shaking (100 rpm), and then light-induced (~21 µmole photons/m^2/s or ~1500 lux) for 15, 30, 45, 60, 120 or 240 min in a Percival (Perry, IA) incubator.

Circadian time course experiments. For rhythmic analysis, the clock was synchronized by a light-to-dark transition in mycelial mats grown in shaking liquid culture at 25ºC, according to the procedure described by Correa et al. (2003), with modifications. The light-to-dark transfer sets the clock to dusk or circadian time (CT) 12 and the clock follows its endogenous rhythm. By convention, CT0 represents the subjective dawn, and CT12 represents the subjective dusk. The times of light-to-dark transfer were set such that the age of the cultures at harvesting were approximately the same, but the CTs varied. Specifically, conidia were inoculated in Petri dishes containing 25 mL VM medium, 2% glucose, 0.5% arginine, pH 6.0, and incubated under constant light at 30ºC for 48 h to prepare mycelia mats. Mycelial mats were cut, and individually inoculated into Erlenmeyer 125 mL flasks containing 75 mL of growth media and incubated under light at 25ºC with shaking (100 rpm) on day 1. The flasks were transferred to constant darkness at 25ºC in Percival (Perry, IA) incubators at different times on day 1 (for collection at DD 36, 40, 44, 48, and 52), day 2 (for collection at DD 12, 16, 20, 24, 28, and 32), day 3 (for collection at DD 8), and harvested in constant darkness either at 9:00 a.m. (DD 12, 16, 20, 36, 40, and 44) or 5:00 p.m. (DD 8, 24, 28, 32, 48, and 52) on day 3.

Glycogen and protein quantification. Glycogen was quantified according to Freitas et al. (2010), with slight modifications. Frozen mycelia pads were ground to a fine powder in a pre-chilled mortar in liquid nitrogen and extracted in lysis buffer (50 mM Tris-HCl, pH 8.0, 50 mM NaF, 1 mM EDTA, 0.5 mM PMSF, and 1 µg/mL each of pepstatin A, leupeptin and aprotinin). Cellular extracts were clarified by centrifugation at 10,000 X *g*, for 10 min at 4ºC, and the supernatants were used for glycogen and protein quantifications. Briefly, the crude extract was precipitated with TCA, resuspended in acetate solution and digested with α-amylase and amyloglucosidase. Free glucose was quantified using a glucose oxidase kit (glucose liquiform, Labtest) and the glycogen content was normalized to total protein. Free glucose and total protein were quantified using a NanoDrop® ND-1000 spectrophotometer at 505 nm

and 280 nm, respectively. The glycogen content was calculated using a standard glycogen curve and the results were expressed in µg of glycogen/mg total protein.

RNA extraction. RNA was extracted from frozen mycelial pads ground to a fine powder in RNA extraction buffer (0.1 M sodium acetate, pH 6.5, 10 mM EDTA, 1% SDS) with 0.5 mm glass beads (BioSpec Products, Inc.) and acid phenol:chloroform (5:1 solution, pH 4.5, Ambion). After extraction, total RNA was suspended in formamide:water (1:1) (Ambion), and quantified using a NanoDrop® ND-1000 spectrophotometer.

Gene expression assays by northern blotting. Total RNA (15 µg) was separated on a 1% agarose-formaldehyde denaturing gel at 175 V for 2 h. The RNA was transferred to nitrocellulose membranes (NitroPure, GE) using 5 x SSC, and the RNA was fixed onto the membranes in a UV Stratalinker™ 2400 on the autocrosslink setting. The DNA probes were amplified by PCR using the oligonucleotides pairs NCU06687F/NCU06687R for *gsn* gene, NCU07027F/NCU07027R for *gpn* gene and NCU05964NF/NCU05964NR for *vos-1* gene (Table S1). The *ccg-1* fragment (382 bp), cloned into pKL119 plasmid, was obtained after digestion with *Eco*RV and *Hind*III. Blots were probed with the 994 bp *gsn* DNA, 1,024 bp *gpn* DNA, 633 bp *vos-1* DNA and *ccg-1* DNA fragments radiolabeled with [α-^{32}P]-dCTP (3,000 Ci/mM) (PerkinElmer) in 25 mL of hybridization buffer (50 mM Tris-HCl, pH 7.5, 0.1% Na-pyrophosphate, 1 M NaCl, 10 x Denhardt's, 50% formamide, 100 µg/mL salmon sperm DNA) at 42ºC overnight. After hybridization, the membranes were washed in 2 x SSC containing 0.1% SDS for 30 min at RT, 0.5 x SSC containing 0.1% SDS for 15 min at 42ºC, and 0.1 x SSC containing 0.1% SDS for 15 min at 42ºC, followed by exposure to X-ray film. Densitometry was performed using the NIH ImageJ software, and signals were normalized to the ribosomal RNA detected by ethidium bromide staining.

Protein expression assays by western blots. Proteins from the VOS-1-V5-tagged cells were extracted from ground tissue (Garceau et al., 1997), and 100 mg of total protein was run on SDS-PAGE, and electro-transferred to polyvinylidene difluoride membranes (Millipore). VOS-1 protein was hybridized with primary mouse monoclonal anti-V5 antibody (Invitrogen), recognized with an anti-mouse horseradish

peroxide 2 conjugated secondary antibody (BioRad), and visualized with SuperSignal Femto Maximum Sensitivity Substrate (Thermo Scientific, Waltham, MA). After detecting by Western blotting, membranes were stained with an amido black solution (0.1% amido black, 10% acetic acid, 25% isopropanol) to reveal all proteins as an indication of protein transfer.

ChIP-PCR assay. ChIP assays were performed as described by Tamaru et al. (2003), with modifications. Briefly, conidia from the VOS-1-V5-tagged strain were inoculated into liquid growth media for either light induction or circadian time course experiments, as described above. To crosslink the VOS-1-V5 to genomic DNA, 1% (v/v) formaldehyde was added and the flasks were incubated for 30 min at 25ºC with shaking (100 rpm). Formaldehyde was quenched using 125 mM glycine, at 25ºC, 100 rpm, for 10 min. Tissue was transferred to tubes containing ChIP lysis buffer (50 mM Hepes, pH 7.5, 90 mM NaCl, 1 mM EDTA, pH 8.0, 1% Triton X-100, 0.1% Na deoxycholate, 0.172 mM PMSF, 1 µg/mL each of leupeptin and pepstatin). The tissue was homogenized and the chromatin was sheared to an average size of 0.5-0.8 kb using a Branson Digital Sonifier S-250D microtip probe (3 cycles: 10 sec, 40% amplitude, 0.8 sec pulse ON, 0.2 sec pulse OFF; and 6 cycles: 30 sec, 30% amplitude, 0.8 sec pulse ON, 0.2 sec pulse OFF). Extracts were clarified by centrifugation and the samples were immunoprecipitated with mouse monoclonal anti-V5 antibody (Invitrogen) and Dynabeads® Protein G (Life Technologies). The DNA concentration was quantified either by NanoDrop or by fluorescence using Quant-iT™ PicoGreen® dsDNA reagent (Invitrogen). Amplification reactions were performed using the pairs of primers NCU06687F1_VOS1/NCU06687R1_VOS1 for *gsn* promoter and NCU07027F_VOS1/NCU07027R_VOS1 for *gpn* promoter (Table S1). The primers were designed to amplify specific VOS-1 binding regions in *gsn* and *gpn* promoters as previously identified by ChIP-seq. Input DNA was used as positive control of PCR and a region from the 60S ribosomal L6 gene (ORF NCU04068) as negative control, using the primers pair rtPCRintL6f/rtPCRintL6r (Table S1). According to ChIP-seq data, the 60S ribosomal L6 gene is not a target of the transcription factor VOS-1. 20 ng of DNA from the anti-V5 (IP), no Ab and Input amplification reactions was utilized for amplifications. The amplification products were analyzed on a 2% agarose gel and visualized by ethidium bromide. Densitometry

was performed using NIH ImageJ software, and signals were normalized to the negative control (either no Ab or 60S ribosomal L6).

Bioluminescence assay. To monitor the expression of the FRQ protein, strains carrying a FRQ-LUC translational fusion were analyzed. Solid medium containing 1 x VM medium, 0.01% glucose, 0.03% arginine, 0.1% M quinic acid, pH 6.0, 1.5% agar and 25 µM luciferin (LUCNA-300; Gold Biotechnology, St. Louis, MO) was used to quantify the luciferase activity. Quinic acid was added to the media to increase the amplitude of the luciferase rhythms (Larrondo et al., 2015). 96-well microtiter plates were inoculated with 5 µL of 10^6 conidia/mL and incubated in the light for 24 h at 30ºC. The plates were then transferred to DD at 25ºC and the bioluminescence was measured with a TopCount NXT™ Microplate Scintillation and Luminescence Counter (PerkinElmer Life Sciences, Boston, MA) at intervals of 90 min for 4-5 days. Data were collected and analyzed using the Import and Analysis (I&A) program (Plautz et al., 1997). In our analyses, we did the detrended profile graphs to plot the luciferase levels using linear regression.

Bioluminescence was also performed using standard race tubes containing VM medium, pH 5.8, with 0.1% glucose, 0.17% arginine, 50 ng/mL biotin, 1.5% agar and 12.5 µM luciferin. The strains were inoculated and grown at 25°C in constant light (LL) overnight and the tubes were transferred into constant dark (DD) at 25°C. Bioluminescence was collected every hour with a PIXIS CCD camera (Princeton Instruments) controlled by Winview/32 software (Roper Scientific). The collected images were analyzed and plotted by ImageJ software and the customized Excel macro (gift by Dr. Luis Larrondo's lab), respectively.

Statistical data. Nonlinear regression to fit the circadian time course data to a sine wave (fitting period, phase, and amplitude) or a line (fitting slope and intercept), as well as the Akaike's information criteria tests to compare the fit of each data set to the 2 equations were carried out using the Prism software package (Prism version 4.0c, GraphPad Software, San Diego, CA). The P values reflect the probability that, for instance, the sine wave fits the data better than a straight line. This software analyzes the data using the equation Y=amplitude*sin[6.2831853*(X-phase-8)/(PerSixteen+16)] for morning sine test, Y=amplitude*sin[6.2831853*(X-phase-

19.5)/(PerSixteen+16)] for evening sine test and Y=M*X+B for line test. X means hours in DD, M means intercept, and B means slope of the line.

RESULTS

Circadian clock controls glycogen accumulation and the genes involved in the regulation of glycogen synthesis (*gsn*) and degradation (*gpn*)

Several studies have demonstrated that glycogen accumulation is rhythmic in different organisms (Ishikawa and Shimazu, 1976; Doi et al., 2010; Pattanayak et al., 2014, Diamond et al., 2015), although the mechanism for this regulation is unknown. The circadian clock in *N. crassa* is well defined, and the regulation of glycogen metabolism has been investigated (Gonçalves et al., 2011; Candido et al., 2014; Cupertino et al., 2015; Freitas et al., 2016). Therefore, to better understand how the clock controls glycogen metabolism, we first examined if glycogen accumulates rhythmically. In the wild-type cells, glycogen accumulated rhythmically with a period of 26 ± 2 hours and an amplitude of 0.59 ± 0.09 ($p<0.0001$; Fig. 1A, left panel), peaking in the subjective night. The rhythm in glycogen accumulation was abolished in the clock deficient Δ*frq* strain (Fig. 1A, right panel), demonstrating that the circadian clock influences the rhythmic glycogen accumulation.

To begin to determine the mechanism for clock control of glycogen levels, we examined the mRNA levels over a circadian time course of *gsn* and *gpn,* encoding glycogen synthase and glycogen phosphorylase, enzymes involved in glycogen biosynthesis and degradation, respectively. Both *gsn* and *gpn* mRNA accumulated rhythmically in wild-type cells. The period of the rhythm for *gsn* was 22.8 ± 1.3 hours with amplitude of 0.62 ± 0.14 ($p=0.0001$) (Fig. 1B, left panel), and for *gpn* was 22.3 ± 1.5 hours with amplitude of 0.59 ± 0.18 ($p=0.0051$) (Fig. 1C, left panel). Similar to glycogen accumulation, the rhythmic expression of both genes was abolished in the Δ*frq* strain (Figs. 1B and C, right panels), suggesting that FRQ-dependent circadian clock may control the circadian glycogen accumulation via rhythmic expression of *gsn* and *gpn* genes.

The clock-controlled VOS-1 transcription factor binds to the *gsn* and *gpn* promoters

To investigate the mechanism of clock control of *gpn* and *gsn*, we focused our attention on transcription factors that are directly controlled by the circadian clock. Several transcription factors were demonstrated by high-throughput sequencing analyses to be regulated by light and/or clock (Smith et al., 2010; Wu et al., 2014), and a subset of them was described as putative regulators of glycogen metabolism (Gonçalves et al., 2011), which led us to speculate that some transcription factors could connect glycogen metabolism to circadian clock. The *N. crassa* homolog of the *Aspergillus nidulans* VosA transcription factor (NCU05964, called VOS-1) was identified as a WCC target (Smith et al., 2010). A near consensus *A. nidulans* VosA DNA binding site (5'-CTGGCCAAGGC-3') (Ahmed et al., 2013) was present in the promoters of *N. crassa gsn* and *gpn* genes, suggesting that VOS-1 may directly regulate the expression of these genes. Consistent with this idea, the *gsn* (Fig. S1A) and *gpn* (Fig. S1B) promoters were targets of VOS-1 binding in constant dark (DD) and after exposure to light in ChIP-seq analyses (manuscript in preparation). Therefore, we analyzed binding of VOS-1 to *gsn* and *gpn* promoters in DD and after light exposure to investigate if the *gsn* and *gpn* expression and glycogen accumulation were light induced.

First, light responses of VOS-1 were examined at transcript levels and in cells containing the VOS-1-V5-tagged protein. The *vos-1* mRNA levels were light induced in wild-type cells and induction was abolished in cells containing a deletion of the blue-light photoreceptor *wc-1* (Δ*wc-1* strain) (Fig. 2A). Induction of the *ccg-1* gene, which is a late light induced gene (Loros and Dunlap, 1991), was also abolished in the Δ*wc-1* strain (Fig. 2A). Protein expression was also analyzed and a protein band with a molecular weight of ~48 kD was observed in the tagged strain, but not in the control wild-type strain, consistent with the predicted size of VOS-1 (447 aa) (Fig. 2B). While VOS-1-V5 levels were low in DD, the levels increased about 2.5-fold following 45-60 min of light exposure (Fig. 2B), confirming light induction of VOS-1.

To determine if VOS-1 binds to the *gsn* and *gpn* promoters *in vivo*, we performed ChIP-PCR assays using oligonucleotides (Table S1) designed to amplify genomic DNA fragments predicted to be bound by VOS-1 by the previous ChIP-seq analyses [Figs. S1A (*gsn* promoter) and S1B (*gpn* promoter)]. Based on the *A. nidulans* VosA binding site we identified, within the amplified DNA fragments, putative VOS-1 motifs located at -1806 (5'-CTTGGCC-3') and -338 (5'-CCTTGG-3') bp in *gsn* and *gpn* promoters, respectively, relative to the ATG start codon. Cross-

linked chromatin was collected from mycelia of VOS-1-V5 cells grown in DD and exposed to light for varying times. VOS-1 bound to both promoter regions in DD and after light exposure (Figs. 3A and 3B, left panels), confirming the ChIP-seq results, and suggesting that the VosA and VOS-1 DNA binding sites may be similar. Plots of the band intensities normalized to no Ab samples are shown in the right panels for *gsn* (Fig. 3A) and *gpn* (Fig. 3B) promoters. VOS-1 strongly bound to both promoters in DD, with a slight increase in binding to the *gsn* promoter after 45 min of light exposure. The binding of VOS-1 to the *gpn* promoter after light exposure, while still enriched, was significantly lower than the binding observed in DD. These results confirm that VOS-1 binds to the *gsn* and *gpn* promoters in DD and after light exposure, likely leading to the regulation of expression of these genes in both conditions.

We next investigated if *gsn* and *gpn* gene expression and glycogen accumulation were light induced in wild-type and cells containing a deletion of the blue-light photoreceptor (Δ*wc-1*) cells exposed to light. Surprisingly, while the positive control *ccg-1* gene was normally light induced in wild-type, but not Δ*wc-1* cells, as expected, neither *gsn* nor *gpn* transcripts were induced by light in wild-type cells (Fig. S1C). The same samples were used for glycogen quantification, and similar to *gsn* and *gpn* mRNA levels, glycogen levels were not light induced (Fig. S1D). Thus, although VOS-1 is light regulated, this regulation is not transduced to all of its direct targets. Instead, these data suggested that VOS-1, which is directly bound by the core clock component WC-1 (Smith et al., 2010), and binds to *gpn* and *gsn* promoters in the dark and in the light, primarily signals time of day information to *gpn* and *gsn*.

The *vos-1* mRNA is clock-controlled and VOS-1 binds rhythmically to the *gsn* and *gpn* promoters

To investigate if *vos-1* expression is clock-controlled, *vos-1* mRNA and protein levels were examined in a circadian time course. To analyze *vos-1* mRNA levels, a codon optimized firefly luciferase (Gooch et al., 2008) was fused downstream of the *vos-1* promoter (p*vos-1-luc*). The mRNA cycled in DD peaking around subjective dusk (DD 42) (Fig. 4A). To analyze protein expression, VOS-1-V5 was assayed by western blot

using anti-V5 antibody and the protein also cycled in DD with a period of about 22 h and peaking a few hours later than the mRNA (DD 28) (Figs. 4B and S2A).

The rhythmic binding of VOS-1 to the *gsn* and *gpn* promoters was assayed by ChIP-PCR using the circadian time course samples (Figs. 4C and D, and S2B). VOS-1 bound rhythmically to the *gsn* (Fig. 4C) and *gpn* (Fig. 4D) promoters showing binding peak in the subjective night at DD 28, consistent with the nighttime peak levels of *vos-1* mRNA and protein, and preceding the peak in *gsn* and *gpn* mRNA levels (Figs. 1B and C).

Glycogen accumulation and the *gsn* and *gpn* genes have low amplitude rhythms in the *vos-1* deletion strain

Our demonstration that VOS-1 accumulation and binding to the *gsn* and *gpn* promoters are rhythmic, support the idea that VOS-1 signals temporal information from the oscillator to *gsn* and *gpn*. To test this idea, glycogen levels were quantified in Δ*vos-1* cells in a circadian time course. Surprisingly, glycogen accumulation remained rhythmic in the VOS-1 deletion cells (Fig. 5A and S3B) similar to what is observed in wild-type strain (Fig. S3A), peaking in the subjective night. In addition, the total glycogen levels observed in Δ*vos-1* cells were similar to those obtained in wild-type cells (compare Figs. S3A and B). However, the period was slight shorter (21.89 ± 1.6 hours) when compared to glycogen accumulation in the wild-type cells (26 ± 2 hours), and the amplitude of the rhythm was reduced ~2-fold, from 0.59 ± 0.09 in wild-type cells to 0.3 ± 0.08 in the mutant (compare Figs. 1A, left panel and 5A).

We tested the impact of *vos-1* deletion in the expression of *gsn* and *gpn* by constructing bioluminescent reporters to investigate the expression of the *gsn* and *gpn* genes in wild-type and ∆*vos-1* mutant strains. The rhythmic expression of *gsn* and *gpn* observed in the wild-type strain (solid line) was maintained in ∆*vos-1* mutant strain (dashed line) (Figs. 5B and C, respectively), although the transcript levels were of at least 2-fold lower amplitude when compared to the wild-type strain. These data indicate that while VOS-1 functions as an activator of *gsn* and *gpn* expression, controlling the overall levels and amplitude of the rhythm of *gsn* and *gpn,* there are additional components regulating the rhythmic expression of the genes, and the rhythmic accumulation of glycogen.

GSN, GPN and VOS-1 are part of a circadian output pathway

To investigate if *gsn*, *gpn* and *vos-1* feed back to the core oscillator to regulate its function, the rhythmic accumulation of FRQ-LUC was monitored in Δ*gsn*, Δ*gpn* and Δ*vos-1* strains (Fig. 6). No change in rhythmic expression of FRQ protein was observed in the Δ*gsn*, Δ*gpn* and Δ*vos-1* mutant strains as compared to wild-type cells. These data support the idea that VOS-1 functions in an output pathway from the clock to regulate the expression of *gsn* and *gpn*.

DISCUSSION

In the last years, a large number of reports have described the functional link between circadian clock and cellular metabolism, revealing that most of the metabolism is under circadian control (Bass and Takahashi, 2010; Eckel-Mahan and Sassone-Corsi, 2013; Hurley et al., 2014; Hurley et al., 2016) and that, in human, disruption of the circadian clock impacts health and disease (Green et al., 2008; Bass, 2012). However, the molecular mechanisms coupling both processes are starting to be investigated and have been only characterized in higher eukaryotic organisms. The mechanisms relay on the dependence of intermediary metabolites, including ATP, NAD+, among others, which connect the metabolic state of cells to the biological clock via signaling pathways and/or protein modifications (reviewed in Asher and Schibler, 2011; Peek et al., 2013; Rey and Reddy, 2013; Etchegaray and Mostoslavsky, 2016). One of the major links between metabolism and circadian clock is the metabolite NAD+, whose levels are regulated via circadian rhythms. Recently, SIRT6, a member of the sirtuin family with (NAD+)-dependent deacetylase activity, was reported to control the recruitment of the CLOCK:BMAL1 complex to chromatin and to define the circadian oscillations of hepatic genes related to fatty acid and carbohydrate metabolism in mouse (Masri et al., 2014).

The filamentous fungus *Neurospora crassa* is a model organism for circadian systems studies and the core components of the biological clock have been well characterized. A genome-wide transcriptional profile by RNA-seq revealed that a high number of genes can be expressed under circadian control and that much of metabolism is clock-controlled; daytime favoring catabolism and nighttime the

biosynthesis of cellular components (Hurley et al., 2014). We demonstrated here that glycogen metabolism in *N. crassa* is clock controlled. Glycogen was accumulated and degraded during the subjective night and day, respectively, and the circadian accumulation was lost in cells without a functional circadian clock (Δ*frq*). These findings are similar to the results of circadian accumulation of glycogen in rats: increased glycogen levels during the dark period and consumption during the light (Ishikawa and Shimazu, 1976). However, they are opposite to what was reported for the cyanobacteria *Synechococcus elongates,* which accumulates glycogen during the subjective day and break it down during the subjective night (Pattanayak et al., 2014; Diamond et al., 2015), consistent with the diurnal metabolism centered on photosynthesis. Thus, clock may coordinate the glycogen accumulation at different times of the day, depending on the metabolic activities of the organism.

The *gsn* and *gpn* genes encoding the regulatory enzymes glycogen synthase (GSN) and glycogen phosphorylase (GPN), respectively, also showed circadian rhythmicity in *N. crassa*, and both transcripts accumulated during the subjective day. However, both transcripts accumulated in the same phase, and this result is not correlated with the activities of the enzymes since glycogen synthase and glycogen phosphorylase are the regulatory enzymes in two opposite metabolic pathways: glycogen biosynthesis and degradation, respectively. Therefore, it is expected that the rhythmic glycogen accumulation should result from the balance between both enzymes. The *gsn* and *gpn* rhythmic expression results and the enzymes activities regulation led us to speculate that the rhythmic glycogen accumulation may result, not only from transcript levels, but from additional factors, such as regulation of the enzymes GSN and GPN.

The GSN and GPN enzymes are both regulated by allosterism, in which glucose-6-phosphate (G6P) is the modulator for glycogen synthase and AMP the effector for glycogen phosphorylase. The G6P levels, in a certain time, depends on the balance between the hexoquinase and glucose-6-phosphatase enzymes activities and should be important to investigate whether both enzymes are under circadian control in *N. crassa*. Glycogen synthase is also highly regulated by phosphorylation, and at least four phosphorylation sites have been identified in the *N. crassa* enzyme (unpublished results) whereas glycogen phosphorylase is phosphorylated in a single residue. The phosphorylation activates glycogen phosphorylase enzyme and inhibits glycogen synthase enzyme (Téllez-Iñón and

Torres, 1970; Fletterick and Madsen, 1980), leads to reversible regulation of both enzymes. Additionally, several protein kinases were identified to affect glycogen levels in *N. crassa* (Freitas et al., 2010; Candido et al., 2014), and should be also interesting to investigate whether their activities are under clock control.

Here, we investigated whether the VOS-1 TF could play a role in the link between glycogen accumulation and the circadian clock in *N. crassa.* VOS-1 is a protein containing a *velvet* domain, belongs to a new class of transcription factors classified under the *velvet* family (Ni and Yu, 2007), and is a putative target of the blue-light photoreceptor WCC (Smith et al., 2010). In this work, we demonstrated that although *vos-1* and VOS-1 expression is light-induced and binds to glycogenic gene promoters under dark and light conditions, the *gsn* and *gpn* transcripts and the glycogen accumulation are not light-induced. VOS-1 TF also binds rhythmically to the *gsn* and *gpn* promoters during a circadian time course; however, glycogen accumulation and the expression of *gsn* and *gpn* genes are still rhythmic, although at low amplitude, in the absence of VOS-1. These data suggest that VOS-1 contributes to the robustness of *gsn* and *gpn* rhythmic expression regulation, though additional components participate in a rhythmic accumulation of glycogen in wild-type cells. Thus, VOS-1 could be part of a transcription factor network that connects glycogen metabolism to the *N. crassa* clock.

Based on our findings, we propose a preliminary model, which is described in Fig. 7. According this model, WCC controls the expression of *vos-1* under light and in a circadian time course. VOS-1 is rhythmically expressed peaking in the dark and binds rhythmically to the *gsn* and *gpn* promoters in the dark. Both genes are rhythmically expressed peaking in the subjective morning. Glycogen is also accumulated in a circadian rhythm, peaking in the subjective evening, suggesting that the rhythmicity of *gsn* and *gpn* genes, encoding the rate-limiting enzymes in glycogen metabolism, could affect the glycogen accumulation in *N. crassa*. In summary, our results show that glycogen accumulates during the night and is degraded during the day to supply the appropriate levels of energy to cells at the right time of the day, and that this regulation is, in part, through the control of *gsn* and *gpn* expression by the VOS-1 transcription factor.

Our results demonstrate the first evidence of the VOS-1 TF role in a metabolic process and the circadian-clock regulation of the glycogen content in *N. crassa*,

529 although some questions remain unanswered. The results described here reveal new
530 insights about glycogen metabolism that deserve to be further investigated.
531
532 **ACKNOWLEDGMENTS**
533
534 We thank J. Dunlap and the Neurospora Genome Project group for strains, and for
535 sharing VOS-1 ChIP-seq data prior to publication. In addition, we thank the Fungal
536 Genetics Stock Center (Kansas City, MO) for strains. We deeply thank Bell-
537 Pedersen's lab members for discussions, and particularly T. Lamb for help with
538 experiments. This work was supported by the Fundação de Amparo à Pesquisa do
539 Estado de São Paulo (FAPESP), the Conselho Nacional de Desenvolvimento
540 Científico e Tecnológico (CNPq) for grants and fellowships to M.C.B. and S.V., and
541 the National Institute of Health P01 GM068087 grant subcontract to D.B.P.
542
543 **REFERENCES**
544
545 Ahmed YL, Gerke J, Park HS, Bayram Ö, Neumann P, Ni M, Dickmanns A, Kim SC,
546 Yu JH, Braus GH, Ficner R. (2013) The velvet family of fungal regulators contains
547 a DNA-binding domain structurally similar to NF-κB. *PLoS Biol.* 11: e1001750
548 Asher G, Sassone-Corsi P. (2015) Time for food: the intimate interplay between
549 nutrition, metabolism, and the circadian clock. *Cell* 161: 84-92
550 Asher G, Schibler U. (2011) Crosstalk between components of circadian and
551 metabolic cycles in mammals. *Cell Metab*. 13: 125-137
552 Baker CL, Kettenbach AN, Loros JJ, Gerber SA, Dunlap JC. (2009) Quantitative
553 proteomics reveals a dynamic interactome and phase-specific phosphorylation in
554 the Neurospora circadian clock. *Mol Cell.* 34(3): 354-363
555 Ballario P, Vittorioso P, Magrelli A, Talora C, Cabibbo A, Macino G. (1996) White
556 collar-1, a central regulator of blue light responses in Neurospora, is a zinc finger
557 protein. *EMBO J.* 15(7): 1650-1657
558 Bardiya N, Shiu PK. (2007) Cyclosporin A-resistance based gene placement system
559 for *Neurospora crassa*. *Fungal Genet Biol.* 44(5): 307-314
560 Bass J. (2012) Circadian topology of metabolism. *Nature* 491: 348-356
561 Bass J, Takahashi JS. (2010) Circadian integration of metabolism and energetics.
562 *Science* 330: 1349-1354
563 Candido TS, Gonçalves RD, Freitas FZ, Cupertino FB, Felicio AP, Carvalho ACGV,
564 Bertolini MC. (2014) A screening of *Neurospora crassa* mutant strains in protein
565 kinases reveals SNF1 as a protein kinase likely phosphorylating glycogen
566 synthase *Biochem. J.* 464, 323-334

Chen CH, Ringelberg CS, Gross RH, Dunlap JC, Loros JJ. (2009) Genome-wide analysis of light-inducible responses reveals hierarchical light signaling in Neurospora. *EMBO J.* 28: 1029-1042

Cheng P, He Q, He Q, Wang L, Liu Y. (2005) Regulation of the Neurospora circadian clock by an RNA helicase. *Genes Dev.* 19(2): 234-241

Cheng P, Yang Y, Gardner KH, Liu Y. (2002) PAS domain-mediated WC-1/WC-2 interaction is essential for maintaining the steady-state level of WC-1 and the function of both proteins in circadian clock and light responses of Neurospora. *Mol Cell Biol.* 22(2): 517-524

Colot HV, Park G, Turner GE, Ringelberg C, Crew CM, Litvinkova L, Weiss RL, Borkovich KA, Dunlap J. (2006) A high-throughput gene knockout procedure for Neurospora reveals functions for multiple transcription factors. *Proc Natl Acad Sci USA* 103(27): 10352-10357

Correa A, Lewis ZA, Greene AV, March IJ, Gomer RH, Bell-Pedersen D. (2003) Multiple oscillators regulate circadian gene expression in *Neurospora*. *Proc. Natl. Acad. Sci. U.S.A.* 100: 13597-13602

Cupertino FB, Virgilio S, Freitas FZ, Candido TS, Bertolini MC. (2015) Regulation of glycogen metabolism by the CRE-1, RCO-1 and RCM-1 proteins in *Neurospora crassa.* The role of CRE-1 as the central transcriptional regulator. *Fungal Genet. Biol.* 77: 82-94.

Denault DL, Loros JJ, Dunlap JC. (2001) WC-2 mediates WC-1-FRQ interaction within the PAS protein-linked circadian feedback loop of Neurospora. *EMBO J.* 20(1-2): 109-117

Diamond S, Jun D, Rubin BE, Golden SS. (2015) The circadian oscillator in *Synechococcus elongates* controls metabolite partitioning during diurnal growth. *Proc. Natl. Acad. Sci. U.S.A.* 112: E1916-25

Doi R, Oishi K, Ishida N. (2010) CLOCK regulates circadian rhythms of hepatic glycogen synthesis through transcriptional activation of Gys2. *J Biol Chem.* 285: 22114-22121

Eckel-Mahan K, Sassone-Corsi P. (2013) Metabolism and the circadian clock converge. *Physiol Rev.* 93: 107-135

Etchegaray JP, Mostoslavsky R. (2016) Interplay between Metabolism and Epigenetics: A Nuclear Adaptation to Environmental Changes. *Mol Cell.* 62: 695-711

Fletterick RJ, Madsen NB. (1980) The structures and related functions of phosphorylase a. *Annu Rev Biochem.* 49: 31-61

Freitas FZ, de Paula RM, Barbosa LC, Terenzi HF, Bertolini MC. (2010) cAMP signaling pathway controls glycogen metabolism in *Neurospora crassa* by regulating the glycogen synthase gene expression and phosphorylation. *Fungal Genet Biol* 47: 43-52

Freitas FZ, Virgilio S, Cupertino FB, Kowbel DJ, Fioramonte M, Gozzo FC, Glass NL, Bertolini M. (2016) The SEB-1 Transcription factor binds to the STRE motif in *Neurospora crassa* and regulates a variety of cellular processes including the

stress response and reserve carbohydrate metabolism. *G3* (Bethesda) 6(5):1327-1343

Froehlich AC, Liu Y, Loros JJ, Dunlap JC. (2002) White-Collar-1, a circadian blue light photoreceptor, binding to the *frequency* promoter. *Science* 297(5582): 815-819

Garceau NY, Liu Y, Loros, JJ, Dunlap, JC. (1997) Alternative initiation of translation and time-specific phosphorylation yield multiple forms of the essential clock protein FREQUENCY. *Cell* 89: 469-476

Gonçalves RD, Cupertino FB, Freitas FZ, Luchessi AD, Bertolini MC. (2011) A genome-wide screen for *Neurospora crassa* transcription factors regulating glycogen metabolism. *Mol Cell Proteomics* 10(11): M111.007963

Gooch VD, Mehra A, Larrondo LF, Fox J, Touroutoutoudis M, Loros JJ, Dunlap JC. (2008) Fully codon-optimized luciferase uncovers novel temperature characteristics of the Neurospora clock. *Eukaryot Cell.* 7(1): 28-37

Green CB, Takahashi JS, Bass J. (2008) The meter of metabolism. *Cell* 134: 728-742

He Q, Cheng P, Yang Y, He Q, Yu H, Liu Y. (2003) FWD1-mediated degradation of FREQUENCY in Neurospora establishes a conserved mechanism for circadian clock regulation. *EMBO J.* 22(17): 4421-4430

He Q, Liu Y. (2005) Degradation of the Neurospora circadian clock protein FREQUENCY through the ubiquitin-proteasome pathway. *Biochem Soc Trans.* 33(Pt 5): 953-956

Hong CI, Zámborszky J, Baek M, Labiscsak L, Ju K, Lee H, Larrondo LF, Goity A, Chong HS, Belden WJ, Csikász-Nagy A. (2014) Circadian rhythms synchronize mitosis in *Neurospora crassa*. *Proc Natl Acad Sci U S A.* 111(4): 1397-1402

Hurley JM, Dasgupta A, Emerson JM, Zhou X, Ringelberg CS, Knabe N, Lipzen AM, Lindquist EA, Daum CG, Barry KW, Grigoriev IV, Smith KM, Galagan JE, Bell-Pedersen D, Freitag M, Cheng C, Loros JJ, Dunlap JC. (2014) Analysis of clock-regulated genes in Neurospora reveals widespread posttranscriptional control of metabolic potential. *Proc Natl Acad Sci U S A.* 111: 16995-17002

Hurley JM, Loros JJ, Dunlap JC. (2016) The circadian system as an organizer of metabolism. *Fungal Genet Biol.* 90: 39-43

Ishikawa K, Shimazu T. (1976) Daily rhythms of glycogen synthetase and phosphorylase activities in rat liver: Influences of food and light. *Life Sci.* 19: 1873-1878

Larrondo LF, Olivares-Yañez C, Baker CL, Loros JJ, Dunlap JC. (2015) Circadian rhythms. Decoupling circadian clock protein turnover from circadian period determination. *Science* 347(6221): 1257277

Lee K, Dunlap JC, Loros JJ. (2003) Roles for WHITE COLLAR-1 in circadian and general photoperception in *Neurospora crassa*. *Genetics* 163(1): 103-114

Liu Y, Loros J, Dunlap JC. (2000) Phosphorylation of the Neurospora clock protein FREQUENCY determines its degradation rate and strongly influences the period length of the circadian clock. *Proc Natl Acad Sci U S A.* 97(1): 234-239

Loros JJ, Dunlap JC. (1991) *Neurospora crassa* clock-controlled genes are regulated at the level of transcription. *Mol Cell Biol.* 11: 558-563

Marcheva B, Ramsey KM, Buhr ED, Kobayashi Y, Su H, Ko CH, Ivanova G, Omura C, Mo S, Vitaterna MH, Lopez JP, Philipson LH, Bradfield CA, Crosby SD, JeBailey L, Wang X, Takahashi JS, Bass J. (2010) Disruption of the clock components CLOCK and BMAL1 leads to hypoinsulinaemia and diabetes. *Nature* 466: 627-631

Masri S, Rigor P, Cervantes M, Ceglia N, Sebastian C, Xiao C, Roqueta-Rivera M, Deng C, Osborne TF, Mostoslavsky R, Baldi P, Sassone-Corsi P. (2014) Partitioning circadian transcription by SIRT6 leads to segregated control of cellular metabolism. *Cell* 158: 659-672

McCluskey K, Wiest A, Plamann M. (2010) The Fungal Genetics Stock Center: a repository for 50 years of fungal genetics research. *J Biosci.* 35(1): 119-126

Miller BH, McDearmon EL, Panda S, Hayes KR, Zhang J, Andrews JL, Antoch MP, Walker JR, Esser KA, Hogenesch JB, Takahashi JS. (2007) Circadian and CLOCK-controlled regulation of the mouse transcriptome and cell proliferation. *Proc. Natl. Acad. Sci. U.S.A.* 104(9): 3342-3347

Ni M, Yu JH. (2007) A novel regulator couples sporogenesis and trehalose biogenesis in *Aspergillus nidulans. PLoS One* 10: e970

Olmedo M, Navarro-Sampedro L, Ruger-Herreros C, Kim SR, Jeong BK, Lee BU, Corrochano LM. (2010) A role in the regulation of transcription by light for RCO-1 and RCM-1, the Neurospora homologs of the yeast Tup1-Ssn6 repressor. *Fungal Genet Biol.* 47: 939-952

Pall ML. (1993) The use of Ignite (Basta;glufosinate;phosphinothricin) to select transformants of bar-containing plasmids in *Neurospora crassa*. *Fungal Genet Newsl.* 40: 58

Panda S, Antoch MP, Miller BH, Su AI, Schook AB, Straume M, Schultz PG, Kay SA, Takahashi JS, Hogenesch JB. (2002) Coordinated transcription of key pathways in the mouse by the circadian clock. *Cell* 109: 307-320

Pattanayak GK, Phong C, Rust MJ. (2014) Rhythms in energy storage control the ability of the cyanobacterial circadian clock to reset. *Curr Biol.* 24: 1934-1938

Peek CB, Affinati AH, Ramsey KM, Kuo HY, Yu W, Sena LA, Ilkayeva O, Marcheva B, Kobayashi Y, Omura C, Levine DC, Bacsik DJ, Gius D, Newgard CB, Goetzman E, Chandel NS, Denu JM, Mrksich M, Bass J. (2013) Circadian clock NAD^+ cycle drives mitochondrial oxidative metabolism in mice. *Science* 342: 1243417

Plautz JD, Straume M, Stanewsky R, Jamison CF, Brandes C, Dowse HB, Hall JC, Kay SA. (1997) Quantitative analysis of *Drosophila period* gene transcription in living animals. *J Biol Rhythms* 12: 204-217

Rey G, Reddy AB. (2013) Protein acetylation links the circadian clock to mitochondrial function. *Proc Natl Acad Sci U S A.* 110: 3210-3211

Rudic RD, McNamara P, Curtis AM, Boston RC, Panda S, Hogenesch JB, Fitzgerald GA. (2004) BMAL1 and CLOCK, two essential components of the circadian clock, are involved in glucose homeostasis. *PLoS Biol.* 2: e377

Sancar G, Sancar C, Brügger B, Ha N, Sachsenheimer T, Gin E, Wdowik S, Lohmann I, Wieland F, Höfer T, Diernfellner A, Brunner M. (2011) A global circadian repressor controls antiphasic expression of metabolic genes in Neurospora. *Mol. Cell* 44: 687-697

Schafmeier T, Diernfellner A, Schäfer A, Dintsis O, Neiss A, Brunner M. (2008) Circadian activity and abundance rhythms of the Neurospora clock transcription factor WCC associated with rapid nucleo-cytoplasmic shuttling. *Genes Dev.* 22(24): 3397-3402

Schafmeier T, Haase A, Káldi K, Scholz J, Fuchs M, Brunner M. (2005) Transcriptional feedback of Neurospora circadian clock gene by phosphorylation-dependent inactivation of its transcription factor. *Cell* 122(2): 235-246

Shi M, Collett M, Loros JJ, Dunlap JC. (2010) FRQ-interacting RNA helicase mediates negative and positive feedback in the Neurospora circadian clock. *Genetics* 184(2): 351-361

Smith KM, Sancar G, Dekhang R, Sullivan CM, Li S, Tag AG, Sancar C, Bredeweg EL, Priest HD, McCormick RF, Thomas TL, Carrington JC, Stajich JE, Bell-Pedersen D, Brunner M, Freitag M. (2010) Transcription factors in light and circadian clock signaling networks revealed by genome wide mapping of direct targets for Neurospora white collar complex. *Eukaryot Cell* 9: 1549-1556

Tamaru H, Zhang X, McMillen D, Singh PB, Nakayama J, Grewal SI, Allis CD, Cheng X, Selker EU. (2003) Trimethylated lysine 9 of histone H3 is a mark for DNA methylation in *Neurospora crassa*. *Nat Genet.* 34: 75-79

Téllez-Iñón MT, Torres HN. (1970) Interconvertible forms of glycogen phosphorylase in *Neurospora crassa*. *Proc Natl Acad Sci U S A.* 66(2): 459-463

Vogel HJ. (1956) A convenient growth medium for *Neurospora crassa* (medium N). *Microbiol Genet Bull.* 13: 42-43

Westergaard M, Mitchell HK. (1947) Neurospora V. A synthetic medium favoring sexual reproduction. *Am J Bot.* 34: 573-577

Wu C, Yang F, Smith KM, Peterson M, Dekhang R, Zhang Y, Zucker J, Bredeweg EL, Mallappa C, Zhou X, Lyubetskaya A, Townsend JP, Galagan JE, Freitag M, Dunlap JC, Bell-Pedersen D, Sachs MS. (2014) Genome-wide characterization of light-regulated genes in *Neurospora crassa*. *G3* (Bethesda) 4: 1731-1745

Zarrinpar A, Chaix A, Panda S. (2016) Daily Eating Patterns and Their Impact on Health and Disease. *Trends Endocrinol Metab.* 27: 69-83

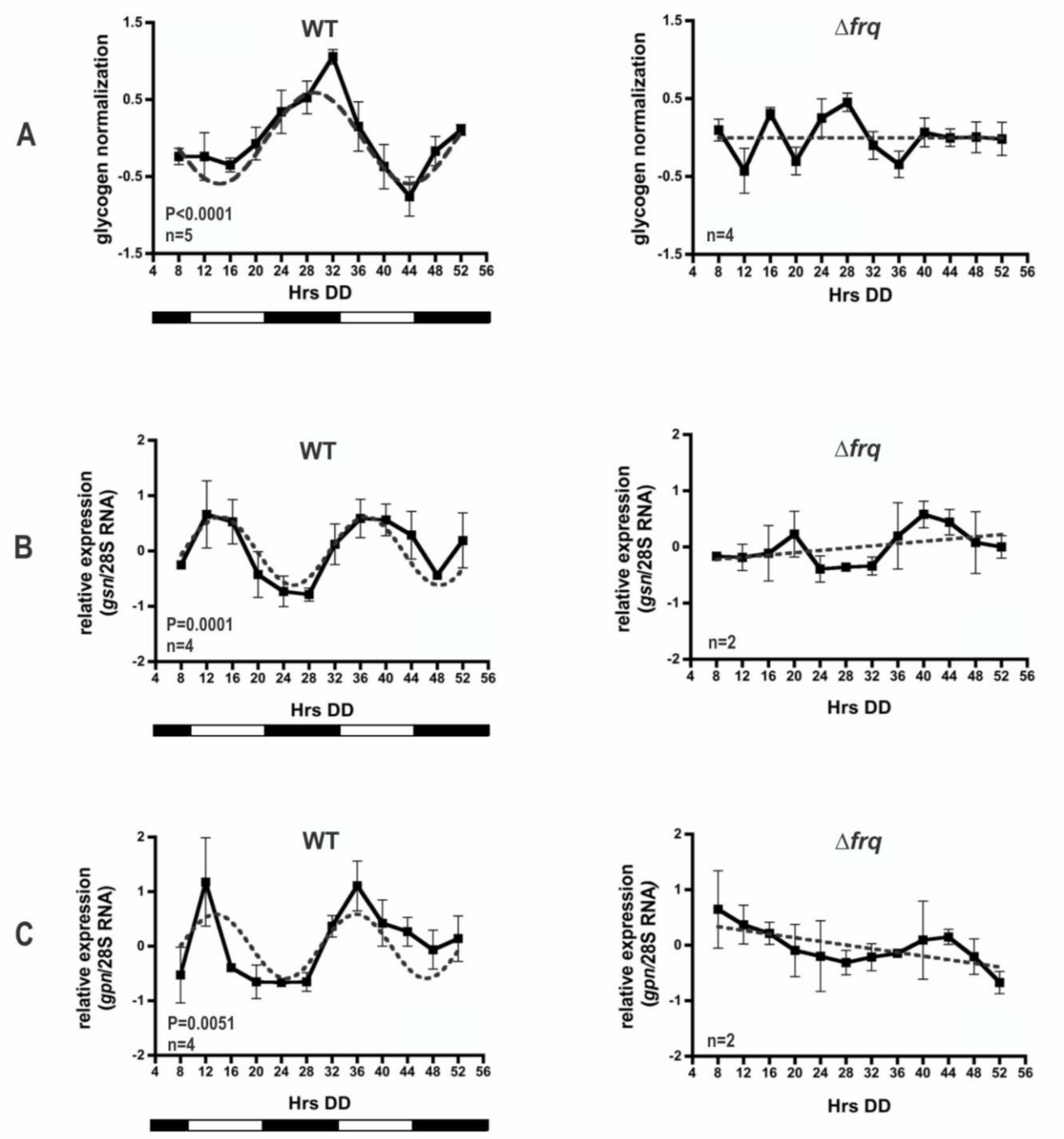

Fig. 1. Glycogen accumulation and mRNA levels of *gsn* and *gpn* are controlled by the circadian clock. (A) Glycogen levels were determined from wild-type (left graph) and Δ*frq* (right graph) cells harvested at the indicated times in constant darkness (DD) and plotted (±SEM, n≥4). mRNA levels of *gsn* (B) and *gpn* (C) were examined by northern blot from wild-type and Δ*frq* cells in the same conditions from (A), and the results (±SEM, n≥2) were normalized using 28S rRNA as internal loading control. The bars represent the phase that the circadian clock is experiencing, with subjective night in black, and subjective day in white. The glycogen levels panels show that wild-type cells fit a sine wave with p<0.0001 (dotted line) with an amplitude of 0.59 ± 0.09, but in Δ*frq* cells the best fit of the glycogen levels (solid line) is a line (dotted). Gene expression levels in the wild-type strain (solid line) fit a sine wave with p<0.006 (dotted line) with an amplitude of 0.62 ± 0.14 for *gsn* and 0.59 ± 0.18 for *gsn*, but in Δ*frq* cells the best fit of the mRNA levels (solid line) is a line (dotted line).

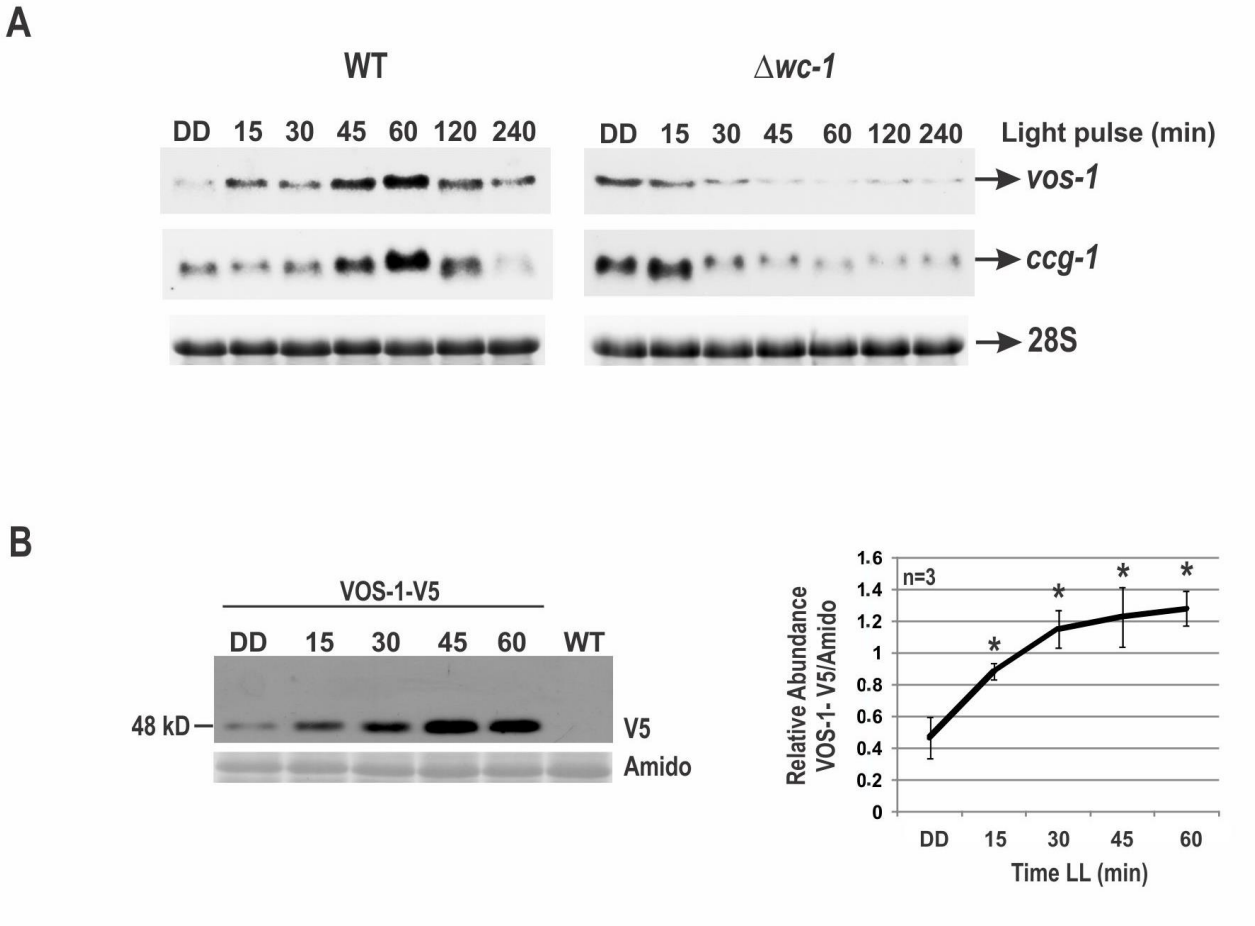

Fig. 2. The *vos-1* mRNA and VOS-1 protein are light-induced. (A) mRNA levels of *vos-1* was assayed by northern blot in wild-type and Δ*wc-1* cells harvested in DD and after light exposure. The 28S rRNA was used as internal loading control. The *ccg-1* gene expression was used as control of light induction. The data represent 1 of 2 independent experiments. (B) VOS-1 protein was detected by western blot in extracts from VOS-1-V5-tagged cells harvested in DD and after light exposure for the indicated times (min). Amido black staining of proteins (Amido) on the membrane was used as loading control and the wild-type cellular extract without V5 tag was used as the negative control. Relative VOS-1 expression from three biological replicates is plotted (right panel). The asterisks indicate significant differences compared to DD condition (Student's *t*-test, $p<0.005$).

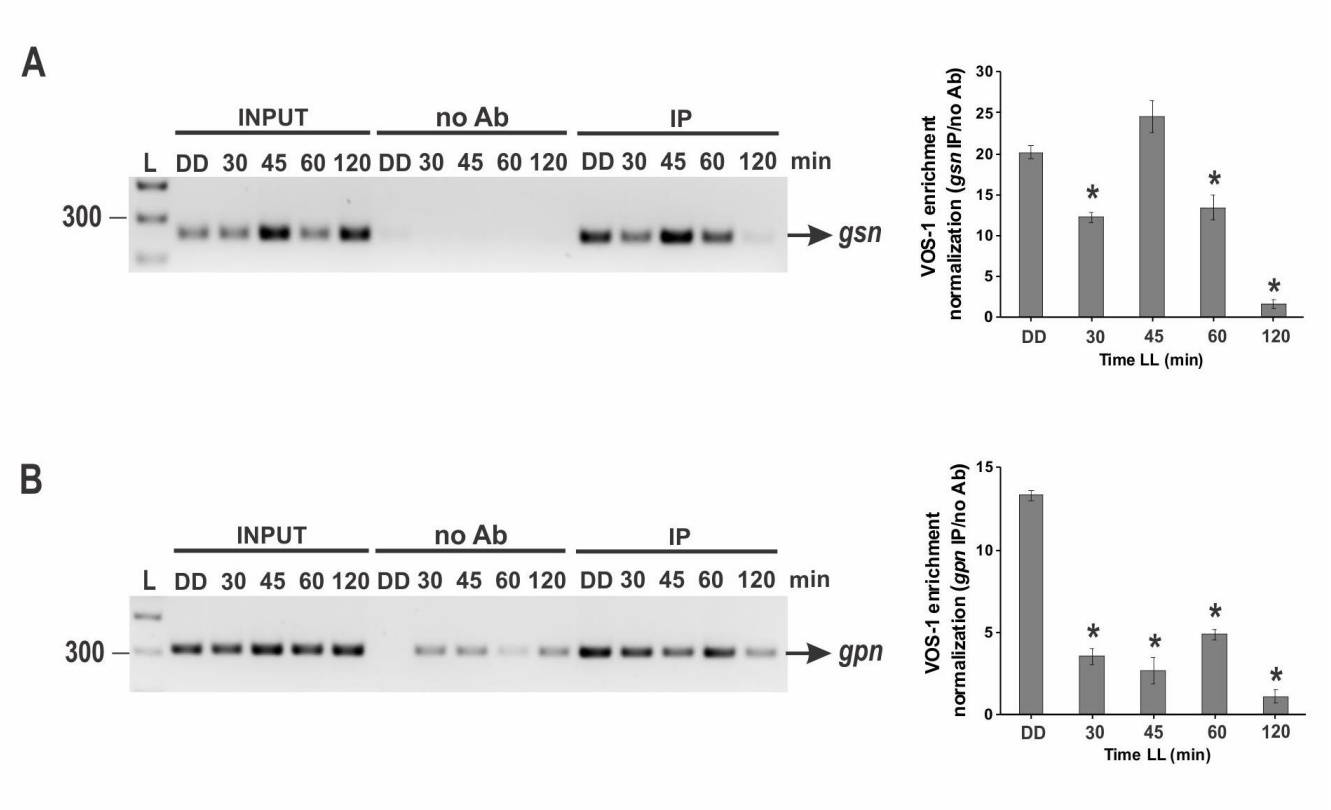

Fig. 3. VOS-1 binds to the *gsn* and *gpn* promoters in the dark and after light exposure. Binding of VOS-1 to the *gsn* (A) and *gpn* (B) genomic regions was analyzed by ChIP-PCR in cultures harvested in DD and following light exposure for the indicated times. Input DNA was used as the positive control, and the non-immunoprecipitated reactions (no Ab) were used as the negative control. The panels represent one of the two independent experiments, in which similar results were obtained. The right panels show the IP signals normalized to the negative control (±SEM, n=2). L is a 1 kb DNA ladder. The asterisks indicate significant differences compared to DD condition (Student's *t*-test, $p<0.001$).

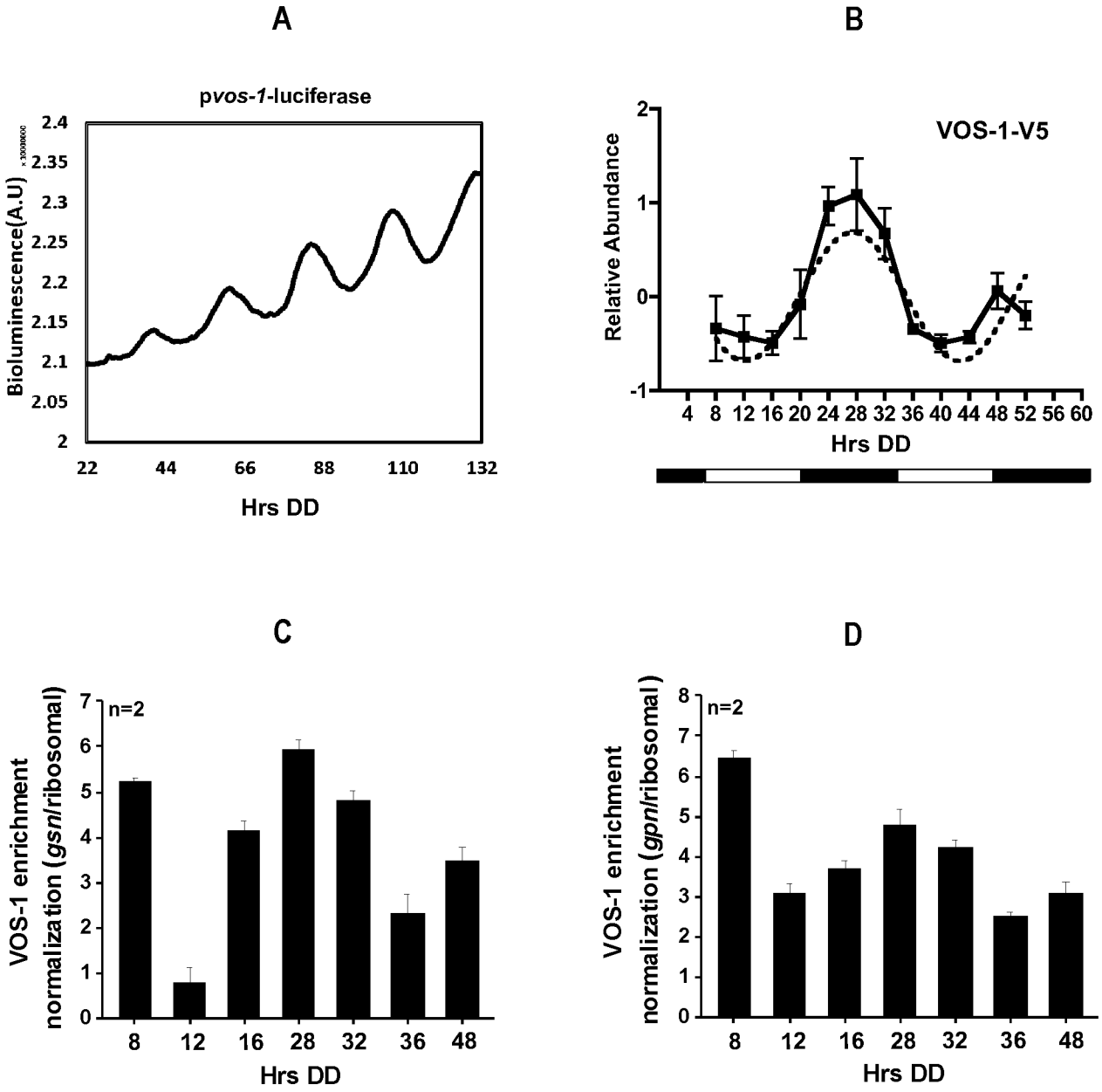

Fig. 4. VOS-1 is clock-controlled and binds rhythmically to the *gsn* and *gpn* promoters. (A) Quantification of bioluminescence of the p*vos-1-luc* in wild-type cells harvested in DD is plotted. (B) Levels of VOS-1 protein detected by western blot in extracts from VOS-1-V5-tagged cells harvested at the indicated times in the dark (DD) and plotted. The bar below graph represents the phase of the clock in DD, as described in Fig. 1. The relative abundance of VOS-1 expression levels (solid line) fit a sine wave. Binding of VOS-1-V5 to the promoters of *gsn* (C) and *gpn* (D) from cells harvested in DD and determined by ChIP-PCR. The relative IP signals were normalized to the negative control and are plotted (±SEM, n=2).

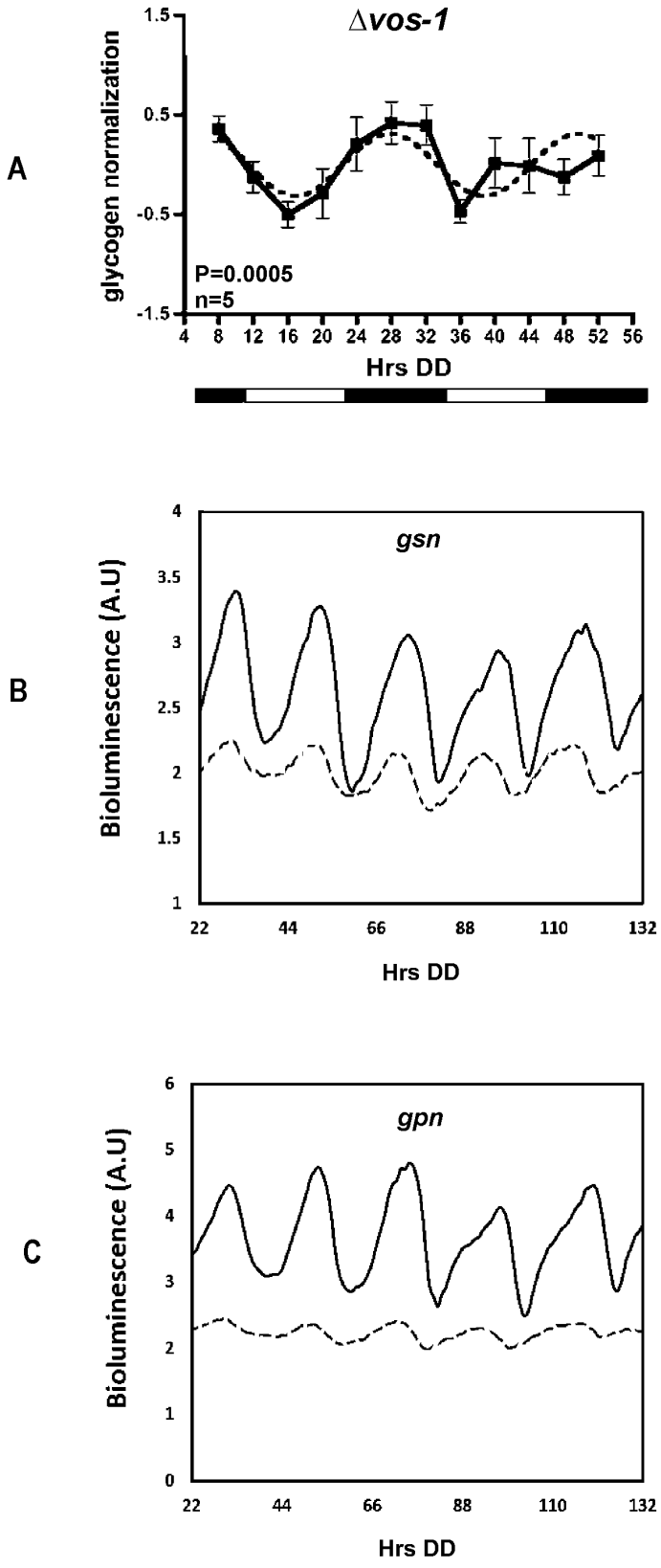

Fig. 5. Glycogen accumulation and the expression of the *gsn* and *gpn* genes have reduced amplitude rhythms in Δ*vos-1* cells. (A) Glycogen levels in Δ*vos-1* cells harvested in DD at the indicated times. The data (solid line) was plotted (±SEM, n=5), and glycogen levels fit a sine wave (p=0.0005) (dotted line), with amplitude of 0.3 ± 0.08. The bar below graph represents the phase of the clock in DD, as described in Fig. 1. Quantification of bioluminescence of the p*gsn-luc* (B) and p*gpn-luc* (C) in wild-type (solid line) and Δ*vos-1* (dashed line) cells harvested in DD is plotted.

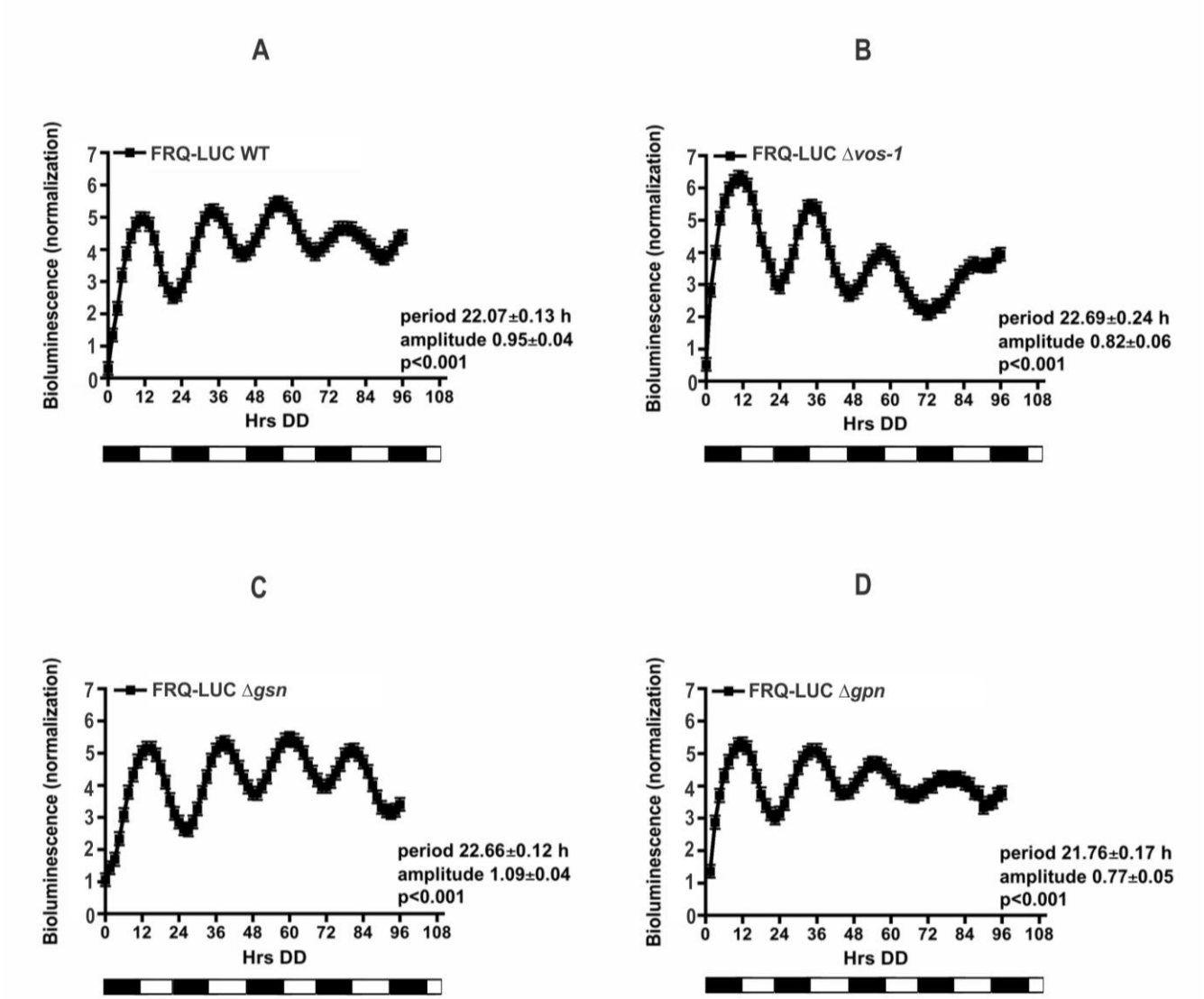

Fig. 6. The FRQ/WCC oscillator functions normally in cells deleted for *vos-1, gsn,* and *gpn*. Detrended luciferase levels are plotted from FRQ-LUC WT (wild-type control) (A), FRQ-LUC Δ*vos-1* (B), FRQ-LUC Δ*gsn* (C), and FRQ-LUC Δ*gpn* (D) cells. Each line represents the average of at least 5 independent experiments from at least two biological replicates. The bars below each plot represent the phase of the clock in DD as described in Fig. 1. The period and amplitude of the rhythms are shown.

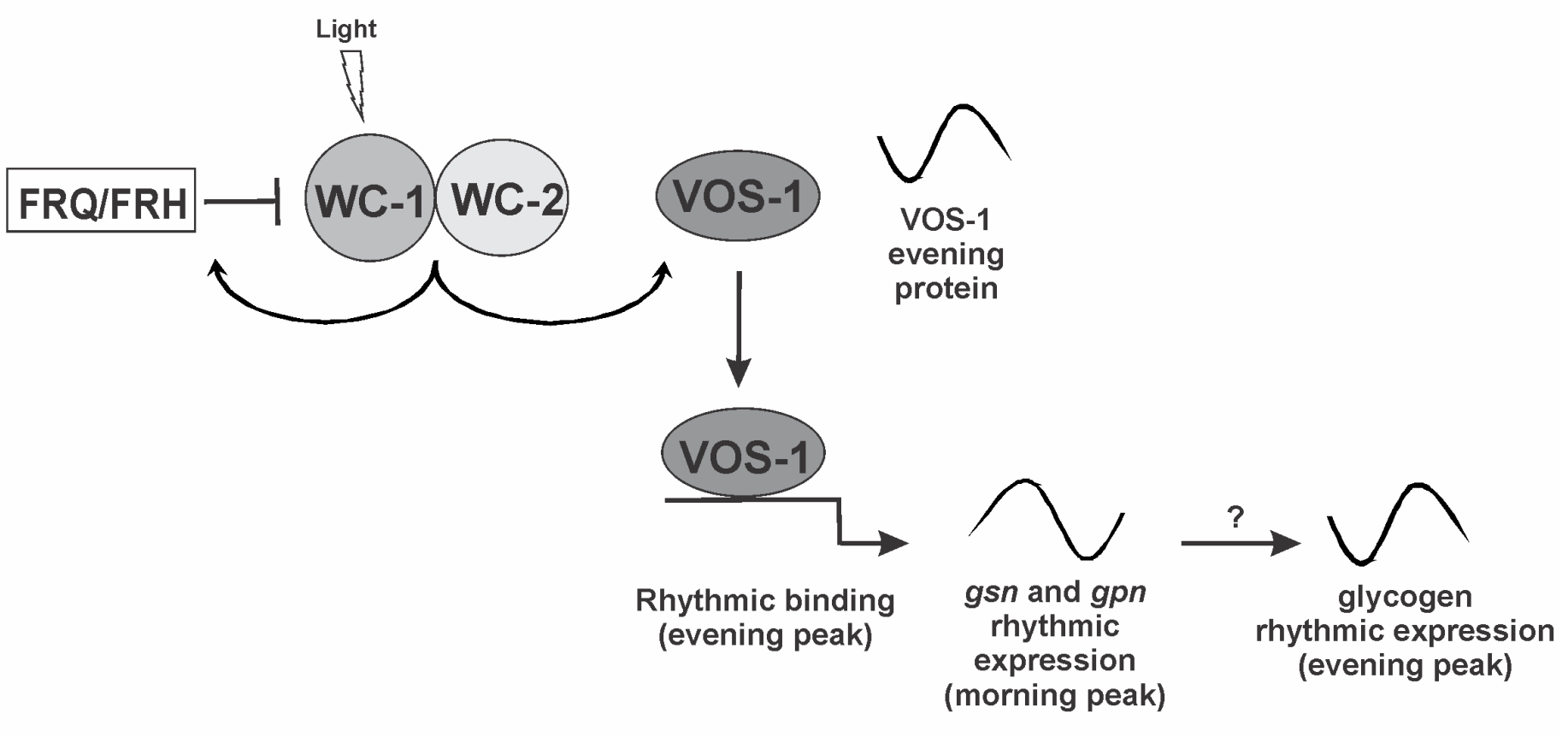

Fig. 7. Proposed model for clock regulation of glycogen levels. The WCC complex regulates the expression of the *vos-1* gene and VOS-1 binds rhythmically to the *gsn* and *gpn* promoters during the evening phase. Glycogen accumulation is clock-controlled and the VOS-1 transcription factor regulates the robustness of rhythmic expression of *gsn* and *gpn* genes. The mechanism of regulation is discussed in the text.

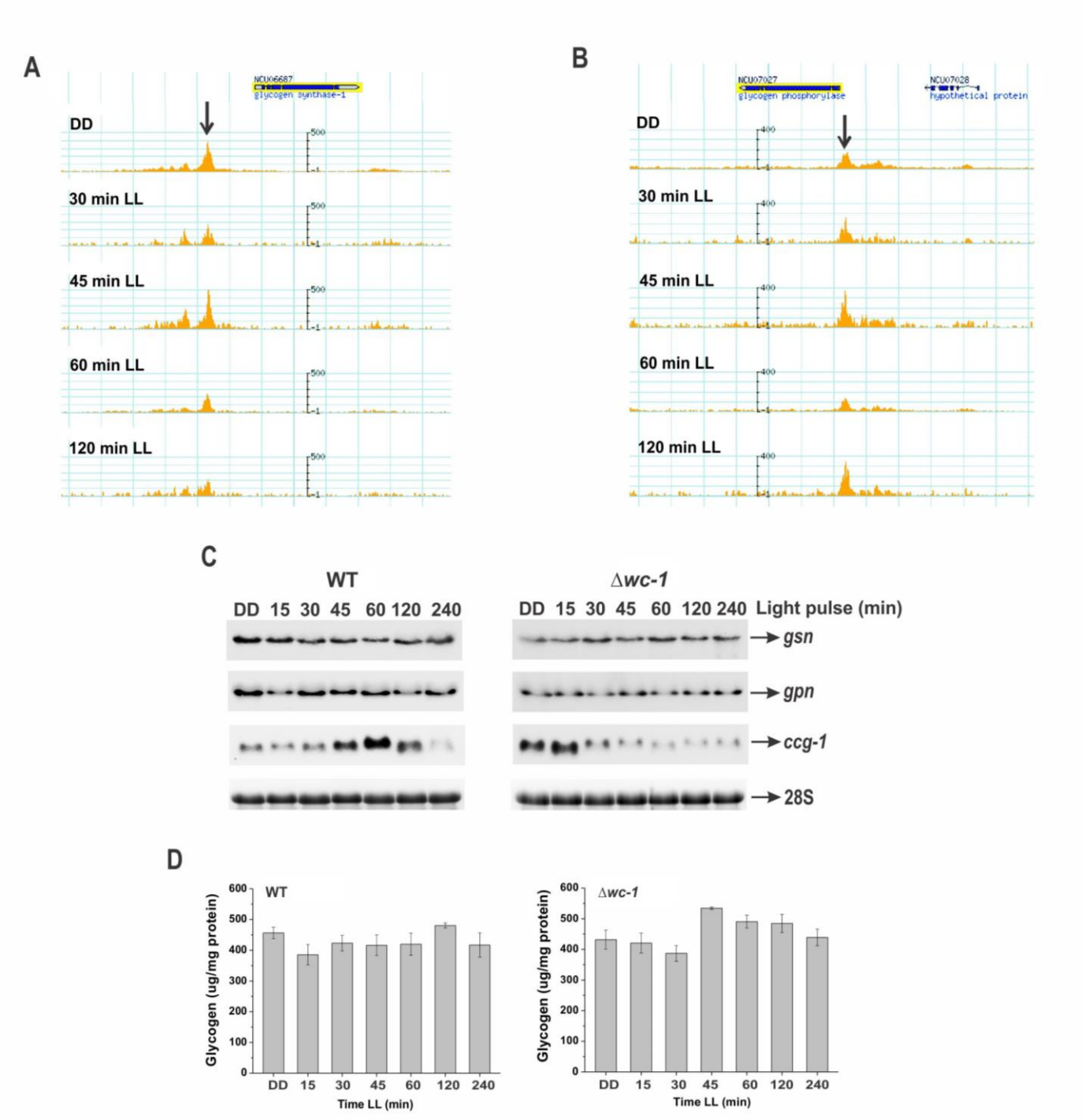

Fig. S1. VOS-1 binds to the *gsn* and *gpn* promoters, however mRNA levels and glycogen accumulation are not light induced. The plots show the ChIP-seq reads for VOS-1-V5 at the *gsn* (A) and *gpn* (B) genomic regions in DD and after light treatment for the indicated times. The black arrows indicate regions where the transcription factor VOS-1 likely binds to *gsn* and *gpn* promoters, and the direction of each gene is shown with an arrow. These regions were analyzed in independent experiments by ChIP-PCR. (C) Northern blots of the indicated genes in wild-type and Δ*wc-1* cells harvested in DD and after light exposure for the indicated times. 28S rRNA was used as an internal loading control. The data represent 1 of 2 independent experiments. (D) Plot of glycogen accumulation in the indicated strains harvested as in Fig. 1 (±SEM, n=2). No statistical difference was found in glycogen levels in wild-type versus Δ*wc-1* cells (Student's *t*-test, $p>0.01$).

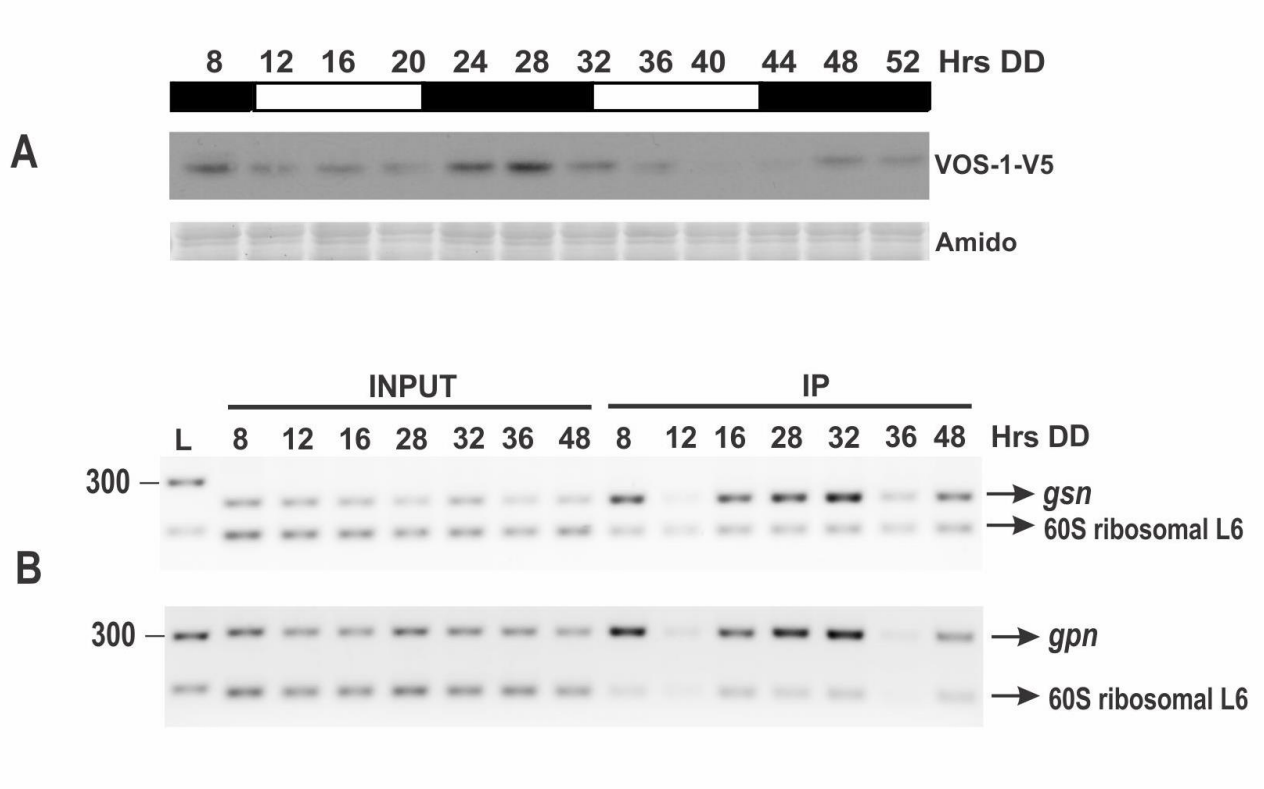

Fig. S2. The VOS-1 is clock-controlled and binds to *gsn* and *gpn* expression. (A) Levels of VOS-1 protein were detected by western blot in extracts from VOS-1-V5-tagged cells harvested at the indicated times in the dark (DD). The amido black staining (Amido) of the membrane in the lower panel demonstrates equal protein loading. The plot represents 1 of 3 independent experiments. (B) Binding of VOS-1-V5 to *gsn* (upper panel) and *gpn* (lower panel) promoters in cells harvested in DD at the indicated times. The input DNA was used as the positive control and a region from the 60S ribosomal L6, not bound by VOS-1, as the negative control. The data represent 1 of 2 independent experiments, where similar results were obtained. The bars represent circadian phase as described in Fig. 1.

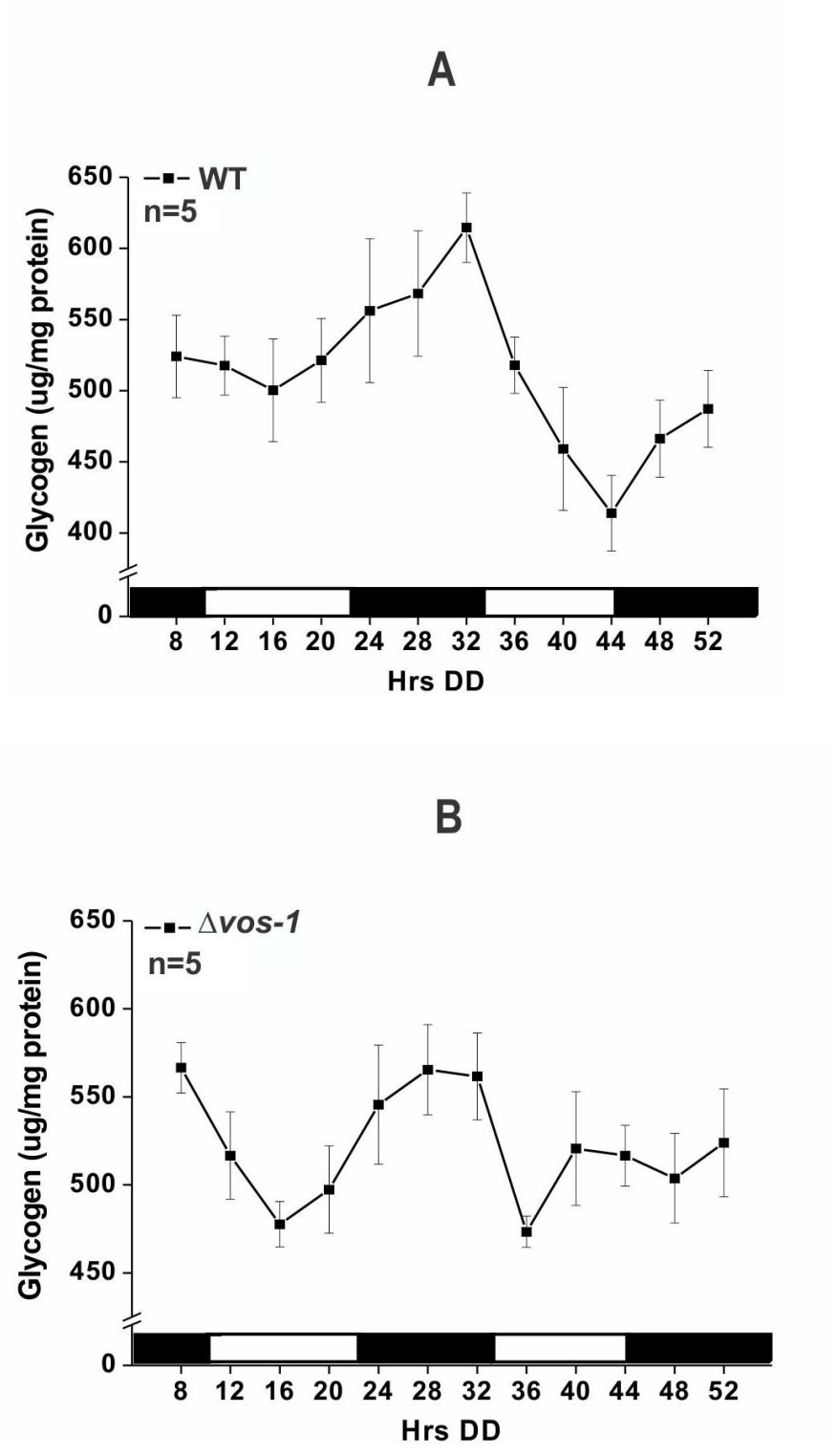

Fig. S3. Total glycogen accumulation in wild-type and Δ*vos-1* cells. The total glycogen levels were determined from WT (A) and Δ*vos-1* cells (B) harvested at the indicated times in constant darkness (DD) (±SEM, n=5). The bars represent circadian phase as described in Fig. 1.

Table S1. Oligonucleotides used in this study.

Primer	Sequence (5'→3')	Name	Position[a]
Northern blotting			
NCU06687F	CGCCGGCTCAGTAGACTTCTA	*gsn*	+777 to +797
NCU06687R	GAGTTCCTCCATGTAGCAGCCG	*gsn*	+1749 to +1770
NCU07027F	AGACTACTGGCTCGACTTCAACC	*gpn*	+768 to +790
NCU07027R	AATCTTGGCCAGCTCCGTCA	*gpn*	+1772 to +1791
NCU05964NF	ATGCGCCATCAAATACACAA	*vos-1*	+252 to +271
NCU05964NR	GGCTAGGGTGGTGTTGAT	*vos-1*	+867 to +884
CHIP-PCR			
NCU06687F1_VOS1	CCGTCTTTGGGCCAGCTTG	*gsn*	-1827 to -1806
NCU06687R1_VOS1	GTCCTCCAGATCTGTGCAGTGC	*gsn*	-1591 to -1570
NCU07027F_VOS1	CAGTCACGGTGCAGCATTCCA	*gpn*	-419 to -399
NCU07027R_VOS1	CAACAACAGATATAGCTTGGGGAAC	*gpn*	-135 to -111
rtPCRintL6f	ATCGACTTGGCAAAAGGACCA	60S ribosomal L6	+308 to +328
rtPCRintL6r	GTGAAAAAGCACACGCACACG	60S ribosomal L6	+482 to +502

[a]Primers are positioned according to the ATG start codon from genomic DNA.

Chapter 2

Chapter 2: Regulation by the PAC-3 transcription factor and the protein components of the *N. crassa* pH signaling pathway

In this chapter, we characterized the PAL signaling pathway in the filamentous fungus *N. crassa*. We described the pH sensitivity of null mutants in the pathway, since they were unable to grow in alkaline pH, and showed the role of PAL signaling in melanin production, by demonstrating the pH and PAL pathway-dependence of tyrosinase gene expression. Most of mutant strains accumulated brown pigments under normal growth conditions in flask. Similarly, the ChIP-PCR experiments strongly suggested that PAC-3 recognizes the *N. crassa* motif (5'-BGCCVAGV-3') by directly binding to many of the *pal* gene promoters, and this binding is responsible for the pH-dependent alteration in gene expression. We showed that PAC-3 undergoes a single proteolytic event in response to alkaline pH and translocates to nucleo-cytoplasmic depending on pH. Finally, we showed that the PAC-3 translocation process to the nucleus at alkaline pH may occur by the classical nuclear import pathway, in which *N. crassa* importin-α binds to the PAC-3 nuclear localization site (NLS). Our data show that the pH signaling pathway in *N. crassa* presented differences when compared to other filamentous fungi and yeasts, and some results clearly demonstrated that the PAL pathway could regulate the PAC-3 expression and processing.

This work was published in *PLoS ONE,* v. 11, n. 8, 2016 (doi:10.1371/journal.pone.0161659).

Observation: According to "Alterações das Normas Internas para a defesa da Dissertação de Mestrado ou da Tese de Doutorado, aprovadas pelo Conselho de Pós-Graduação em Biotecnologia do Instituto de Química, UNESP, Araraquara, em nov/2010 e pela Congregração em reunião de dez/2010" (Appendix), the results are presented in chapter format similar to the published article.

Molecular components of the *Neurospora crassa* pH signaling pathway and their regulation by pH and the PAC-3 transcription factor

Authors' names: Stela Virgilio[1], Fernanda Barbosa Cupertino[1], Natália Elisa Bernardes[2], Fernanda Zanolli Freitas[1], Agnes Alessandra Sekijima Takeda[2], Marcos Roberto de Mattos Fontes[2], Maria Célia Bertolini[1*]

[1]Departamento de Bioquímica e Tecnologia Química, Instituto de Química, Universidade Estadual Paulista, UNESP, 14.800-060, Araraquara, São Paulo, Brazil.
[2]Departamento de Física e Biofísica, Instituto de Biociências, Universidade Estadual Paulista, UNESP, 18.618-970, Botucatu, São Paulo, Brazil.

Running title: pH signaling pathway components in *Neurospora crassa*

***Corresponding author:** Maria Célia Bertolini
Instituto de Química, UNESP
Departamento de Bioquimica e Tecnologia Química
R. Prof. Francisco Degni, 55
14,800-060, Araraquara, São Paulo, Brazil
Phone: +55-16-33019675
Fax: +55-16-33222308
e-mail: mcbertol@iq.unesp.br

Abstract

Environmental pH induces a stress response triggering a signaling pathway whose components have been identified and characterized in several fungi. *Neurospora crassa* shares all six components of the *Aspergillus nidulans* pH signaling pathway, and we investigate here their regulation during an alkaline pH stress response. We show that the *N. crassa pal* mutant strains, with the exception of Δ*pal-9,* which is the *A. nidulans palI* homolog, exhibit low conidiation and are unable to grow at alkaline pH. Moreover, they accumulate the pigment melanin, most likely via regulation of the tyrosinase gene by the pH signaling components. The PAC-3 transcription factor binds to the tyrosinase promoter and negatively regulates its gene expression. PAC-3 also binds to all *pal* gene promoters, regulating their expression at normal growth pH and/or alkaline pH, which indicates a feedback regulation of PAC-3 in the *pal* gene expression. In addition, PAC-3 binds to the *pac-3* promoter only at alkaline pH, most likely influencing the *pac-3* expression at this pH suggesting that the activation of PAC-3 in *N. crassa* results from proteolytic processing and gene expression regulation by the pH signaling components. In *N. crassa,* PAC-3 is proteolytically processed in a single cleavage step predominately at alkaline pH; however, low levels of the processed protein can be observed at normal growth pH. We also demonstrate that PAC-3 preferentially localizes in the nucleus at alkaline pH stress and that the translocation may require the *N. crassa* importin-α since the PAC-3 nuclear localization signal (NLS) has a strong *in vitro* affinity with importin-α. The data presented here show that the pH signaling pathway in *N. crassa* shares all the components with the *A. nidulans* and *S. cerevisiae* pathways; however, it exhibits some properties not previously described in either organism.

Introduction

All organisms adapt and survive under different environmental conditions using cellular mechanisms that integrate environmental sensing and signal transduction pathways. Extracellular pH is an environmental condition to which microorganisms need to adapt, and the signal transduction pathway mediating this adaptation has been extensively characterized in model organisms, such as the filamentous fungi *Aspergillus nidulans* and the yeast *Saccharomyces cerevisiae.* More recently, additional contributions to the role of the pH signaling pathway have been made from

studies on *Candida albicans, Aspergillus fumigatus, Cryptococcus neoformans*, *Yarrowia lipolytica* and also plant pathogens, such as *Ustilago maydis.* As a consequence, their similarities and divergences and the cellular processes influenced by this signaling pathway in different organisms have been described [1, 2]. The involvement of the pH signaling pathway and the influence of the pH response for pathogenesis and virulence in pathogenic fungi have also been described, and this was first reported in *C. albicans* [3]. Additional studies have established that this signaling pathway plays an important role in the virulence of organisms such as *A. fumigatus* [4] and *C. neoformans* [5].

The PacC/Rim101 transcription factor in *A. nidulans* [6] and in *S. cerevisiae* [7], respectively, is the major effector that mediates the pH response. Upon a neutral to alkaline pH transition, a signaling pathway is activated leading to the activation of this transcription factor by proteolysis (reviewed in [1, 8, 9]). The Pal/Rim protein components of the pH signaling pathway are conserved among different fungal species, and three components are involved in the ambient pH sensing, the PalI/Rim9, PalH/Rim21 and PalF/Rim8 proteins in *A. nidulans* and *S. cerevisiae*, respectively. In *A. nidulans,* the activation of the $PacC^{72}$ protein precursor occurs by two successive proteolytic cleavage steps [10], resulting in the active $PacC^{27}$ protein, which translocates to the nucleus to activate alkaline-regulated genes and to repress acid-regulated genes [11]. The first step is pH dependent and is activated by the products of the six *pal* genes, while the second is proteasome-mediated and pH independent [10, 12]. Alkaline pH triggers the pH signaling pathway at cortical structures in the plasma membrane by recruiting all Pal proteins and several ESCRT (endosomal sorting complex required for transport) proteins, leading to the activation of PacC by proteolysis [1, 13-15] in a process that does not involve endocytosis, as has been recently demonstrated [16].

Although the major components of the pH signaling pathway are conserved among different organisms, there are differences between the PacC and Rim101 pathways, and one major difference is that the Rim101 transcription factor requires only a single proteolytic cleavage step to be activated in *S. cerevisiae* [17] and *C. albicans* [18]. Additionally, in *A. nidulans* and *S. cerevisiae,* PalF/Rim8, respectively, are post-translationally modified by ubiquitination, while *C. albicans* Rim8 is phosphorylated in response to a neutral-alkaline pH transition, and this modification correlates with Rim101 activation [19]. In *A. nidulans,* ubiquitination of PalF plays a

key role in pH signaling, promoting the downstream events of the pathway [20]. More recently, new components in the pH response pathway have been described. Thus, in *A. nidulans*, the zinc binuclear DNA binding protein PacX was identified and characterized, and the authors suggested that PacX plays a role in *pacC* gene repression and in $PacC^{27}$ activity [21]. Interestingly, this protein is absent in Saccharomycotina [21]. In *C. neoformans,* the RRA1 protein, which has a predicted structure similar to PalH/Rim21, was shown to be required for Rim101 activation [22].

In *Neurospora crassa,* the influence of the pH signaling pathway in metabolism was first described by demonstrating that the PACC transcription factor affects glycogen levels, more likely by controlling the expression of the gene encoding glycogen synthase (*gsn*), the regulatory enzyme involved in glycogen synthesis [23]. The PACC pathway was reported to be involved in glycosylation of Pi-repressible acid phosphatase [24], the transcription of the *hsp70* gene [25] and the requirement for female development [26] in *N. crassa*. Although this signaling pathway influences several cellular processes in *N. crassa,* no studies have evaluated the components of this signaling pathway in the pH response. In this work, we describe the characterization of the protein components of this signaling pathway in *N. crassa,* and we demonstrate that all mutant strains, with the exception of Δ*pal-9,* overproduce melanin, most likely due to high expression of the tyrosinase gene in these mutant strains. We further describe the modulation of the expression of the *pal* genes by alkaline pH and by the PAC-3 transcription factor and demonstrate the existence of feedback regulation involving PAC-3 at alkaline pH. Finally, we show that PAC-3 migrated to the nucleus at alkaline pH and that this translocation may occur by the classical nuclear import pathway [27] through the interaction between the *N. crassa* importin-α and a specific basic region of PAC-3, which has a nuclear localization signal (NLS).

Materials and Methods

Neurospora crassa strains and culture conditions

Neurospora crassa FGSC#9718 (*mat a*, *mus-51*::*bar*), the wild-type background strain, and the FGSC#21931 (Δ*pal-1*, *mat a*), FGSC#15867 (Δ*pal-2*, *mat A*), FGSC#16419 (Δ*pal-3*, *mat a*), FGSC#22412 (Δ*pal-6*, *mat a*), FGSC#16099 (Δ*pal-8*, *mat a*) and FGSC#13378 (Δ*pal-9*, *mat a*) mutant strains were purchased from the

Fungal Genetics Stock Center (FGSC, University of Missouri, Kansas City, MO, USA, http://www.fgsc.net) [28]. The Δ*pac-3* strain was generated as described in Cupertino et al. [23]. Details for all mutant strains can be found in S1 Table. The gene knockout in all mutant strains was confirmed by PCR using specific oligonucleotides (S2 Table, real-time PCR primers) by comparing to the amplification of genomic DNA from the wild-type strain. The strains were maintained on solid Vogel's minimal (VM) medium, pH 5.8 [29] containing 2% sucrose at 30ºC. Conidia from 10-day old cultures of wild-type and mutant strains were suspended in sterile water and counted. For morphology analyses, 10^7 conidia/mL were inoculated into flasks containing solid VM medium plus 2% sucrose, pH 5.8. For radial growth analyses, 10^7 conidia/mL were inoculated onto Petri dishes containing solid VM medium plus 2% sucrose at pH 5.8 and 7.8 for 24 h at 30ºC. Images of colony morphology were captured after 24 h.

For pH stress, 10^9 conidia/mL were first germinated in 1 L of VM medium, pH 5.8, at 30ºC and 200 rpm for 24 h. After this period, the culture was filtered and the mycelia were divided into two samples. One was frozen in liquid nitrogen and stored at -80ºC for further processing (control sample, not submitted to stress), while the remaining sample was transferred to 500 mL of fresh VM medium containing 0.5% sucrose at pH 7.8 (for alkaline pH stress). Sample from mycelia submitted to pH stress was harvested after 1 h incubation. The mycelial samples were used for RNA extraction and gene expression assays.

Construction of the Δ*pac-3* complemented strain

For complementation, the strain Δ*pac-3*::*bar* [23] was crossed with the *his-3* mutant strain (FGSC#6103, *A his-3*) to generate the Δ*pac-3 his-3* double mutant strain. A DNA fragment of 2,041 bp was amplified by PCR with the primers N-mChPACC-F and N-mChPACC-R (S2 Table) using genomic DNA from the wild-type strain as a template. The N-mChPACC-F oligonucleotide contains the sequence that codifies for 6-Gly between the nucleotide sequences encoding mCherry and the PAC-3 protein. PCR was performed using a Phusion High-Fidelity PCR kit (Finzymes), and the DNA fragment was purified with a QIAquick Gel Extraction Kit (Qiagen, CA) according to the manufacturer's instructions. The purified DNA fragment was cloned into the *Spe*I and *Xba*I sites of the pTSL48-B plasmid (a donation from N. L. Glass, University of California at Berkeley, Berkeley, CA, USA), generating the pTSL48-B-*pac-3* plasmid.

The pTSL48-B plasmid allows the constitutive expression of the N-terminus mCh-PAC-3 fusion protein, as the *ccg-1* promoter drives the *pac-3* gene expression. The pTSL48-B-*pac-3* construction was used to transform competent conidia from the recipient Δ*pac-3 his-3* double mutant strain. The transformants (Δ*pac-3 his-3::ccg-1-mCh-pac-3*) were selected on VM media containing basta without histidine and confirmed by PCR using the primers N-mChPACC-F and N-mChPACC-R (S2 Table). The progeny were analyzed by fluorescence microscopy and by evaluating the growth on Petri dishes and tubes for the production of melanin. The complemented strain (Δ*pac-3 pac-3*$^{+}$) was evaluated by growing on solid VM medium containing 2% sucrose at pH 5.8 and 7.8 and comparing to the wild-type and *pac-3* mutant strains.

RNA extraction and gene expression assays

For the RT-qPCR analysis, total RNA from the wild-type strain and the Δ*pac-3*, Δ*pal-1*, Δ*pal-2*, Δ*pal-3*, Δ*pal-6*, Δ*pal-8* and Δ*pal-9* mutants was prepared using mycelia samples cultured at pH 5.8 for 24 h at 30ºC and mycelia grown at pH 5.8 and shifted to pH 7.8 for 1 h, according to Sokolovsky et al. [30]. Expression of the tyrosinase (NCU00776) gene and the *pal-1* (NCU05876), *pal-2* (NCU00317), *pal-3* (NCU03316), *pal-6* (NCU03021), *pal-8* (NCU00007), *pal-9* (NCU01996) and the *pac-3* (NCU00090) genes was evaluated by RT-qPCR using specific oligonucleotides (S2 Table). For this, total RNA (10 µg) samples were first treated with RQ1 RNase-free DNase (Promega) and subjected to cDNA synthesis by using SuperScript III First-Strand Synthesis kit (Invitrogen) and an oligo (dT) primer, according to manufacturer's instructions. The cDNA libraries were subjected to RT-qPCR on a StepOnePlus™ Real Time PCR System (Applied Biosystems) using the Power SYBR® Green PCR Master Mix (Applied Biosystems) and specific primers for each gene amplicon (S2 Table). Reactions were performed under the following conditions: 95ºC for 10 min, 40 cycles of 95ºC for 15 s, 60ºC for 1 min to calculate cycle threshold (Ct) values, followed by 95ºC for 15 s, 60ºC for 1 min and then 95ºC for 15 s to obtain melt curves. Data analysis was performed by the StepOne Software (Applied Biosystems) using the comparative CT (ΔΔCT) method [31]. At least three biological replicates, with three experimental replicates per sample were performed, and reactions with no template were used as a negative control. The fluorescent dye ROX™ was used as the passive reference to normalize the SYBR green reporter dye fluorescence signal.

The PCR products were subjected to melting curves analysis to verify the presence of a single amplicon. All reaction efficiencies varied from 94 to 100%. We used the expression of the beta-tubulin gene as the reference gene (β-*tub-2* gene, NCU04054).

Protein expression

Conidia (10^8/mL) from the Δ*pac-3* complemented and wild-type strains were grown in 500 mL of VM liquid medium containing 2% sucrose, pH 5.8 at 30ºC and 200 rpm for 24 h. After that, the culture was filtered, and the mycelia were divided into three samples. The control sample was not subjected to pH stress and was frozen in liquid nitrogen and stored at -80ºC. The remaining samples were transferred into 250 mL of fresh VM medium containing 0.5% sucrose either at pH 4.2 (for acid stress) or 7.8 (for alkaline stress). Samples were harvested after 1 h incubation at 30ºC and 200 rpm and frozen at -80ºC. Mycelia pads were disrupted by grinding in a mortar with liquid nitrogen, and proteins were extracted with extraction buffer (50 mM HEPES, pH 7.4, 137 mM NaCl, 10% glycerol, 1 mM PMSF, 0.1 mM TCLK, 1 mM benzamidine, and 1 µg/ml of each pepstatin and antipain) [32] plus 200 µL of glass beads (710-1180 μm, Sigma) and quantified by the Hartree method [33] using BSA as standard. The amounts of 50 and 70 µg of total protein were separated by 10% SDS-PAGE gels [34] and electro-transferred to nitrocellulose blotting membrane (GE Healthcare). Immunoblotting was performed with a polyclonal anti-mCherry antibody (BioVision). Blots were subsequently probed with HRP-conjugated secondary antibodies (Sigma) and developed with luminol reagent.

Chromatin immunoprecipitation-PCR assays

Chromatin immunoprecipitation assays were performed as described by Tamaru et al. [35], with modifications. Briefly, conidia from the Δ*pac-3* complemented strain were grown in 250 mL of VM liquid medium containing 2% sucrose pH 5.8 at 30ºC and 200 rpm for 24 h. After that, mycelium from half of the culture was collected by filtration and transferred into 125 mL of fresh VM medium containing 0.5% sucrose pH 7.8 and incubated at 30ºC and 200 rpm for 1 h. The remaining sample (control, not subjected to pH stress) and the sample subjected to pH stress were fixed by adding formaldehyde (Sigma) to final concentration of 1%, followed by incubation for

30 min at 30ºC and 200 rpm. Formaldehyde was quenched using 125 mM glycine at 30ºC and 200 rpm during 10 min. Both samples were subsequently harvested by filtration and suspended in ChIP lysis buffer (50 mM HEPES, pH 7.9, 90 mM NaCl, 1 mM EDTA pH 8.0, 1% Triton X-100, 0.1% sodium deoxycholate, 1 mM PMSF, 0.1 mM TCLK, 1 mM benzamidine, and 1 µg/ml of each pepstatin and antipain). The chromatin was sheared to an average size of 0.3-0.8 kb using Vibra Cell Sonics ultrasonic processor (10 cycles: 1 min, 40% amplitude, 8.0 s pulse ON, 9.9 s pulse OFF on ice). Extracts were clarified by centrifugation, and the sonicated chromatin was pre-cleared with Dynabeads Protein A (Novex) pre-blocked with 0.5% BSA in PBS 1x and then immunoprecipitated with the anti-mCherry polyclonal antibody (BioVision) and Dynabeads Protein A. The DNA was quantified using NanoVue Plus spectrophotometer (GE Healthcare), and 25 ng of input DNA (I), no Ab (N, reaction without antibody) and IP (immunoprecipitated DNAs with anti-mCherry antibody) samples were amplified by PCR using primers specific for each promoter (S2 Table). Input DNA was used as a positive control of the experiment, and no Ab was used as a negative control.

PCR was performed using a Phusion High-Fidelity PCR kit (Finzymes) and specific oligonucleotides (S2 Table) for the tyrosinase (tyrp-F/tyrp-R), *pal-1* (pal1p-F/pal1p-R), *pal-2* (pal2p-F/pal2p-R), *pal-3* (pal3p-F/pal3p-R), *pal-6* (pal6p-F/pal6p-R), *pal-8* (pal8p-F/pal8p-R), *pal-9* (pal9p-F/pal9p-R) and *pac-3* (pac3p-F/pac3p-R) promoters. An ubiquitin gene fragment (NCU05995) amplified by the primers qUbi-F/qUbi-R was used as a negative control for binding. The ubiquitin fragment does not have the PAC-3 motif. Reactions were performed under the following conditions: 98ºC for 10 s, 25 cycles of 98ºC for 1 s, 60ºC for 5 s and 72ºC for 30 s, and then 72ºC for 5 min. The reaction products were analyzed on a 2% agarose gel and visualized by ethidium bromide. Densitometry was performed using ImageJ software [36], and the IP signals were compared to the negative control (no Ab).

Subcellular localization

To determine the subcellular localization of the fluorescent mCh-PAC-3 protein at different pH conditions, 40 µL of a 3 x 10^8 conidia/mL suspension from the Δ*pac-3* complemented strain was inoculated onto coverslips, covered with VM liquid plus 1% sucrose, pH 5.8 and incubated at 30ºC for 12 h. After this period, the coverslips were

transferred to fresh VM media containing 1% sucrose, pH 7.8 at 30°C and incubated for 30 min and 1 h. For nuclei analysis, mycelia were fixed [1% phosphate buffered saline (PBS), 3.7% formaldehyde, 5% DMSO], washed twice with PBS and stained with 100 µl DAPI (4',6-diamidino-2-phenylindole, 0.5 mg/mL) for 5 min. DAPI fluorescence was visualized using a fluorescence microscope with excitation and emission wavelengths of 358 nm and 463 nm, respectively, and mCherry fluorescence was visualized using excitation and emission wavelengths of 563 nm and 581 nm, respectively. The images were captured using an AXIO Imager.A2 Zeiss microscope, at a magnification of 100 X, coupled to an AxioCam MRm camera and processed using the AxioVision software, version 4.8.2. Further processing was performed using Corel®PHOTO-PAINT™ X7.

Expression and purification of importin-α and synthesis of PAC-3 NLS

The gene (NCU01249) encoding importin-α was cloned into the pET28a expression vector, and the recombinant protein was expressed as a truncated protein consisting of residues 75–529 fused to a 6-His tag at N-terminus, as previously described [37]. The protein was expressed in the *Escherichia coli* host strain RosettaTM (DE3) pLysS (Novagen) and purified by affinity chromatography [37]. The protein was eluted with a 0.15-3.0 M imidazole linear gradient, followed by dialysis in buffer (20 mM Tris-HCl, pH 8.0 and 100 mM NaCl) and stored at cryogenic temperatures. The PAC-3 NLS peptide (281FDARKRQFDDLNDFFGSVKRRQIN304) used in the experiments was synthesized with purity higher than 95% (GenOne). The peptide contained additional residues at the N- and C-termini compared with the minimally identified NLS to avoid artifactual binding at the termini [38].

Isothermal titration calorimetry (ITC)

ITC experiments were carried out to verify the binding affinity of importin-α to the putative NLS peptide of PAC-3 (PAC-3 NLS). The experiments were performed with a MicroCal iTC200 microcalorimeter (GE Healthcare). The protein and the PAC-3 NLS peptide were diluted in buffer (20 mM Tris-HCl, pH 8.0 and 100 mM NaCl) at a concentration of 50 µM and 500 µM for protein and peptide (protein:peptide molar ratio of 1:10), respectively. The protein sample was added to the cell, and the peptide was titrated into the cell with a syringe. Titrations were conducted at 20°C and

consisted of 20 injections of 2.0 μL in an interval of 240 s with an 800 rpm homogenization speed. The heat of the dilution was determined in a control assay by titration of the peptide sample into the protein sample buffer and was subtracted from the corresponding titrations. The data were processed using MicroCal Origin Software to obtain values for stoichiometry (N), dissociation constants (K_d), and enthalpy (ΔH). The binding-type input parameters were adjusted to obtain the best fitting model. The values of K_d and ΔH were used to calculate free energy (ΔG) and entropy (ΔS) values.

Results

The Δ*pal* and Δ*pac-3* mutant strains show impaired growth at alkaline pH and high production of melanin

In *A. nidulans,* the pH signaling pathway includes the central regulator PacC, which undergoes proteolytic processing at a neutral to alkaline pH transition in a process mediated by the pH-dependent *pal* gene cascade and the proteasome [11]. *N. crassa* has the six *A. nidulans pal* gene homologs, and to characterize the putative *N. crassa* PAL proteins, we first analyzed the morphology of the Δ*pal* mutant strains. The gene knockout in all strains was confirmed by PCR using the oligonucleotides described in S2 Table (Real-time PCR primers). All *N. crassa pal* and *pacC* mutant strains were renamed considering the Neurospora nomenclature [39], replacing the letters on the *A. nidulans* gene names by numbers (S1 Table, last column). S1 Table also shows the FGSC number and the mating type of the mutant strains, the ORF number, the theoretical MW and pI, the protein family or domain of the PAL and PAC-3 proteins and the annotation of ortholog proteins in fungi and yeast.

To assess the effects of the knockout genes, we analyzed the Δ*pal*-1, Δ*pal-2*, Δ*pal-3*, Δ*pal-6*, Δ*pal-8*, Δ*pal-9* and Δ*pac-3* strains morphology at normal (5.8) and alkaline (7.8) pH. Ten-day old flask cultures at pH 5.8 exhibited reduced aerial growth, low conidiation and high production of a dark pigment, except Δ*pal-9* (the *palI* homolog), compared to the wild-type strain (Fig 1A). The Δ*pac-3* (the *pacC* homolog) and Δ*pal-6* (the *palF* homolog) strains showed the highest pigmentation among all the Δ*pal* mutants. Basal hyphae growth was examined after cultivating the strains on Petri dishes at pH 5.8 and 7.8 for 24 h. All mutant strains, except Δ*pal-9* (the *palI* homolog), were able to growth at pH 5.8; however, they were unable to grow at

alkaline pH (7.8) (Fig 1A). Notably, all mutant strains showed reduced radial growth compared to the wild-type strain. The apical extension of the colonies at different pH values was measured and is presented in Fig 1B. These results suggest that PAC-3 and the PAL proteins, except PAL-9 (the PalI homolog), are required for growth under alkaline conditions, confirming that the *N. crassa pal* genes are involved in the response to alkaline pH stress as in *A. nidulans*. As most of the mutant strains showed high production of a dark pigment, likely melanin, we analyzed the levels of the tyrosinase gene (NCU00776) in the strains at pH 5.8 and 7.8 by RT-qPCR. Tyrosinase is a rate-limiting enzyme that controls the production of melanin [40]. The β-tubulin gene (*tub-2*, NCU04054) was used as the endogenous control. The tyrosinase gene was expressed in all mutant strains at normal growth pH (5.8) and over-expressed at alkaline pH ($P < 0.01$), except in Δ*pal-9*, which did not produce the dark pigment. These results indicate that the expression of the gene was also regulated by alkaline pH (Fig 2A) and that the PAC-3 and PAL proteins may control the melanin biosynthesis by negatively regulating the tyrosinase expression. It is important to observe the high tyrosinase gene expression in the Δ*pac-3* strain, indicating that PAC-3, the final component of the pH signaling pathway, plays a key regulatory role in the tyrosinase expression.

An *in silico* analysis of the tyrosinase gene promoter revealed the existence of four *N. crassa* PAC-3 DNA binding preference (5'-BGCCVAGV-3') [41] in its 5'-flanking region (Fig 2B). ChIP-PCR assays were performed to confirm the regulation of the tyrosinase gene by PAC-3. One PAC-3 motif was analyzed for *in vivo* binding (the dashed box in Fig 2B). In these experiments, we used the Δ*pac-3* complemented strain (Δ*pac-3 his-3::Pccg-1-mCh-pac-3*) and an anti-mCherry antibody. Chromatin was collected from the mycelial samples grown for 24 h at pH 5.8 for 1 h after transfer to pH 7.8. The input DNA (I) and the reactions without antibody (no Ab) were used as positive and negative controls of the experiment, respectively. The results showed that PAC-3 bound to the tyrosinase promoter *in vivo,* under normal and alkaline pH conditions (Fig 2B). This DNA-protein binding may explain the high expression of the tyrosinase gene and most likely the high melanin biosynthesis by the mutant strains.

pac-3 **complementation rescues the wild-type phenotype**

To confirm that the morphological changes in the Δ*pac-3* (the *pacC* homolog) strain were due to the *pac-3* knockout, we constructed the Δ*pac-3* complemented strain (Δ*pac-3 his-3::Pccg-1-mCh-pac-3*) by inserting the *pac-3* genomic sequence from the wild-type strain into the *his-3* locus. When cultured under the same conditions as the mutant and the wild-type strains, the complemented strain (Δ*pac-3 pac-3*$^{+}$) restored the wild-type phenotype, confirming that the morphological aspects observed in the mutant strain are indeed due to the *pac-3* deletion (S1 Fig). We first analyzed growth of the Δ*pac-3* and the Δ*pac-3* complemented strains in tubes of 10-day cultures at pH 5.8. The complemented strain did not show melanin pigmentation and exhibited a similar phenotype to the wild-type strain (S1A Fig). To investigate the pH response in the complemented strain, we evaluated its sensitivity to pH stress in cultures after 24 h of growth at 30°C and compared the results to the Δ*pac-3* and wild-type strains. The Δ*pac-3* mutant strain was sensitive to both pH analyzed, exhibiting lower radial growth than the wild-type strain at pH 5.8 and an inability to grow at alkaline pH (7.8), while the rescued strain exhibited a wild-type phenotype at both pH values (S1B Fig). The results confirm that the effects of pH on the growth sensitivity and melanin production were indeed due to the lack of the active PAC-3 transcription factor.

PAC-3 processing is pH-dependent

The *A. nidulans* PacC undergoes two proteolytic cleavage steps, while the *S. cerevisiae* Rim101p undergoes only one cleavage step for activation after transfer to alkaline pH. Therefore, we investigated whether PAC-3 undergoes proteolytic cleavages, resulting in isoforms with different molecular masses, and we used the Δ*pac-3* complemented strain in this experiment. The presence of PAC-3 was analyzed in cellular extracts from mycelia from wild-type and complemented strains cultivated at pH 5.8 (not subjected to pH stress) and from mycelia collected after transferring to pH 4.2 and 7.8 (for acid and alkaline stress, respectively) for 1 h. The protein was detected using the anti-mCherry antibody. In the complemented strain, PAC-3 is fused to mCherry having a final molecular weight of approximately 100 kD, which corresponds to 67.3 kD of the full-length PAC-3 protein (621 amino acid residues) along with 28.8 kD of mCherry (237 amino acid residues). The mCh-PAC-3 protein was predominantly detected in 50 µg of total protein from crude cellular

extracts prepared from cultures grown at pH 5.8 and 4.2 and was barely detected at pH 7.8 (Fig 3A). A single proteolytic cleavage was observed only at pH 7.8, leading to the production of a fused protein showing a molecular mass close to 80 kD (Fig 3A), indicating that the size of the PAC-3 processed form is similar to the intermediate PacC form from *A. nidulans* grown at alkaline pH (53 kD). It is important to mention that the *N. crassa* PAC-3 processed form was detected in cell extracts prepared from mycelium subjected to alkaline pH stress for 1 h, the time necessary for full PacC processing in *A. nidulans.* The second processed PacC form ($PacC^{27}$) described in *A. nidulans* was not detected in *N. crassa*.

We also analyzed 70 µg of total protein and observed the predominant full-length form of mCh-PAC-3 and one proteolytically processed form at pH 7.8 (Fig 3B). However, the same PAC-3 processed form was also observed at lower levels at pH 5.8 and 4.2 (arrows), indicating that PAC-3 may be proteolytically processed independent of the alkaline pH signaling pathway (Fig 3B). As expected, the mCh-PAC-3 protein was not detected in the wild-type cellular extracts. The blot probed with anti-α-tubulin antibody was used as loading control (Fig 3C). Based on these results, we conclude that PAC-3 undergoes only one pH-dependent proteolytic cleavage, similar to what is described for the *S. cerevisiae* and *C. albicans* Rim101 processing at alkaline pH. Interestingly, our results also show that PAC-3 could be processed in a pH-independent manner (pH 5.8 and pH 4.2), most likely independent of the *pal* signaling cascade.

The PAC-3 transcription factor binds to all *pal* gene promoters *in vivo* and influences their expression

To investigate whether PAC-3 feedback controls the pH signaling by regulating the *pal* and *pac-3* genes, we analyzed the expression of all genes in mycelia from Δ*pac-3* and wild-type strains grown at pH 5.8 for 24 h and in mycelia shifted to pH 7.8 for 1 h. The expression of all genes was analyzed by RT-qPCR using specific oligonucleotides described in S2 Table. The *tub-2* gene was used as the reference gene and the wild-type sample at pH 5.8 as the reference sample. Expression of the *pac-3* gene in the wild-type strain was significantly higher at alkaline pH ($P < 0.01$), as expected (Fig 4) and consistent with previous results obtained by Cupertino et al. [23]. Additionally, the *pal-1* (the *palA* homolog)*, pal-2* (the *palB* homolog)*,* and *pal-9*

(the *palI* homolog) genes were over-expressed at alkaline pH in the wild-type strain, and their expression was dependent on the PAC-3 transcription factor since they were down-regulated in Δ*pac-3* strain under the same pH (Fig 4). Curiously, the Δ*pal-9* strain grew well at pH 7.8 and did not produce melanin, although the *pal-9* expression was regulated by alkaline pH. On the other hand, the expression of the *pal-6* (the *palF* homolog) gene was significantly down-regulated in the wild-type strain at pH 7.8 ($P < 0.01$) and dependent on the PAC-3 transcription factor. Finally, the expression of the *pal-3* (the *palC* homolog) gene however, was not influenced by PAC-3 or pH 7.8, and while the expression of *pal-8* (the *palH* homolog, the pH sensor) gene was dependent on PAC-3, it was not influenced by pH 7.8 in the wild-type strain (Fig 4). In summary, the expression of *pal* genes was differentially regulated by alkaline pH and by the PAC-3 transcription factor.

An *in silico* analysis of the *pal* gene promoters revealed the existence of the *N. crassa* PAC-3 motif in all promoters, either adjacent to or distant from each other (Fig 5A), suggesting that the *N. crassa* PAC-3 transcription factor could directly regulate the expression of these genes. Many PAC-3 motifs were also identified within the *pac-3* gene promoter. A ChIP-PCR assay was performed to analyze whether PAC-3 could bind to DNA fragments containing some of these motifs *in vivo*. The PAC-3 motifs analyzed are shown in the dashed boxes in Fig 5A. In these experiments, we used the Δ*pac-3* complemented strain and the anti-mCherry antibody. Chromatin was collected from mycelia subjected to alkaline pH stress or not, and the binding of PAC-3 to all gene promoters was analyzed by PCR using the oligonucleotides described in S2 Table. As a positive control of the experiments, the input DNA (I) was analyzed, and as negative controls, a fragment of the ubiquitin gene lacking the PAC-3 motif and the non-immunoprecipitated reactions (N) were used. The DNA fragments amplified in the ChIP-PCR assays (Fig 5B) were quantified by ImageJ and the results are shown in the graphs (Fig 5C). PAC-3 was able to significantly bind to all motifs analyzed both before and after pH stress, with the exception of the motifs in the *pal-2* (the *palB* homolog) and *pac-3* (the *pacC* homolog) promoters, which were bound only at alkaline pH (Fig 5B and C). Notably, PAC-3 bound to its own gene promoter suggesting a feedback regulation of PAC-3 under this pH (Fig 5C).

The comparison of the *pal* gene expressions with PAC-3 binding to their promoters allowed us to observe that the promoters of genes whose expression was dependent on PAC-3, such as *pal-1* (the *palA* homolog), *pal-2* (the *palB* homolog),

pal-6 (the *palF* homolog), *pal-8* (the *palH* homolog), and *pal-9* (the *palI* homolog) genes, as shown in Fig 4, were bound *in vivo* by PAC-3 at alkaline pH. Although the expression of the *pal-3* (the *palC* homolog) gene was not influenced by alkaline pH or by PAC-3 (Fig 4), the transcription factor bound to its gene promoter under both conditions (Fig 5C). In this case, PAC-3 was able to bind to the promoter although did not influence its expression. Finally, PAC-3 did not bind to the ubiquitin gene fragment, which has no PAC-3 motif (Fig 5B and 5C) ($P < 0.01$), showing the specificity of the transcription factor binding. All these results show that PAC-3 binds to most of the *pal* promoters *in vivo*, including its own gene promoter, and may influence their expression at normal and alkaline pH.

Since the PAC-3 transcription factor bound to *pac-3* and to the *pal* promoters at alkaline pH, and that *pac-3* was highly expressed in the wild-type strain grown under the same condition, we asked whether the *pac-3* expression could be influenced by the PAL components of the signaling pathway. To investigate this, we analyzed the expression of the *pac-3* gene in mycelia samples from the wild-type and all Δ*pal* strains grown at pH 5.8 for 24 h (control) and in mycelia grown at pH 5.8 and shifted to pH 7.8 for 1 h (Fig 6). We observed very high expression of *pac-3* in the wild-type strain at pH 7.8, in agreement with the results shown in Fig 4. However, very low expression was observed in most of the Δ*pal* mutants at both pH, indicating a negative effect of the PAL components on the *pac-3* expression. These results also suggest that a functional pH signaling pathway is required for proper *pac-3* expression. Thus, we hypothesized that PAC-3 activation in *N. crassa* results from proteolytic processing and gene expression regulation by the PAL and PAC-3 components. Interestingly, PAL-9 (the PalI homolog), which did not influence growth at pH 7.8, as shown in Fig 1, also did not influence the *pac-3* expression. However, it was bound by PAC-3 (see Fig 5C) and its expression was influenced by PAC-3 at both pH values.

PAC-3 shuttles between the nucleus and cytoplasm and may require importin-α

Since the PAC-3 transcription factor binds to the *pal* and *pac-3* promoters at normal and/or alkaline pH and likely regulates their gene expression under the same conditions, we decided to analyze the subcellular localization of PAC-3 under pH stress. To assess this, we used the Δ*pac-3* complemented strain, in which PAC-3 is

produced as an N-terminus mCherry-tagged fusion protein under the control of the *ccg-1* promoter. For this, conidia were germinated at pH 5.8 for 12 h and then transferred to pH 7.8 for 30 min and 1 h. The mCh-PAC-3 was predominantly located in the cytoplasm at pH 5.8; however, after 1 h of transfer to pH 7.8, PAC-3 was detected predominantly in the nuclei (Fig 7A). These data are consistent with the results of PAC-3 binding to the *pal* and *pac-3* promoters and the expression modulation of these genes at alkaline pH, a condition where PAC-3 should be predominantly located in the nucleus. Our results are also in agreement with those described for *A. nidulans* by Peñalva et al. [8], who observed a preferential nuclear localization of the $PacC^{27}$ and $PacC^{53}$ forms under the same condition.

Since importin-α, together with importin-β, recognizes cargo proteins that contain nuclear localization sequences (NLS) and translocates into nucleus, we investigated the PAC-3 translocation by analyzing *in vitro* the interaction between importin-α and a peptide corresponding to the putative nuclear localization signal (NLS) of PAC-3. For this assay, recombinant *N. crassa* importin-α from *E. coli* was produced, and its interaction with the PAC-3 NLS peptide was analyzed by ITC to obtain the dissociation constant and the thermodynamic values for the formation of this complex. ITC data analyses resulted in a single binding site model indicating that one peptide binds to one protein with strong affinity (Fig 7B), with a dissociation constant (K_d) of 0.39 ± 0.074 μM, enthalpy (ΔH) of -12.10 ± 0.17 kcal mol^{-1} and entropy (ΔS) of -12.20 cal mol^{-1}. The negative enthalpy and entropy suggest that the hydrogen bonds play an important role in this interaction and that conformational changes are unfavorable, which are consistent with the interaction between the NLS sequences and importin-α [42] and in other organisms [27]. The data obtained from the titration of the PAC-3 NLS peptide to importin-α showed similar K_d values to ITC assays of importin-α and NLS peptides from other analyses [42-44].

Discussion

All microorganisms need to develop the ability to adapt to environmental pH since it strongly impacts cell growth and development. The Pac/Rim in filamentous fungi and yeast is the best-characterized signaling pathway involved in the pH stress response, and numerous reports have described its importance in different cellular processes. *N. crassa* shares all six *A. nidulans* Pal orthologs along with the ESCRT proteins

required for signal sensing and proteolytic activation of PAC-3 in response to ambient alkaline pH. In this work, we investigated the components of the *N. crassa* pH signaling pathway regarding their characterization upon transition from neutral to alkaline pH conditions. All Δ*pal* mutant strains showed reduced growth and low conidiation at normal growth pH, consistent with previously reported results [26]. In addition, the mutant strains showed an inability to grow at alkaline pH, the same phenotype described for the *A. nidulans pal* mutants [45]. The Δ*pal-9* strain, however, exhibited a wild-type phenotype. PAL-9 is the *A. nidulans* PalI component, which is located in the plasma membrane and together with PalH and PalF establishes the ambient pH signal. Although unnecessary for growth at alkaline pH, *pal-9* expression is regulated by the PAC-3 transcription factor following transition from normal to alkaline pH in *N. crassa*. This is quite surprising because in *A. nidulans* the PalI component is required for normal growth at pH 8 compared to the wild-type strain under the same condition [45].

An interesting characteristic of the *N. crassa* mutant strains, which has not been reported in any of the mutant strains of the pH signaling pathway, is the high production of the pigment melanin, which is important for cell protection in diverse microorganisms and is associated with virulence in many human pathogenic fungi [46, 47]. In *N. crassa,* melanin accumulation by most of the mutant strains in the pH signaling pathway could not be attributed to cell protection under adverse conditions, since the pigment accumulation was high at normal growth pH. This result suggests that the components of the signaling pathway, either directly or indirectly, affect the melanin production under normal growth conditions. To identify a regulatory mechanism connecting both processes, pH signaling and melanin accumulation, we demonstrated that the tyrosinase gene was over-expressed in all mutant strains, mainly in the Δ*pac-3* (the *pacC* homolog) strain, but not in Δ*pal-9* (the *palI* homolog) strain. Thus, PAC-3 appears to be the main regulator of tyrosinase expression; it is the final component of the signaling pathway whose activation results from an active signaling cascade. All data are coincident with the high number of PAC-3 motifs in the tyrosinase promoter and with the ability of PAC-3 to bind to the promoter in a pH-independent manner. Melanin is an insoluble compound and is associated with virulence in numerous fungal pathogens, such as *C. neoformans* [48] and *Paracoccidioides brasiliensis* [49], among others. In *N. crassa,* protoperithecia differentiation was previously correlated with tyrosinase activity and melanin

559 formation [50]. More recently, Park et al. [51] suggested a role for the MAK-1
560 pathway in melanin production in *N. crassa* by modulating the tyrosinase gene
561 expression under nitrogen starvation. Mutant strains in two components of this
562 pathway (Δ*mek-1* and Δ*mak-1*) exhibited high tyrosinase gene expression and
563 accumulated melanin [51]. In addition to the MAK-1 pathway, the pH signaling
564 pathway, among other pathways, was also reported to be required for protoperithecia
565 formation [26], indicating the requirement of different signaling pathways for female
566 development in *N. crassa.* The results presented in this work connect all these data
567 by demonstrating that the pH signaling pathway controls tyrosinase gene expression
568 and, as a consequence, the melanin accumulation, which is required for female
569 development. However, the influence of the pH signaling pathway in both processes,
570 protoperithecia formation and melanin production, may be modulated by different
571 regulatory mechanisms because the mutant strains in this pathway are unable to
572 develop protoperithecia but they over-express tyrosinase and accumulate melanin.
573 Additional signaling pathways could play a role in connecting both processes.

574 We showed here that most of the pH signaling pathway components, but not
575 all, were regulated at the gene expression level by ambient pH, which suggests the
576 existence of feedback regulation on these genes. Such regulation in the pH pathway
577 components was previously reported only for the *C. albicans RIM8* gene, which was
578 described as transcriptionally repressed at alkaline pH [19, 52]. In *N. crassa,* the
579 expression of the *pal-6* homolog was also negatively regulated by alkaline pH,
580 consistent with the results described in *C. albicans.* However, alkaline pH also
581 positively regulates several *pal* genes (*pal-1, pal-2,* and *pal-9*) in *N. crassa*,
582 suggesting that opposing regulatory mechanisms affect the pH signaling
583 components. Interestingly, while the *pal-9* expression was regulated by alkaline pH,
584 the PAL-9 protein appears to play a minor role in pH signaling transduction in *N.*
585 *crassa* since the Δ*pal-9* mutant strain did not display growth defects at alkaline pH.
586 This is in contrast to what was reported in *S. cerevisiae* and *C. albicans,* where the
587 Rim9 homolog is necessary for Rim101 cleavage and therefore fully required for pH
588 signaling transduction [17, 53]. The expression of several *pal* genes, including *pal-6,*
589 *pal-8* and *pal-9,* was also dependent on the PAC-3 transcription factor, which
590 indicates that they require an active signaling pathway for normal expression. This
591 result may be a consequence of the ability of PAC-3 to bind to all *pal* promoters at
592 both pH conditions, likely regulating the expression of most *pal* genes.

The *pac-3* expression was also negatively modulated irrespective of both pH by the PAL components in *N. crassa*, with the exception of PAL-9, indicating the existence of a cross-regulation among all components of this signaling pathway and a self-regulation on *pac-3* expression. Considering this result, we may suggest that this regulation may be a consequence of the lack of an active PAC-3 in the *pal* mutant strains, which, once activated, could bind to its own promoter at alkaline pH, activating its expression. In *A. nidulans,* Trevisan et al. [54] described the existence of alternative RNA splicing of the *palB* gene, depending on the growth conditions, which could affect the PacC protein activity. We also cannot preclude the existence of additional proteins involved in such cross-regulation, similar to what was recently described for the PacX protein in *A. nidulans* [21], which was identified to play a role in *pacC* gene repression.

We demonstrated here that PAC-3 may be processed in a single proteolytic step, similar to what was described for *S. cerevisiae* [17] and *C. albicans* [18]. In addition, as in *C. albicans,* PAC-3 processing was also observed at acidic pH, which could explain the localization of PAC-3 to the nucleus at normal pH growth conditions and its regulatory function at the same pH. The results presented here regarding the protein processing at acidic pH confirm previous results obtained by our group [23] using different experimental approaches. However, we previously were unable to detect the unprocessed PAC-3 [23]. We also showed here that PAC-3 translocates to the nucleus at alkaline pH and that this process may occur by the classical nuclear import pathway, in which importin-α binds to a specific NLS, known as classical NLSs. ITC assays between PAC-3 NLS and importin-α demonstrated that these molecules have an affinity compatible with the interaction between a classical NLS peptide and importin-α [42]. A classical bipartite NLS presents two basic clusters that binds to different regions of the importin-α [38] with a stoichiometry of 1:1, and its consensus sequence is generally accepted as **KR**X_{10-12}**K**(K/R)X(K/R), where X corresponds to any residue, and residues in bold indicate critical residues [55]. PAC-3 NLS displays all these critical requirements, except for the last position (K/R) (Fig 8A), for its sequence to be classified as a classical bipartite NLS. ITC results also supported this identification because a stoichiometry of 1:1 for the NLS peptide/importin-α complex is characteristic of a bipartite NLS, while most classical monopartite NLSs bind with a stoichiometry of 1:2 (protein:peptide). Thus, the data presented here indicate that this NLS region is responsible for the recognition of the

PAC-3 transcription factor by importin-α, and these components may form a complex that permits PAC-3 to be translocated to the nucleus under specific conditions. The *N. crassa* importin-α used in our work was first identified by Foss et al. [56] as important for DNA methylation, and later described as required for heterochromatic formation and DNA methylation [57, 58].

Finally, we may conclude that the *N. crassa* PAC-3 transcription factor cycles between the cytoplasm and nucleus under pH alkaline stress, either up- or down-regulating the expression of pH-responsive genes. Based on our findings, we propose a model of the pH signaling pathway in *N. crassa* (Fig 8B). According to the results, the pathway requires the same Pal/Rim components described in *A. nidulans* and *S. cerevisiae,* sharing characteristics with both organisms. We suggest that the PAC-3 transcription factor, once activated, regulates the *pal* gene expression and that this regulation may be directly mediated by PAC-3 because it binds to all *pal* promoters.

Acknowledgments

We thank Dr. Trevor Lee Starr, University of California at Berkeley, Laboratory of Plant and Microbial Biology, Berkeley, CA, USA, for the plasmid pTSL48-B and the Fungal Genetics Stock Center (Kansas City, MO) for the Neurospora strains. We thank Jonatas E. M. Campanella for helping with the microscopy analysis and Antonio Tarcisio Delfino for technical assistance.

Author Contributions

Conceived and designed the experiments: SV NEB FBC MRMF MCB. Performed the experiments: SV NEB FBC FZF AAST. Analyzed the data: SV NEB AAST FBC MRMF MCB. Contributed reagents/materials/analysis tools: MRMF MCB. Wrote the paper: SV NEB MRMF MCB.

References

1. Peñalva MA, Lucena-Agell D, Arst HN Jr. Liaison alcaline: Pals entice non-endosomal ESCRTs to the plasma membrane for pH signaling. Curr Opin Microbiol. 2014; 22:49-59.
2. Cornet M, Gaillardin C. pH signaling in human fungal pathogens: a new target for antifungal strategies. Eukaryot Cell. 2014; 13(3):342-352.

3. Davis, D. Adaptation to environmental pH in *Candida albicans* and its relation to pathogenesis. Curr Genet. 2003; 44(1):1-7.

4. Bertuzzi M, Schrettl M, Alcazar-Fuoli L, Cairns TC, Muñoz A, Walker LA, et al. The pH-responsive PacC transcription factor of *Aspergillus fumigatus* governs epithelial entry and tissue invasion during pulmonary aspergillosis. PLoS Pathog. 2014; 10(10):e1004413 doi: 10.1371/journal.ppat.1004413.

5. O'Meara TR, Xu W, Selvig KM, O'Meara MJ, Mitchell AP, Alspaugh JA. The *Cryptococcus neoformans* Rim101 transcription factor directly regulates genes required for adaptation to the host. Mol Cell Biol. 2014; 34(4):673-684.

6. Tilburn J, Sarkar S, Widdick DA, Espeso EA, Orejas M, Mungroo J, et al. The *Aspergillus* PacC zinc finger transcription factor mediates regulation of both acid- and alkaline-expressed genes by ambient pH. EMBO J. 1995; 14(4):779-790.

7. Su SS, Mitchell AP. Identification of functionally related genes that stimulate early meiotic gene expression in yeast. Genetics 1993; 133(1):67-77.

8. Peñalva MA, Tilburn J, Bignell E, Arst HN Jr. Ambient pH gene regulation in fungi: making connections. Trends Microbiol. 2008; 16(6):291-300.

9. Ariño J. Integrative responses to high pH stress in *S. cerevisiae.* OMICS. 2010; 14(5):517-523.

10. Díez E, Alvaro J, Espeso EA, Rainbow L, Suárez T, Tilburn J, et al. Activation of the *Aspergillus* PacC zinc finger transcription factor requires two proteolytic steps. EMBO J. 2002; 21(6):1350-1359.

11. Arst HNJr, Peñalva MA. pH regulation in *Aspergillus* and parallels with higher eukaryotic regulatory systems. Trends Genet. 2003; 19(4):224-231.

12. Peñas MM, Hervás-Aguilar A, Múnera-Huertas T, Reoyo E, Peñalva MA, Arst HN Jr, et al. Further characterization of the signaling proteolysis step in the *Aspergillus nidulans* pH signal transduction pathway. Eukaryot Cell. 2007; 6(6): 960-970.

13. Rodríguez-Galán O, Galindo A, Hervás-Aguilar A, Arst HN Jr, Peñalva MA. Physiological involvement in pH signaling of Vps24-mediated recruitment of Aspergillus PalB cysteine protease to ESCRT-III. J Biol Chem. 2009; 284(7):4404-4412.

14. Calcagno-Pizarelli AM, Hervás-Aguilar A, Galindo A, Abenza JF, Peñalva MA, Arst HN Jr. Rescue of *Aspergillus nidulans* severely debilitating null mutations in ESCRT-0, I, II and III genes by inactivation of a salt-tolerance pathway allows examination of ESCRT gene roles in pH signalling. J Cell Sci. 2011; 124(Pt 23):4064-4076.

15. Galindo A, Calcagno-Pizarelli AM, Arst HN Jr, Peñalva MÁ. An ordered pathway for the assembly of fungal ESCRT-containing ambient pH signalling complexes at the plasma membrane. J Cell Sci. 2012; 125(Pt 7):1784-1795

16. Lucena-Agell D, Galindo A, Arst HN Jr, Peñalva MA. *Aspergillus nidulans* ambient pH signaling does not require endocytosis. Eukaryot Cell. 2015; 14(6):545-553.

17. Li W, Mitchell AP. Proteolytic activation of Rim1p, a positive regulator of yeast sporulation and invasive growth. Genetics. 1997; 145(1):63-73.

18. Li M, Martin SJ, Bruno VM, Mitchell AP, Davis DA. *Candida albicans* Rim13p, a protease required for Rim101p processing at acidic and alkaline pHs. Eukaryot Cell. 2004; 3(3):741-751.

19. Gomez-Raja J, Davis DA. The β-arrestin-like protein Rim8 is hyperphosphorylated and complexes with Rim21 and Rim101 to promote adaptation to neutral-alkaline pH. Eukaryot Cell. 2012; 11(5): 683-693.

20. Hervás-Aguilar A, Galindo A, Peñalva MA. Receptor-independent ambient pH signaling by ubiquitin attachment to fungal arrestin-like PalF. J Biol Chem. 2010; 285(23):18095-18102.

21. Bussink HJ, Bignell EM, Múnera-Huertas T, Lucena-Agell D, Scazzocchio C, Espeso EA, et al. (2015) Refining the pH response in *Aspergillus nidulans*: a modulatory triad involving PacX, a novel zinc binuclear cluster protein. Mol Microbiol. 2015; 98(6):1051-1072.

22. Ost KS, O'Meara TR, Huda N, Esher SK, Alspaugh JA. The *Cryptococcus neoformans* alkaline response pathway: identification of a novel rim pathway activator. PLoS Genet. 2015; 11(4):e1005159 doi: 10.1371/journal.pgen.1005159.

23. Cupertino FB, Freitas FZ, de Paula RM, Bertolini MC. Ambient pH controls glycogen gevels by regulating glycogen synthase gene expression in *Neurospora crassa*. New insights into the pH signaling pathway. Plos One. 2012; 7(8):e44258 doi: 10.1371/journal.pone.0044258.

24. Nozawa SR, Ferreira-Nozawa MS, Martinez-Rossi NM, Rossi A. The pH-induced glycosylation of secreted phosphatases is mediated in *Aspergillus nidulans* by the regulatory gene *pacC*-dependent pathway. Fungal Genet Biol. 2003; 39(3): 286-295.

25. Squina FM, Leal J, Cipriano VT, Martinez-Rossi NM, Rossi A. Transcription of the *Neurospora crassa* 70-kDa class heat shock protein genes is modulated in response to extracellular pH changes. Cell Stress Chaperones 2010; 15(2):225-231.

26. Chinnici JL, Fu C, Caccamise LM, Arnold JW, Free SJ. *Neurospora crassa* female development requires the PACC and other signal transduction pathways, transcription factors, chromatin remodeling, cell-to-cell fusion, and autophagy. PLoS One. 2014; 9(10):e110603 doi: 10.1371/journal.pone.0110603.

27. Christie M, Chang CW, Róna G, Smith KM, Stewart AG, Takeda AAS, et al. Structural biology and regulation of protein import into the nucleus. J Mol Biol. 2016; 428:doi:10.1016/j.jmb.2015.10.023.

28. McCluskey K. The Fungal Genetics Stock Center: from molds to molecules. Adv Appl Microbiol. 2003; 52: 245-262.

29. Vogel HJ. A convenient growth medium for *Neurospora crassa* (medium N). Microbiol Genet Bull. 1956; 13:42-43.

30. Sokolovsky V, Kaldenhoff R, Ricci M, Russo VEA. Fast and reliable mini-prep RNA extraction from *Neurospora crassa*. Fungal Genet Newsl*.* 1990; 37:41-43.

31. Livak KJ, Schmittgen TD. Analysis of relative gene expression data using real-time quantitative PCR and the 2(-Delta Delta C(T)) method. Methods. 2001; 25(4):402-408.

748 **32.** Garceau NY, Liu Y, Loros JJ, Dunlap JC. Alternative initiation of translation and
749 time-specific phosphorylation yield multiple forms of the essential clock protein
750 FREQUENCY. Cell. 1997; 89(3):469-476.
751 **33.** Hartree EF. Determination of protein: a modification of the Lowry method that
752 gives a linear photometric response. Anal Biochem. 1972; 48(2):422-427.
753 **34.** Laemmli UK. Cleavage of structural proteins during the assembly of the head of
754 bacteriophage T4. Nature. 1970; 227(5259):680-685.
755 **35.** Tamaru H, Zhang X, McMillen D, Singh PB, Nakayama J, Grewal SI, et al.
756 Trimethylated lysine 9 of histone H3 is a mark for DNA methylation in *Neurospora*
757 *crassa*. Nat Genet. 2003; 34(1):75-79.
758 **36.** Abràmoff MD, Magalhães PJ, Ram SJ. Image processing with ImageJ.
759 Biophotonics Intern. 2004; 11(7):36-42.
760 **37.** Takeda AAS, Freitas FZ, Magro AJ, Bernardes NE, Fernandes CAH, Gonçalves
761 RD, et al. Biophysical characterization of the recombinant importin-α from
762 *Neurospora crassa*. Protein Pept Lett. 2013; 20(1):8-16.
763 **38.** Fontes MR, Teh T, Kobe B. Structural basis of recognition of monopartite and
764 bipartite nuclear localization sequences by mammalian importin-alpha. J Mol Biol.
765 2000; 297(5):1183-1194.
766 **39.** Perkins DD, Radford A, Newmeyer D, Björkman M. Chromosomal loci of
767 *Neurospora crassa*. Microbiol Rev. 1982; 46(4):426-570.
768 **40.** Sánchez-Ferrer A, Rodríguez-López JN, García-Cánovas F, García-Carmona F.
769 Tyrosinase: a comprehensive review of its mechanism. Biochim Biophys Acta.
770 1995; 1247(1):1-11.
771 **41.** Weirauch MT, Yang A, Albu M, Cote AG, Montenegro-Montero A, Drewe P, et al.
772 Determination and inference of eukaryotic transcription factor sequence specificity.
773 Cell. 2014; 158(6):1431-1443.
774 **42.** Bernardes NE, Takeda AAS, Dreyer TR, Freitas FZ, Bertolini MC, Fontes MRM.
775 Structure of Importin-α from a filamentous fungus in complex with a classical
776 nuclear localization signal. PLoS One. 2015; 10:e0128687 doi:
777 10.1371/journal.pone.0128687.
778 **43.** Lott K, Bhardwaj A, Sims PJ, Cingolani G. A minimal nuclear localization signal
779 (NLS) in human phospholipid scramblase 4 that binds only the minor NLS-binding
780 site of importin alpha1. J Biol Chem. 2011; 286(32):28160–28169.
781 **44.** Cutress ML, Whitaker HC, Mills IG, Stewart M, Neal DE. Structural basis for the
782 nuclear import of the human androgen receptor. J Cell Sci. 2008; 121(Pt 7):957–
783 968.
784 **45.** Peñalva MA, Arst HN Jr. Regulation of gene expression by ambient pH in
785 filamentous fungi and yeasts. Microbiol Mol Biol Rev. 2002; 66(3):426-446.
786 **46.** Gómez BL, Nosanchuk JD. Melanin and fungi. Curr Opin Infect Dis. 2003;
787 16(2):91-96.
788 **47.** Nosanchuk JD, Stark RE, Casadevall A. Fungal melanin: What do we know
789 about structure? Front Microbiol. 2015; 6: 1463 doi: 10.3389/fmicb.2015.01463.
790 **48.** Casadevall A, Rosas AL, Nosanchuk JD. Melanin and virulence in *Cryptococcus*
791 *neoformans*. Curr Opin Microbiol. 2000; 3(4):354–358.

792 **49.** Silva MB, Thomaz L, Marques AF, Svidzinski AE, Nosanchuk JD, Casadevall A,
793 et al. Resistance of melanized yeast cells of *Paracoccidioides brasiliensis* to
794 antimicrobial oxidants and inhibition of phagocytosis using carbohydrates and
795 monoclonal antibody to CD18. Mem Inst Oswaldo Cruz. 2009; 104(4):644–648.
796 **50.** Hirsch HM. Environmental factors influencing the differentiation of protoperithecia
797 and their relation to tyrosinase and melanin formation in *Neurospora crassa*.
798 Physiol Plant. 1954; 7(1):72–97.
799 **51.** Park G, Pan S, Borkovich KA. Mitogen-activated protein kinase cascade required
800 for regulation of development and secondary metabolism in *Neurospora crassa*.
801 Eukaryot Cell. 2008; 7(12):2113-2122.
802 **52.** Porta A, Ramon AM, Fonzi WA. PRR1, a homolog of *Aspergillus nidulans* palF,
803 controls pH-dependent gene expression and filamentation in *Candida albicans*. J
804 Bacteriol. 1999; 181(24):7516-7523.
805 **53.** Cornet M, Richard ML, Gaillardin C. The homologue of the *Saccharomyces*
806 *cerevisiae* RIM9 gene is required for ambient pH signalling in *Candida albicans*.
807 Res Microbiol. 2009; 160(3):219-293.
808 **54.** Trevisan GL, Oliveira EH, Peres NT, Cruz AH, Martinez-Rossi NM, Rossi A.
809 Transcription of *Aspergillus nidulans pacC* is modulated by alternative RNA
810 splicing of *palB*. FEBS Lett. 2011; 585(21):3442-3445.
811 **55.** Marfori M, Lonhienne TG, Forwood JK, Kobe B. Structural basis of high-affinity
812 nuclear localization signal interactions with importin-α. Traffic. 2012; 13(4):532-
813 548.
814 **56.** Foss HM, Roberts CJ, Claeys KM, Selker EU. Abnormal chromosome behavior in
815 Neurospora mutants defective in DNA methylation Science. 1993;
816 262(5140):1737-1741.
817 **57.** Klocko AD, Rountree MR, Grisafi PL, Hays SM, Adhvaryu KK, Selker EU.
818 Neurospora importin α is required for normal heterochromatic formation and DNA
819 methylation. PLoS Genet. 2015; 11(3):e1005083.
820 **58.** Galazka JM, Klocko AD, Uesaka M, Honda S, Selker EU, Freitag M. Neurospora
821 chromosomes are organized by blocs of importin alpha-dependent
822 heterochromatin that are largely independent of H3K9me3. Genome Res. 2016;
823 26(8):1069-1080.

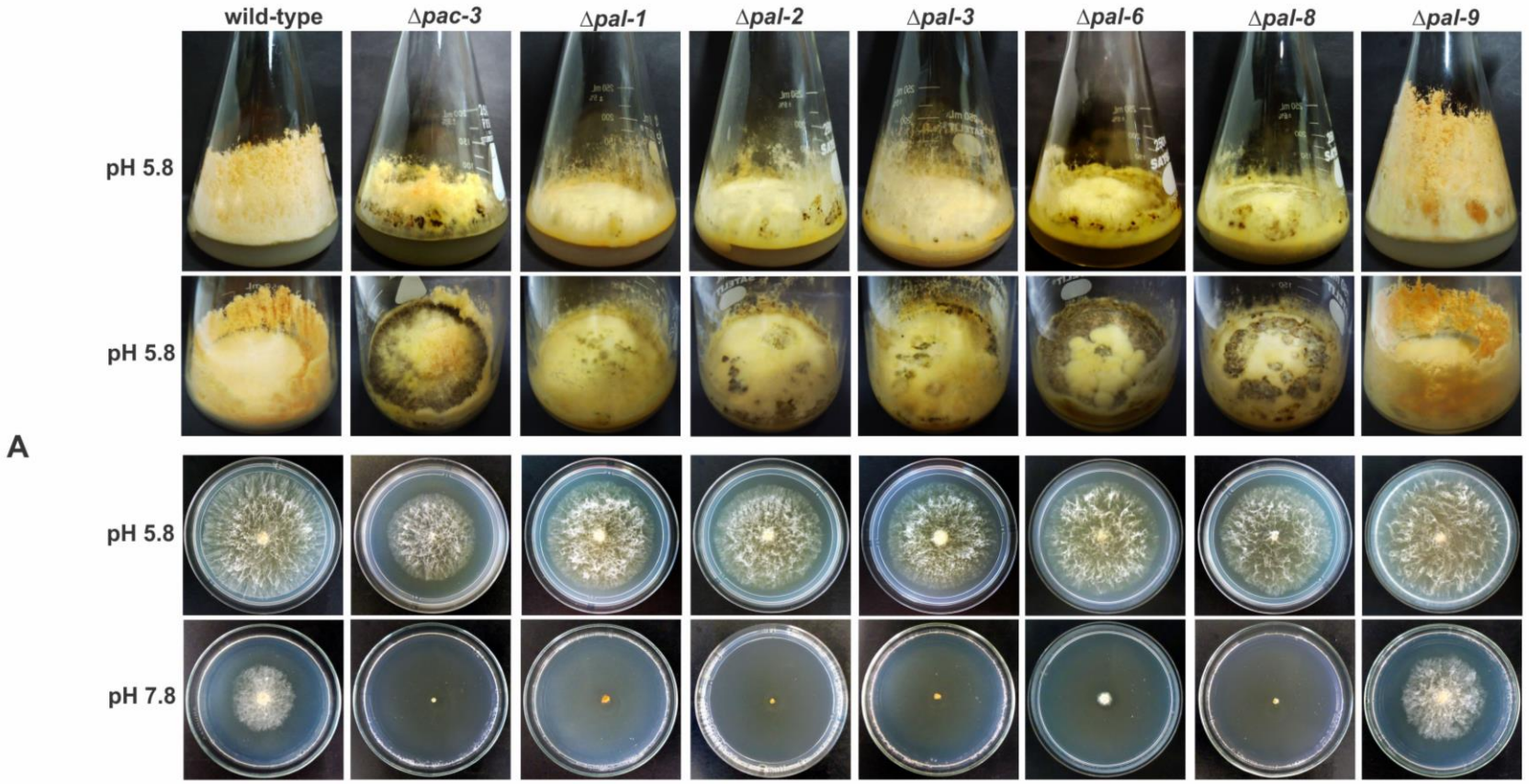

B

Apical extension at different pH[a]

	wild-type	Δpac-3	Δpal-1	Δpal-2	Δpal-3	Δpal-6	Δpal-8	Δpal-9
pH 5.8	8.0 ± 0.32	5.2 ± 0.07 *	6.2 ± 0.47 *	6.5 ± 0.14 *	6.2 ± 0.28 *	7.0 ± 0.14 *	6.9 ± 0.28 *	8.5 ± 0.40
pH 7.8	4.5 ± 0.29	0.7± 0.21 *	0.8 ± 0.28 *	0.7 ± 0.35 *	0.5 ± 0.14 *	1.1 ± 0.07 *	0.8 ± 0.07 *	5.0 ± 0.38

a. Apical extension of basal hyphae was represented by the radial growth of the colonies (cm).

Fig 1. Morphological analyses of the *pal* mutant strains. (A) The strains (10^7 conidia/mL) were cultured in Erlenmeyer flasks containing solid VM medium plus 2% sucrose at pH 5.8 for 8-10 days. Basal hyphae growth was examined after cultivating the strains on Petri dishes containing solid VM medium plus 2% sucrose at pH 5.8 and 7.8 for 24 h at 30ºC. **(B)** Radial growth of the colonies measured in cm. The results represent at least two independent experiments. *Indicates significant difference between wild-type and mutant strains at the same pH (Student's *t*-test, $P < 0.01$).

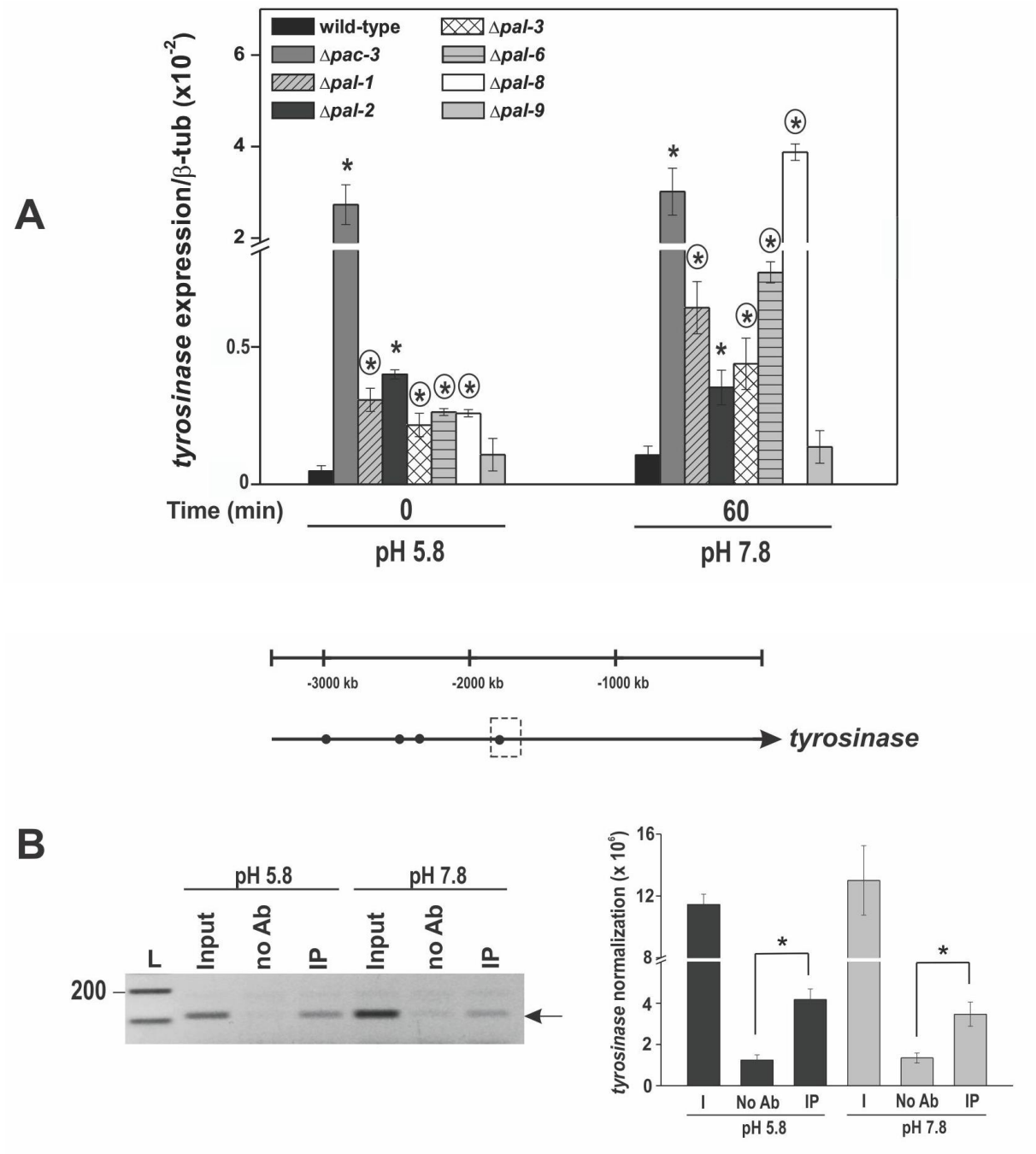

Fig 2. Expression of the tyrosinase gene in the wild-type and the Δ*pal* mutant strains at normal (5.8) and alkaline (7.8) pH. (A) Mycelial samples from the wild-type and Δ*pal* mutant strains cultured at pH 5.8 for 24 h and shifted to pH 7.8 for 1 h were used to extract total RNA. Gene expression analysis was performed by RT-qPCR on the StepOnePlus™ Real-Time PCR system (Applied Biosystems) using Power SYBR® Green and specific primers. The *tub-2* gene was used as the reference gene. The asterisks indicate significant differences compared to the wild-type strain at the same pH, and circles indicate significant differences between the same mutant strain cultured at a different pH (Student's *t*-test, $P < 0.01$). **(B)** Representation of the PAC-3 motifs (black circles) in the tyrosinase gene promoter. Dashed boxes indicate the region analyzed by ChIP-PCR. Genomic DNA samples from the Δ*pac-3* complemented strain subjected to pH stress or not were immunoprecipitated with an anti-mCherry antibody and subjected to PCR using specific primers. The input DNA (I) was used as the positive control, and the reactions without any antibody (no Ab) were used as the negative control. The intensity of the DNA bands in the gel (left side, arrow) was quantified by ImageJ and the results are shown in the right figure. L, 1 kb DNA ladder. *Asterisks indicate significant differences between the no Ab and IP samples at the same pH (Student's *t*-test, $P < 0.01$). All results represent the average of at least three independent experiments. Bars indicate the standard deviation from the biological experiments.

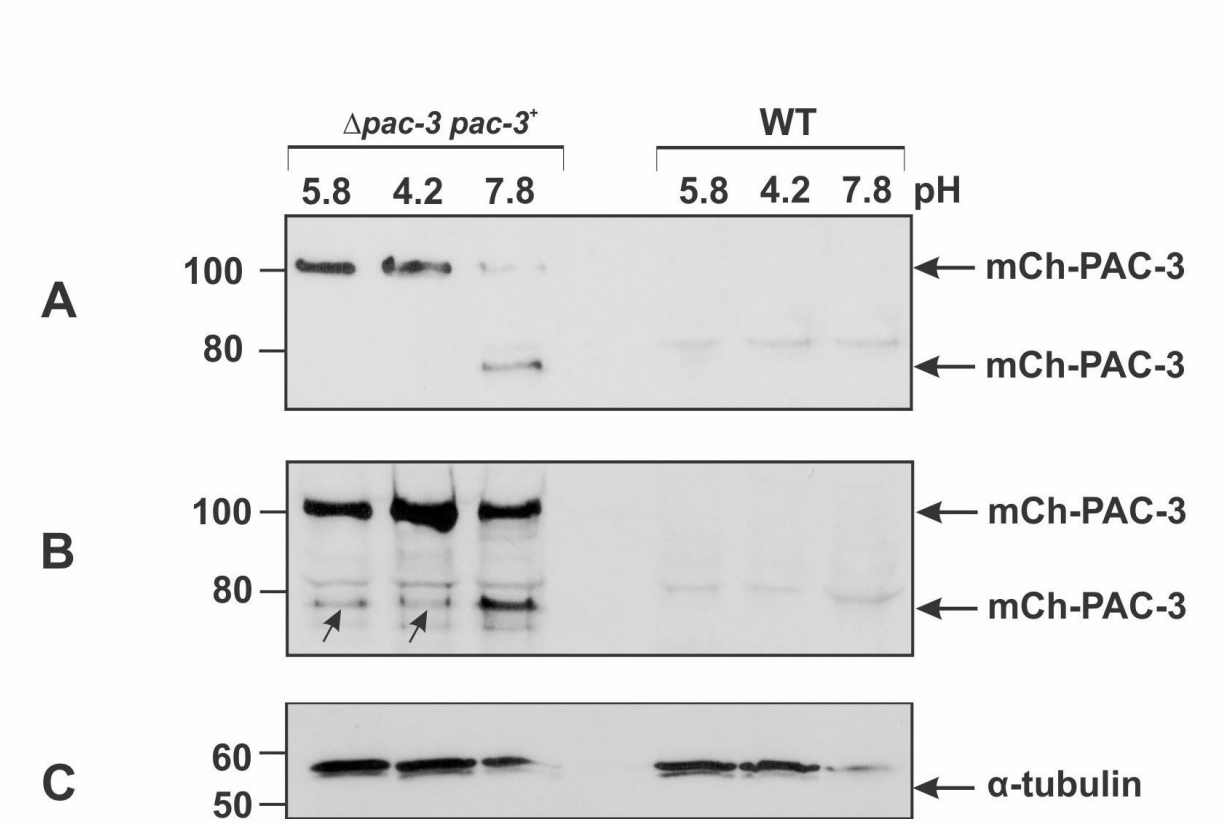

Fig 3. PAC-3 proteolytic processing at alkaline pH. PAC-3 protein levels were detected by western blot using the polyclonal anti-mCherry antibody and cell extracts from the wild-type and complemented (Δ*pac-3 pac-3*$^{+}$) strains cultivated at pH 5.8 at 30ºC for 24 h and then shifted to pH 4.2 and 7.8 at 30ºC for 1 h. **(A)** Aliquots of 50 µg of total protein were loaded onto the gel. **(B)** Aliquots of 70 µg of total protein were loaded onto the gel. The arrows indicate the processed mCh-PAC-3 form at pH 5.8 and 4.2. **(C)** The protein α-tubulin was used as the loading control. The plots represent one of the three independent experiments. The numbers on the left represent the molecular weight in kD.

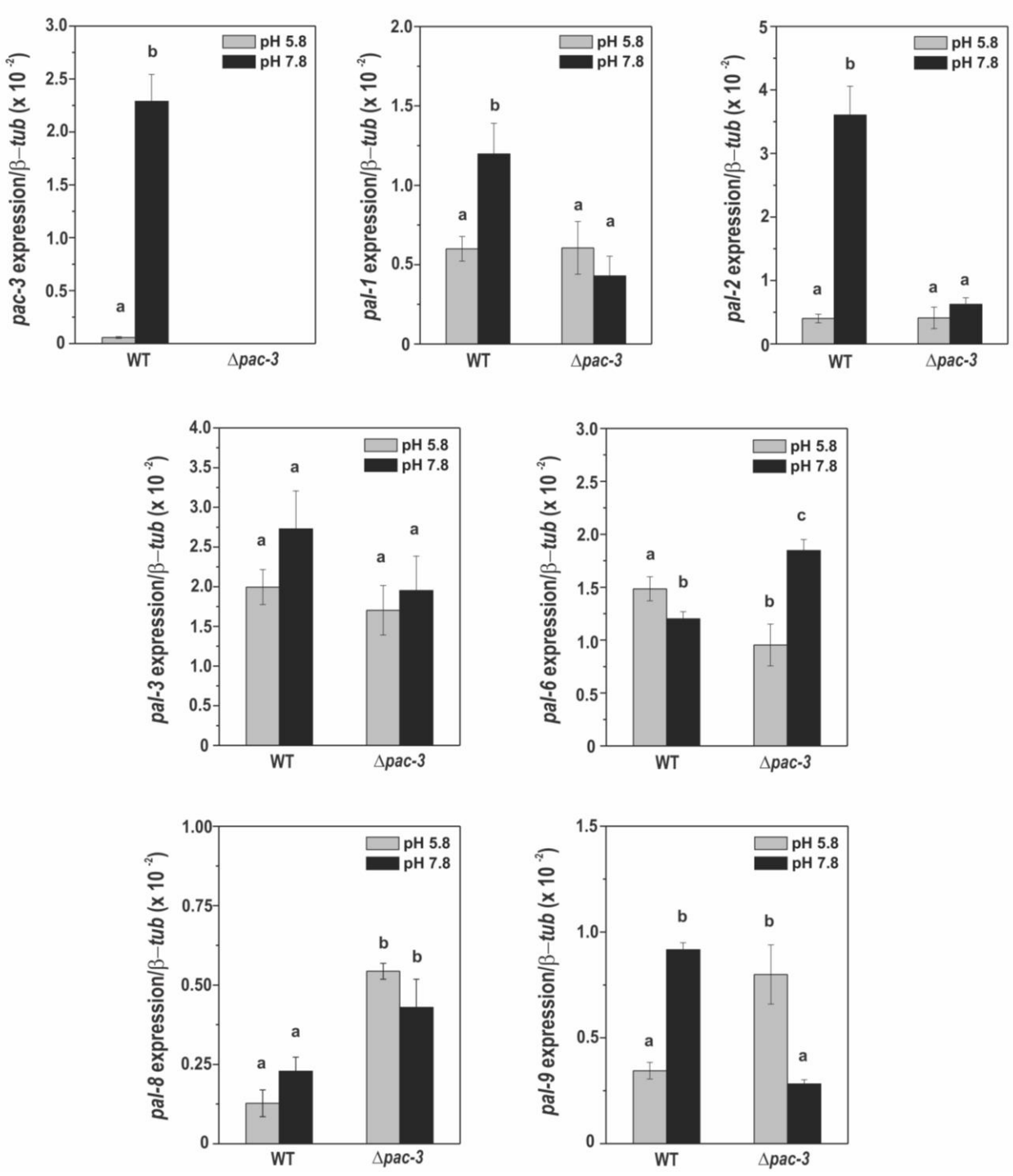

Fig 4. Expression of the *pal* genes in the wild-type and Δ*pac-3* strains at normal and alkaline pH. Cells from the wild-type and Δ*pac-3* strains were cultured at pH 5.8 for 24 h and shifted to pH 7.8 for 1 h. Mycelial samples were collected and used to extract total RNA. Gene expression analysis was performed by RT-qPCR in the StepOnePlus™ Real-Time PCR system (Applied Biosystems) using the Power SYBR® Green and specific primers. The *tub-2* gene was used as the reference gene, and the pH 5.8 wild-type was used as the reference sample. At least three biological replicates were performed, and the data were analyzed using the relative quantification standard curve method. Bars indicate the standard deviation from the biological experiments. **a, b, c:** Letters above the bars indicate statistical significance; different letters indicate significant differences between two samples and similar letters indicate no significant difference between two samples at the same or different pH (Student's *t*-test, $P < 0.01$).

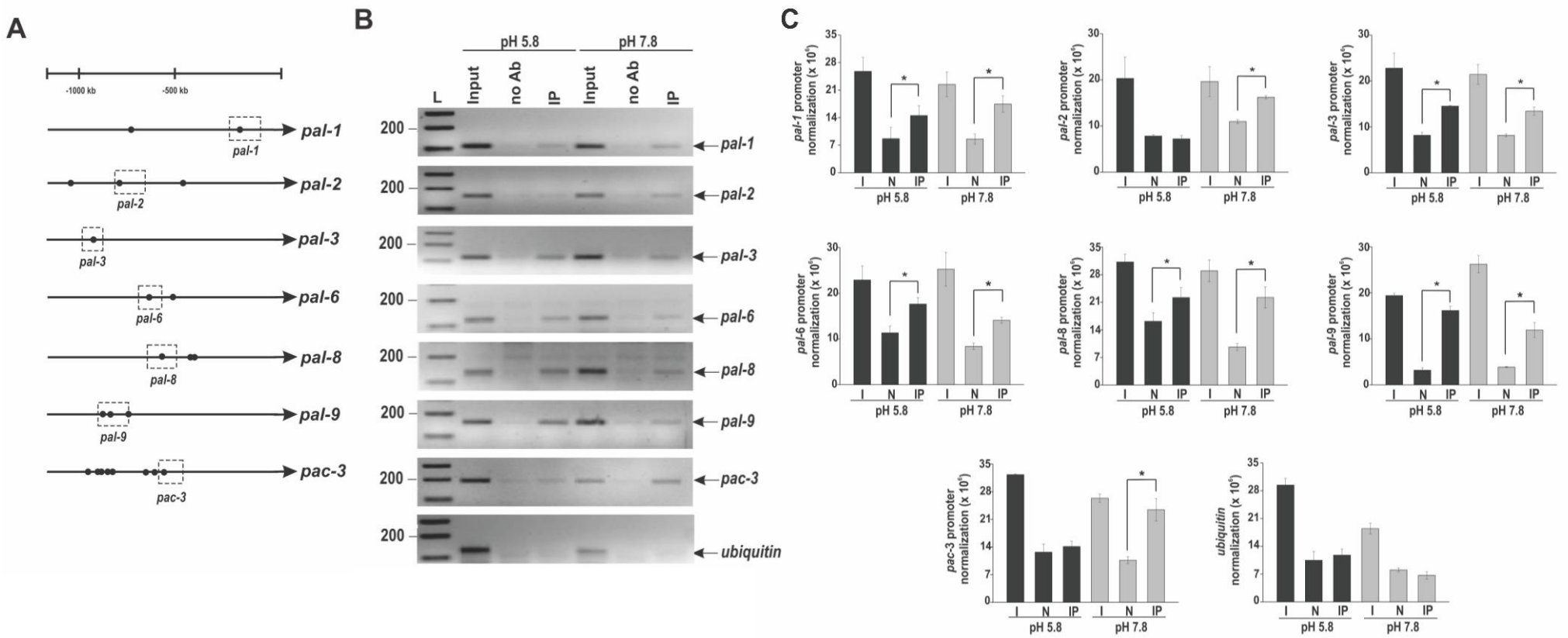

Fig 5. Binding of PAC-3 to the *pal* gene promoters at normal and alkaline pH. (A) Representation of the PAC-3 motifs in the *pal* gene promoters. The black dots indicate the position of the PAC-3 motifs, and the dashed boxes indicate regions that were analyzed by ChIP-PCR. **(B)** Genomic DNA samples from the Δ*pac-3* complemented strain both subjected to alkaline pH stress or not were immunoprecipitated with the anti-mCherry antibody and subjected to PCR to amplify DNA fragments containing the PAC-3 motif. A DNA fragment from the ubiquitin gene, which does not have a PAC-3 motif, was used as a negative control of binding. The input DNA (I) was used as a positive control and the non-immunoprecipitated reaction (no Ab) as the negative control. L, 1 kb DNA ladder. **(C)** The DNA bands after ChIP-PCR were quantified by ImageJ and the results are shown in the graphs. *Asterisks indicate significant differences between no Ab and IP at the same pH (Student's *t*-test, $P < 0.01$). All results represent the average of at least two independent experiments. Bars indicate the standard deviation from the biological experiments.

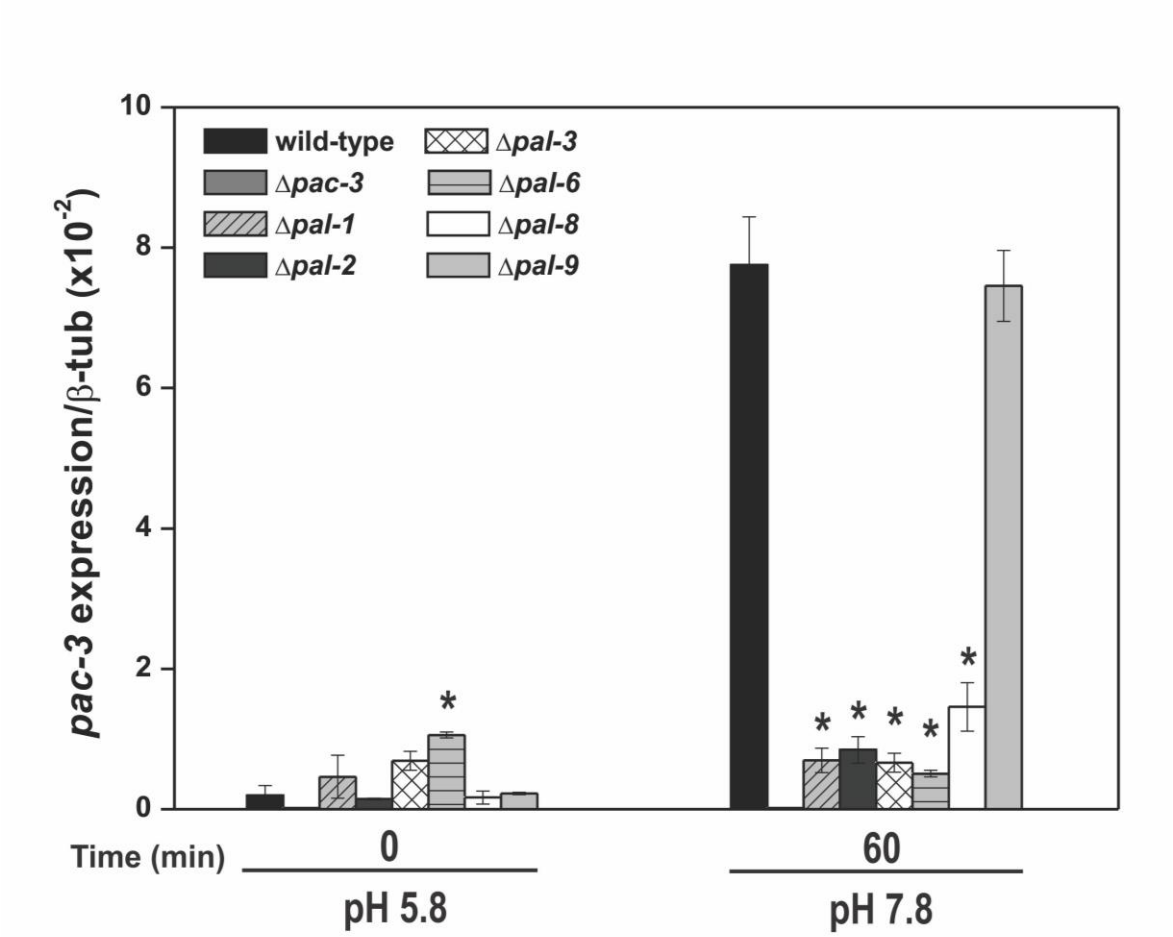

Fig 6. The expression of the *pac-3* gene at normal and alkaline pH. Samples from the wild-type and from all *pal* mutant strains cultured at pH 5.8 for 24 h and then shifted to pH 7.8 for 1 h were used to extract total RNA. Gene expression analysis was performed by RT-qPCR in the StepOnePlus™ Real-Time PCR system (Applied Biosystems) using the Power SYBR® Green and specific primers. At least three biological replicates were carried out, and the data were analyzed using the relative quantification standard curve method. Bars indicate the standard deviation from the biological experiments. The *tub-2* gene was used as the reference gene, and the pH 5.8 wild-type was used as the reference sample. *Asterisks indicate significant differences compared to the wild-type at the same pH (Student's *t*-test, $P < 0.01$).

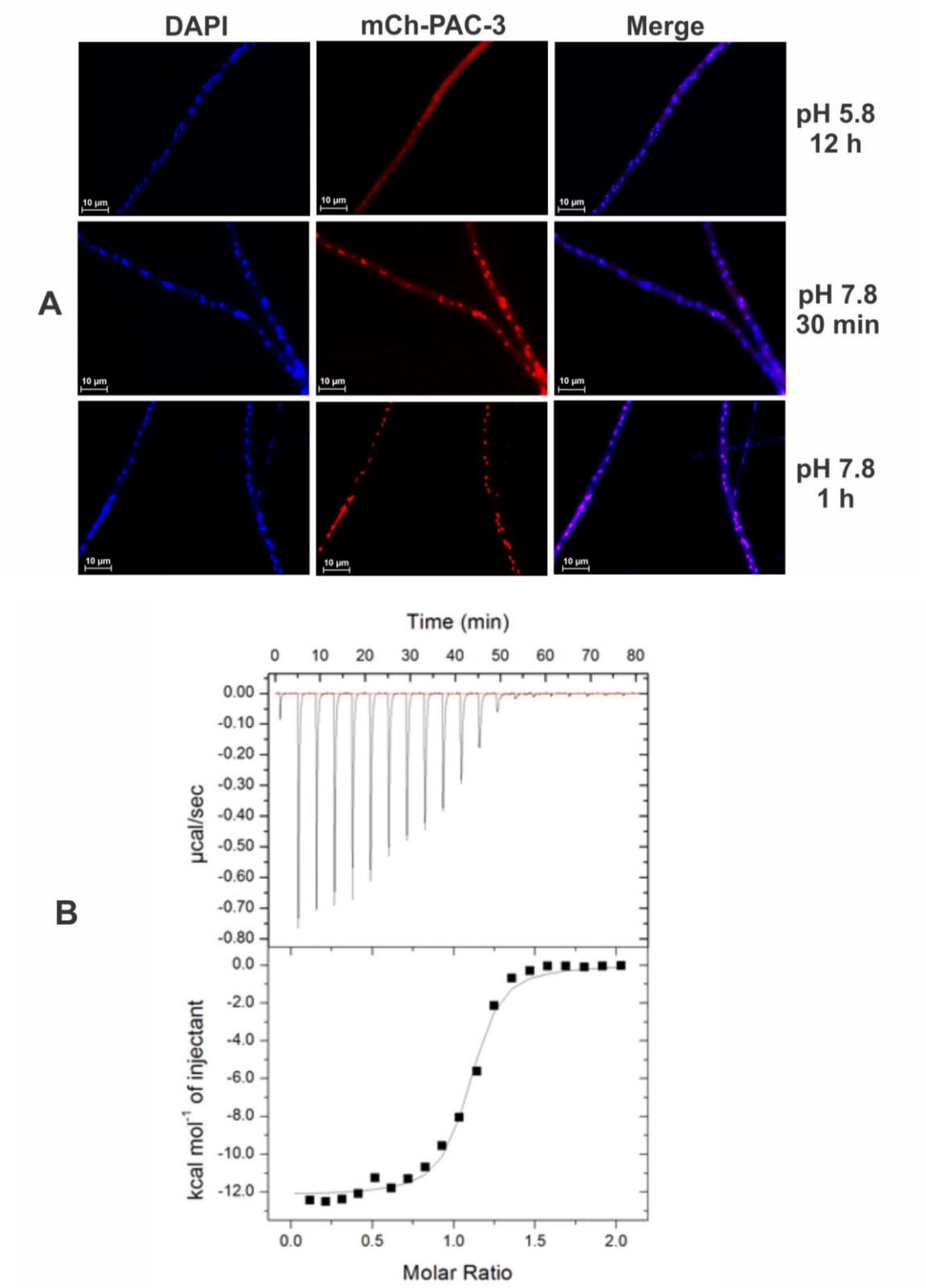

Fig 7. Subcellular localization of PAC-3. (A) The PAC-3 protein translocates to the nucleus at alkaline pH. Conidia from the Δ*pac-3* complemented strain were grown onto coverslips in liquid VM medium containing 1% sucrose, pH 5.8 at 30ºC for 12 h. After this period, mycelia were transferred to VM medium containing 1% sucrose, pH 7.8 at 30ºC (alkaline pH) for 30 min and 1 h. The mycelia were fixed with formaldehyde in PBS, the nuclei were stained with DAPI, and the fluorescence was visualized. Fluorescence was evaluated using the microscope AXIO Imager.A2 (Zeiss) at a magnification of 100 X. The results from one of three independent experiments are shown. **(B)** Isothermal Titration Calorimetry analysis of the PAC-3 NLS peptide binding to importin-α at 20ºC. The upper panel corresponds to the thermogram of the replicate titrations (thermal power as a function of time). The lower panel displays the binding isotherm integrated data (kcal mol^{-1} of injectant versus molar ratio of PAC-3 NLS to importin-α).

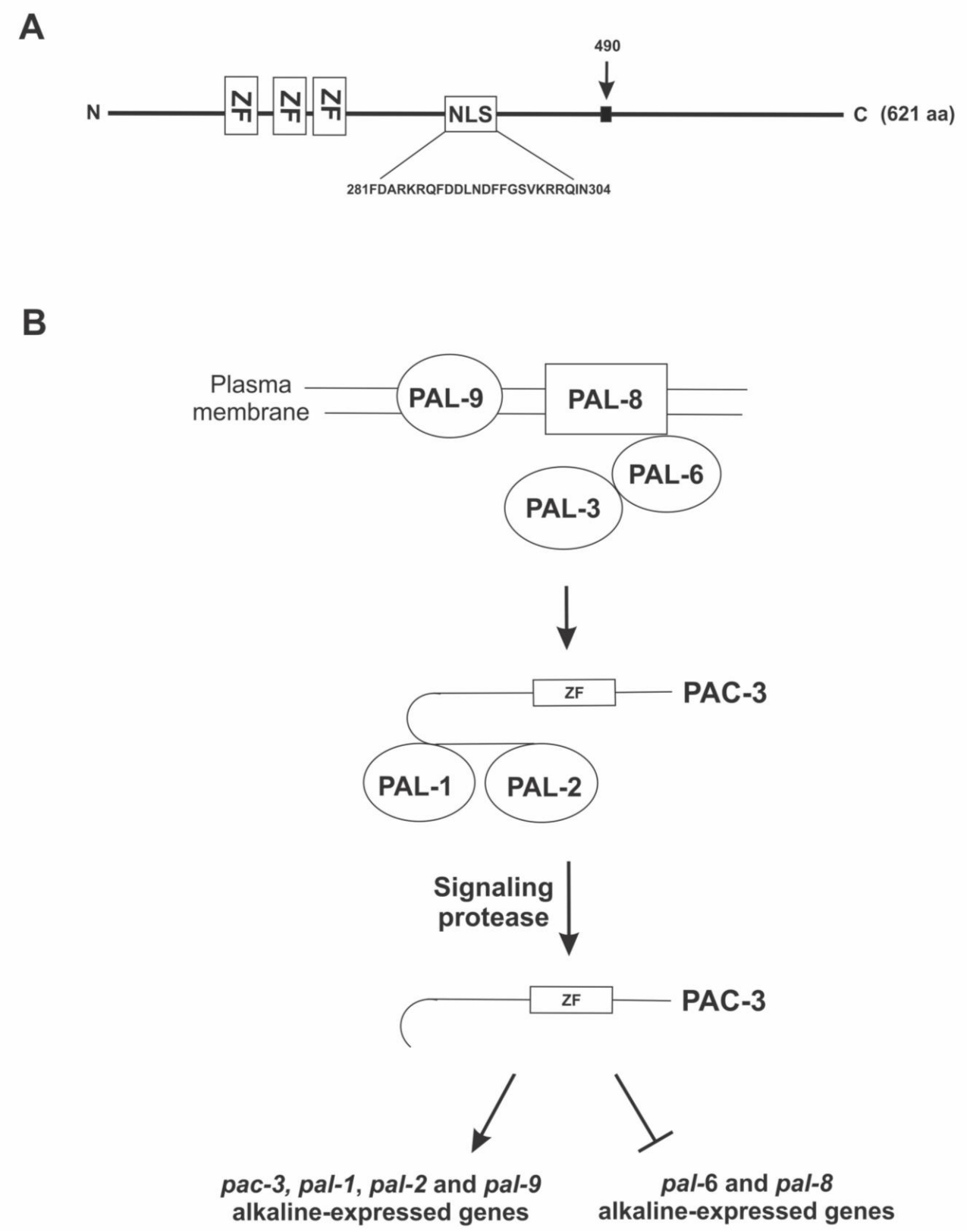

Fig 8. Proposed model for the alkaline pH signaling in *N. crassa*. (A) The PAC-3 protein contains 621 amino acid residues and has three C_2H_2 zinc-finger domains encompassing the amino acid from 95 to 183. The NLS sequence is shown between amino acid residues 281 and 304. The black arrow indicates the putative protease-processing site at amino acid 490. **(B)** *N. crassa* has the six *A. nidulans* Pal homologues. External pH signaling may involve the PAL-8, PAL-9, PAL-6 and PAL-3 complex. PAL-1 may act together with PAL-2 and may recruit the PAC-3 protein. PAC-3 undergoes only one proteolytic processing and is likely involved in the activation of the *pal-1*, *pal-2*, *pal-9,* and *pac-3* genes and the repression of the *pal-6* and *pal-8* genes at alkaline conditions. aa, amino acid; ZF, C_2H_2 zinc finger; NLS, nuclear localization signal.

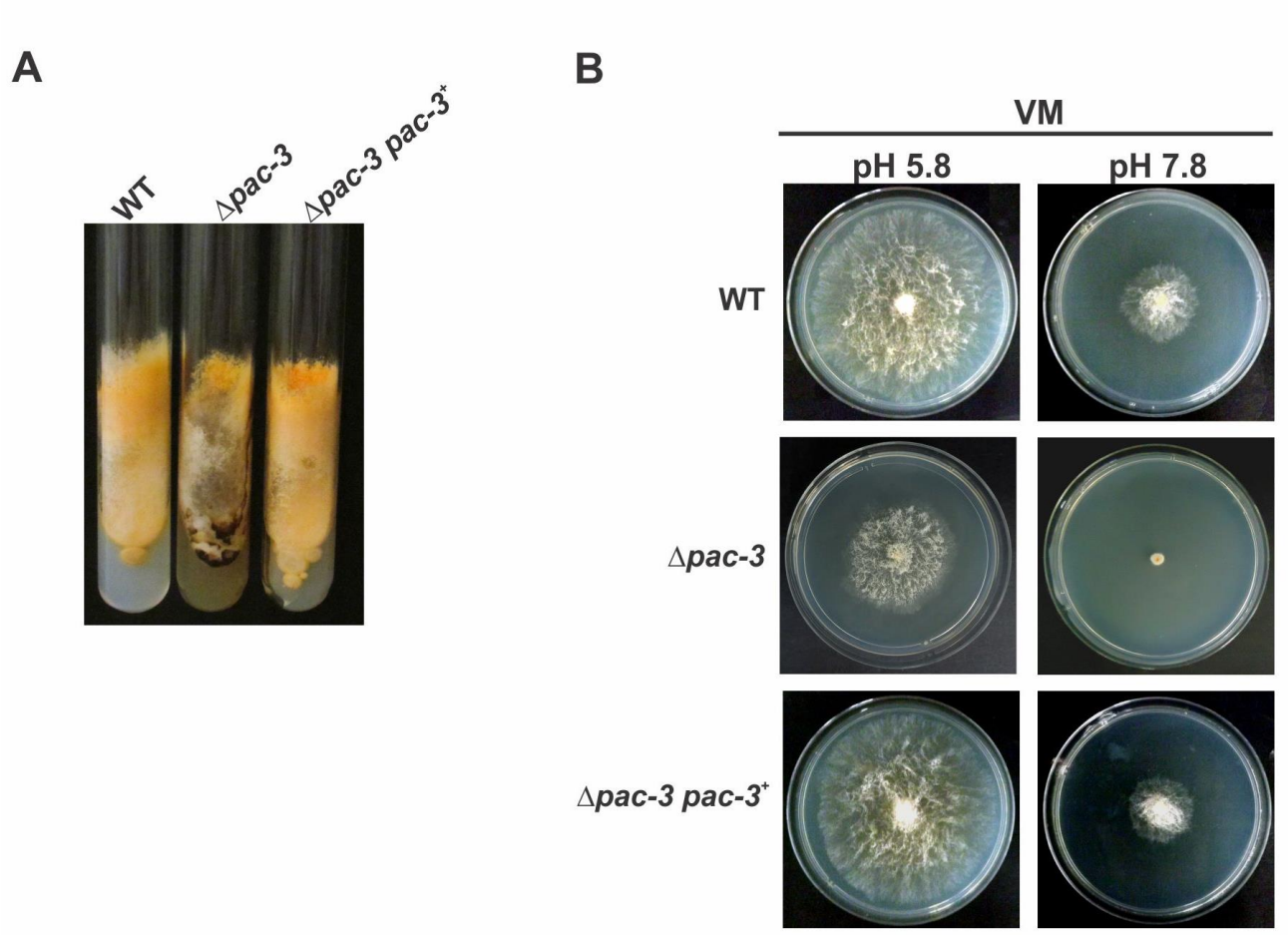

S1 Fig. Morphological analysis of the Δ*pac-3* complemented strain. (A) Growth of the wild-type, Δ*pac-3* and Δ*pac-3* complemented (Δ*pac-3 pac-3*$^{+}$) strains in tubes containing solid VM medium plus 2% sucrose at pH 5.8. **(B)** Growth of the same strains in Petri dishes containing solid VM medium plus 2% sucrose at pH 5.8 and 7.8 for 24 h.

S1 Table. Protein family or domain classification, annotation, biochemistry and structural characteristics of the proteins[a].

FGSC#	Mating type	ORF	Protein family or domain	Theoretical MW/pI	Annotation of orthologs	Gene names in *N. crassa*[b]	Gene names in *N. crassa*[c]
21931	a	NCU05876	BRO-1 and ALIX V	96.9/6.29	pH-response regulator protein PalA/Rim20	*prr-1*	*pal-1*
15867	A	NCU00317	Peptidase C2 and Calpain III	101.46/5.93	calpain signaling protease PalB/Rim13	*cpr-8*	*pal-2*
16419	a	NCU03316	BRO-1	53.45/6.77	pH-response regulator protein PalC/YGR122W	*prr-2*	*pal-3*
22412	a	NCU03021	Arrestin	102.83/5.69	pH-response regulator protein PalF/Rim8	*prr-3*	*pal-6*
16099	a	NCU00007	PalH	83.99/9.09	pH-response regulator protein PalH/Rim21	*prr-4*	*pal-8*
13378	a	NCU01996	SUR7/PalI	73.56/8.99	pH-response regulator protein PalI/Rim9	*prr-5*	*pal-9*
	a	NCU00090	C_2H_2 zinc finger	67.3/7.19	pH-response transcription factor PacC/Rim101	*pacc-1*	*pac-3*[d]

[a]The identification of each strain was made according to the Fungal Genetics Stock Center (www.fgsc.net) number. Theoretical estimative of physical and chemical characteristics was performed according to ProtPAram tools (www.expasy.org/tools/protpar-ref.html). The protein family or domains were classified according to Pfam 28.0 (pfam.sanger.ac.uk). MW, molecular weight; pI, isoeletric point. Annotation of ortholog proteins in *Aspergillus nidulans* and *Saccharomyces cerevisiae*, respectively.

[b]Nomenclature proposed by Alan Radford (http://www.bioinf.leeds.ac.uk/~gen6ar/newgenelist/genes/browse.html)

[c]Nomenclature proposed in this work based on the nomenclature proposed by Perkins et al. [39].

[d]The construction of the knockout strain was described in Cupertino et al. [23]. The gene was named as *pacC;* we renamed here as *pac-3* gene according to the *Neurospora crassa* nomenclature [39].

S2 Table. Oligonucleotides used in this study.

Primer	Sequence[a] (5'→3')	Source	Name	Position[b]
Δpac-3 complementation				
N-mChPACC-F	GCACTAGT**GGAGGAGGAGGAGG AGGA**ATGTCGTCCACACCAGCCC	NCU00090	-	+1 to +19
N-mChPACC-R	CTAGTCTAGATTAGTTGATGCGAG GAAGAAC	NCU00090	-	+2021 to +2041
Real-time PCR				
tyrosinase_F	CGACGAGTATAATCTGGAGGA	NCU00776	-	+2044 to +2064
tyrosinase_R	CTGGCGAGAGTAATGTGG	NCU00776	-	+2126 to +2143
qPac3-F	CAAGCATCGACCCGTATCAT	NCU00090	-	+1377 to +1396
qPac3-R	TGGTGAGTGACCCGAAGTA	NCU00090	-	+1486 to +1504
qPal1-F	CTGGATGCGGCCTATTACAA	NCU05876	-	+2065 to +2084
qPal1-R	CCCTCCACTGTTCTACAATCTG	NCU05876	-	+2143 to +2164
qPal2-F	GGGATTGGAGGTGGACATATAC	NCU00317	-	+2719 to +2740
qPal2-R	CTCCCTCGTTCTTAAACCTAGAC	NCU00317	-	+2804 to +2826
qPal3-F	GGCGATTGCTTGGTTGAATG	NCU03316	-	+981 to +1000
qPal3-R	AACCTCCGCTCCTCTTACT	NCU03316	-	+1048 to +1066
qPal6-F	GAAGATTATCACGGTGGTGGAT	NCU03021	-	+2639 to +2660
qPal6-R	GACCCAGGGCGATGATTATT	NCU03021	-	+2744 to +2763
qPal8-F	ATGGCACGCACTTACACCAACA	NCU00007	-	+1725 to +1746
qPal8-R	TTGCTGCGAACTCCTCAACT	NCU00007	-	+1836 to +1855
qPal9-F	AAGAAGGGCCCAACGACGTTTA	NCU01996	-	+1696 to +1717
qPal9-R	AATCACTGGCCACTGTAGCTGT	NCU01996	-	+1812 to +1833
4054Tub-F	CCTCCACCTTCGTCGGTAACTCC	NCU04054	-	+1669 to +1691
4054Tub-R	GGTACTGCTGGTACTCGGAGACG	NCU04054	-	+1832 to +1854
ChIP-PCR				
pal1p-F	GCATTCGTACCTCTACCCACCG	p*pal-1*	*pal-1* (129 bp)	-247 to -226
pal1p-R	TGACATCAATCAACCACCAGCCC	p*pal-1*	*pal-1* (129 bp)	-141 to -119
pal2p-F	CCAACGACGTTTACGTGCCGCC	p*pal-2*	*pal-2* (162 bp)	-794 to -775
pal2p-R	CAGTGTCGGTGGAGATTCTGGC	p*pal-2*	*pal-2* (162 bp)	-654 to -633
pal3p-F	GAGGAGGATAGTCGAGACCCCAC	p*pal-3*	*pal-3* (119 bp)	-963 to -941
pal3p-R	ACCACCTCTGTTTGGCGACTAC	p*pal-3*	*pal-3* (119 bp)	-866 to -845
pal6p-F	CTTCCCTTTCTCCTCCACCGTC	p*pal-6*	*pal-6* (121 bp)	-691 to -670
pal6p-R	TGGACAAGCAAGGCCTGGA	p*pal-6*	*pal-6* (121 bp)	-589 to -571
pal8p-F	GTTCCCTCGACCACTTCCCA	p*pal-8*	*pal-8* (135 bp)	-662 to -643
pal8p-R	GGGAATATTGCGCCGCGG	p*pal-8*	*pal-8* (135 bp)	-545 to -528
pal9p-F	CTCCTCCATCTGCCCTTTCCAA	p*pal-9*	*pal-9* (159 bp)	-914 to -893
pal9p-R	CCAAGATTACAGCCGGGAGTGG	p*pal-9*	*pal-9* (159 bp)	-777 to -756
pac3p-F	GCTGCCAAGTCTTTTCGCCAG	p*pac-3*	*pac-3* (196 bp)	-617 to -597
pac3p-R	CGCGCGCAGGAAGAATCG	p*pac-3*	*pac-3* (196 bp)	-439 to -422
tyrp-F	TTTAGCGCCCGGTGTCCA	ptyrosinase	tyrosinase (111 bp)	-1852 to -1835
tyrp-R	ACAAGTAGTCCCGATCCGTGG	ptyrosinase	tyrosinase (111 bp)	-1762 to -1742
qUbi-F	CGAGTCTTCGGATACGATTG	*ubiquitin* gene	*ubiquitin* (108 bp)	+805 to +824
qUbi-R	CCATCCTCCAACTGCTTAC	*ubiquitin* gene	*ubiquitin* (108 bp)	+894 to +912

[a]The *Spe*I and *Xba*I restriction sites are underlined in the N-mChPACC-F and N-mChPACC-R sequences, respectively. The nucleotides in bold in the oligonucleotides N-mChPACC-F represent the nucleotide sequence encoding for 6-Gly.

[b]The DNA oligonucleotides are positioned according to the gene ATG start site from genomic DNA.

Chapter 3

Chapter 3: Effects of alkaline pH and calcium concentration on glycogen and trehalose metabolism regulation by PAC-3

In this chapter, we investigated the role of the PAC-3 transcription factor and the PAL components of the pH signaling in other biological processes, such as glycogen and trehalose metabolism regulation under alkaline pH and calcium stresses. We described here that *pac-3* and most of *pal* mutants showed higher glycogen and trehalose accumulation than wild-type cells under normal and alkaline pH. This result suggests that PAC-3 is a repressor of glycogen and trehalose accumulation. PAC-3 bound *in vivo* to promoters of genes involved in glycogen and trehalose synthesis and degradation, and the binding was responsible for the pH-dependent changes in gene expression. The *pac-3* mutant showed high growth under calcium stress compared to wild-type cells and gene expression was induced in the presence of Ca^{2+}. We also analyzed glycogen and trehalose accumulation under calcium stress, and the results showed that the accumulation was influenced by the presence of calcium. Finally, some glycogenic and trehalose genes were differently regulated by PAC-3 in the presence of low and high calcium concentration. Our data suggest that PAC-3 likely connects pH and the calcium signaling pathway in the regulation of the reserve carbohydrates metabolism in *N. crassa*.

This is a manuscript in preparation.

Observation: According to “Alterações das Normas Internas para a defesa da Dissertação de Mestrado ou da Tese de Doutorado, aprovadas pelo Conselho de Pós-Graduação em Biotecnologia do Instituto de Química, UNESP, Araraquara, em nov/2010 e pela Congregração em reunião de dez/2010” (Appendix), the results are presented in chapter format similar to a manuscript.

Regulation of the reserve carbohydrate metabolism by alkaline pH and calcium in *Neurospora crassa* reveals a possible cross-regulation of both signaling pathways

Authors' names: Stela Virgilio, Fernanda Barbosa Cupertino and Maria Célia Bertolini*

Address: Departamento de Bioquímica e Tecnologia Química, Instituto de Química, UNESP, Universidade Estadual Paulista, 14800-060, Araraquara, SP, Brazil

Short title: Reserve carbohydrate regulation by pH and calcium

Keywords: PAC-3, glycogen, trehalose, gene expression, calcium

***Corresponding author:** Maria Célia Bertolini

Instituto de Química, UNESP

Departamento de Bioquimica e Tecnologia Química

R. Prof. Francisco Degni, 55

14,800-060, Araraquara, São Paulo, Brazil

Phone: +55-16-33019675

Fax: +55-16-33222308

e-mail: mcbertol@iq.unesp.br

INTRODUCTION

Glycogen and trehalose are storage carbohydrates found in many microorganisms and their contents vary dynamically, not only in response to changes in environmental conditions, but also throughout their life cycle. Glycogen is a polymer of glucose linked by α-1,4-linear and α-1,6-branched glycosidic bonds, while trehalose is a disaccharide consisting of two units of glucose linked by α-1,1-glycosidic bonds. The filamentous fungus *Neurospora crassa* accumulates glycogen during exponential growth and degrades it when its growth rate decreases (de Paula *et al.*, 2002). Trehalose is highly accumulated in sexual spores, accounting for up to 14% of their dry weight (Hecker and Sussman, 1973). While glycogen functions as a carbon source and energy reserve, trehalose appears to be mainly involved in stress protection in yeast and filamentous fungi (reviewed in Wiemken, 1990 and *Jorge et al.*, 1997).

In eukaryotic cells, glycogen is synthesized by the action of the enzymes glycogenin, glycogen synthase, and branching enzyme, while its degradation requires glycogen phosphorylase and debranching enzyme (Roach *et al.*, 2001). Glycogen synthase and glycogen phosphorylase are regulated by reversible covalent modification, such that phosphorylation activates glycogen phosphorylase and inhibits glycogen synthase (Téllez-Iñón *et al.*, 1969; Fletterick and Madsen, 1980). These two enzymes are also regulated by allosterism, such that glucose-6-phosphate and adenosine monophosphate modulate glycogen synthase and glycogen phosphorylase, respectively.

Trehalose, on the other hand, is synthesized by a large complex consisting of trehalose-phosphate synthase and trehalose-phosphate phosphatase subunits (Bell *et al.*, 1998) and is hydrolyzed by two unrelated trehalases, which differ in their optimal pH, localization and regulation. The acid trehalase (also referred to as nonregulatory trehalase) is a vacuolar enzyme, while the neutral trehalase (also referred to as regulatory trehalase) is cytosolic and is specifically phosphorylated by the cAMP-dependent protein kinase PKA (Thevelein, 1984; reviewed in Jorge *et al.*, 1997). In *N. crassa*, both glycogen and trehalose contents vary under heat shock; glycogen is degraded under heat stress, while trehalose accumulates under such condition (Noventa-Jordão *et al.*, 1996; de Paula *et al.*, 2002).

We have been studying the molecular mechanisms involved in glycogen and trehalose metabolism regulation in *N. crassa* under different conditions (Freitas and Bertolini, 2004; Cupertino *et al.*, 2012; Cupertino *et al.*, 2015; Freitas *et al.*, 2016). Using a collection of N. crassa mutant strains in transcription factors, we identified PAC-3 as a transcription factor likely involved in glycogen metabolism regulation (Gonçalves *et al.*, 2011). Further investigation showed that PAC-3 down regulates the expression of the *gsn* gene under alkaline pH, which is the gene encoding glycogen synthase, the regulatory enzyme in glycogen synthesis. This is consistent with the low glycogen accumulation under the same condition (Cupertino *et al.*, 2012). The *Saccharomyces cerevisiae* GSY1 orthologous gene is also repressed under alkaline stress (Serrano *et al.*, 2002). PAC-3 is the *Aspergillus nidulans* and *S. cerevisiae* PacC/Rim101p homolog, respectively, which are the central regulators of the pH signaling pathway mediated by a gene cascade responsive to alkaline pH (reviewed in Peñalva *et al.*, 2008 and Serra-Cardona *et al.*, 2015). In yeast, response to high pH also involves the signaling pathway mediated by the protein phosphatase calcineurin, which is triggered by an increase in cytosolic calcium. Calcineurin dephosphorylates the Crz1 transcription factor, which migrates to the nucleus leading to the regulation of calcium-responsive genes. Alkali-regulated genes were also described to be dependent on calcineurin in *S. cerevisiae* showing that the signaling pathway triggered by calcium can be involved in the pH response (Serrano *et al.*, 2002; Viladevall *et al.*, 2004). Recently, many genes responsive to pH stress were identified as targets of Crz1 in yeast, and among them there were genes related to glucose utilization, which includes those involved in glycogen and trehalose metabolism (Roque *et al.*, 2016).

In this work, we investigated in *N. crassa* the regulation of glycogen and trehalose metabolism by alkaline pH and calcium stresses, and we demonstrated that the accumulation of both reserve carbohydrates is modulated under both conditions. The expression of most genes encoding enzymes involved in the carbohydrate synthesis and degradation is regulated by alkaline pH and most gene promoters are bound by the PAC-3 transcription factor. We also showed that Ca^{2+} induces the expression of *pac-3* and of some genes involved in glycogen and trehalose metabolism in a wild-type strain. Additionally, glycogen and trehalose accumulation is differently regulated under low (10 mM) and high (300 mM) calcium concentration and is PAC-3-dependent. These data suggest a cross regulation

between the pH and calcium signaling pathways regarding the control of the reserve carbohydrates metabolism in *N. crassa*, which may be mediated by the PAC-3 transcription factor.

MATERIALS AND METHODS

Neurospora crassa strains and growth conditions

Neurospora crassa FGSC#9718 (*mus-51*::*bar*), used as wild-type strain, and the FGSC#21931 (Δ*pal-1*, NCU 05876), FGSC#15867 (Δ*pal-2*, NCU00317), FGSC#16419 (Δ*pal-3*, NCU03316), FGSC#22412 (Δ*pal-6*, NCU03021), FGSC#16099 (Δ*pal-8*, NCU00007), and FGSC#13378 (Δ*pal-9*, NCU01996) mutant strains were purchased from the Fungal Genetics Stock Center (FGSC, University of Missouri, Kansas City, MO, USA, http://www.fgsc.net) (McCluskey, 2003). The Δ*pac-3* strain (NCU00090) was generated as described in Cupertino *et al.* (2012) and the Δ*pac-3 pac-3*$^{+}$ complemented strain was constructed as described in Virgilio *et al.* (2016). The characteristics of all mutant strains and the gene and protein data were described in Virgilio *et al.* (2016). All strains were maintained on solid Vogel's minimal (VM) medium, pH 5.8 (Vogel, 1956) containing 2% sucrose at 30ºC. Conidia from 10-day old culture of wild-type, mutant, and complemented strains were suspended in sterile water and counted. For radial growth analyses, 10^7 conidia ml^{-1} were inoculated onto Petri dishes containing solid VM medium plus 2% sucrose either under different pH or different concentration of Ca^{2+} with or without cyclosporin A (Sigma) at 30ºC. Images of colony morphology were captured after 24 h of growth.

For pH and calcium stresses, 10^9 conidia ml^{-1} were first germinated in 1 l of VM medium containing 2% sucrose, pH 5.8 (time zero), at 30ºC, 200 rpm, for 24 h. After this period, the culture was filtered and the mycelia were divided in samples. One was frozen in liquid nitrogen and stored at -80ºC for further processing (control sample, not subjected to stress), while the remaining samples were individually transferred into 500 ml of fresh VM medium containing 0.5% sucrose at pH 7.8 (for alkaline pH stress) and 10 and 300 mM of $CaCl_2$ (for calcium stress). Samples were harvested after 15, 30 and 60 min incubation and stored at -80ºC. The mycelia samples were used for glycogen and trehalose quantification and RNA extraction.

Glycogen, trehalose and protein quantification

Mycelia pads were extracted in lysis buffer (50 mM Tris-HCl, pH 8.0, 50 mM NaF, 1 mM EDTA, 0.5 mM PMSF, 0.1 mM TCLK, 25 mM benzamidine, and 1 µg/mL of each pepstatin and aprotinin). Cellular extracts were clarified and the supernatants were used for glycogen, trehalose and protein quantification. Glycogen content was quantified according to Freitas *et al.* (2010) and trehalose was quantified following the protocol described by Neves *et al.* (1991), with modifications. Glycogen was precipitated with cold ethanol and digested with α-amylase and amyloglucosidase and trehalose was digested with a partially purified trehalase from *Humicola grisea* (Zimmermann *et al.*, 1990). Free glucose was quantified with a glucose oxidase kit (Labtest) and glycogen and trehalose concentrations were normalized to the total protein concentration. Total protein was quantified by the Hartree (1972) method using BSA as standard.

RNA isolation and gene expression analysis

Gene expression was analyzed by RT-qPCR. Total RNA was prepared using mycelia samples according to Sokolovsky *et al.* (1990) method. RNA (10 µg) from each sample was fractionated on agarose gel to assess the rRNAs integrity. RNA samples were first treated with RQ1 RNAse-free DNAse (Promega) and subjected to cDNA synthesis using the SuperScript III First Strand Synthesis kit (Invitrogen) and oligo (dT) primer according to the manufacturer's instructions. The cDNA libraries were subjected to RT-qPCR on a StepOnePlus™Real-Time PCR System (Applied Biosystems) using the Power SYBR® Green PCR Master Mix (Applied Biosystems) and specific primers. For genes involved in glycogen metabolism, the following primers were utilized: *pac-3* (qPac3-F/qPac-3-R), *gsn* (qGSN-F/qGSN-R), *gbn* (qRAMIF-F/qRAMIF-R), *gnn* (qGNN-F/qGNN-R), *gpn* (qGPN-F/qGPN-R) and *gdn* (qDESRAM-F/qDESRAM-R) amplicons (Table S1). For genes involved in trehalose metabolism, the following primers were utilized: *tps-1* (qtps1-F/qtps1-R), *tps-1α* (qtps1alfa-F/qtps1alfa-R), *tps-2* (qtps2-F/qtps2-R), *tre-1* (qtre1-F/qtre1-R) and *tre-2* (qtre2-F/ qtre2-R) amplicons (Table S1).

Reactions were performed under the following conditions: 95ºC for 10 min, 40 cycles of 95ºC for 15 s, 60ºC for 1 min to calculate cycle threshold (Ct) values,

followed by 95ºC for 15 s, 60ºC for 1 min and then 95ºC for 15 s to obtain melt curves. Data analysis was performed by the StepOne Software (Applied Biosystems) using the Comparative CT (ΔΔCT) method (Livak and Schmittgen, 2001). At least four biological replicates, with three experimental replicates per sample were performed, and reactions with non-template were used as a negative control. The fluorescent dye ROX™ was used as the passive reference to normalize the SYBR green reporter dye fluorescent signal. The PCR products were subjected to melting curves analysis to verify the presence of single amplicons. All reaction efficiencies varied from 92 to 100%. The beta-tubulin gene (β-*tub* gene, NCU04054) was used as the reference gene in pH stress analyses and the actin gene (*act* gene, NCU04173) was used as the reference gene in calcium stress.

Chromatin immunoprecipitation-PCR assays

Chromatin immunoprecipitation assays were performed as described in Virgilio *et al.* (2016), using mycelia from the Δ*pac-3 pac-3*$^{+}$ complemented strain, anti-mCherry polyclonal antibody (BioVision) and Dynabeads Protein A (Invitrogen) for immunoprecipitation. After sonication and immunoprecipitation, the DNA was quantified and 25 ng of Input DNA (I), no Ab (N, reaction without antibody) and IP (immunoprecipitated DNA) samples were amplified by PCR using primers specific for each promoter (Table S1, ChIP-PCR). Input DNA was used as positive control of the experiment and no Ab as negative control.

PCR was performed using Phusion High-Fidelity PCR kit (Finzymes) and specific oligonucleotides for *gsn* (PacC-F/SREBP-RP2), *gpn* (pGPNNit-F2/pGPNNit-R2), *gnn* (gnnPAC3-Fp/gnnPAC3-Rp), *gbn* (branch-FP5/branch-RP5), *gdn* (DEBp-F2/DEBp-R2), *tps-1* (tresynt-Fp/tresynt-Rp), *tps-1α* (alfatre-Fp/alfatre-Rp), *tps-2* (trephosp-Fp/ trephosp-Rp), *tre-1* (tre1-Fp/tre1-Rp) and *tre-2* (tre2-Fp/tre2-Rp) promoters. A fragment of the ubiquitin gene (NCU05995), which does not have the PAC-3 motif, was amplified with the primers qUbi-F/qUbi-R and used as negative control of binding. Reactions were performed under the following conditions: 98ºC for 10 s, 25 cycles of 98ºC for 1 s, 60ºC for 5 s and 72ºC for 30 s, and then 72ºC for 5 min. The reaction products were analyzed on a 2% agarose gel and visualized by ethidium bromide. Densitometry was performed using ImageJ software (Abramoff *et al.*, 2004), and the IP signals were compared to the negative control (no Ab).

RESULTS

The pH-signaling pathway controls accumulation of the reserve carbohydrate glycogen and trehalose in N. crassa

We previously identified the PAC-3 transcription factor as a putative regulator of glycogen metabolism (Gonçalves *et al.*, 2011), and later we showed that PAC-3 is required for proper glycogen accumulation by down-regulating the expression of *gsn*, the gene encoding glycogen synthase, the regulatory enzyme in glycogen synthase (Cupertino *et al.*, 2012). To better investigate the role of the pH signaling pathway in the control of the reserve carbohydrate metabolism, we quantified the levels of glycogen and trehalose, another reserve carbohydrate, in mutant strains in each component of the pH pathway. The pH signaling pathway includes a pH sensor located in the plasma membrane, which once activated by ambient alkaline pH, recruits five downstream protein components to activate the PacC and Rim101 transcription factors in *A. nidulans* and *S. cerevisiae*, respectively. *N. crassa* shares all components (PAL proteins) with the *A. nidulans* and *S. cerevisiae* pH pathways and all of them, except PAL-9, are required for growth at alkaline pH (7.8) (Virgilio *et al.*, 2016). Here, we quantified both carbohydrates in mycelial samples from all mutant strains grown at pH 5.8 and in samples harvested at different times after shifting to pH 7.8. The pH 5.8 and 7.8 were used as normal and alkaline condition, respectively, considering the wild-type and Δ*pac-3* strains growth. The wild-type grew well under acid-to-normal condition, and reduced the growth under alkaline pH. The Δ*pac-3* mutant strain showed progressively reduction of growth at pH 4.5 until 7.3 (P <0.01) and unable to grow at pH 7.8 (Fig. S1).

The levels of both carbohydrates were significantly higher in all mutant strains at pH 5.8, with exception of the Δ*pal-9* mutant, compared to the wild-type strain (Fig. 1). These results suggest that a functional pH signaling pathway is required for proper carbohydrate accumulation at normal pH. On the other hand, transfer to alkaline pH led to a decrease in the levels of both carbohydrates and the repression was stronger regarding trehalose levels indicating that pH stress has a negative effect in the reserve carbohydrate accumulation in *N. crassa*, different from heat stress, which induces trehalose and repress the glycogen accumulation (Noventa-Jordão *et al.*, 1996; Freitas *et al.*, 2016). From these results, we observed two

independent results: the requirement of an active pH signaling pathway to maintain proper levels of the reserve carbohydrate in a pH independent manner, and the repressor effect of alkaline pH on the carbohydrate levels.

To confirm the results, we quantified the glycogen levels in the Δ*pac-3 pac-3*$^{+}$ complemented strain at pH 5.8 and after shifting the mycelia to alkaline pH for 1 h. The wild-type and the complemented strains showed similar glycogen levels (Fig. S2), indicating that pac-3 complementation rescues the wild-type phenotype.

Alkaline pH and PAC-3 modulate the expression of genes encoding enzymes of glycogen metabolism

Here we demonstrated that glycogen accumulation is modulated by the protein components of the pH signaling pathway. In addition, we broadly investigated the expression of all genes directly involved in glycogen metabolism. Gene expression of *gsn* (encodes glycogen synthase), *gbn* (encodes glycogen branching enzyme), *gnn* (encodes glycogenin), *gpn* (encodes glycogen phosphorylase), and *gdn* (encodes glycogen debranching enzyme) genes was analyzed in mycelia from Δ*pac-3* and wild-type strains grown at pH 5.8 for 24 h and in mycelia shifted to pH 7.8 for 1 h. All genes were repressed at pH 7.8, with exception of *gnn*, which was up-regulated, consistent with the repression in glycogen accumulation under the same condition (Fig. 2). In addition, expression was dependent on the PAC-3 transcription factor under normal and alkaline pH since most of genes were up-regulated in Δ*pac-3* strain at both pH, and also consistent with the higher glycogen accumulation observed in the Δ*pac-3* strain at both pH (compare with Fig. 1). These results suggest that PAC-3 acts as a repressor of glycogen accumulation by down-regulation the expression of most genes encoding the enzymes required for glycogen metabolism.

An *in silico* analysis of the promoter region of the genes involved in glycogen synthesis/degradation revealed the existence of the *N. crassa* PAC-3 DNA binding preference sequence (5'-BGCCVAGV-3') (Weirauch *et al.*, 2014) in all glycogenic promoters, except in *gpn* promoter, suggesting that PAC-3 could directly regulate the expression of these genes. A schematic representation of the gene promoters is shown in Fig. 3A. A ChIP-PCR assay was performed to analyze PAC-3 binding to DNA fragments containing some of these motifs *in vivo*. The PAC-3 motifs analyzed

are shown in dashed boxes in Fig. 3A. In these experiments, we used Δ*pac-3 pac-3*$^{+}$ complemented strain and the anti-mCherry antibody. Chromatin was collected from mycelia submitted or not to alkaline pH stress, and binding of PAC-3 to all promoters was analyzed by PCR using the oligonucleotides described in Table S1 (ChIP-PCR). As a positive control of the experiments, the input DNA (I) was analyzed, and as negative controls, a region of the *gpn* promoter, which lacks the PAC-3 motif and the non-immunoprecipitated reactions (N) were used. The DNA fragments amplified in the ChIP-PCR assays (Fig. 3B) were quantified by ImageJ and the results are shown in graphs (Fig. 3C). PAC-3 was able to significantly bind to all gene promoters containing PAC-3 motif under normal and alkaline pH (Fig. 3B and 3C, $P < 0.01$) and, surprisingly, binding seemed to be more intense at normal pH (Fig. 3C). The *gpn* promoter was not bound by PAC-3, as expected, confirming that this gene is not regulated by PAC-3 at alkaline pH (see Fig. 2). Although the expression of the *gnn* gene was not influenced by PAC-3 under pH 7.8 (Fig. 2), the transcription factor bound to its gene promoter under both conditions (Fig. 3C). In this case, PAC-3 could to bind to the promoter although but not to influence its expression.

Binding of PAC-3 to gene promoters and gene expression regulation by PAC-3 at normal growth pH (5.8), suggest the existence in *N. crassa* of an active pH signaling pathway at this pH and agree with previous results showing the presence of processed, therefore active, PAC-3 transcription factor in the same pH (Virgilio *et al.*, 2016).

Alkaline pH and PAC-3 modulate the expression of genes encoding enzymes of trehalose metabolism

As the trehalose accumulation was also influenced by PAC-3 and the PAL components of the signaling pathway under normal and alkaline pH, we analyzed the expression of the genes encoding enzymes of trehalose metabolism under the same conditions. We assayed the expression of the *tps-1* (encodes trehalose phosphate synthase), *tps-1α* (encodes alpha-trehalose phosphate synthase), *tps-2* (encodes trehalose phosphatase), *tre-1* (encodes trehalase-1) and *tre-2* (encodes neutral trehalase-2) genes in mycelia samples from the wild-type and Δ*pac-3* strains grown at pH 5.8 for 24 h (control) and shifted to pH 7.8 for 1 h. We observed that only *tre-1* and *tre-2* genes, which encode enzymes involved in trehalose degradation, were

regulated by both alkaline pH and PAC-3 (Fig. 4). It is notable to observe the high expression levels of *tps-2* and *tre-2* in Δ*pac-3* strain under normal pH (Fig. 4). These results, similar to those observed for genes encoding enzymes of glycogen metabolism, show that PAC-3 and alkaline pH independently influence the glycogen and trehalose accumulation by regulating gene expression.

The existence of the PAC-3 motif in all trehalose gene promoters was also confirmed by *in silico* analysis (Fig. 5A), and binding *in vivo* to one of such motifs was investigated by ChIP-PCR using the same extracts prepared to assay the glycogen gene promoters. As a positive control, the input DNA (I) was analyzed, and as negative controls, a fragment of the ubiquitin gene lacking the PAC-3 motif and the non-immunoprecipitated reactions (N) were used. The DNA fragments amplified in the ChIP-PCR assays (Fig. 5B) were quantified by ImageJ and the results are shown in graphs (Fig. 5C). PAC-3 was able to bind significantly to *tps-1*, *tps-2* and *tre-1* gene promoters under normal and alkaline pH; however, bound to *tre-2* promoter only under normal pH (Fig. 5B and 5C). Although the expression of the *tps-1* gene was not influenced by PAC-3 under normal pH (see Fig. 4), the transcription factor bound to its gene promoter under both pH (Fig. 5C). In this case, PAC-3 was able to bind to the promoter at pH 5.8 although did not influence its expression. On the other hand, while the expression of *tre-2* was influenced by PAC-3 under both pH, PAC-3 was able to bind *in vivo* to its promoter only under normal pH (Fig. 5). Interestingly, PAC-3 was unable to bind to *tps-1α* under both pH, in agreement with the results of gene expression, which showed that the *tps-1α* expression was not regulated by the transcription factor under the same conditions (see Fig. 4).

Response to calcium stress may involve PAC-3

We described here the requirement of an active pH signaling pathway to maintain proper levels of the reserve carbohydrate and showed that their levels are decreased at alkaline pH. PAC-3 has been studied in different cellular processes and no work has reported the PAC-3 action combined with other(s) protein(s) or pathway in *N. crassa*. In *Candida albicans*, Rim101 acts in parallel to Crz1, via calcineurim, for adaptation to alkaline pH (Kullas *et al.*, 2007). In *S. cerevisiae*, the transcriptional response to alkaline pH involves different signaling mechanisms, and the calcium signaling seems have a role in this response (Serrano *et al.*, 2002). The

Rim101/PacC pathway inhibition could be used in a combinatorial approach with the calcineurin pathway inhibitors, especially in therapeutic target for combating pathogenic fungi (Kullas *et al.*, 2007). Thus, it is very interesting analyze the glycogen and trehalose metabolism regulation under calcium addition and try correlate the transcriptional response to calcium by PAC-3 in *N. crassa*.

In the first experiment, we analyze the effects of the Δ*pac-3* knockout gene in the morphology growth after calcium addition. Basal hyphae growth was examined after cultivating the wild-type, Δ*pac-3* mutant and Δ*pac-3 pac-3*$^{+}$ complemented strain on Petri dishes with 2% sucrose as the sole carbon source and different calcium concentration (0, 10, 50, 100, 200 and 300 mM final concentration) for 24 h. At concentrations of 10, 50 and 100 mM of Ca^{2+} significantly stimulated the hyphal growth of the Δ*pac-3* mutant ($P < 0.01$), however, in high concentration of Ca^{2+} (200 and 300 mM) the hyphal growth was repressed when compared to the control without addition of calcium in the Δ*pac-3* mutant (Fig. 6A). The wild-type and Δ*pac-3 pac-3*$^{+}$ complemented strain showed the same profile in presence of Ca^{2+}. In 10, 50 and 100 mM of Ca^{2+}, they showed a constant radial growth compared to the control without Ca^{2+} addition. In higher concentration of Ca^{2+} both strains showed reduced radial growth (Fig. 6A). In Fig. 6B the radial growth of the wild-type and Δ*pac-3* strain from Fig. 6A was measured and the percentage of growth was determined considering the condition without Ca^{2+} as 100% of growth. We observed that wild-type showed constant radial growth under lower calcium concentration and significantly reduced growth in 200 and 300 mM of Ca^{2+} when compared to the condition without Ca^{2+} in the same strain (asterisks indication, $P < 0.01$). However, the Δ*pac-3* mutant strain showed increased radial growth in 10, 50 and 100 mM Ca^{2+} and reduced radial growth in 300 mM of Ca^{2+} when compared to the condition without Ca^{2+} in the same strain (asterisks indication, $P < 0.01$). The circles in the Fig. 6B indicate significant differences in all calcium concentration in the Δ*pac-3* mutant strain compared to the wild-type strain at the same Ca^{2+} condition ($P < 0.01$), indicating that in all calcium addition conditions analyzed the radial growth was increased in Δ*pac-3* mutant strain.

To verify whether the stimulation or reduction of radial growth by addition of Ca^{2+} was dependent on calcineurin pathway, we analyze the radial growth of the wild-type and Δ*pac-3* mutant strain on Petri dishes with 2% sucrose and different concentration of cyclosporin A (CsA), a specific inhibitor of calcineurin, in 0, 0.1, 10 and 25 µM final concentration for 24 h. In the Fig. 6C we observed a very reduced

growth in 0.1 µM of CsA and incapacity to growth under 10 and 25 µM of CsA in both strains, suggesting that calcineurin pathway is the unique pathway in *N. crassa* involved in calcium regulation. We selected the 10 µM CsA final concentration to further experiments. Finally the radial growth of the wild-type, Δ*pac-3* mutant and Δ*pac-3 pac-3*$^{+}$ complemented strain was observed on Petri dishes with 2% sucrose with addition of 10 µM of CsA and different concentration of Ca^{2+} (0, 10, 50, 100, 200 and 300 mM). In the Fig. 6D, it is possible to see that no strains growth in presence of CsA and Ca^{2+}, showing that calcineurin inhibitors affect the growth of the strains analyzed.

Effects of Ca^{2+} on the reserve carbohydrate accumulation and the expression levels

To determine the effects of calcium on glycogen and trehalose accumulation, mycelia samples from the Δ*pac-3* mutant and wild-type strain were collected after growth in normal growth for 24 h (time 0) and after shifted the mycelia to 10 and 300 mM of Ca^{2+} for 15, 30 and 60 min. The Fig. 7 shows that the addition of 10 mM of Ca^{2+} significantly stimulated the glycogen and trehalose accumulation in 30 and 60 min of inoculation in the wild-type compared to the condition without calcium ($P < 0.01$). The trehalose levels were also up accumulated at 300 mM calcium in the wild-type strain ($P < 0.01$, Fig. 7). After calcium addition, the reserve carbohydrates accumulation was reduced (10 mM of Ca^{2+}, $P < 0.01$) in Δ*pac-3* mutant strain. In 300 mM of Ca^{2+}, glycogen down accumulated in Δ*pac-3* mutant and trehalose showed the same content when compared to the condition without calcium (Fig. 7). Our data show that PAC-3 is involved to glycogen and trehalose metabolism regulation, presented different profiles when compared to the wild-type in low and high calcium concentration. Curiously, the trehalose regulation seems to be different under alkaline and calcium stresses. Whereas the trehalose content was reduced in the wild-type strain in alkaline condition (Fig. 1), in calcium addition it was stimulated (Fig. 7).

To investigate the effects of Ca^{2+} addition and regulation by PAC-3, some genes involved in glycogen and trehalose metabolism were analyzed under calcium stress. We verified the expression of *pac-3*, *gsn*, *gdn*, *tps-1*, *tre-1* and *tre-2* genes in mycelia from ∆*pac-3* mutant and wild-type strains grown at normal growth for 24 h (time 0) and after shifted the mycelia to 10 and 300 mM of Ca^{2+} for 15, 30 and 60

min. The expression of all genes was analyzed by RT-qPCR using specific oligonucleotides described in Table S1 (qPCR). The actin gene was used as the reference gene and the wild-type sample at time 0 as the reference sample. In the Fig. 8, we observed that the *pac-3* gene expression was significantly induced under 10 mM for 15 min incubation and in all time of 300 mM of Ca^{2+} incubation ($P < 0.01$). The expression of *gsn*, *gdn*, *tps-1*, *tre-1* and *tre-2* was significantly over-expressed at 300 mM of Ca^{2+}, especially for 15 min incubation in the wild-type ($P < 0.01$). All glycogenic and trehalose gene expression was down-expressed at 10 mM of Ca^{2+} for 60 min incubation in the wild-type. The other hand, the expression in the Δ*pac-3* mutant strain showed different profiles when compared to the wild-type. For example, the glycogenic *gsn* and *gdn* gene expression was repressed and over-expressed in some times of 10 mM and 300 mM of Ca^{2+} in the wild-type, respectively, while the genes was stimulated and repressed in some times of 10 mM and 300 mM of Ca^{2+} in the Δ*pac-3* strain, respectively. Additionally, the expression of *tre-1* was over-expressed in the Δ*pac-3* mutant strain under calcium addition when compared to the same condition in the wild-type ($P < 0.01$). It is important to observe that *tre-2* expression showed very high level under 300 mM of Ca^{2+} for 15 min incubation in the wild-type ($P < 0.01$, Fig. 8, last graph). In summary, the expression of glycogenic and trehalose genes was differentially regulated by Ca^{2+} and by PAC-3, suggesting a PAC-3 action in calcium response.

ACKNOWLEDGMENTS

We thank the Fungal Genetics Stock Center (Kansas City, MO) for Neurospora strains and Antonio Tarcisio Delfino for technical assistance. This work was supported by the Fundação de Amparo à Pesquisa do Estado de São Paulo (FAPESP) and the Conselho Nacional de Desenvolvimento Científico e Tecnológico (CNPq) for grants and fellowships.

REFERENCES

Abramoff, M.D., Magalhaes, P.J., and Ram, S.J. (2004) Image Processing with ImageJ. *Biophotonics Intern* **11**: 36-42.

Bell, W., Sun, W., Hohmann, S., Wera, S., Reinders, A., De Virgilio, C., *et al.* (1998) Composition and functional analysis of the *Saccharomyces cerevisiae* trehalose synthase complex. *J Biol Chem* **273**: 33311-33319.

Cupertino, F.B., Freitas, F.Z., de Paula, R.M., and Bertolini, M.C. (2012) Ambient pH controls glycogen levels by regulating glycogen synthase gene expression in *Neurospora crassa*. New insights into the pH signaling pathway. PLoS One **7**. doi:10.1371/journal.pone.0044258.

Cupertino, F.B., Virgilio, S., Freitas, F.Z.; Candido, T.S., and Bertolini, M.C. (2015) Regulation of glycogen metabolism by the CRE-1, RCO-1 and RCM-1 proteins in *Neurospora crassa*. The role of CRE-1 as the central transcriptional regulator. *Fungal Genet Biol* **77**: 82-94.

de Paula, R., de Pinho, C.A., Terenzi, H.F., and Bertolini, M.C. (2002) Cloning and molecular characterization of the gsn cDNA encoding glycogen synthase in *Neurospora crassa*. *Mol Genet Genomics* **267**: 241-253.

Fletterick, R.J., and Madsen, N.B. (1980) The structures and related functions of phosphorylase a. *Annu Rev Biochem* **49**: 31-61.

Freitas, F.Z., and Bertolini, M.C. (2004) Genomic organization of the *Neurospora crassa gsn* gene. Possible involvement of the STRE and HSE elements in the modulation of gene transcription during heat shock. *Mol Genet Genomics* **272**: 550-561.

Freitas, F.Z., de Paula, R.M., Barbosa, L.C.B., Terenzi, H.F., and Bertolini, M.C., (2010) cAMP signaling pathway controls glycogen metabolism in *Neurospora crassa* by regulating the glycogen synthase gene expression and phosphorylation. *Fungal Genet Biol* **47**: 43-52.

Freitas, Z.F., Virgilio, S., Cupertino, F.B., Kowbel, D.J., Fioramonte, M., Gozzo, F.C., *et al.*, (2016) The SEB-1 transcription factor binds to the STRE motif in *Neurospora crassa* and regulates a variety of cellular processes including the stress response and reserve carbohydrate metabolism. *G3* **6**: 1327-1343.

Gonçalves, R.D., Cupertino, F.B., Freitas, F.Z., Luchessi, A.D., and Bertolini, M.C. (2011) A genome-wide screen for *Neurospora crassa* transcription factors regulating glycogen metabolism. *Mol Cell Proteomics* **10**. doi:10.1074/mcp.M111.007963.

Hartree, E.F. (1972) Determination of protein: a modification of the Lowry method that gives a linear photometric response. *Anal Biochem* **48**: 422-427.

Hecker, L.I., and Sussman, A.S. (1973) Localization of trehalase in the ascospores of Neurospora: relation to ascospore dormancy and germination. *J Bacteriol* **115**: 592-599.

Jorge, J.A., Polizeli, M.L., Thevelein, J.M., and Terenzi, H.F. (1997) Trehalases and trehalose hydrolysis in fungi. *FEMS Microbiol Lett* **154**: 165-171.

Kullas, A.L., Martin, S.J., and Davis, D. (2007) Adaptation to environmental pH: integrating the Rim101 and calcineurin signal transduction pathways. *Mol Microbiol* **66**: 858-871.

Livak, K.J., and Schmittgen, T.D. (2001) Analysis of relative gene expression data using real-time quantitative PCR and the 2(-Delta Delta C(T)) Method. *Methods* **25**: 402-408.

McCluskey, K., (2003) The Fungal Genetics Stock Center: from molds to molecules. *Adv Appl Microbiol* **52**: 245-262.

Neves, M.J., Jorge, J.A., François, J.M., and Terenzi, H.F. (1991) Effects of heat shock on the level of trehalose and glycogen, and on the induction of thermotolerance in *Neurospora crassa*. *FEBS Lett* **183**: 19-22.

Noventa-Jordão, M.A., Polizeli, M.L.T.M., Bonini, B.M., Jorge, J.A., and Terenzi, H.F. (1996) Effects of temperature shifts on the activities of *Neurospora crassa* glycogen synthase, glycogen phosphorylase and trehalose-6-phosphate synthase. *FEBS Lett* **378**: 32-36.

Peñalva, M.A., Tilburn, J., Bignell, E, and Arst. H.N.Jr. (2008) Ambient pH gene regulation in fungi: making connections. *Trends Microbiol* **16**: 291-300.

Roach, P.J., Skurat, A.V., and Harris, R.A. (2001) Regulation of glycogen metabolism. In: Jefferson LS, Cherrington AD (eds) Handbook of physiology. The endocrine pancreas and regulation of metabolism, vol II. Oxford University Press, p. 609-647.

Roque, A., Petrezsélyová, S., Serra-Cardona, A., and Ariño, J. (2016) Genome-wide recruitment profiling of transcription factor Crz1 in response to high pH stress. *BMC Genomics* **17**: 662. doi:10.1186/s12864-016-3006-6.

Serra-Cardona, A., Canadell, D., and Ariño, J. (2015) Coordinate responses to alcaline pH stress in budding yeast. *Microbial Cell* **2**: 182-196.

Serrano, R., Ruiz, A., Bernal, D., Chambers, J.R., and Ariño, J. (2002) The transcriptional response to alkaline pH in *Saccharomyces cerevisiae*: evidence for calcium-mediated signalling. *Mol Microbiol* **46**:1319-1333.

Sokolovsky, V., Kaldenhoff, R., Ricci, M., and Russo, V.E.A., (1990) Fast and reliable mini-prep RNA extraction from *Neurospora crassa*. *Fungal Genet Newsl* **37**: 41-43.

Téllez-Iñón, M.T., Terenzi, H., and Torres, H.N. (1969) Interconvertible forms of glycogen synthetase in *Neurospora crassa*. *Biochim Biophys Acta* **191**: 765-768.

Thevelein, J.M. (1984) Regulation of trehalose mobilization in fungi. *Microbiol Rev* **48**: 42-59.

Viladevall, L., Serrano, R., Ruiz, A., Domenech, G., Giraldo, J., *et al.* (2004) Characterization of the calcium-mediated response to alkaline stress in *Saccharomyces cerevisiae*. *J Biol Chem* **279**: 43614-43624.

Virgilio, S., Cupertino, F.B., Bernardes, N.E., Freitas, F.Z., Takeda, A.A.S., Fontes, M.R.M., *et al.* (2016) Molecular components of the *Neurospora crassa* pH signaling pathway and their regulation by pH and the PAC-3 transcription factor. *PLoS One* **11**. doi:10.1371/journal.pone.0161659.

Vogel, H.J. (1956) A convenient growth medium for *Neurospora crassa* (medium N). *Microbiol Gene Bull* **13**: 42-43.

Weirauch, M.T., Yang, A., Albu, M., Cote, A.G., Montenegro-Montero, A., Drewe, P., *et al.* (2014) Determination and inference of eukaryotic transcription factor sequence specificity. *Cell* **158**: 1431-1443.

Wiemken, A. (1990) Trehalose in yeast, stress protectant rather than reserve carbohydrate. *Antonie Van Leeuwenhoek* **58**: 209-217.

Zimmermann, N.A., Terenzi, H.F., and Jorge, J. A. (1990) Purification and properties of an extracellular conidial trehalase from *Humicola grisea var. thermoidea*. *Biochim Biophys Acta* **1036**: 41-46

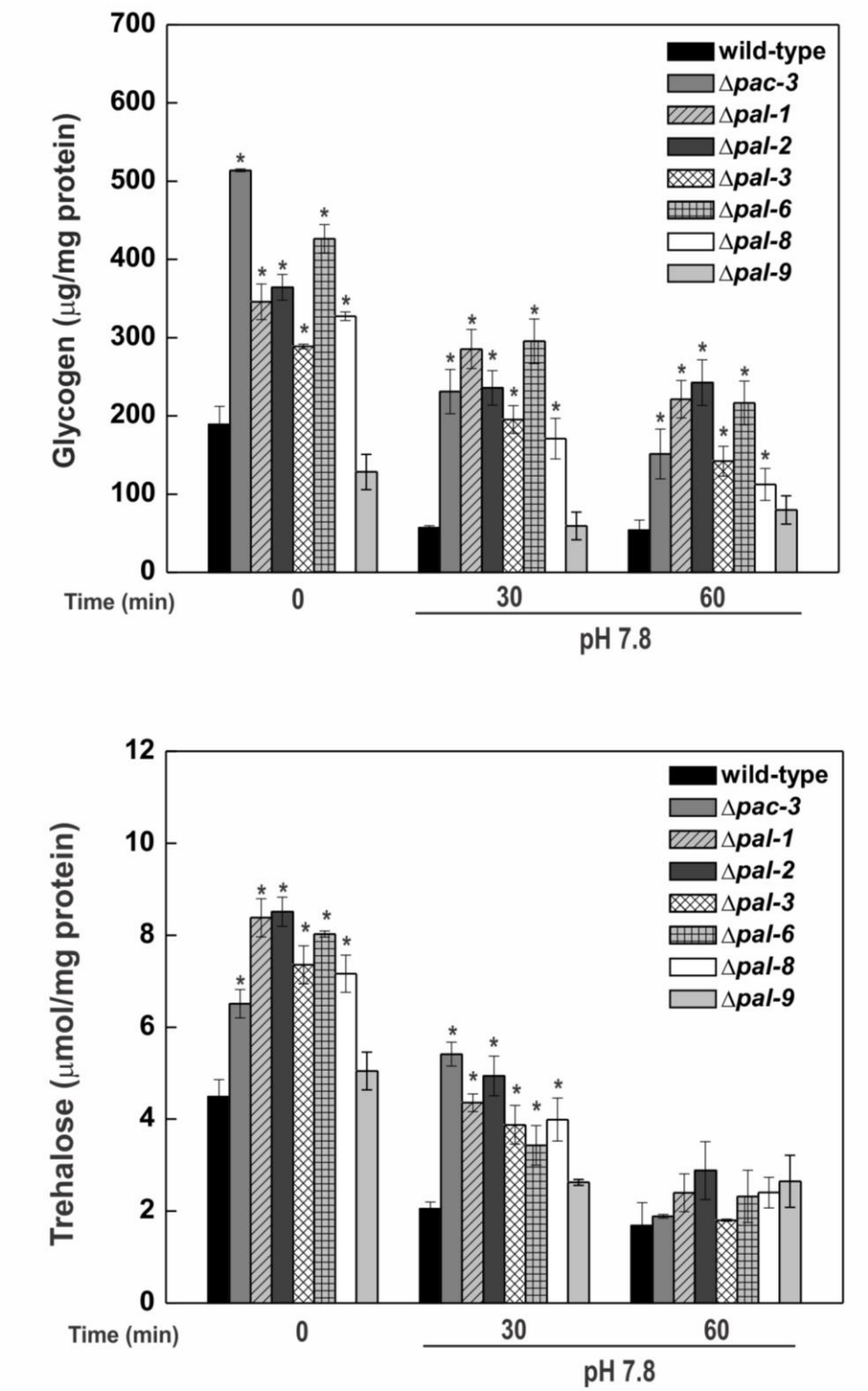

Fig 1. Glycogen and trehalose accumulation in the Δ*pal* mutant strains and in the wild-type strain under normal and alkaline pH. Mycelia samples from the wild-type and Δ*pal* mutant strains cultivated at pH 5.8 at 30ºC for 24 h and shifted to pH 7.8 for 30 and 60 min were used for glycogen and trehalose quantification. Glycogen was digested with α-amylase and amyloglucosidase after precipitation with cold ethanol and trehalose was digested with a partially purified trehalase from *Humicola grisea*. Free glucose was quantified and the glycogen and trehalose concentrations were normalized to the total protein concentration. The asterisks indicate significant differences compared to the wild-type strain at the same condition (Student's *t*-test, $P < 0.01$). All results represent the average of at least three independent experiments. Bars indicate the standard deviation from the biological experiments. 0, sample before pH shifting (control sample, 24 h of growth at pH 5.8).

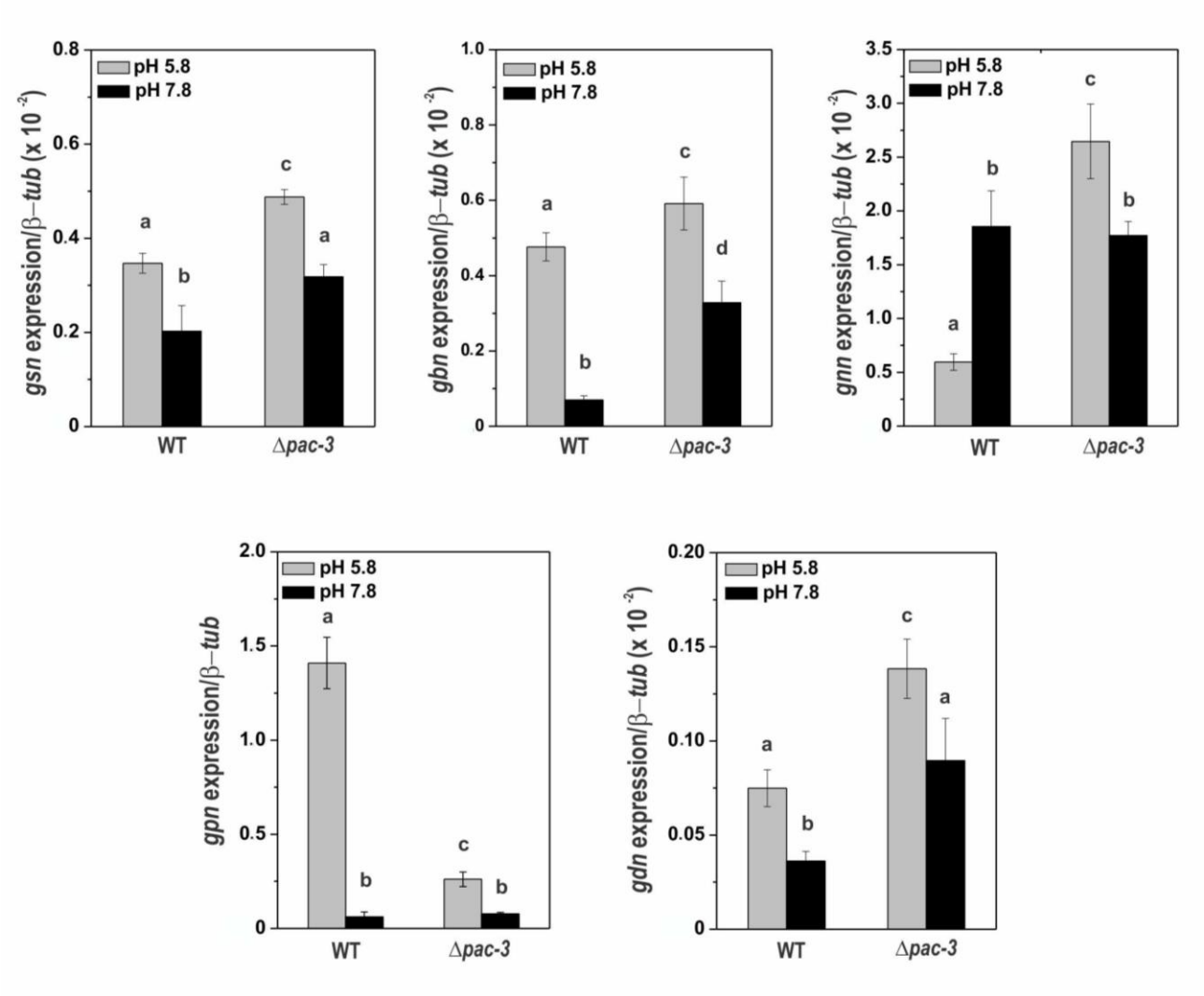

Fig 2. The glycogenic gene expression in the wild-type and Δ*pac-3* mutatn strain at normal and alkaline pH. Cells from the wild-type and Δ*pac-3* strain were cultured at pH 5.8 for 24 h and shifted to pH 7.8 for 1 h. Mycelial samples were collected and used to extract total RNA. Gene expression analysis was performed by RT-qPCR in the StepOnePlus™ Real-Time PCR system (Applied Biosystems) using the Power SYBR® Green and specific primers. The β-*tub* gene was used as the reference gene, and the wild-type at pH 5.8 was used as the reference sample. At least three biological replicates were performed in triplicate, and the data were analyzed using the relative quantification standard curve method. Bars indicate the standard deviation from the biological experiments. **a, b, c, d:** Letters above the bars indicate statistical significance; different letters indicate significant differences between two samples and similar letters indicate no significant difference between two samples at the same or different pH (Student's *t*-test, $P < 0.01$).

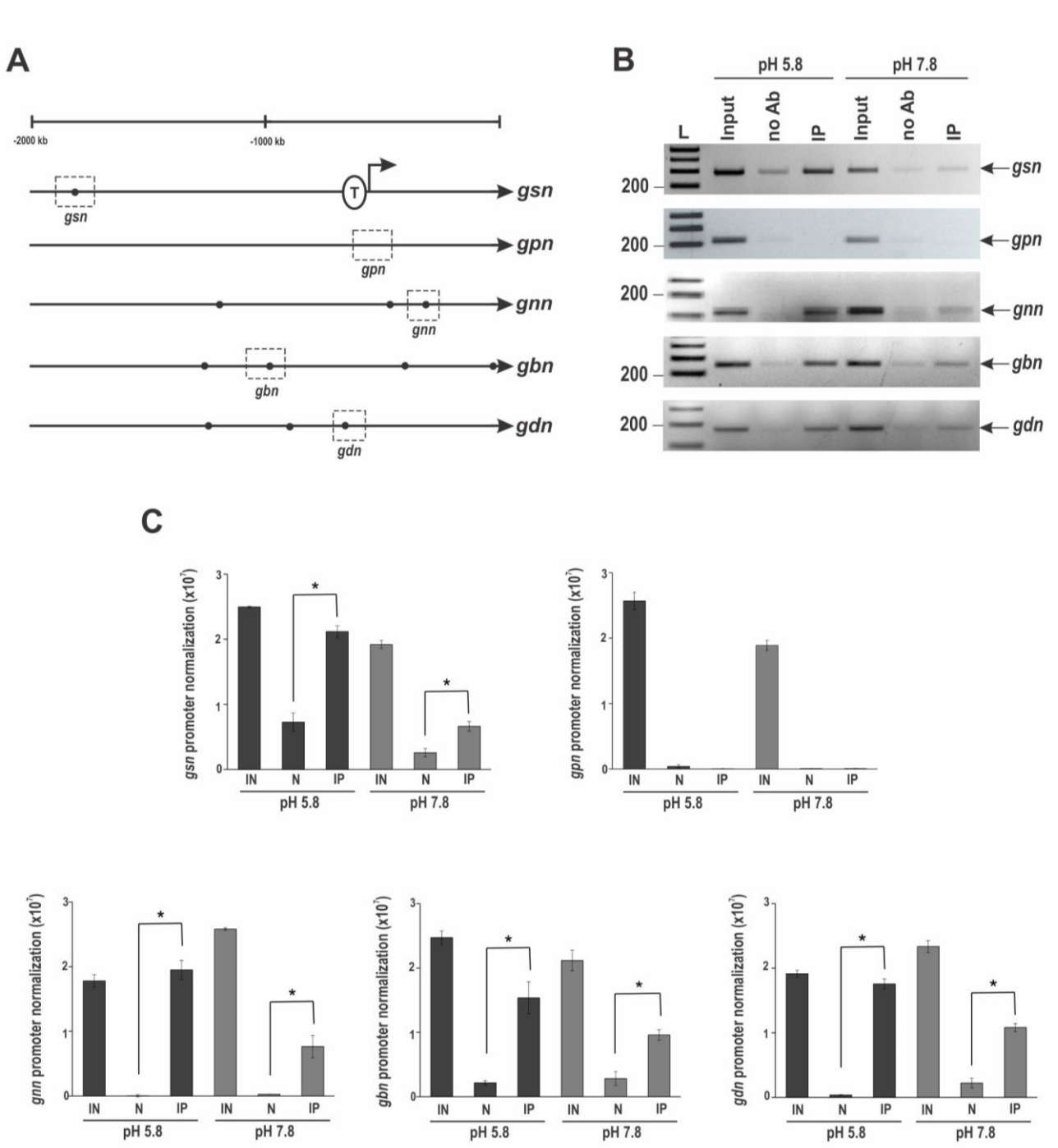

Fig 3. Binding of PAC-3 to the glycogenic gene promoters at normal and alkaline pH. (A) Schematic representation of the PAC-3 DNA binding preference in the 5'-flanking regions of the glycogenic gene promoters. The black dots indicate the position of the PAC-3 motifs (5'-BGCCVAGV-3') (Weirauch *et al.*, 2014) identified and the dashed boxes indicate regions that were analyzed by ChIP-PCR. The transcription initiation site (T) in *gsn* was experimentally determined (Freitas and Bertolini, 2004) **(B)** Genomic DNA samples from the Δ*pac-3 pac-3*$^{+}$ complemented strain both subjected to 7.8 alkaline pH stress or not (pH 5.8) were immunoprecipitated with anti-mCherry antibody and subjected to PCR to amplify DNA fragments containing the PAC-3 motif. A DNA fragment from the *gpn* promoter, which does not have a PAC-3 motif, was used as a negative control of binding. The input DNA (I) was used as a positive control and the non-immunoprecipitated reaction (no Ab, N) as the negative control. L, 1 kb DNA ladder. **(C)** The DNA bands after ChIP-PCR were quantified by ImageJ and the results are shown in the graphs. Asterisks indicate significant differences between no Ab and IP at the same pH (Student's *t*-test, $P < 0.01$). All results represent the average of at least two independent experiments. Bars indicate the standard deviation from the biological experiments.

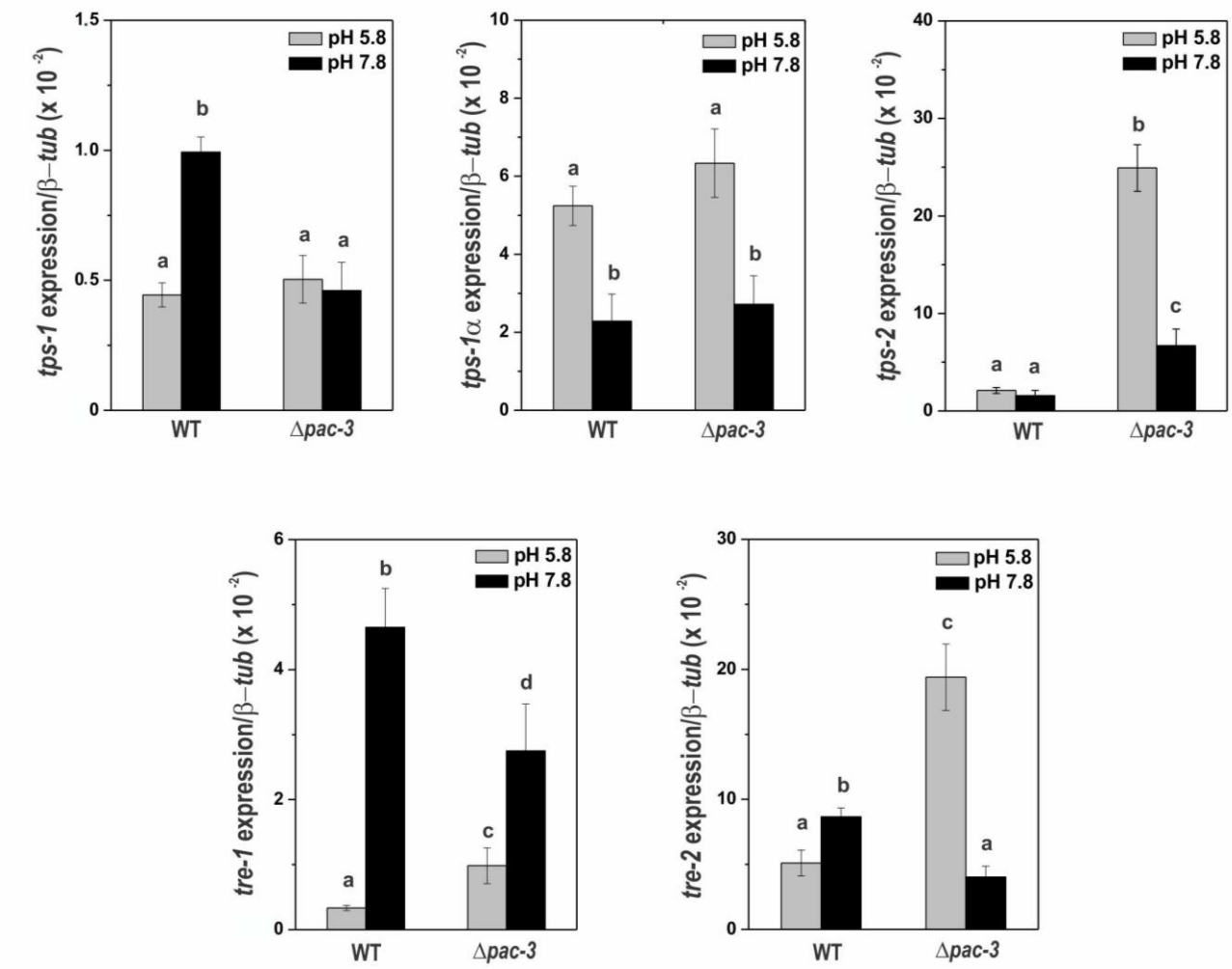

Fig 4. The expression of trehalose genes in the wild-type and Δ*pac-3* strain at normal and alkaline pH. Cells from the wild-type and Δ*pac-3* strain were cultured at pH 5.8 for 24 h and shifted to pH 7.8 for 1 h. Mycelial samples were used to extract total RNA. Gene expression analysis was performed by RT-qPCR in the StepOnePlus™ Real-Time PCR system (Applied Biosystems) using the Power SYBR® Green and specific primers described in Table S1. The β-*tub* gene was used as the reference gene, and the wild-type pH 5.8 was used as the reference sample. At least four biological replicates were performed, and the data were analyzed using the relative quantification standard curve method. Bars indicate the standard deviation from the biological experiments. **a, b, c, d:** Letters above the bars indicate statistical significance; different letters indicate significant differences between two samples and similar letters indicate no significant difference between two samples at the same or different pH (Student's *t*-test, $P < 0.01$).

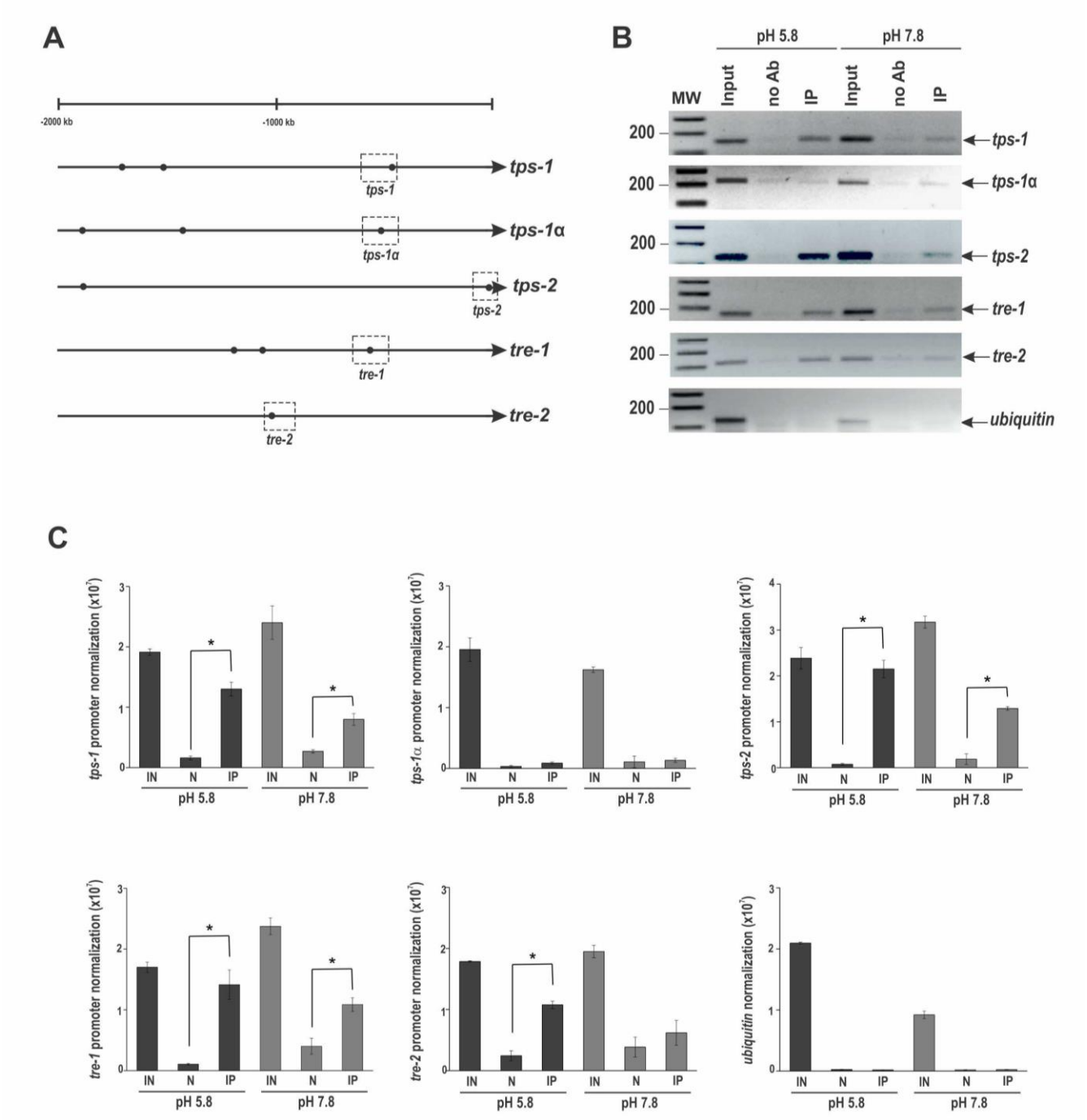

Fig 5. Binding of PAC-3 to the trehalose gene promoters at normal and alkaline pH. (A) Representation of the PAC-3 motif in the trehalose gene promoters. The black dots indicate the position of the PAC-3 motifs and the dashed boxes indicate regions that were analyzed by ChIP-PCR. **(B)** Genomic DNA samples from the Δ*pac-3 pac-3*$^{+}$ complemented strain subjected to alkaline or normal pH stress were immunoprecipitated with anti-mCherry antibody and subjected to PCR to amplify DNA fragments containing the PAC-3 motif. A DNA fragment from the ubiquitin gene, which does not have a PAC-3 motif, was used as a negative control of binding. The input DNA (I) was used as a positive control and the non-immunoprecipitated reaction (no Ab, N) as the negative control. L, 1 kb DNA ladder. **(C)** The DNA bands after ChIP-PCR were quantified by ImageJ and the results are shown in the graphs. Asterisks indicate significant differences between no Ab and IP at the same pH (Student's *t*-test, $P < 0.01$). All results represent the average of at least two independent experiments. Bars indicate the standard deviation from the biological experiments.

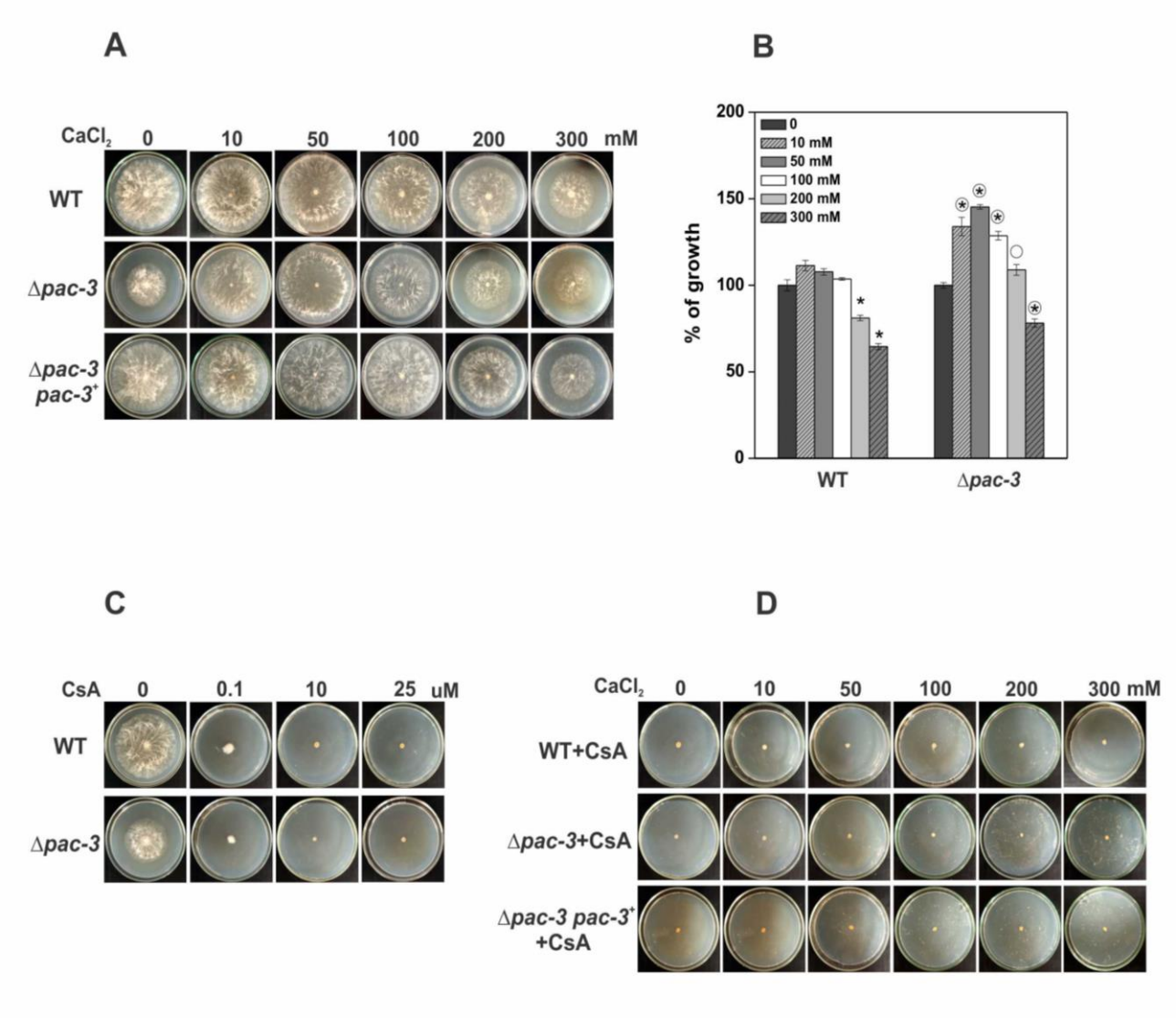

Fig 6. The effects of Ca^{2+} on morphological growth of the Δ*pac-3* mutant strain. (A) The wild-type, Δ*pac-3* and Δ*pac-3 pac-3*$^{+}$ strains (10^7 conidia ml^{-1}) were inoculated on Petri dishes containing solid VM medium plus 2% sucrose and added Ca^{2+} at a final concentration of 0, 10, 50, 100, 200 or 300 mM at 30ºC. Radial growth of the colonies was examined after 24 h growth. **(B)** Radial growth of the wild-type and Δ*pac-3* strain was measured and the percentage of growth was determined considering the condition without Ca^{2+} as 100% of growth. The results represent at least three independent experiments in duplicate. The asterisks indicate significant differences between the same strain cultured without Ca^{2+} and with different calcium concentrations and the circles indicate significant differences compared to the wild-type strain at the same Ca^{2+} condition (Student's *t*-test, $P < 0.01$). Error bars indicate standard deviation. **(C)** The effects of 0.1, 10 and 25 μM of calcineurin inhibitor (cyclosporin A, CsA) on the wild-type and Δ*pac-3* radial growth. **(D)** The effects of different concentration of Ca^{2+} plus 10 μM of CsA on the wild-type, Δ*pac-3* and Δ*pac-3 pac-3*$^{+}$ radial growth for 24 h at 30°C.

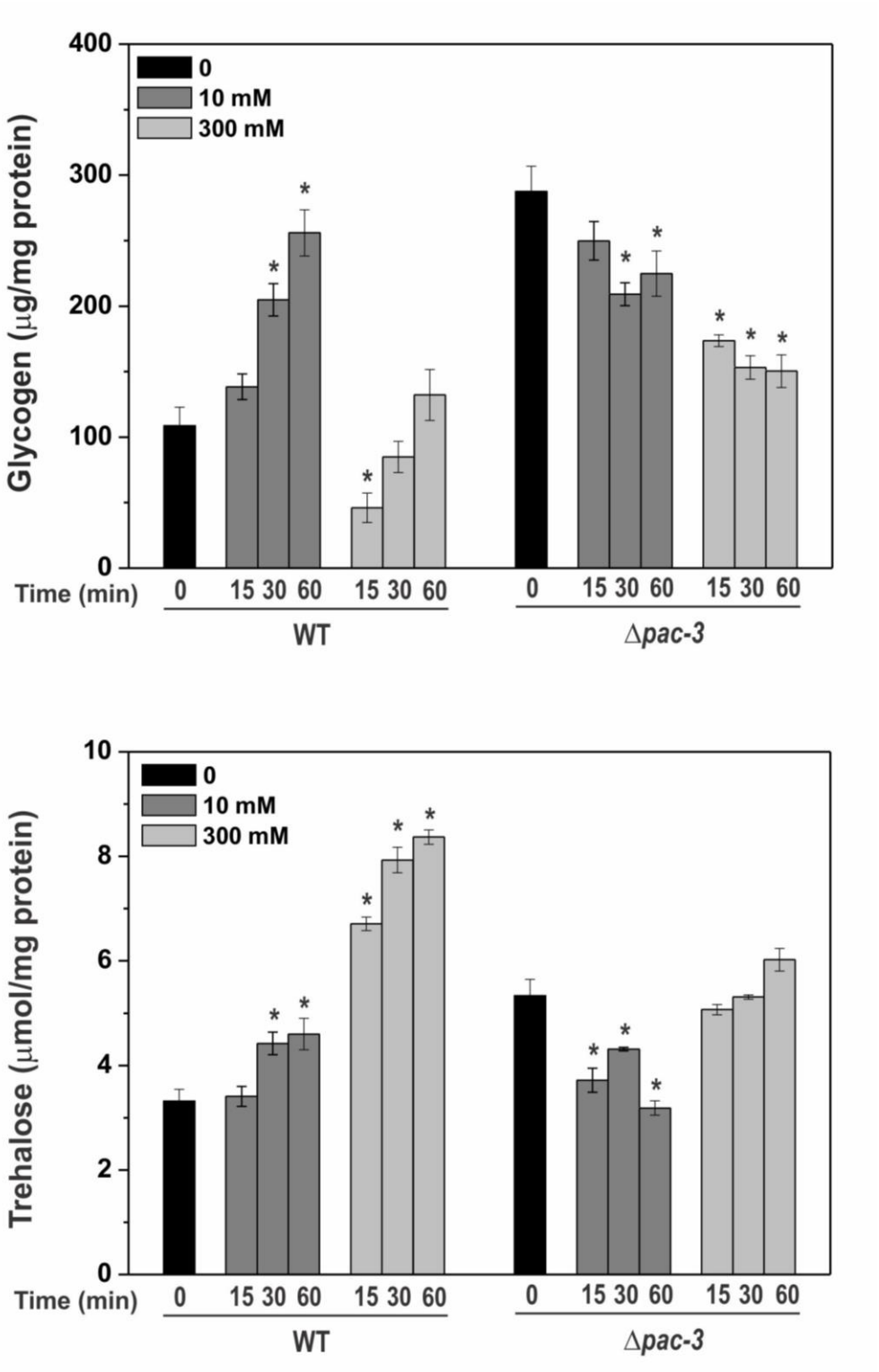

Fig 7. Glycogen and trehalose accumulation in the wild-type and Δ*pac-3* mutant strain at 10 and 300 mM of $CaCl_2$. Mycelial samples from the wild-type and Δ*pac-3* mutant strain cultured at normal condition (zero) at 30ºC for 24 h and shifted to calcium stress (10 mM or 300 mM of Ca^{2+}) for 15, 30 and 60 min were used to glycogen and trehalose quantification. The asterisks indicate significant differences compared to zero sample in the wild-type or mutant strain (Student's *t*-test, $P < 0.01$). All results represent the average of at least four independent experiments. Bars indicate the standard deviation from the biological experiments.

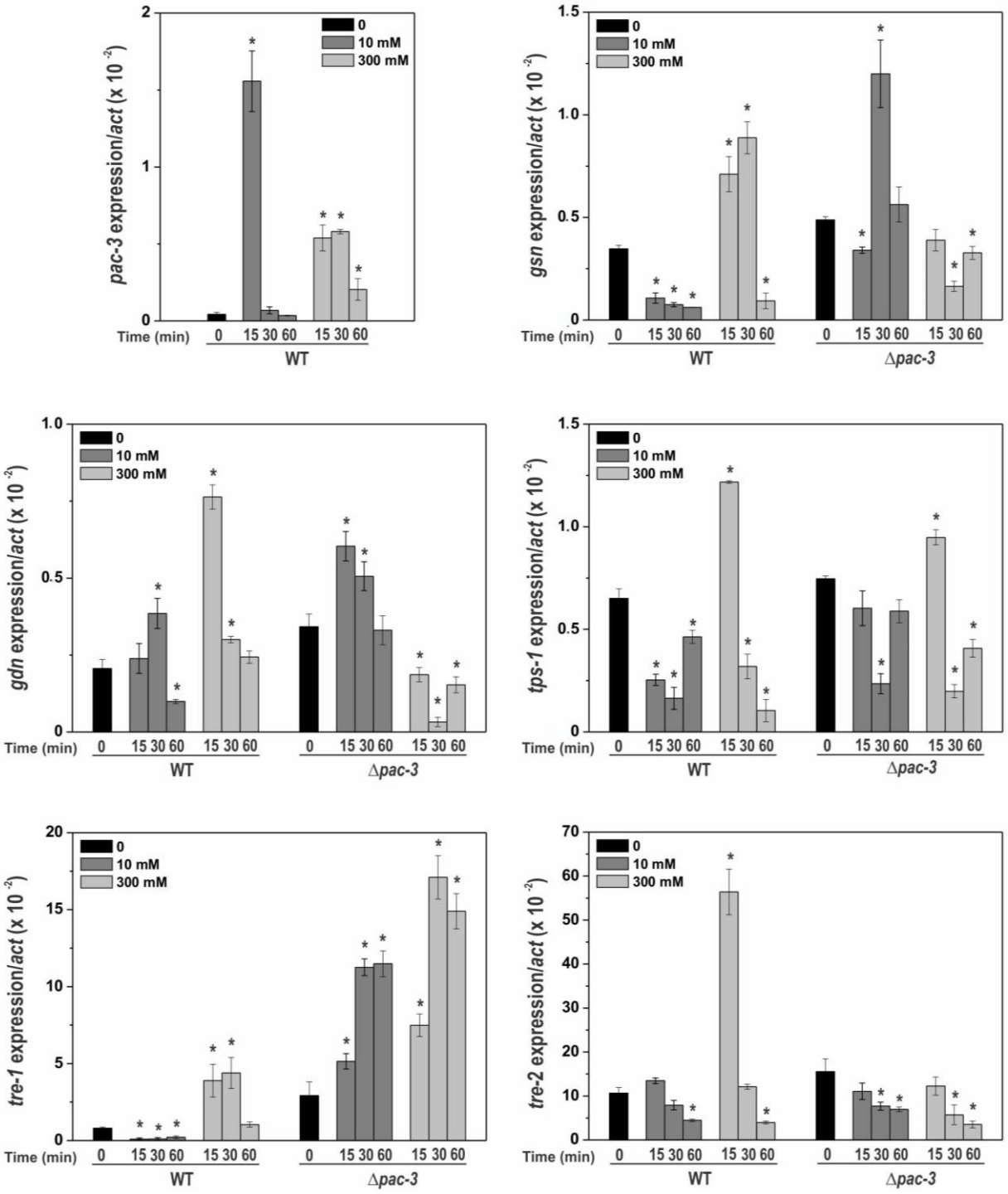

Fig 8. The influence of Ca^{2+} on the expression levels of same genes related to glycogen and trehalose regulation in the wild-type and Δ*pac-3* strain. Cells from the wild-type and Δ*pac-3* strain were cultured at pH 5.8 (0, normal condition) for 24 h and shifted to 10 mM or 300 mM of Ca^{2+} for 15, 30 and 60 min. Mycelial samples were used to extract total RNA. Gene expression analysis was performed by RT-qPCR in the StepOnePlus™ Real-Time PCR system (Applied Biosystems) using the Power SYBR® Green and specific primers (Table S1, qPCR). The actin gene was used as the reference gene, and the zero condition in the wild-type was used as the reference sample. At least four biological replicates were performed, and the data were analyzed using the relative quantification standard curve method. Bars indicate the standard deviation from the biological experiments. The asterisks indicate significant differences compared to zero sample in the wild-type or mutant strain (Student's *t*-test, $P < 0.01$).

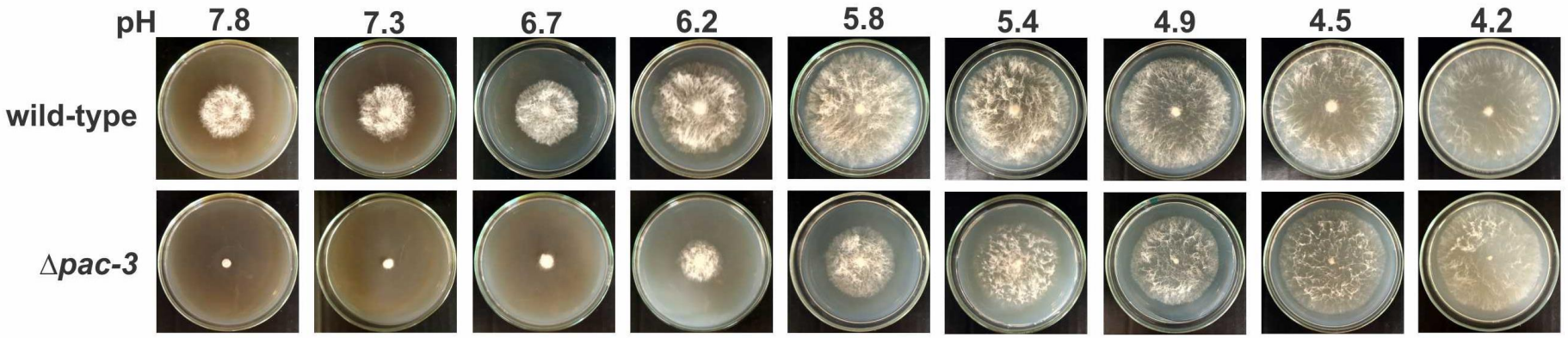

Apical extension at different pH[a]

	pH 7.8	pH 7.3	pH 6.7	pH 6.2	pH 5.8	pH 5.4	pH 4.9	pH 4.5	pH 4.2
WT	3.8 ± 0.09	3.9 ± 0.02	4.5 ± 0.01	6.5 ± 0.03	7.9 ± 0.28	7.8 ± 0.33	7.8± 0.26	8.3 ± 0.20	8.0 ± 0.17
Δpac-3	0.6 ± 0.00*	0.7± 0.13*	1.6 ± 0.01*	3.0 ± 0.08*	5.5 ± 0.25*	6.1 ± 0.35*	6.4 ± 0.21*	7.3 ± 0.21*	7.5 ± 0.13

a. apical extension of basal hyphae was represented by the radial growth of the colonies (cm).
* significant different compared to wild-type in the same pH (T-test student, p<0.01).

Fig S1. Morphological analyses of the wild-type and Δ*pac-3* mutant strain under different pH conditions. The strains (10^7 conidia ml^{-1}) were inoculated on Petri dishes containing solid VM medium plus 2% sucrose at pH 4.2 (acid condition) until pH 7.8 (alkaline condition) at 30ºC. Images of colony morphology were captured after 24 h. Apical extension was measured in centimeters and showed in the table below to the radial growth pictures. The results represent at least two independent experiments in duplicate. *Indicates significant difference between wild-type and mutant strain at the same pH (Student's *t*-test, $P < 0.01$).

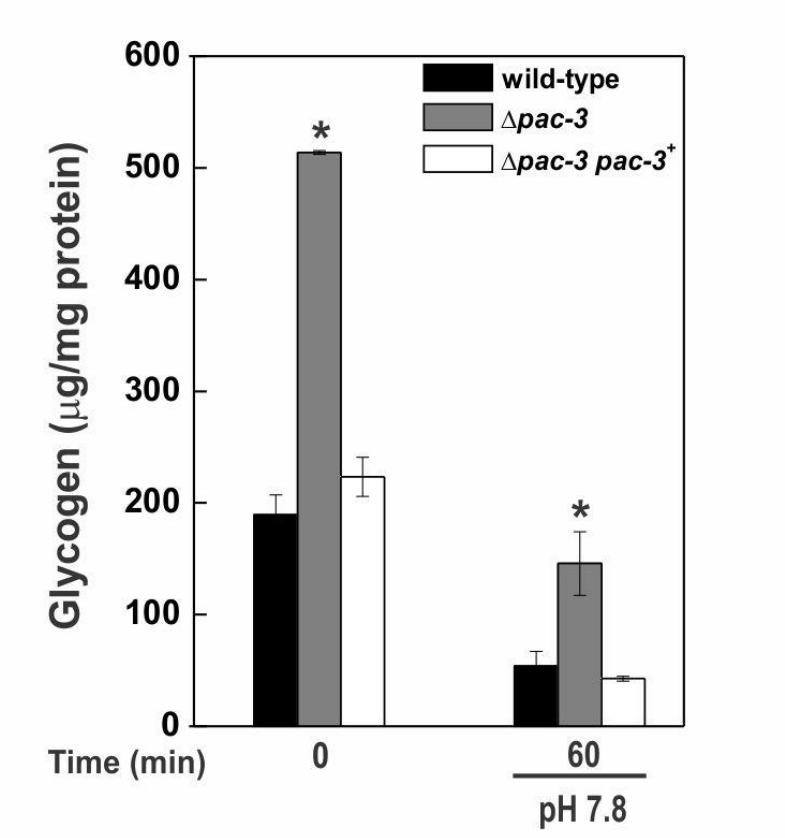

Fig S2. Glycogen quantification in the wild-type, Δ*pac-3* mutant and Δ*pac-3* *pac-3*$^{+}$ complemented strain at normal and alkaline pH. Mycelial samples cultured at pH 5.8 (zero) at 30ºC for 24 h and shifted to pH 7.8 for 1 h were used to glycogen quantification. The asterisks in the Δ*pac-3* indicate significant difference compared to the wild-type strain at the same condition (Student's *t*-test, $P < 0.01$). The results represent the average of three independent experiments. Bars indicate the standard deviation from the biological experiments.

Table S1. *Oligonucleotides used in this study*.

Primer	Sequence (5'→3')	Source	Name	Position[a]
qPCR				
qPac3-F	CAAGCATCGACCCGTATCAT	NCU00090	–	+1203 to +1222
qPac3-R	TGGTGAGTGACCCGAAGTA	NCU00090	–	+1312 to +1330
qGSN-F	TACCAAGCATCACCACCAACCTCT	NCU06687	–	+1541 to +1564
qGSN-R	TGTCTGCGGCTCTTCTGGGTAAAT	NCU06687	–	+1689 to +1712
qRAMIF-F	TCTGCGATGCCGAGTTGT	NCU05429	–	+1487 to +1504
qRAMIF-R	ACTCGTTGCCCTCGAAGT	NCU05429	–	+1616 to +1633
qGNN-F	ACAAGCACCCGAACCCAC	NCU06698	–	+1134 to +1151
qGNN-R	AAGGGTGGGCGATGCTGT	NCU06698	–	+1234 to +1251
qGPN-F	TGCCAATATCGAAATCACCCGCGA	NCU06687	–	+2247 to +2270
qGPN-R	TCTCGATGGCCTCAAACACCTTGA	NCU06687	–	+2375 to +2398
qDESRAM-F	TCGGCGGTAATCAAGCCA	NCU00743	–	+3794 to +3811
qDESRAM-R	TGAATTTGCCGGCTTCGT	NCU00743	–	+3950 to +3967
qtps1-F	GGTTGACTTCCTCATGGTGGTTG	NCU00793	–	+2529 to +2551
qtps1-R	GTCGCCTTAGCCTCAGTGTTTCT	NCU00793	–	+2647 to +2669
qtps1alfa-F	TGCCGAGCTGACAAGGATAAGC	NCU09715	–	+1410 to +1431
qtps1alfa-R	GGCATCCGTCACACCCTCAATA	NCU09715	–	+1512 to +1533
qtps2-F	CGAGATCAAGCCCGAGAACTGC	NCU05041	–	+2817 to +2838
qtps2-R	CATCCTCAGGTTCCAACAAGTGCC	NCU05041	–	+2885 to +2908
qtre1-F	CAAGAGGGCCGACATCACTATGG	NCU00943	–	+1944 to +1966
qtre1-R	CCCCTTCCTGGCGAACTTCTT	NCU00943	–	+2011 to +2031
qtre2-F	CGCTCGGCACTCTGACTCC	NCU04221	–	+2153 to +2171
qtre2-R	CTCAGAGAGCGCCTTGTTCCG	NCU04221	–	+2206 to +2226
4054Tub-F	CCTCCACCTTCGTCGGTAACTCC	NCU04054	–	+1091 to +1113
4054Tub-R	GGTACTGCTGGTACTCGGAGACG	NCU04054	–	+1254 to +1276
4173ACT-F	CCATGTACCCTGGTCTCTCCGAC	NCU04173	–	+911 to +933
4173ACT-R	CCACCGATCCAGACGGAGTACTTG	NCU04173	–	+1005 to +1028
ChIP-PCR				
PacC-F	GACCCAACAGCCCAACTT	p*gsn*	*gsn*	-1918 to -1901
SREBP-RP2	TCTGACCTTTCCCAATCAG	p*gsn*	*gsn*	-1645 to -1627
pGPNNit-F2	CTGGCTGGCTCCGTCTTA	p*gpn*	*gpn*	-725 to -708
pGPNNit-R2	GAGGTAAGTGGGGCAGTC	p*gpn*	*gpn*	-527 to -510
gnnPAC3-Fp	CTTGGGGCTCTCTCGTCTGTG	p*gnn*	*gnn*	-380 to -360
gnnPAC3-Rp	CAGTCGAAGGAGGCTGCAGTG	p*gnn*	*gnn*	-288 to -268
branch-FP5	TAAATGGGAAGCTAGAAGGGACGAC	p*gbn*	*gbn*	-973 to -949
branch-RP5	GGAGCTTCAACAAACACGGACATG	p*gbn*	*gbn*	-747 to -724
DEBp-F2	GCCTGTTTTCTGACGGGT	p*gdn*	*gdn*	-692 to -675
DEBp-R2	TTGGCTGTGATAGGACCG	p*gdn*	*gdn*	-536 to -519
tresynt-Fp	GCTCAAGTTCCTCAGCGCTACATT	p*tps-1*	*tps-1*	-856 to -833
tresynt-Rp	CTTGACATCTTCTGCCCAGACACA	p*tps-1*	*tps-1*	-727 to -704
alfatre-Fp	CGACAACCCGCCAATCAGC	p*tps-1α*	*tps-1α*	-547 to -529
alfatre-Rp	AAGATCGGAAACTTGGAATGGCTGG	p*tps-1α*	*tps-1α*	-351 to -327
trephosp-Fp	GATCTGTTTACATCCTTCGTCCCGC	p*tps-2*	*tps-2*	-119 to -95
trephosp-Rp	TGTTGTCCTTGTGTCATCTTGGCG	p*tps-2*	*tps-2*	-7 to +17
tre1-Fp	CACACATTTCTCAGTCTCGTTCCCC	p*tre-1*	*tre-1*	-737 to -713
tre1-Rp	GCTTGTTCCCCTGCTTCCCT	p*tre-1*	*tre-1*	-586 to -567
tre2-Fp	CCAGCCTCATCTGCGTCCT	p*tre-2*	*tre-2*	-1064 to -1046
tre2-Rp	TGGCGATGGAAAGCGGGAT	p*tre-2*	*tre-2*	-942 to -924
qUbi-F	CGAGTCTTCGGATACGATTG	NCU05995	*ubiquitin*	+805 to +824
qUbi-R	CCATCCTCCAACTGCTTAC	NCU05995	*ubiquitin*	+894 to +912

[a]Primers are positioned according to the ATG start codon from cDNA (qPCR) or genomic DNA (ChIP-PCR).

Chapter 4

Chapter 4: CRE-1 transcription factor and RCO-1 and RCM-1 corepressor proteins regulating glycogen metabolism

In this chapter, we investigated the role of the CRE-1 transcription factor and the corepressor complex RCO-1/RCM-1 in Neurospora glycogen metabolism. We found strong evidence for CRE-1 repression of glycogen synthesis: increased glycogen levels and expression of *gsn* (encoding glycogen synthase), *gbn* (encoding branching enzyme), *gdn* (encoding debranching enzyme), and *gnn* (encoding glycogenin) and decreased expression of *gpn* (encoding glycogen phosphorylase) in the *cre-1* deletion strain. CRE-1 bound *in vitro* and *in vivo* to promoters of genes in the glycogen synthesis and degradation pathways. We also confirmed the regulatory role of CRE-1 in Carbon Catabolite Repression (CCR) and its nuclear localization under repressing condition. Disruption of *rco-1* or *rcm-1* resulted in significant differences in glycogen accumulation and misregulation of some genes involved in glycogen metabolism, but the individual mutants did not affect glycogen metabolism in the same way. Finally, we conclude that CRE-1 is a repressor of glycogenic gene expression and plays a role in the regulation of glycogen synthase activity.

This work was published in *Fungal Genetics and Biology* (Elsevier), v. 77, p. 82-94, 2015 (doi:10.1016/j.fgb.2015.03.011).

Observation: According to “Alterações das Normas Internas para a defesa da Dissertação de Mestrado ou da Tese de Doutorado, aprovadas pelo Conselho de Pós-Graduação em Biotecnologia do Instituto de Química, UNESP, Araraquara, em nov/2010 e pela Congregração em reunião de dez/2010” (Appendix), the results are presented in chapter format similar to the published article.

Regulation of glycogen metabolism by the CRE-1, RCO-1 and RCM-1 proteins in *Neurospora crassa.* The role of CRE-1 as the central transcriptional regulator

Authors' names: Fernanda Barbosa Cupertino[1], Stela Virgilio[1], Fernanda Zanolli Freitas, Thiago Souza Candido, Maria Célia Bertolini*

[1]Both authors contributed equally to this work

Address: Departamento de Bioquímica e Tecnologia Química, Instituto de Química, Universidade Estadual Paulista, UNESP, 14800-060, Araraquara, SP, Brazil

***Corresponding author:** Maria Célia Bertolini, Instituto de Química
Universidade Estadual Paulista, UNESP
Rua Professor Francisco Degni 55
14800-060, Araraquara, SP, Brazil
Phone: +55-16-3301-9675
Fax: +55-16-3322-2308
e-mail: mcbertol@iq.unesp.br

ABSTRACT

The transcription factor CreA/Mig1/CRE-1 is a repressor protein that regulates the use of alternative carbon sources via a mechanism known as Carbon Catabolite Repression (CCR). In *Saccharomyces cerevisiae,* Mig1 recruits the complex Ssn6-Tup1, the *Neurospora crassa* RCM-1 and RCO-1 orthologous proteins, respectively, to bind to promoters of glucose-repressible genes. We have been studying the regulation of glycogen metabolism in *N. crassa* and the identification of the RCO-1 corepressor as a regulator led us to investigate the regulatory role of CRE-1 in this process. Glycogen content is misregulated in the *rco-1*^{KO}, *rcm-1*^{RIP} and *cre-1*^{KO} strains, and the glycogen synthase phosphorylation is decreased in all strains, showing that CRE-1, RCO-1 and RCM-1 proteins are involved in glycogen accumulation and in the regulation of GSN activity by phosphorylation. We also confirmed the regulatory role of CRE-1 in CCR and its nuclear localization under repressing condition in *N. crassa*. The expression of all glycogenic genes is misregulated in the *cre-1*^{KO} strain, suggesting that CRE-1 also controls glycogen metabolism by regulating gene expression. The existence of a high number of the *Aspergillus nidulans* CreA motif (5'-SYGGRG-3') in the glycogenic gene promoters led us to analyze the binding of CRE-1 to some DNA motifs both *in vitro* by DNA gel shift and *in vivo* by ChIP-qPCR analysis. CRE-1 bound *in vivo* to all motifs analyzed demonstrating that it down-regulates glycogen metabolism by controlling gene expression and GSN phosphorylation.

Keywords: *Neurospora crassa*, Glycogen, Gene expression, CRE-1, ChIP-qPCR

1. Introduction

Microorganisms can grow in a variety of environmental conditions due to their wide range of adaptative responses that ensure survival and their use of energy-saving mechanisms. Nutrient responses can influence different regulatory mechanisms, including those related to the use of carbon sources. In general, filamentous fungi use glucose as their preferred carbon source while the alternative sugar metabolizing enzymes are repressed in a mechanism known as Carbon Catabolite Repression (CCR) (Ruijter and Visser, 1997; Vinuselvi et al., 2012). In

recent years, numerous studies have demonstrated the importance of CCR mechanism, especially in the secretory control of hydrolytic enzymes by industrial microorganisms such as *Trichoderma reesei* (*Hypocrea jecorina*) and *Aspergillus* species (reviewed in Aro et al., 2005). The production of cellulolytic and xylanolytic enzymes is regulated by glucose through the action of the transcription factor CreA (*Aspergillus nidulans*), CRE-1 (*Neurospora crassa*) or CRE1 (*T. reesei*). This transcription factor is a repressor protein that regulates the transcription of genes related to the use of alternative carbon sources when glucose is present (de Vries et al., 1999; Mach-Aigner et al., 2008; Sun and Glass, 2011).

The action of the C_2H_2-zinc finger protein CreA/CRE-1/Mig1 is well conserved among different fungi. CreA/CRE-1 binds to the 5'-SYGGRG-3' motif (Sun and Glass, 2011; Kulmburg et al., 1993) that displays strong identity to the motif recognized by Mig1 (5'-SYGGGG-3') (Lundin et al., 1994). However, the regulation of Cre-mediated repression is complex and apparently varies among fungi. Transcriptional and post-transcriptional events regulate *A. nidulans* CreA function (Strauss et al., 1999) and phosphorylation regulates *H. jecorina* CRE1 activity (Cziferszky et al., 2002). Although protein kinases that phosphorylate this transcription factor are unknown, the involvement of the AMPK/Snf1 kinase in the regulation by phosphorylation has been demonstrated (Vautard-Mey and Fèvre, 2000; Ostling and Ronne, 1998). This kinase phosphorylates *in vitro* the yeast Mig1, however the own *H. jecorina* CRE1 was not phosphorylated by the same kinase (Cziferszky et al., 2003). The cellular compartmentalization of CreA/CRE-1/Mig1 also differs among fungi. Mig1 location was initially reported to be glucose-dependent, being nuclear in conditions of CCR and translocating to the cytoplasm under glucose-limiting conditions (De Vit et al., 1997). The *A. nidulans* GFP-tagged CreA location was demonstrated to be nuclear in the presence of high glucose (Vautard-Mey et al., 1999; Roy et al., 2008; Brown et al., 2013), however the cytoplasmic localization was strongly influenced by the nature of the derepressing carbon source (Brown et al., 2013). Similar results have been described for the *Fusarium oxysporum* GFP-Cre1 fusion protein, which showed nuclear localization during growth on ethanol, a derepressing condition (Jonkers and Rep, 2009). More recently, the *T. reesei* CRE1 was described to recycle between nucleus and cytoplasm depending on the carbon source (Lichius et al., 2014).

This transcription factor plays a direct role controlling the expression of a large number of genes encoding cell wall degrading enzymes. In *T. reesei* and *Aspergillus*

species, CRE1/CreA, respectively, regulates the gene expression of celullases, hemicelullases and xylanases (Ilmén et al., 1997; Orejas et al., 1999; reviewed in Ruijter and Visser, 1997), while in *N. crassa*, deletion of the *cre-1* gene led to an increase in the production of hydrolytic enzymes involved in cellulose degradation (Sun and Glass, 2011). We have been investigating the regulatory mechanisms involved in *N. crassa* glycogen metabolism and in a screening of a mutant strains set in transcription factors we identified the corepressor RCO-1 protein (Gonçalves et al., 2011). RCO-1 was first identified in *N. crassa* by Yamashiro et al. (1996) as a protein that mediates the repression of conidiation and it is orthologous to the *Sacchamoryces cerevisiae* Tup1, a protein component of the Ssn6-Tup1 complex (Keleher et al., 1992). This complex mediates the repression of genes related to different cellular processes, depending on the DNA-binding protein that recruits it to DNA. In yeast, such complex regulates glucose-repressible genes in a Mig1-dependent way, a process involving chromatin remodeling and nucleosome compaction (Treitel and Carlson, 1995; reviewed in Smith and Johnson, 2000).

In *N. crassa,* RCM-1 is the *S. cerevisiae* Ssn6 orthologous protein and, together with RCO-1, may have a role in regulating glucose-repressible genes. Lee and Ebbole (1998) demonstrated the regulation of the *N. crassa con-10* gene by RCO-1 in a medium without glucose. More recently, the RCO-1-RCM-1 complex was described to have a role in photoadaptation (Olmedo et al., 2010) and was identified as a partner of the transcription factor CSP1, a clock-controlled repressor (Sancar et al., 2011). The identification of RCO-1 as likely regulating the glycogen metabolism in *N. crassa* and the high number of CreA motifs (5'-SYGGRG-3') in the promoter region of genes codifying for glycogen metabolism enzymes prompted us to start investigating the regulatory role of CRE-1, RCO-1 and RCM-1 in the regulation of glycogen metabolism in *N. crassa*.

In this report, we demonstrate that CRE-1, RCO-1 and RCM-1 proteins regulate glycogen metabolism by a process in which CRE-1 may play a central role since the gene expression of all glycogen enzymes was misregulated in the *cre-1*^{KO} mutant strain. Gel mobility assays showed that the recombinant GST::CRE-1 recognized and bound specifically to the *gsn* and *gpn* promoters *in vitro* and ChIP-qPCR analysis confirmed CRE-1 binding to all glycogenic gene promoters. In addition, CRE-1::GFP bound *in vivo* to its own promoter but was not able to bind to a DNA fragment lacking a CRE-1 motif.

2. Materials and methods

2.1. Neurospora crassa strains and growth conditions

The *N. crassa* FGSC#9718 (*mat a, mus-51::bar*), *cre-1*^{KO} (FGSC#10372), *rco-1*^{KO} (FGSC#11371) and *rcm-1*^{RIP} (FGSC#10215) strains were purchased from the Fungal Genetics Stock Center (FGSC) (McCluskey, 2003). The *his-3::Pn-cre-1-gfp* strain was a gift from N. L. Glass, University of California, Berkeley, CA, USA (Sun and Glass, 2011). All strains were maintained on solid Vogel's minimal (VM) medium, pH 5.8 (Vogel, 1956) containing 2% sucrose. Conidia from 10-day culture were collected, suspended in sterile water and counted. For vegetative growth, 10^7 conidia/mL or hyphae homogenates (for *rco-1*^{KO} and *rcm-1*^{RIP} strains) were first germinated in 60 mL of VM medium +2% sucrose at 30 ºC, 250 rpm, for 24 h. After this period, cultures were harvested and the mycelia were frozen in liquid nitrogen and stored at -80 ºC. For growth in different carbon sources, 10^9 conidia/mL were first germinated in 1 L of VM medium +2% fructose (non-repressing carbon source) (Ziv et al., 2008) at 30 ºC, 250 rpm, for 24 h. After this period, cultures were harvested and the mycelia were divided in four samples: one was frozen in liquid nitrogen and stored at -80 ºC for further processing (control sample) and the remaining were transferred into 400 mL of fresh VM medium containing 2% of glucose, or xylose or glycerol. Samples (125 mL) were harvested after incubation for 2, 4, and 8 h and processed as before. To analyze the effect of 2-deoxy-D-glucose (2-DG) in catabolic repression, conidia (10^7/mL) from wild-type and *cre-1*^{KO} strains were inoculated into 20 mL of VM medium containing 1% sucrose, or glucose or xylose with or without 1 mM 2-DG and incubated at 30 ºC, 250 rpm, for 24 h. The mycelia were harvested, filtered and dried at 98 ºC for 16 h. The biomass weight was expressed as a percentage relative to samples grown without 2-DG.

2.2. Glycogen and protein quantification

Mycelia pads were ground to a fine powder in a pre-chilled mortar in liquid nitrogen and extracted in lysis buffer (50 mM Tris-HCl, pH 7.6, 100 mM NaF, 1 mM EDTA, 1 mM PMSF, 0.1 mM TCLK, 1 mM benzamidine, and 1 µg/mL each of pepstatin and aprotinin). Cellular extracts were clarified by centrifugation at 10,000*g*,

for 10 min at 4 ºC, and the supernatants were used for glycogen and protein quantifications. Glycogen content was measured according to Freitas et al. (2010). Briefly, 100 µL of the crude extract was precipitated with 20% TCA (final concentration) and centrifuged (5000*g*, 10 min, 4 ºC). The glycogen in the supernatant was precipitated with 500 µL of 95% cold ethanol, collected by centrifugation, washed twice with 66% ethanol, dried and digested with α-amylase (10 mg/mL) and amyloglucosidase (30 mg/mL). Free glucose was measured using a glucose oxidase kit and the glycogen content was normalized to total protein. Total protein was quantified by the Hartree (1972) method, using BSA as standard.

2.3. Glycogen synthase activity

The activity of glycogen synthase was determined by [^{14}C]-glucose incorporation, as described by Thomas et al. (1968). Briefly, mycelia pads were ground to a fine powder in nitrogen liquid in a pre-chilled mortar and 200 mg of each sample was extracted in 1 mL of lysis buffer (50 mM Tris HCl, pH 7.5, 100 mM NaF, 1 mM EDTA, 1 mM PMSF, 1 mM benzamidine, 1 mM β-mercaptoethanol and 1 µg/mL each of aprotinin, pepstatin and TLCK). Cellular extracts were clarified (7000*g*, 10 min, 4ºC) and total proteins were quantified (Hartree, 1972) using BSA as standard. To assay glycogen synthase activity, a volume of 15 µL, containing approximately 30 µg of total protein, was added to 30 µL of reaction buffer [50 mM Tris-HCl, pH 7.8, 20 mM EDTA, 25 mM NaF, 0.67% glycogen, 3 mM UDP-[^{14}C]-glucose (1.8 mCi/mmol), with or without 7.2 mM glucose-6-phosphate (G6P)] and incubated at 30 ºC during 15 min. After incubation, 75 µL of each reaction were withdrawn, placed on Whatmann 3 MM filter paper and washed with cold ethanol (70%) under stirring for 15 min. Two additional washes in ethanol (70%) were done, the first for 60 min and the second for 15 min. After washing, the filters containing the reaction product were dried and radioactivity was quantified in a LS 6500 Scintillation Counter (Beckman CoulterTM). One unit of glycogen synthase activity was defined as the amount of enzyme that transferred 1 µmol of glucose to glycogen per minute.

2.4. RNA isolation and gene expression analysis

Total RNA was prepared from mycelia samples according to Sokolovsky et al. (1990) method. RNA (10 µg) from each sample was fractionated on a 2.2 M formaldehyde 1.2% (w/v) agarose gel, stained with ethidium bromide and visualized under UV light to assess the rRNAs integrity. Gene expression analysis was performed by quantitative PCR (qPCR). RNA samples (10 µg) were treated with RQ1 RNAse-free DNAse (Promega) and subjected to cDNA synthesis by using the SuperScript III First Strand Synthesis kit (Invitrogen) and oligo (dT) primers, according to the manufacturers' instructions. qPCR was performed on the StepOnePlus ™Real-Time PCR system (Applied Biosystems) using the Power SYBR® Green PCR Master Mix (Applied Biosystems) and specific primers for glycogen synthase (*gsn*), glycogen phosphorylase (*gpn*), glycogenin (*gnn*), 1,4-α-glucan branching enzyme (*gbn*), glycogen debranching enzyme (*gdn*) and β-tubulin (*tub-2*) mRNA amplicons (Table 1). Five biological replicates were run and the data were analyzed using the StepOne™ Software v2.1 (Applied Biosystems) in the relative quantification standard curve method. The fluorescent dye ROX™ was used as a passive reference to normalize the SYBR green reporter dye fluorescent signal. All PCR products had melting curves indicating the presence of a single amplicon. The tubulin β chain (*tub-2* gene, NCU04054) was used as the endogenous control in all experiments.

2.5. Cellular localization

For microscopy experiments, conidia from the *cre-1*^{KO} complemented strain (*his-3::Pn-cre-1-gfp*) were inoculated onto a coverslip and incubated in liquid VM containing 1% sucrose for 16 h at 30 ºC. After this time, the cells were transferred to the following media: VM without carbon source, VM plus 1% sucrose and VM plus 1% xylose and incubated for 1 h at 30 ºC. Before transferring, the cells were washed in the same transfer media to remove traces of sucrose. After incubation, mycelia on the coverslips were fixed (3.7% formaldehyde, 50 mM NaH_2PO_4, pH 7.0, 0.2% (v/v) tween 80), washed with phosphate buffered saline (PBS) and stained with 0.5 µg/mL DAPI for 5 min. The mycelia were washed again in PBS and examined in an AXIO Imager.A2 Zeiss microscope. Images were captured with the AxioCam MRm camera and processed using the AxioVision software. Further processing was done using Adobe Photoshop 7.0.

228 *2.6. cre-1 cDNA cloning and production and purification of the recombinant protein*
229
230 The *N. crassa cre-1* gene (ORF NCU08807) encodes a 430 amino acid
231 protein with a theoretical molecular mass of 47 kD. The entire *cre-1* cDNA fragment
232 (1293 bp) was amplified from the pYADE5 cDNA plasmid library (Brunelli and Pall,
233 1993) with the oligonucleotides 8807-F and 8807-R (Table 1) and subcloned into the
234 pMOS*Blue* cloning vector (GE Healthcare) leading to the pMOS-8807 plasmid. A
235 ~1.3 kb *Bam*HI-*Eco*RI fragment was removed from pMOS-8807 and inserted into the
236 pGEX-4T1 vector (GE Healthcare) resulting in the pGEX-8807 plasmid. For
237 expression of the non-fused GST and the GST::CRE-1 recombinant protein,
238 *Escherichia coli* Rosetta (DE3) pLysS cells harboring the pGEX-4T1 or pGEX-8807
239 plasmid constructions were used, respectively. Cells were grown at 37 ºC in 1 L of LB
240 medium to an OD_{600} of 0.7 and induced with IPTG (final concentration 0.4 mM) for 4
241 h at 37 ºC and 200 rpm. For purification, cells were suspended in buffer A (10 mM
242 NaH_2PO_4, 1.8 mM KH_2PO_4, pH 7.3, 140 mM NaCl, 2.7 mM KCl, 1 mM DTT, 1 mM
243 PMSF and 10 mM benzamidine) containing 0.5% Triton X-100 and 0.5% Tween 20
244 and lysed by sonication (5 cycles of 30 s sonication and 30 s on ice). After
245 centrifugation, the supernatant was subjected to affinity chromatography on a
246 GSTrap HP column (GE Healthcare) using the ÄKTA Prime purification system. The
247 recombinant protein was eluted in buffer B (50 mM Tris-HCl, pH 8.0, 10 mM
248 glutathione) and dialyzed twice against 1 L of dialysis buffer (10 mM Tris-HCl, pH 7.9,
249 100 mM KCl, 10% v/v glycerol, 1 mM EDTA and 0.5 mM DTT). The purified protein
250 was analyzed by 10% SDS-PAGE (Laemmli, 1970) followed by Coomassie Brilliant
251 blue staining and quantified by the Hartree (1972) method using BSA as standard.
252
253 *2.7. Electrophoretic mobility shift assay (EMSA)*
254
255 DNA-protein binding reactions were carried out in 30-80 µL of 1x binding
256 buffer (25 mM HEPES-KOH, pH 7.9, 20 mM KCl, 10% v/v glycerol, 1 mM DTT, 0.2
257 mM EDTA, 0.5 mM PMSF, 12.5 mM benzamidine, and 5 µg/mL each of antipain and
258 pepstatin A) containing 2 µg of poly(dI-dC).(dI-dC) as non-specific competitor and 3-
259 10 µg of either GST or GST::CRE-1 recombinant protein. A radiolabeled DNA probe
260 (~10^4 cpm) was added and the reactions were incubated at room temperature for 20
261 min. Free probe was separated from DNA-protein complexes by electrophoresis on a

native 5% polyacrylamide gel in 0.5x TBE buffer at 300 V, 10 mA and 10 ºC. After electrophoresis, the gel was dried and autoradiographed. For competition assays, an excess of specific DNA competitor was added to the binding reactions 10 min prior to incubation with the radiolabeled probe.

2.8. DNA probe and competitors for EMSA

A high number of CreA motif (5'-SYGGRG-3') was identified in the 5'-flanking region of the *gsn*, *gpn*, *gnn*, *gbn* and *gdn* genes by *in silico* analysis. To obtain the *gsn* and *gpn* probes, DNA fragments containing the CreA motif were amplified from genomic DNA using the oligonucleotides described in Table 1, in the presence of [α-^{32}P]-dATP (3000 Ci/mmol). The probes were purified on a 2% low-melting point agarose gel. The unlabeled probes were used as specific DNA competitors. A 27 bp DNA oligonucleotide was also used as a competitor after annealing the complementary oligonucleotides oligoCRE-1-F and oligoCRE-1-R (Table 1). The specific competitors were quantified by measuring the absorbance at 260 nm. For competition assays, the specific competitors and the dsDNA CRE-1 oligonucleotide were added to the binding reactions in 10-30-fold and 3-10-fold molar excess, respectively.

2.9. ChIP-qPCR analysis

Chromatin immunoprecipitation assays were performed as described by Tamaru et al. (2003) with modifications. Briefly, conidia from the *his-3::Pn-cre-1-gfp* strain were grown in 125 mL of liquid VM medium containing 2% sucrose at 30 ºC, 250 rpm, for 24 h and the chromatin was fixed by adding formaldehyde to 1% final concentration, followed by incubation for 30 min at 30 ºC and 250 rpm. Formaldehyde was quenched using 125 mM glycine, at 30 ºC, 250 rpm, for 10 min. Sonicated chromatin prepared from each sample was pre-cleared with protein A Mag Sepharose (GE Healthcare) pre-blocked with 0.5% BSA in PBS and then immunoprecipitated with anti-GFP antibody (Sigma) and protein A Mag Sepharose. As a negative control, a mock reaction without antibody was run (no Ab). The DNA concentration was quantified and 25 ng of each reaction: input DNA, no Ab and IPs (immunoprecipitated DNAs with anti-GFP) were analyzed by absolute quantification

by quantitative PCR (qPCR). qPCR was performed on the StepOnePlus ™Real-Time PCR system (Applied Biosystems) using the Power SYBR® Green PCR Master Mix (Applied Biosystems) and specific oligonucleotides for *gsn*, *gpn*, *gnn*, *gbn*, and *gdn* promoter regions (Table 1). A *cre-1* promoter region containing the CreA motif was used as positive control of binding and an ubiquitin region, lacking the motif were used as negative control of binding. All PCR products had melting curves indicating the presence of a single amplicon.

3. Results

3.1. CRE-1, RCO-1, and RCM-1 proteins regulate glycogen accumulation, glycogen synthase activity and expression of genes encoding glycogenic enzymes

We previously screened a set of *N. crassa* knockout strains in genes encoding transcription factors and identified the RCO-1 as a protein that regulates glycogen metabolism (Gonçalves et al., 2011). This protein is the *S. cerevisiae* Tup1 orthologue. In yeast, Tup1 requires Ssn6, the called Ssn6-Tup1 complex, which, together with the Mig1 transcription factor, acts as a repressor of glucose-repressible genes (Smith and Johnson, 2000). Since the *N. crassa* CRE-1, RCO-1 and RCM-1 proteins correspond to the *S. cerevisiae* Mig1, Tup1 and Ssn6 orthologous proteins, respectively, we investigated the glycogen metabolism in the corresponding knockout strains. The *rcm-1*^{RIP} is a mutant strain, in which the gene was partially inactivated by RIP (Repeat Induced Point Mutation); the knockout strain is not viable (Olmedo et al., 2010). Glycogen accumulation and *gsn* gene expression were previously analyzed in a wild-type strain of *N. crassa* during vegetative growth (30 °C), and the results showed higher levels after ~24 h of growth (de Paula et al., 2002). Here, we analyzed the glycogen content, the glycogen synthase phosphorylation (the rate-limiting enzyme in glycogen synthesis) and the expression of genes encoding the glycogenic enzymes glycogenin (*gnn*), glycogen synthase (*gsn*), branching enzyme (*gbn*), glycogen phosphorylase (*gpn*), and debranching enzyme (*gdn*) in the *cre-1*^{KO}, *rco-1*^{KO} and *rcm-1*^{RIP} strains after 24 h of growth.

All mutant strains presented significant differences in glycogen accumulation compared to the wild-type strain (Fig. 1A). However, whereas the *cre-1*^{KO} strain showed increased glycogen levels (two times), the *rcm-1*^{RIP} strain showed a

reduction of three times in glycogen content. The *rco-1*^{KO} strain showed only a slight increase in glycogen level, in agreement with our previous findings (Gonçalves et al., 2011). Glycogen synthase phosphorylation was analyzed in the presence and absence of the allosteric modulator G6P (-/+ G6P ratio), lower values corresponding to higher phosphorylation and, then, less active enzyme. All mutant strains displayed higher ratio when compared to the wild-type strain showing that the enzyme is less phosphorylated, and then more active in the mutant strains (Fig. 1B). The relative gene expression was also analyzed for all genes encoding glycogenic enzymes (Fig. 1C). The *cre-1*^{KO} strain showed misregulation in the expression of all glycogenic genes. The CRE-1 protein appeared to act as a repressor of glycogen synthesis since *gsn*, *gbn* and *gnn* expression (genes encoding enzymes for the glycogen synthesis) was higher in the mutant strain than in the wild-type strain. In addition, *gpn* expression (encodes a degradation enzyme) was lower in the same strain, likely contributing to the high glycogen accumulated by the mutant strain (Fig. 1A). The *gnn* and *gpn* expression was dramatically increased in the *rco-1*^{KO} strain, in agreement with previous results on *gpn* expression in this mutant strain (Bertolini et al., 2012). Finally, the *gbn, gpn* and *gdn* expression was not substantially changed in the *rcm-1*^{RIP} strain and the gene expression results did not explain the levels of the glycogen accumulated by this strain. It is likely that the lower *gsn* gene expression contributed to the reduced glycogen levels in this mutant strain.

Based on these results, we concluded that the transcription factor CRE-1 could act as a repressor of the glycogen metabolism in *N. crassa,* likely by regulating the expression of genes encoding glycogenic enzymes.

3.2. CRE-1 mediates repression of glycogen metabolism under carbon repressing and non-repressing conditions

Since the transcription factor CreA/CRE-1/Mig1 mediates the CCR mechanism in most fungi and CRE-1 regulates glycogen metabolism in *N. crassa* we decided to investigate whether the regulation was dependent on the growth conditions. First, we confirmed that CRE-1 protein mediates CCR by growing the wild-type and *cre-1*^{KO} strains in VM medium containing either glucose or sucrose (for repressing condition) and in VM containing xylose (for non-repressing condition), in the absence and presence of 2-DG (Fig. 2A). This compound is a non-metabolizable glucose analog

that can be phosphorylated but cannot be further isomerized. The wild-type strain showed reduced growth in xylose medium containing 2-DG while the growth of the mutant strain was unaffected by the presence of 2-DG. These results confirmed that, like in other fungi, *N. crassa* CRE-1 plays an important regulatory role in CCR.

To analyze whether the repressing and non-repressing carbon sources influenced the regulation of glycogen metabolism by CRE-1 protein, conidia were first grown for 24 h in fructose (derepressor carbon source) medium and then transferred to glucose (repressor carbon source), xylose or glycerol (non-repressing carbon sources). The *rco-1*^{KO} and *rcm-1*^{RIP} mutant strains were included in this assay in order to assess whether RCO-1 and RCM-1 proteins were required, together with CRE-1, in the regulation. The Fig. 2B shows that the *cre-1*^{KO} strain accumulated the highest levels of glycogen regardless of the carbon source, indicating that CRE-1 negatively regulates glycogen metabolism under repressing and non-repressing growth conditions. However, the glycogen accumulation in the *cre-1*^{KO} was more pronounced in the presence of fructose and glucose, the preferable carbon source for glycogen accumulation. The glycogen accumulated by the *rco-1*^{KO} and *rcm-1*^{RIP} mutant strains followed the same pattern presented in Fig. 1A, with some variations. In general, the *rco-1*^{KO} strain showed slightly higher levels while the *rcm-1*^{RIP} strain showed slightly lower levels than those presented by the wild-type strain ($p < 0.01$). These results suggest that both RCO-1 and RCM-1 proteins may not have a role in the glycogen metabolism repression mediated by CRE-1. Although the *cre-1*^{KO} strain accumulated high levels of glycogen in the presence of glucose (repressing condition), the glycogen levels accumulated in the presence of glycerol (non-repressing condition) were very similar to those of the other mutant strains, mainly to the *rco-1*^{KO} strain. Finally, comparison of the different growth conditions, it was possible to observe that alternative carbon sources such as those used in this work (xylose or glycerol) are not good substrates for glycogen synthesis.

We analyzed the cellular localization of CRE-1 under repressing and derepressing conditions in a CRE-1::GFP complemented strain in which the protein expression is under control of the native promoter. For this, conidia were germinated in VM containing sucrose for 16 h and then transferred to medium containing sucrose (repressing condition) and media containing either xylose (non-repressing condition) or lacking any carbon source. In cells grown in sucrose and transferred to sucrose, the CRE-1::GFP localization was predominantly nuclear (Fig. 3A and B), as expected

for a repressor carbon source such as sucrose. However, after 1 h of transfer to medium containing xylose, CRE-1::GFP was detected in nuclei and the cytoplasm (Fig. 3C). In VM lacking any carbon source (C-free) the protein was localized both in the nuclei and cytoplasm after 1 h of transfer (Fig. 3D) and it was predominantly outside the nuclei after later time of transferring (4 h, Fig. 3E). The results demonstrated that CRE-1 protein is present in both the nucleus and the cytoplasm in derepressed and starved conditions, showing that the CRE-1 partial absence of nucleus may induce derepression of glucose-repressible genes. Although cycling was observed, complete absence of CRE-1 from the nucleus seems not be essential for depression in *N. crassa*. Our results were similar to those described for *A. nidulans* by Brown et al. (2013) but differed from those reported by Sun and Glass (2011) in *N. crassa*, although the later experiments were performed in a different way. The authors observed a nuclear CRE-1 localization in agarose medium lacking any carbon source.

3.3. Recombinant GST::CRE-1 binds to gsn and gpn promoters in vitro

The CreA DNA-binding motif was first identified in the *A. nidulans* gene promoters, including the *alcR* and *alcA* for ethanol utilization (Kulmburg et al., 1993) as being the consensus sequence 5'-SYGGRG-3'. In *N. crassa* genome, this sequence is very common in the genome, however, Sun and Glass (2011) described that genes having adjacent motifs in their promoter regions are more likely to be the direct targets of CRE-1. A search for this motif in the promoters of the glycogenic genes (*gnn, gsn, gbn, gpn,* and *gdn*) revealed many motifs in all 5'-flanking regions, either adjacent or not (Fig. 4). Some of these motifs (shaded boxes), containing either two or three CRE-1 adjacent motifs in different position of the promoter regions, were analyzed by DNA shift using the recombinant GST::CRE-1 protein produced in *E. coli*. First, we assayed the binding reaction in the labeled *gsn* 234 bp-probe (*gsn* 2) containing two adjacent motifs (Fig. 5A) located -1578 and -1601 bp from the ATG start codon. Two DNA-protein complexes of different electrophoretic mobility were observed using 3 µg of the recombinant protein (Fig. 5A, lane 3), which were lightly reduced in the presence of unlabeled specific competitor added prior to the probe (Fig. 5A, lane 4). However, the complexes were strongly reduced by adding the 27 bp oligonucleotide *cre-1* (Fig. 5A, lanes 5-8), which is a short dsDNA

oligonucleotide containing a single 5'-SYGGRG-3' motif (see Fig. 5B, upper panel). The complexes were not observed when the GST protein was added (Fig. 5A, lane 9) demonstrating that the binding complexes were specific for CRE-1. An interesting result was obtained when only one motif of the same probe was analyzed (*gsn* 2, 179 bp). A unique DNA-protein complex was visualized (Fig. 5A, lane 12), which was totally removed in the presence of the CRE-1 motif-containing oligonucleotide *cre-1* (Fig. 5A, lanes 15 and 16). A similar result was observed when the *gsn* 3 DNA probe, which contains three adjacent motifs (*gsn* 3, 166 bp) located -228, -293, and -327 bp from the ATG start codon, was used (Fig. 5B). Three DNA-protein complexes exhibiting different molecular masses were visualized (Fig. 5B, lanes 2 and 3), with the lower mass complex showing weak intensity and specificity. The specificity was probed using the same oligonucleotide *cre-1* (Fig. 5B, lane 7) and the GST protein (Fig. 5B, lane 8). The results in Fig. 5A and B showed that *N. crassa* CRE-1 recognized the same DNA motif as in *A. nidulans* but did not require adjacent motifs for binding as previously described (Cubero and Scazzocchio, 1994). From these results, we suggest that each DNA-protein complex may correspond to only one DNA motif.

We also investigated whether GST::CRE-1 was able to recognize and bind *in vitro* to some CreA motifs identified in the *gpn* promoter (see Fig. 4, shaded boxes). Initially, a 190 bp-probe (*gpn* 1) containing three motifs located -1984, -2074 and -2090 bp from the start codon was assayed and three DNA-protein complexes were visualized (Fig. 6A, lane 2). The highest and lowest molecular mass complexes were strongly decreased when the unlabeled probe was added as specific competitor prior to binding (Fig. 6A, lane 3) and the lowest molecular mass complex was completely abolished in the presence of 20-fold molar excess of the DNA oligonucleotide *cre-1* (Fig. 6A, lane 6). Interestingly, the intermediate complex was not removed by adding these competitors, which suggested that it was a high affinity DNA-protein complex. Fig. 6B shows the binding reaction of the GST::CRE-1 protein to the *gpn* 3 probe (138 bp) containing two motifs, localized at -262 and -290 bp from the start codon; three complexes were also visualized (Fig. 6B, lane 2). Similar to the results described in Fig. 5A and B, formation of the complexes was either decreased or abolished in the presence of the specific competitors and the GST protein was unable to bind to the probes (Fig. 6A and B, lanes 7). It is noteworthy that the oligonucleotide *cre-1,* used as a specific competitor in all DNA-binding reactions,

corresponds to a motif present in the *gsn* promoter (*gsn* 3), suggesting that the regions surrounding the DNA motif do not strongly influence the protein binding. In addition, it should be noted that all CRE-1 DNA motifs (5'-SYGGRG-3') analyzed in this work corresponded to different nucleotide sequences. An interesting result was the presence of multiple DNA-protein complexes exhibiting different molecular masses for probes having more than one motif. We speculate that they may represent complexes having distinct conformational structures.

3.4. CRE-1 binds to all glycogenic gene promoters in vivo

Chromatin immunoprecipitation-qPCR assays were done to confirm the binding *in vivo* of CRE-1 to the DNA motifs in the glycogenic genes (Fig. 7). Using ChIP-qPCR we analyzed whether the DNA motifs were indeed the binding targets for CRE-1. In these experiments we used the *cre-1*^{KO} complemented strain (*his-3::Pn-cre-1-gfp*) and anti-GFP antibody. Chromatin was obtained from mycelia grown in VM medium containing sucrose (repressing carbon source), a condition that favors glycogen accumulation in the *cre-1*^{KO} strain (see Fig. 1A). As a negative control, a mock reaction without antibody was run and the input DNA was used as positive control of the experiments. As previously described, many CreA motifs were identified in the 5'-flanking regions of the glycogenic genes and some of them were bound *in vitro* by the recombinant CRE-1 (Figs. 5 and 6).

The ChIP-qPCR was analyzed in *gsn* (Fig. 7A), *gpn* (Fig. 7B), *gdn* (Fig. 7C), *gnn* (Fig. 7D) and *gbn* (Fig. 7E) promoters. The *cre-1* promoter and a region inside the coding sequence of the ubiquitin gene, lacking the motif, were used as positive and negative control of binding, respectively. The Fig. 7A shows that CRE-1 was not able to bind to the single motif located at -2034 bp from the ATG start codon in the *gsn*1 promoter region. However, CRE-1 bound to *gsn*2 and *gsn*3 promoter regions, which possess two and three CreA adjacent motifs, respectively. CRE-1 also bound specifically to all regions in *gpn* (Fig. 7B), *gdn* (Fig. 7C), *gnn* (Fig. 7D), and *gbn* (Fig. 7E) promoters. Interestingly, some regions possess a single motif (*gnn* and *gdn* promoters) showing that the CRE-1 transcription factor can also recognize and bind *in vivo* to one single motif. It is important to observe the high copy number of the *gsn3* (Fig. 7A, right panel), which may suggest a major regulatory role of CRE-1 in the expression of this gene. Finally, CRE-1 bound to its own promoter, which

contains three adjacent CreA motifs (see Fig. 4) but did not bind to the ubiquitin gene fragment, which does not have any CreA motifs (Fig. 7F) (considering $p < 0.001$). These results showed that CRE-1 specifically recognizes and binds to all glycogenic gene promoters *in vivo*, therefore regulating their expression in the presence of sucrose (repressive condition).

4. Discussion

A screening of *N. crassa* strains deleted in transcription factors allowed us to identify transcriptional regulators that are likely involved in glycogen metabolism control. Some of the proteins identified are described in the literature as involved in alternative cellular processes what raised insights concerning the importance of the energy balance provided by glycogen metabolism in different biological processes (Gonçalves et al., 2011). In this work, we investigated the link between glycogen metabolism and carbon repression in *N. crassa*. Carbon catabolic repression (CCR) is a mechanism present in many microorganisms and related to the glucose-preferred effect on the metabolism of other carbon sources. It is mediated by the transcription factor Mig1/CreA/CRE-1, highly conserved among fungal species, and in *S. cerevisiae*, Mig1 recruits the repressor complex Tup1-Ssn6 to promoters of glucose-repressible genes (Treitel and Carlson, 1995). In this study, we used the *cre-1*^{KO} strain to assess the regulation of glycogen metabolism and included the strains *rco-1*^{KO} and *rcm-1*^{RIP}, which are the RCO-1 and RCM-1 mutant strains, the orthologues of *S. cerevisiae* Tup1 and Ssn6, respectively. We previously identified RCO-1 as likely involved in the regulation of glycogen metabolism (Gonçalves et al., 2011) and also observed a severe defect in glycogen accumulation by the *cre-1*^{KO} strain, which suggested that this transcription factor represses glycogen metabolism in *N. crassa.* In this work, we demonstrated that the repressor activity mediated by CRE-1 was observed under repressing and non-repressing carbon conditions, indicating that it was not dependent on the external carbon source. The accumulation of glycogen in *cre-1*^{KO} strain could result from misregulation in the expression of genes encoding glycogenic enzymes. All genes, except *gpn* (encodes glycogen phosphorylase), were up-regulated in *cre-1*^{KO}, indicating that loss of CRE-1 caused derepression of these genes. On the other hand, *gpn* was down-regulated indicating that CRE-1 also plays a role in gene activation, in agreement with Sun and Glass

(2011) and similar to the findings described for this transcription factor in *A. nidulans* (Mogensen et al., 2006) and *T. reesei* (Portnoy et al., 2011). In the Sun and Glass (2011) work, the genes *gsn* and *gpn* were described as putative targets of CRE-1 regulation.

To analyze the regulatory role of CRE-1 on gene expression we examined the 5'-flanking regions of all glycogenic genes and many CreA DNA-binding motifs (5'-SYGGRG-3') were identified. Some motifs were examined for protein binding *in vitro* and *in vivo* based on their positions and number in the genomic region analyzed. DNA shift experiments showed that the *E. coli* recombinant GST-tagged CRE-1 was able to bind to DNA fragments from the *gsn* and *gpn* promoters containing CRE-1 motifs producing DNA-protein complexes with different molecular masses and affinities, depending on the DNA probe. All DNA-binding reactions were specific since binding was reduced or even abolished when the DNA oligonucleotide *cre-1* containing the CRE-1 binding site was used as a specific competitor. These findings revealed that CreA binding sites in the promoters analyzed were indeed the target for the binding of recombinant CRE-1. In addition, the nucleotide sequences in the neighborhood may not play an important role in DNA binding since only a single DNA oligonucleotide competed in all the DNA probes analyzed. Our results are not consistent with findings previously reported in the literature in some aspects. First, the number of complexes formed was independent of the motif orientation; in *A. nidulans* two divergently oriented sequences, separated by one base pair, are necessary for binding (Cubero and Scazzocchio, 1994). Other important difference was related to the number of motifs required for CRE-1 binding; while some reports indicated a requirement for multiple motifs for binding (Cubero and Scazzocchio, 1994; Sun and Glass, 2011), in our work, CRE-1 was able to bind *in vitro* and *in vivo* to only one motif and there seemed to be a correlation between the number of motifs and the number of complexes in the *in vitro* assays. We observed binding *in vivo* of CRE-1 in the motifs present in all promoters, with the exception of a region in the *gsn* promoter, independently of whether a single motif or not. We conclude that under the physiological growth conditions analyzed here (VM medium containing 2% sucrose and 24 h of growth) the majority of CreA motifs existent in the glycogenic gene promoters may be functional *in vivo.* Based on these results we suggest that CRE-1 is a repressor of glycogen synthesis, likely repressing the expression of *gsn* and *gbn* genes, that encode enzymes in the glycogen synthesis, and that in its absence the

repressor activity is released and glycogen accumulates.

Since in *S. cerevisiae* Mig1 recruits the complex Tup1/Ssn6 to glucose-repressed promoters (Treitel and Carlson, 1995), we investigated the role of the RCO-1 and RCM-1 proteins in the regulation of the glycogen metabolism. We demonstrated that both proteins regulate the glycogen metabolism by influencing in the glycogen synthase phosphorylation and in the expression of the genes that encode enzymes of the glycogen metabolism. Taking in consideration the results when repressing and non-repressing conditions were used (Fig. 2B), we conclude that RCO-1 and RCM-1 proteins do not play a regulatory role in the regulation of glycogen metabolism under repressing and non-repressing growth conditions; however, CRE-1 may play a repressor central role in this process. RCO-1 was previously described to have a minor role in CreA-mediated carbon repression in *A. nidulans* (Hicks et al., 2001; García et al., 2008). We have not determined whether these proteins interact to each other and we cannot preclude the possibility of additional proteins being required for binding. The Tup1-Ssn6 complex has been implicated in the repression of a large number of genes in *S. cerevisiae,* although neither Tup1 nor Ssn6 binds directly to DNA (reviewed in Parnell and Stillman, 2011). Different mechanisms have been proposed to explain the repressor function of the Tup1-Ssn6 complex, including interaction with histone deacetylases, inhibition of transcriptional activators and modification of chromatin structures. However, in a recent study, Wong and Struhl (2011) proposed that the Tup1-Ssn6 complex regulates transcription by blocking the activation domains of DNA-binding proteins, thereby preventing their interaction with transcriptional activators rather than by acting as a corepressor. In *N. crassa,* the RCO-1-RCM-1 complex was identified to transiently interact with the clock-controlled transcriptional repressor CSP1 (Sancar et al., 2011), regulating its kinetics of phosphorylation and thus its degradation. Interestingly, the authors described the gene encoding glycogen phosphorylase as a putative target of regulation by CSP-1 and RCO-1.

Our findings show that CRE-1 mediates the repression of glycogen metabolism under carbon repressing and non-repressing conditions, however repressing carbon sources such as glucose are preferred to non-repressing carbon sources such as xylose and glycerol for glycogen accumulation. Glucose is metabolized to pyruvate by glycolysis and further metabolism depends on the growth conditions whether aerobic/anaerobic, whereas xylose is metabolized via the pentose

phosphate pathway. Different organisms, including filamentous fungi, need to regulate the metabolic reprogramming of their glucose/carbon metabolism, although the molecular mechanisms involved are not always well understood. The regulation of galactose metabolism by the *S. cerevisiae* gene *GAL1* provides a good example for understanding such regulation. In glucose-rich medium, *GAL1* is repressed by the Mig1-Tup1-Ssn6 complex (Nehlin et al., 1991), while in galactose-containing medium without glucose, *GAL1* transcription is activated by Gal4 that recruits the SAGA complex (Bhaumik and Green, 2001). The repressed/activated states are the consequence of a distinct chromatin architecture and epigenetic status such that multiple transcriptional regulatory proteins must be required, depending on the DNA region. Han and Emr (2011) showed that in *S. cerevisiae* conversion of the *GAL1* promoter from a repressed state to an activated state is dependent on a cytoplasmic component, phosphatidylinositol 3,5-bisphosphate [PI(3,5)P_2] that interacts with Cti6 protein to assemble the activator complex Cti6-Tup1-Ssn6. More recently, the same group showed that this mechanism controls the reprogramming from glycolysis to gluconeogenesis (Han and Emr, 2013). The genes *FBP1* (encoding fructose-1,6-biphosphatase) and *ICL1* (encoding isocitrate lyase) are under control of Mig1 repressor and the Tup1-Ssn6 corepressor complex and require PI(3,5)P_2 for transcriptional activation.

Although the findings described here represent an important progress in assessing the CRE-1 transcription factor regulating a specific metabolic process in *N. crassa,* more studies are required to understand if there is a role of the RCO-1/RCM-1 complex in this process. One model proposed for the repressor activity of Tup1 protein in yeast suggests that, together with Ssn6, they recruit histone deacetylases for chromatin remodeling at the promoter (Parnell and Stillman, 2011). Since the complex needs to interact with a DNA-binding protein, it is assumed that large protein complexes must be recruited to ensure the repression of target genes. We have previously identified that a histone acetyltransferase protein binds to some regions of the *gsn* promoter (Freitas et al., 2008), a finding that raises interesting questions regarding the role of chromatin architecture in the regulation of this gene. The answer to this question may reveal fundamental aspects of gene regulation in *N. crassa* glycogen metabolism.

Acknowledgments

This work was supported by the Fundação de Amparo à Pesquisa do Estado de São Paulo (FAPESP) and Conselho Nacional de Desenvolvimento Científico e Tecnológico (CNPq), Brazil, for grants and fellowships. We deeply thank NL Glass (University of California, Berkeley, CA, USA) for providing the *cre-1*^{KO} complemented strain. We also thank PA de Castro (from GH Goldman's lab, Faculdade de Ciências Farmacêuticas, USP, Ribeirão Preto, SP, Brazil) and I Malavazi (Universidade Federal de São Carlos, São Carlos, SP, Brazil) for their support on the microscopic analysis.

References

Aro, N., Pakula, T., Penttila, M., 2005. Transcriptional regulation of plant cell wall degradation by filamentous fungi. FEMS Microbiol. Rev. 29, 719-739.

Bertolini, M.C., Freitas, F.Z., de Paula, R.M., Cupertino, F.B., Gonçalves, R.D., 2012. Glycogen Metabolism Regulation in *Neurospora crassa,* in: Witzany G, (Ed.), Biocommunication of Fungi. Springer, Dordrecht, pp. 39-55.

Bhaumik, S.R., Green, M.R., 2001. SAGA is an essential in vivo target of the yeast acidic activator Gal4p. Genes Dev. 15, 1935-1945.

Brown, N.A., de Gouvea, P.F., Krohn, N.G., Savoldi, M., Goldman, G.H., 2013. Functional characterisation of the non-essential protein kinases and phosphatases regulating *Aspergillus nidulans* hydrolytic enzyme production. Biotechnol. Biofuels 6, 91. doi: 10.1186/1754-6834-6-91.

Brunelli, J.P., Pall, M.L., 1993. A series of yeast/*Escherichia coli* lambda expression vectors designed for directional cloning of cDNAs and *cre/lox*-mediated plasmid excision. Yeast 9, 1309-1318.

Cubero, B., Scazzocchio, C., 1994. Two different, adjacent and divergent zinc finger binding sites are necessary for CREA-mediated carbon catabolite repression in the proline gene cluster of *Aspergillus nidulans*. EMBO J. 13, 407-415.

Cziferszky, A., Mach, R.L., Kubicek, C.P., 2002. Phosphorylation positively regulates DNA binding of the carbon catabolite repressor CRE-1 of *Hypocrea jecorina* (*Trichoderma reesei*). J. Biol. Chem. 277, 14688-14694.

Cziferszky, A., Seiboth, B., Kubicek, C.P., 2003. The Snf1 kinase of the filamentous fungus *Hypocrea jecorina* phosphorylates regulation-relevant serine residues in the yeast carbon catabolite repressor Mig1 but not in the filamentous fungal counterpart CRE-1. Fungal Genet. Biol. 40, 166-175.

de Paula, R., de Pinho, C.A., Terenzi, H.F., Bertolini, M.C., 2002. Molecular and biochemical characterization of *Neurospora crassa* glycogen synthase encoded by *gsn* cDNA. Mol. Genet. Genomics 267, 241-253.

De Vit, M.J., Waddle, J.A., Johnston, M., 1997. Regulated nuclear translocation of the Mig1 glucose repressor. Mol. Biol. Cell 8, 1603-1618.

de Vries, R.P., Visser, J., de Graaff, L.H., 1999. CreA modulates the XlnR-induced expression on xylose of *Aspergillus niger* genes involved in xylan degradation. Res. Microbiol. 150, 281-285.

Freitas, F.Z., Bertolini, M.C., 2004. Genomic organization of the *Neurospora crassa gsn* gene: possible involvement of the STRE and HSE elements in the modulation of transcription during heat shock. Mol. Gen. Genomics 272, 550-561.

Freitas, F.Z., Chapeaurouge, A., Perales, J., Bertolini, M.C., 2008. A systematic approach to identify STRE-binding proteins of the *gsn* glycogen synthase gene promoter in *Neurospora crassa*. Proteomics 8, 2052-2061.

Freitas, F.Z., de Paula, R.M., Barbosa, L.C.B., Terenzi, H.F., Bertolini, M.C., 2010. cAMP signaling pathway controls glycogen metabolism in *Neurospora crassa* by regulating the glycogen synthase gene expression and phosphorylation. Fungal Genet. Biol. 47, 43-52.

García, I., Mathieu, M., Nikolaev, I., Felenbok, B., Scazzocchio, C., 2008. Roles of the *Aspergillus nidulans* homologues of Tup1 and Ssn6 in chromatin structure and cell viability. FEMS Microbiol. Lett. 289, 146-154.

Gonçalves, R.D., Cupertino, F.B., Freitas, F.Z., Luchessi, A.D., Bertolini, M.C., 2011. A genome-wide screen for *Neurospora crassa* transcription factors regulating glycogen metabolism. Mol. Cell. Proteomics 10.11. doi: 10.1074/mcp.M111.007963.

Han, B.K., Emr, S.D., 2011. Phosphoinositide [PI(3,5)P_2] lipid-dependent regulation of the general transcriptional regulator Tup1. Genes Dev. 25, 984-995.

Han, B.K., Emr, S.D., 2013. The phosphatidylinositol 3,5-bisphosphate (PI(3,5)P_2)-dependent Tup1 conversion (PIPTC) regulates metabolic reprogramming from glycolysis to gluconeogenesis. J. Biol. Chem. 288, 20633-20645.

Hartree, E.F., 1972. Determination of protein: a modification of the Lowry method that gives a linear photometric response. Anal. Biochem. 48, 422-427.

Hicks, J., Lockington, R.A., Strauss, J., Dieringer, D., Kubicek, C.P., Kelly, J., Keller, N., 2001. RcoA has pleiotropic effects on *Aspergillus nidulans* cellular development. Mol. Microbiol. 39, 1482-1493.

Ilmén, M., Saloheimo, A., Onnela, M.L., Penttilä, M.E., 1997. Regulation of cellulase gene expression in the filamentous fungus *Trichoderma reesei.* Appl. Environ. Microbiol. 63, 1298-1306.

Jonkers, W., Rep, M., 2009. Mutation of CRE-1 in *Fusarium oxysporum* reverts the pathogenicity defects of the FRP1 deletion mutant. Mol. Microbiol. 74, 1100-1113.

Keleher, C.A., Redd, M.J., Schultz, J., Carlson, M., Johnson, A.D., 1992. Ssn6-Tup1 is a general repressor of transcription in yeast. Cell 68, 709-719.

Kulmburg, P., Mathieu, M., Dowzer, C., Kelly, J., Felenbok, B., 1993. Specific binding sites in the alcR and alcA promoters of the ethanol regulon for the CREA repressor mediating carbon catabolite repression in *Aspergillus nidulans*. Mol. Microbiol. 7, 847-857.

Laemmli, U.K., 1970. Cleavage of structural protein during the assembly of the head of bacteriophage T4. Nature 227, 680-685.

720 Lee, K., Ebbole, D., 1998. Tissue-specific repression of starvation and stress
721 responses of the *Neurospora crassa* con-10 gene is mediated by RCO-1. Fungal
722 Genet. Biol. 23, 269-278.
723 Lichius, A., Seidl-Seiboth, V., Seiboth, B., Kubicek, C.P., 2014. Nucleo-cytoplasmic
724 shuttling dynamics of the transcriptional regulators XYR1 and CRE1 under
725 conditions of cellulose and xylanase gene expression in *Trichoderma reesei.* Mol.
726 Microbiol. doi:10.1111/mmi.12824.
727 Lundin, M., Nehlin, J.O., Ronne, H., 1994. Importance of a flanking AT-rich region in
728 target site recognition by the GC box-binding zinc finger protein MIG1. Mol. Cell.
729 Biol. 14, 1979-1985.
730 Mach-Aigner, A.R., Pucher, M.E., Steiger, M.G., Bauer, G.E., Preis, S.J., Mach, R.L.,
731 2008. Transcriptional regulation of xyr1, encoding the main regulator of the
732 xylanolytic and cellulolytic enzyme system in *Hypocrea jecorina*. Appl. Environ.
733 Microbiol. 74, 6554-6562.
734 McCluskey, K., 2003. The Fungal Genetics Stock Center: from molds to molecules.
735 Adv. Appl. Microbiol. 52, 245-262.
736 Mogensen, J., Nielsen, H.B., Hofmann, G., Nielsen, J., 2006. Transcription analysis
737 using high-density micro-arrays of *Aspergillus nidulans* wild-type and creA mutant
738 during growth on glucose or ethanol. Fungal Genet. Biol. 43, 593-603.
739 Nehlin, J.O., Carlberg, M., Ronne, H., 1991. Control of yeast GAL genes by MIG1
740 repressor: a transcriptional cascade in the glucose response. EMBO J. 10, 3373-
741 3377.
742 Olmedo, M., Navarro-Sampedro, L., Ruger-Herreros, C., Kim, S.R., Jeong, B.K., Lee,
743 B.U., Corrochano, L.M., 2010. A role in the regulation of transcription by light for
744 RCO-1 and RCM-1, the *Neurospora* homologs of the yeast Tup1-Ssn6 repressor.
745 Fungal Genet. Biol. 47, 939-952.
746 Orejas, M., MacCabe, A.P., González, J.A.P., Kumar, S., Ramón, D., 1999. Carbon
747 catabolite repression of the *Aspergillus nidulans* xlnA gene. Mol. Microbiol. 31,
748 177-184.
749 Ostling, J., Ronne, H., 1998. Negative control of the Mig1p repressor by Snf1p-
750 dependent phosphorylation in the absence of glucose. Eur. J. Biochem. 252,
751 162-168.
752 Parnell, E.J., Stillman, D.J., 2011. Shields up: the Tup1-Cyc8 repressor complex
753 blocks coactivator recruitment. Genes Dev. 25, 2429-2435.
754 Portnoy, T., Margeot, A., Linke, R., Atanasova, L., Fekete, E., Sándor, E., Hartl, L.,
755 Karaffa, L., Druzhinina, I.S., Seiboth, B., Le Crom, S., Kubicek, C.P., 2011. The
756 CRE-1 carbon catabolite repressor of the fungus *Trichoderma reesei*: a master
757 regulator of carbon assimilation. BMC Genomics 12, 269-280.
758 Roy, P., Lockington, R.A., Kelly, J.M., 2008. CreA-mediated repression in *Aspergillus*
759 *nidulans* does not require transcriptional auto-regulation, regulated intracellular
760 localization or degradation of CreA. Fungal Genet. Biol. 45, 657-670.
761 Ruijter, G.J.G., Visser, J., 1997. Carbon repression in *Aspergilli*. FEMS Microbiol.
762 Lett. 151, 103-114.

763 Sancar, G., Sancar, C., Brügger, B., Ha, N., Sachsenheimer, T., Gin, E., Wdowik, S.,
764 Lohmann, I., Wieland, F., Höfer, T., Diernfellner, A., Brunner, M., 2011. A global
765 circadian repressor controls antiphasic expression of metabolic genes in
766 *Neurospora*. Mol. Cell 44, 687-697.
767 Smith, R.L., Johnson, A.D., 2000. Turning genes off by Ssn6-Tup1: a conserved
768 system of transcriptional repression in eukaryotes. Trends Biochem. Sci. 25, 325-
769 330.
770 Sokolovsky, V., Kaldenhoff, R., Ricci, M., Russo, V.E.A., 1990. Fast and reliable mini-
771 prep RNA extraction from *Neurospora crassa.* Fungal Genet. Newsl. 37, 41-43.
772 Strauss, J., Horvath, H.K., Adballah, B.M., Kindermann, J., Mach, R.L., Kubicek,
773 C.P., 1999. The function of CreA, the carbon catabolite repressor of *Aspergillus*
774 *nidulans,* is regulated at the transcriptional and post-transcriptional level. Mol.
775 Microbiol. 32, 169-178.
776 Sun, J., Glass, N.L., 2011. Identification of the CRE-1 cellulolytic regulon in
777 *Neurospora crassa*. PLoS ONE 6, e25654.
778 Tamaru, H., Zhang, X., McMillen, D., Singh, P.B., Nakayama, J., Grewal, S.I., David
779 Allis, C., Cheng, X., Selker, E.U., 2003. Trimethylated lysine 9 of histone H3 is a
780 mark for DNA methylation in *Neurospora crassa*. Nat. Genet. 34, 75-79.
781 Thomas, J.A., Schlender, K.K., Larner, J., 1968. A rapid filter paper assay for
782 UDPglucose-glycogen glucosyltransferase, including an improved biosynthesis of
783 UDP-^{14}C-glucose. Anal. Biochem. 25, 486-499.
784 Treitel, M.A., Carlson. M., 1995. Repression by SSN6-TUP1 is directed by MIG1, a
785 repressor/activator protein. Proc. Natl. Acad. Sci. USA 92, 3132-3136.
786 Vautard-Mey, G., Fèvre, M., 2000. Mutation of a putative AMPK phosphorylation site
787 abolishes the repressor activity but not the nuclear targeting of the fungal glucose
788 regulator CRE-1. Curr. Genet. 37, 328-332.
789 Vautard-Mey, G., Cotton, P., Fèvre, M., 1999. Expression and compartmentation of
790 the glucose repressor CRE-1 from the phytopathogenic fungus *Sclerotinia*
791 *sclerotiorum*. Eur. J. Biochem. 266, 252-259.
792 Vinuselvi, P., Kim, M.K., Lee, S.K., Ghim, C-M., 2012. Rewiring carbon catabolism
793 repression for microbial cell factory. BMB Rep. 45, 59-70.
794 Vogel, H.J., 1956. A convenient growth medium for *Neurospora crassa* (medium N).
795 Microbiol. Genet. Bull. 13, 42-43.
796 Wong, K.H., Struhl, K., 2011. The Cyc8-Tup1 complex inhibits transcription primarily
797 by masking the activation domain of the recruiting protein. Genes Dev. 25, 2525-
798 2539.
799 Yamashiro, C.T., Ebbole, D.J., Lee, B.U., Brown, R.E., Bourland, C., Madi, L.,
800 Yanofsky, C., 1996. Characterization of *rco-1* of *Neurospora crassa*, a pleiotropic
801 gene affecting growth and development that encodes a homolog of Tup1 of
802 *Saccharomyces cerevisiae*. Mol. Cell Biol. 16, 6218-6228.
803 Ziv, C., Gorovits, R., Yarden, O., 2008. Carbon source affects PKA-dependent
804 polarity of *Neurospora crassa* in a CRE-1-dependent and independent manner.
805 Fungal Genet. Biol. 45, 103-116.
806

807 **Table 1**

808 Oligonucleotides used in this study.

Primers	Sequences[a, b] (5'→3')	Source	Name	Positions
8807-F	***ATG***CAACGCGTACAGTCAGCAG	NCU08807	-	+1 to +22
8807-R	GAATTC***TTA***CAACCGGTCCATCATCTC	NCU08807	-	+1273 to +1293
qGSN-F	TACCAAGCATCACCACCAACCTCT	NCU06687	-	+1541 to +1564
qGSN-R	TGTCTGCGGCTCTTCTGGGTAAAT	NCU06687	-	+1689 to +1712
qGPN-F	TGCCAATATCGAAATCACCCGCGA	NCU07027	-	+2247 to +2261
qGPN-R	TCTCGATGGCCTCAAACACCTTGA	NCU07027	-	+2375 to +2398
qGNN-F	ACAAGCACCCGAACCCAC	NCU06698	-	+1134 to +1151
qGNN-R	AAGGGTGGGCGATGCTGT	NCU06698	-	+1234 to +1251
qRAMIF-F	TCTGCGATGCCGAGTTGT	NCU05429	-	+1487 to +1504
qRAMIF-R	ACTCGTTGCCCTCGAAGT	NCU05429	-	+1616 to +1633
qDESRAM-F	TCGGCGGTAATCAAGCCA	NCU00743	-	+3779 to +3796
qDESRAM-R	TGAATTTGCCGGCTTCGT	NCU00743	-	+3935 to +3952
4054Tub-F	CCTCCACCTTCGTCGGTAACTCC	NCU04054	-	+1091 to +1113
4054Tub-R	GGTACTGCTGGTACTCGGAGACG	NCU04054	-	+1254 to +1276
XLNR-FP2	TGAGGGTGAGAAAGTTGC	p*gsn*	*gsn* 1	-2173 to -2156
XLNR-RP2	TATTCTGCAACGGAACTCC	p*gsn*	*gsn* 1	-2053 to -2035
SREBp-F2	CATGGGAGTATTCGTTGC	p*gsn*	*gsn* 2	-1790 to -1773
GSN-FP4	CTGATTGGGAAAGGTCAGA	p*gsn*	*gsn* 2	-1645 to 1627
emsaSTRE1-F	CACTGCACAGATCTGGAG	p*gsn*	*gsn* 2	-1590 to -1573
emsaSTRE1-R	GAGACATCCATGGGCATT	p*gsn*	*gsn* 2	-1429 to -1412
STRE2i-F	GCTTCAGTGAGGCCCCGT	p*gsn*	*gsn* 3	-350 to -333
STRE2i-R	GCAGATCAGGTCGACGTAGC	p*gsn*	*gsn* 3	-204 to -185
oligoCRE1-F	GAGGCCCCGTT**CCCCGC**TTCCGGCCGG	p*gsn*	oligo *cre-1*	-342 to -316
oligoCRE1-R	CCGGCCGGAA**GCGGGG**AACGGGGCCTC	p*gsn*	oligo *cre-1*	-342 to -316
pGPNNit-F1	CGGTGGGTGGTAGGTTGTG	p*gpn*	*gpn* 1	-2111 to -2093
pGPNNit-R1	CCGACCCCGACTTTGCG	p*gpn*	*gpn* 1	-1938 to -1922
pGPNNit-F3	GTAGTATCACGGTTGGGC	p*gpn*	*gpn* 2	-1287 to -1270
pGPNNit-R3	ACCCCCATTGGCCCCTCC	p*gpn*	*gpn* 2	-1122 to -1105
pGPNxlnr-F	CTAGCCCATCAAGGTACGTG	p*gpn*	*gpn* 3	-321 to -302
pGPNxlnr-R	CCTAGGTGGTGTCTCTGGTC	p*gpn*	*gpn* 3	-203 to -184
GNNp-F3	GTCGCCAAGTTAGGTTCA	p*gnn*	*gnn*	-198 to -181
GNNp-R	CTACTTGACAATCACAAAATTC	p*gnn*	*gnn*	-19 to +3
DEBp-F1	TAACTCTCACAGCGGTCG	p*gdn*	*gdn* 1	-1633 to -1616
DEBp-R1	GCTGACCGCAACAAGACC	p*gdn*	*gdn* 1	-1447 to -1430
DEBp-F2	GCCTGTTTTCTGACGGGT	p*gdn*	*gdn* 2	-707 to -690
DEBp-R2	TTGGCTGTGATAGGACCG	p*gdn*	*gdn* 2	-551 to -534
BRANCH-FP3	GCCCCTCCATGAAGCGAAGA	p*gbn*	*gbn*	-1215 to -1196
BRANCH-RP1	TGGTTGGGCTTCTGGGCG	p*gbn*	*gbn*	-1133 to -1116
pCRE1-F	GCAACGGAGTCTGAACCC	p*cre-1*	*cre-1*	-1226 to -1209
pCRE1-R	CAATACAATACGCAGCAC	p*cre-1*	*cre-1*	-1073 to -1056
qUbi-F	CGAGTCTTCGGATACGATTG	NCU05995	ubiquitin	+735 to +754
pUbi-R	CCATCCTCCAACTGCTTAC	NCU05995	ubiquitin	+842 to +824

809 [a] The *Eco*RI restriction site is underlined in the 8807-R sequence.

810 [b] The ATG start codon and TAA stop codon in the NCU08807-F/R sequences are represented in bold and
811 italic. Primers are positioned according to the ATG start codons. The nucleotides in bold in the
812 oligonucleotides oligoCRE-1-F/R represent the CreA motif.

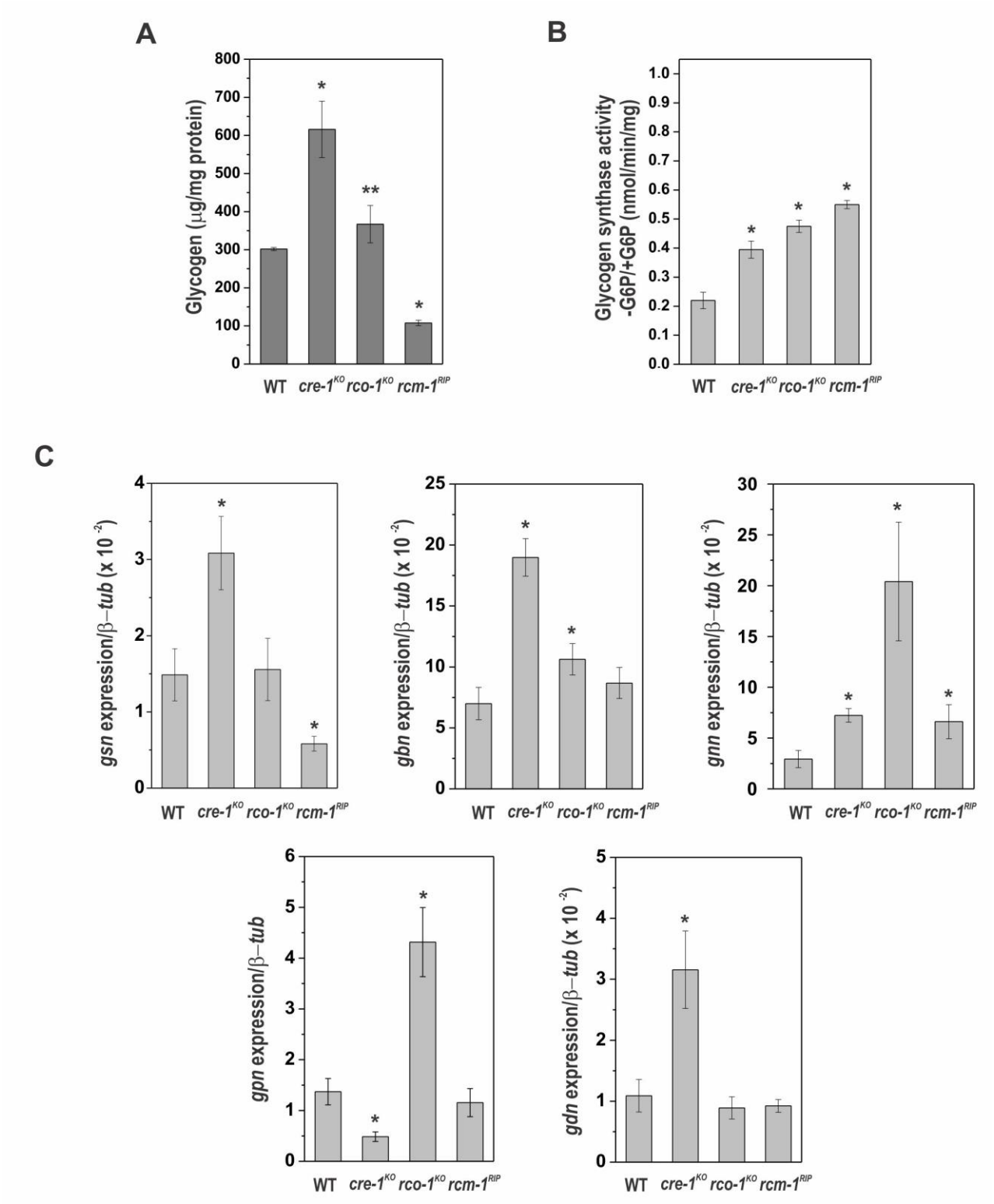

Fig. 1. Glycogen accumulation, glycogen synthase activity and expression of genes encoding glycogen metabolism enzymes under physiological growth. (A) Glycogen accumulation in wild-type and mutant strains. (B) Glycogen synthase activity (-G6P/+G6P ratio) in the same strains. (C) Gene expression analysis of genes *gsn* (NCU006687), *gpn* (NCU07027), *gnn* (NCU06698), *gbn* (NCU05429) and *gdn* (NCU00743) in the same strains. The expression of the tubulin *tub-2* gene (NCU04054) was used as the endogenous control for all genes. Mycelia were grown at 30 °C for 24 h in VM medium containing 2% sucrose. Results represent the average of 3-5 independent experiments. The asterisks indicate significant differences compared to the wild-type strain (*T-test*), **p* < 0.01 and ***p* < 0.05.

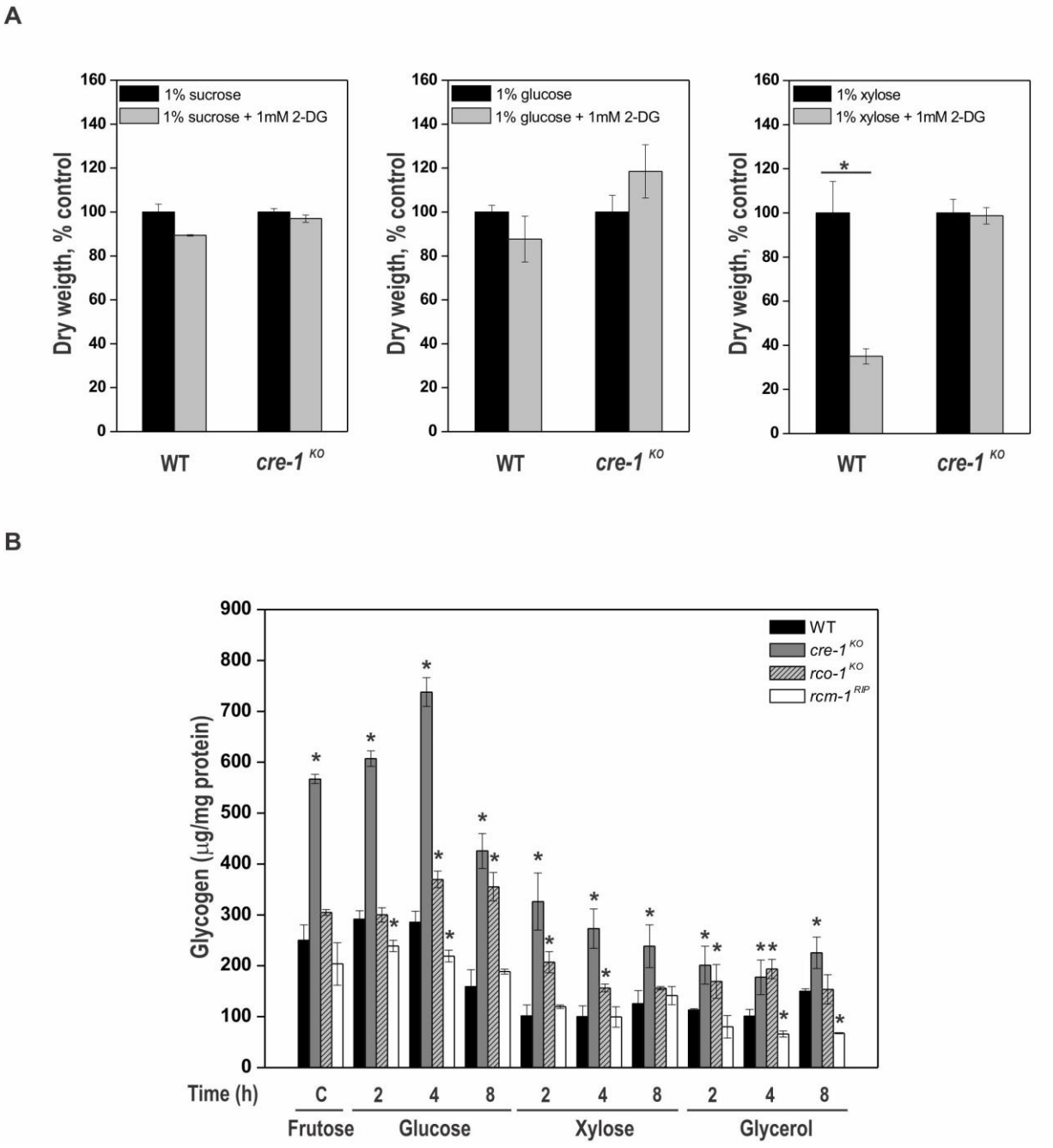

Fig. 2. Glycogen accumulation under different carbon sources. (A) Effect of 2-deoxy-D-glucose (2-DG) on the growth of wild-type and *cre-1*^{KO} mutant strains. Mycelia were grown for 24 h at 30 °C in VM medium containing 1% sucrose (left panel), glucose (middle panel) or xylose (right panel) in the absence or presence of 1 mM 2-DG. Mycelial mats were harvested, dried at 98 ºC for 16 h and weighed. (B) Glycogen content in wild-type and mutant strains. Mycelia were grown at 30 °C for 24 h in VM medium containing 2% fructose (C, control) and then transferred to VM medium containing 2% glucose, xylose or glycerol. Mycelia were collected 2, 4 and 8 h after transferring. Results represent the average of at least three independent experiments. The asterisks indicate significant difference (*T-test*, $p < 0.01$) in the presence and absence of 2-DG (A), and differences between the mutants and wild-type strains in the same growth condition (B).

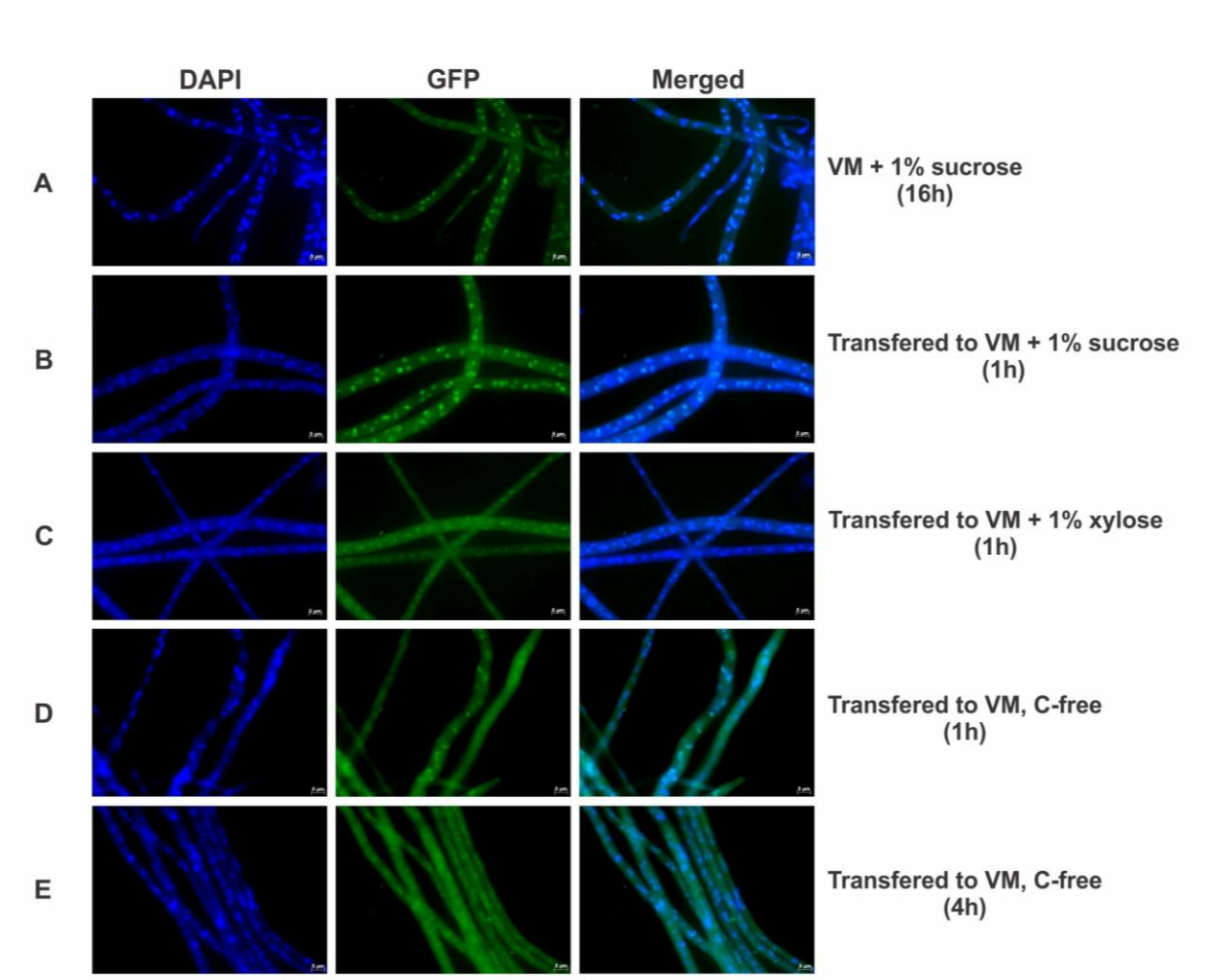

Fig. 3. Subcellular localization of CRE-1::GFP under repressing and derepressing conditions. The *his-3::Pn-cre-1-sfgfp* strain was grown on VM medium containing 1% sucrose for 16 h (A) and then transferred to medium containing sucrose (repressing condition) (B), or xylose (derepressing condition) (C) or a medium lacking carbon source (D and E). Images were taken after 1 and 4 h of incubation. Fluorescence was evaluated using a Zeiss Microscope at a magnification of 100x. Results shown represent one of at least two independent experiments.

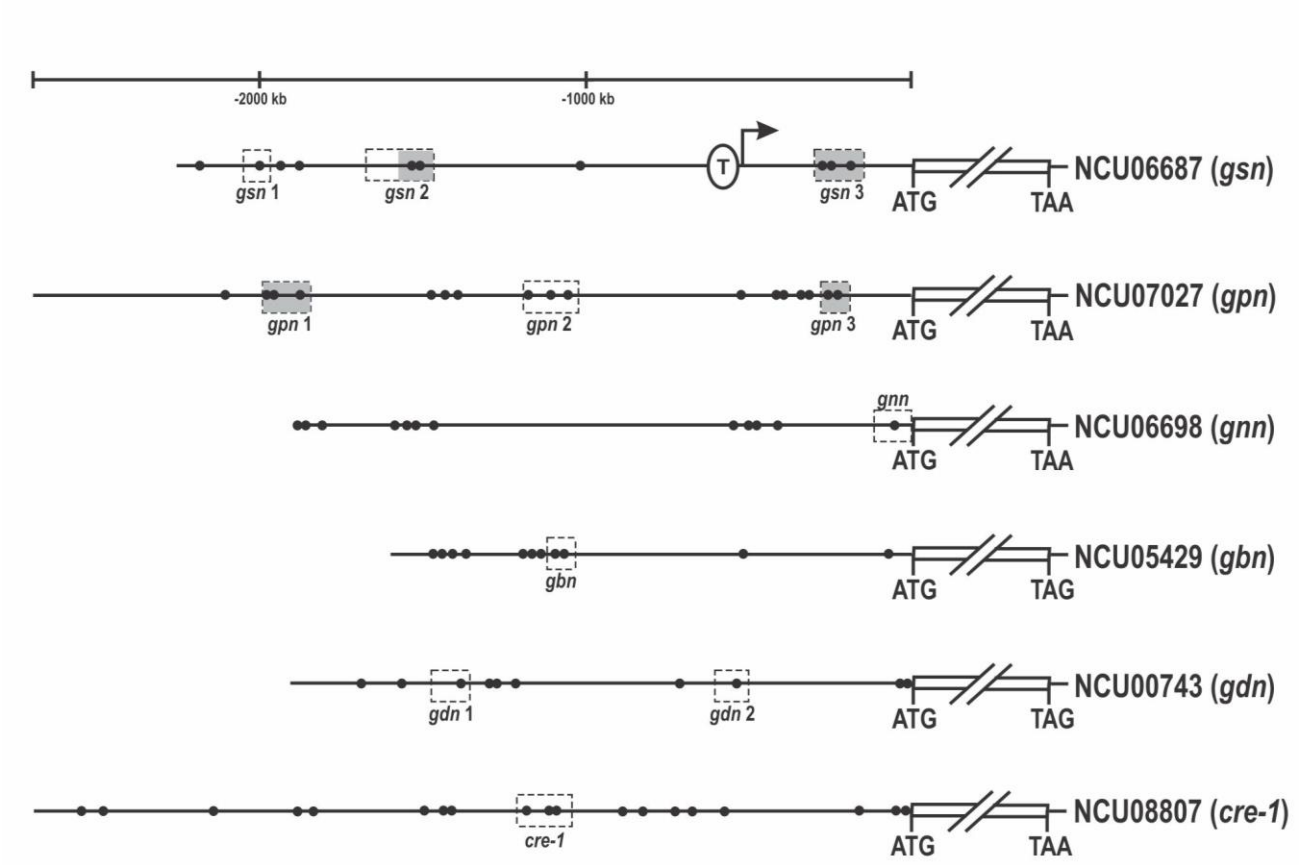

Fig. 4. Schematic representations of CreA motifs in the 5'-flanking regions of the glycogenic genes. The black dots indicate the position of the *A. nidulans* CreA motifs (5'-SYGGRG-3') identified in the 5'-flanking region of the *gsn* (NCU006687), *gpn* (NCU07027), *gnn* (NCU06698), *gbn* (NCU05429), *gdn* (NCU00743) and *cre-1* (NCU08807) genes. The shaded boxes indicate regions that were analyzed by electrophoretic mobility shift assays (EMSA) and the white dashed boxes the regions analyzed by ChIP-qPCR. *gsn* was the only gene whose transcription initiation site (T) was experimentally determined (Freitas and Bertolini, 2004).

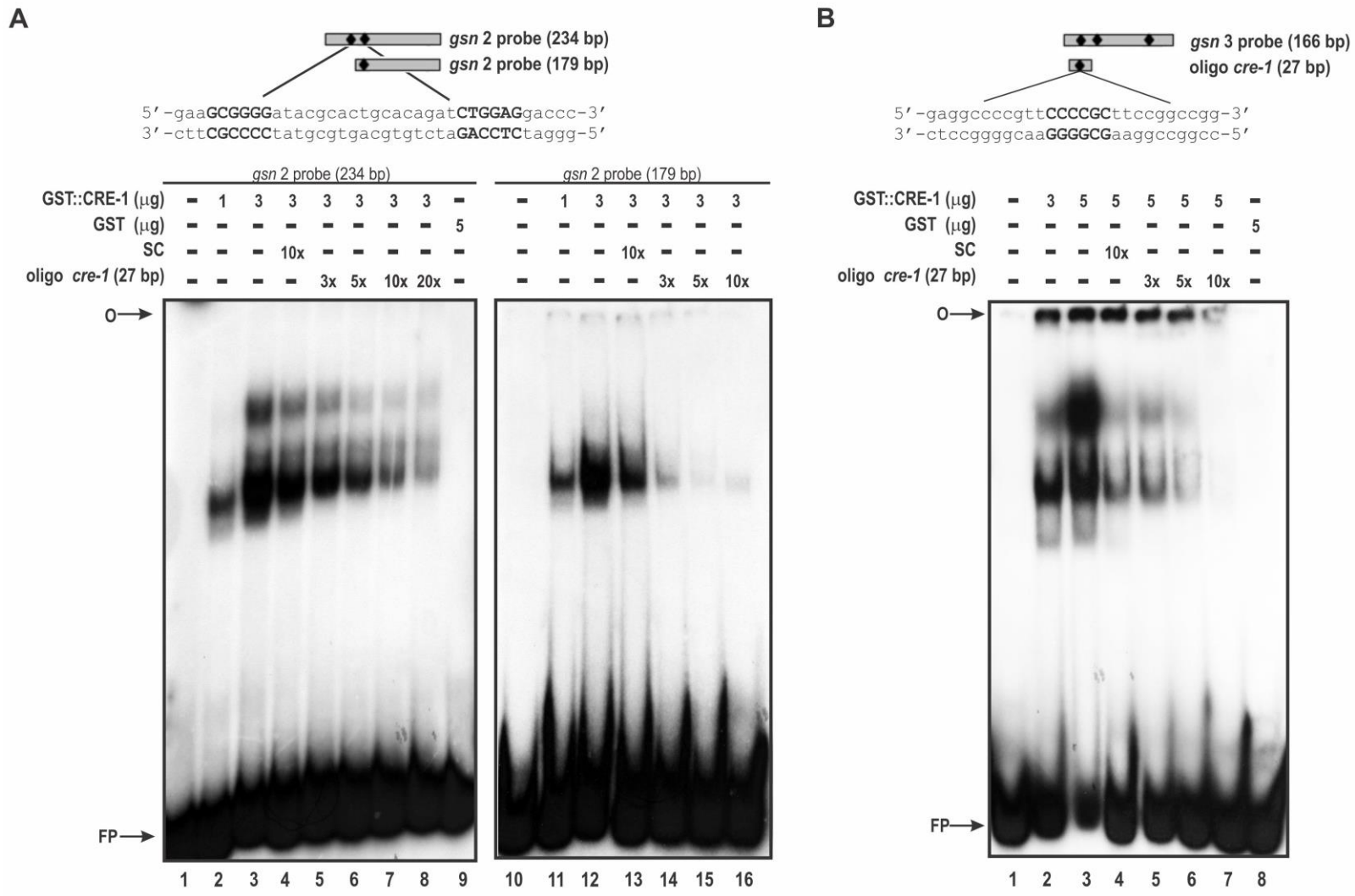

Fig. 5. Binding of recombinant GST::CRE-1 to the *gsn* promoter. (A) Upper panel, schematic representation of the *gsn* 2 probes (179 and 234 bp) with the CreA motifs analyzed. Lower panels, gel shift analysis using different concentrations of GST::CRE-1 and two probes in the absence and presence of specific competitors (SC and oligo *cre-1*). Lanes 1 and 10, *gsn* 2 probe, no protein added. Lane 9, the protein GST was used as a negative control. (B) Upper panel, schematic representation of the *gsn* 3 probe and the oligo *cre-1* with the CreA motifs. Lower panel, gel shift analysis using different concentrations of GST::CRE-1 in the absence and presence of specific competitors (SC and oligo *cre-1*). Lane 1, *gsn* 3 probe, no protein added. Lane 8, the protein GST was used as a negative control. O, gel origin; SC, specific competitor; FP, free probe. Results shown represent one of at least two independent experiments.

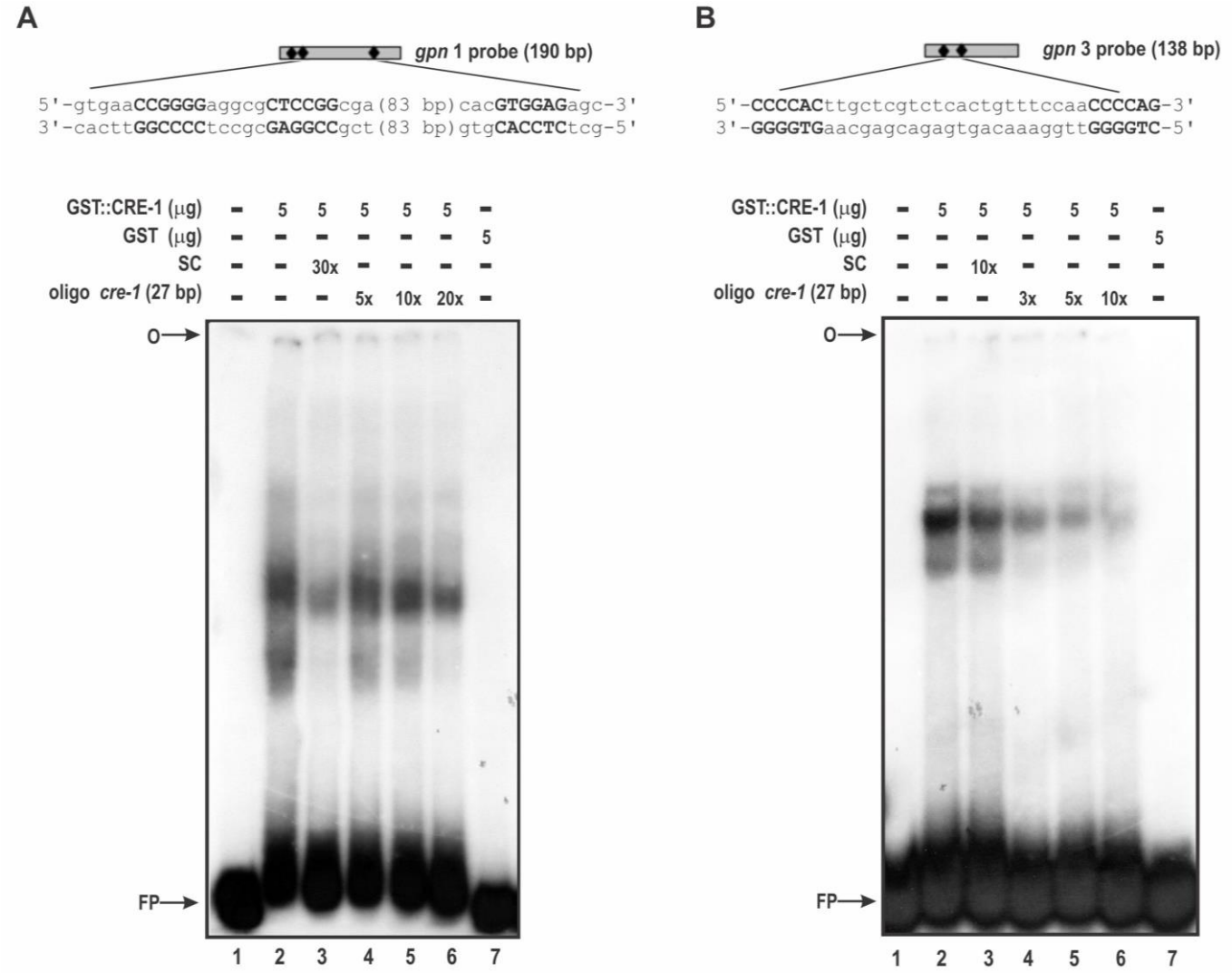

Fig. 6. Binding of recombinant GST::CRE-1 to the *gpn* promoter. (A) Upper panel, schematic representation of the *gpn* 1 probe with the CreA motifs analyzed. Lower panel, gel shift analysis using 5.0 µg of GST::*CRE-1* in the absence and presence of specific competitors (SC and oligo *cre-1*). Lane 1, *gpn* 1 probe, no protein added. Lane 7, the protein GST was used as a negative control. (B) Upper panel, schematic representation of the *gpn* 3 probe with the CreA motif analyzed. Lower panel, gel shift analysis using 5.0 µg of GST::CRE-1 in the absence and presence of specific competitors (SC and oligo *cre-1*). Lane 1, *gpn* 3 probe, no protein added. Lane 7, the protein GST was used as a negative control. O, gel origin; SC, specific competitor; FP, free probe. Results shown represent one of at least two independent experiments.

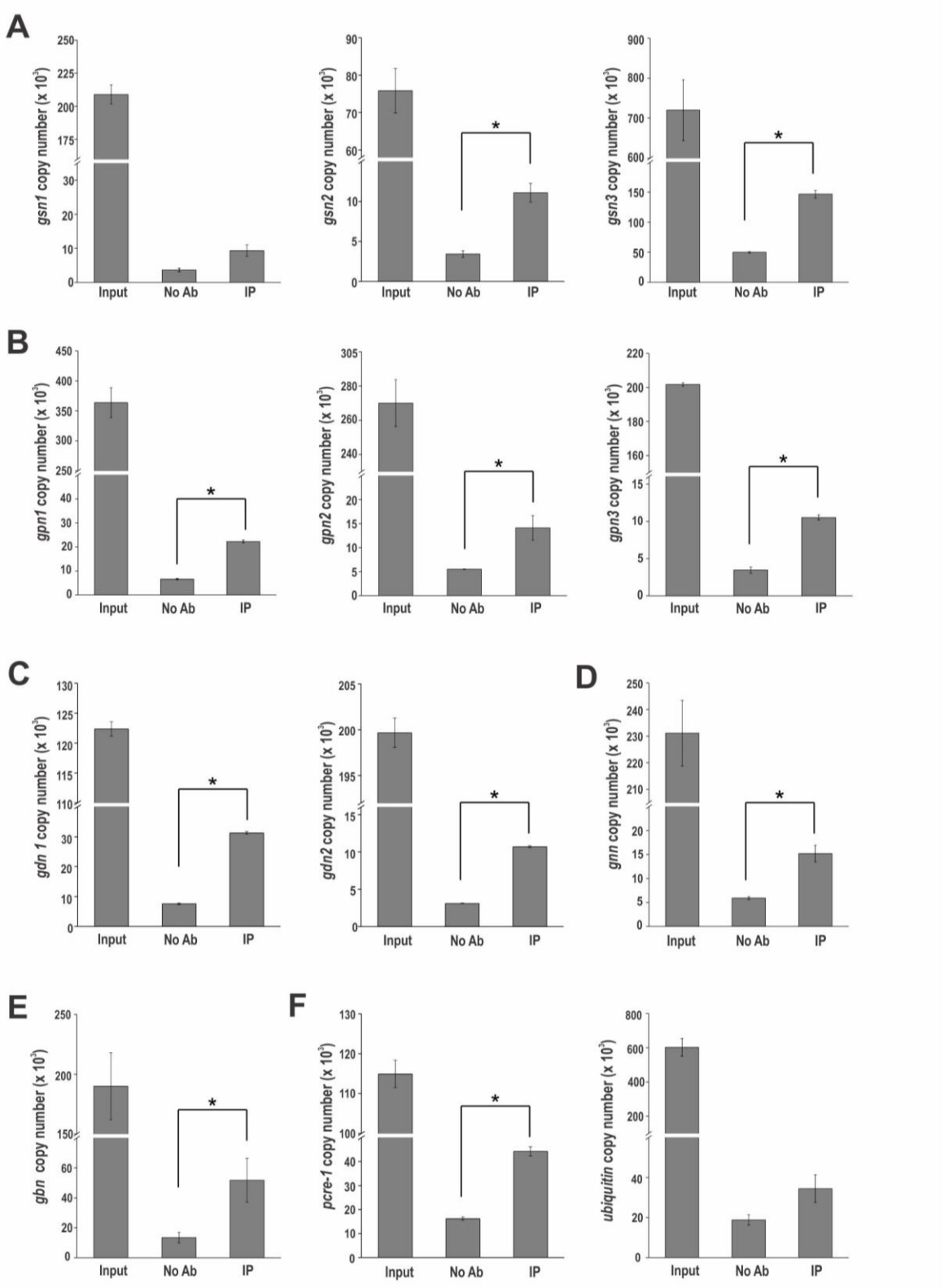

Fig. 7. ChIP-qPCR. Genomic DNA from *his-3::Pn-cre-1-gfp* strain grown at 30 °C for 24 h in VM medium containing 2% sucrose was immunoprecipitated with anti-GFP antibody and subjected to qPCR by absolute quantification to detect direct targets of CRE-1. DNA fragments amplification was analyzed in *gsn* (A), *gpn* (B), *gdn* (C), *gnn* (D), *gbn* (E) and *cre-1* (F) promoters in the genomic DNA. A region inside the coding sequence of the ubiquitin gene was used as negative control of binding (F). The input DNA was used as positive controls of the reactions. As the negative control, the immunoprecipitation reactions were done without antibodies (no Ab). The results represent the average of experimental triplicate in two biological replicates. The asterisks indicate significant differences (*T-test*, $p < 0.001$).

Discussion and Conclusion

In general, the microoganismos has the ability to respond to different environmental conditions, being stressful conditions or not. Although the mechanisms by which cells detect and respond appropriately to these different environmental conditions are oftentimes unknown, a large number of the transcription factors participate in signal transduction pathways involved in the response to these conditions. The methodology for inactivation of genes encoding transcription factors contributed to the use of mutant strains in specific genes in studies of biochemical and molecular characterization, as the reserve carbohydrates regulation.

Glycogen and trehalose are considered main glucose reserve sources in the microorganisms, and their accumulation or degradation is influenced by environmental conditions. In *N. crassa*, glycogen is degraded under heat shock stress and trehalose is accumulated (NOVENTA-JORDÃO et al., 1996; NEVES et al., 1991; DE PINHO et al., 2001). In carbon starvation, the levels of glycogen and trehalose content are reduced (DE PINHO et al., 2001; NOVENTA-JORDÃO et al., 1996). However, few studies have shown how the reserve carbohydrates are regulated, especially regarding the key regulatory enzymes of each process and which transcription factors could be involved in this regulation under different conditions. Transcription factors normally control gene transcription by facilitating recruitment and activation of the transcription machinery or by interacting with activator or repressor proteins.

In this work, we focused in the glycogen and trehalose metabolism regulation by different transcription factors in diverse experimental conditions, such as biological clock, normal and alkaline pH, calcium stress, repressing, non-repressing and depressing carbon sources using *N. crassa* as model organism. Other studies have shown the carbohydrates regulation under heat shock, different nitrogen sources and during vegetative growth.

The circadian clock drives cycles of energy storage and utilization in cyanobacteria, fungi, flies, plants and mammals in anticipation of changes in the external environment, using an internal 24 hours clock system. Human beings are diurnal and conduct most of activities during the day, including feeding, exercising, and working. However, this system has been challenged in modern society by increases in night activites that could disrupt the clock and energy homeostasis, leading to some metabolic diseases (reviewed in FENG; LAZAR, 2012). Recent researches have focused on the crosstalk between the circadian clock and

metabolism. The metabolism is clock regulated in mammals and the accumulation or degradation of nutrients and metabolites lead to the balance of energy disponible during the day. The basic clock machinery is present in most organs, assembled in a hierarchical system in which the central clock can entrain peripheral clocks (reviewed in FENG; LAZAR, 2012). Therefore, the biological clock of mammals involves a complex regulatory network that is regulated by the central clock and by food intake via hormones and nutrients and metabolites. Using a simple organism, we focused our studies in the connection between the regulation of glycogen metabolism and the biological clock in *N. crassa*, trying to understand the transcriptional regulation of the rate-limiting metabolic enzymes, glycogen synthase and glycogen phosphorylase, and the transcription factors that may be involved in this connection.

Our results show that glycogen accumulation and the expression of *gsn* and *gpn* genes are rhythmic, with peaks in subjective night and in subjective morning, respectively. According to ChIP-seq data, VOS-1 and others transcription factors could participate in this connection, but the binding peaks of VOS-1 to *gsn* and *gpn* promoters were more consistent than other proteins and preliminary data from RNA-seq showed that VOS-1 regulates genes involved in metabolism, development, circadian clock, cell wall, MAPK kinase and stress response (data not published). We showed that VOS-1 is light induced and clock regulated and binds to *gsn* and *gpn* promoters. However, the Δ*vos-1* mutant strain showed rhythmic glycogen accumulation and *gsn* and *gpn* expression, though the amplitude of the rhythmicities was reduced when compared to the wild-type strain. Other transcription factors seem to participate in rhythmic glycogen metabolism.

Recently, a collaboration with Dr. Christian I. Hong from University of Cincinnati, Ohio, USA, was proposed. He works with *N. crassa* circadian clock and mathematical modeling to investigate the underlying molecular mechanisms of how circadian clock regulates glycogen metabolism. The results of his research group showed that the CSP-1 transcription factor, that is clock controlled and represses WCC, could act in the *gpn* regulation, since the *gpn* rhythmic gene expression was abolished in absence of *csp-1*. However, the *gsn* expression maintained rhythmic in *csp-1* mutant cells. Combining his results and ours, a mathematical model was proposed in which VOS-1 and CSP-1 transcription factors could act together to maintain the *gsn* and *gpn* rhythmic expression. We not preclude the existence of additional transcription factors acting in parallel under this condition.

Glycogen was also quantified in Δ*csp*-1 and Δ*csp-1* Δ*vos-1* mutant strains and the results showed rhythmic accumulation with peaks in subjective night and period around 22 hours in both strains. Taken together, these data indicate that the absence of VOS-1, or CSP-1 or both transcription factors does not completely abolish the rhythmicity of glycogen accumulation. Other transcription factors were tested in this model, such as SAH-1, but the results were not favorable (data not shown). Our results suggest a complex regulatory mechanism of the circadian glycogen accumulation that involves more than one transcription factor and the participation of the White-Collar-Complex. A new mathematical model predicts that the core clock transcription factors, WC-1/WC-2, could cooperate with clock-controlled transcription factors to regulate the circadian oscillation of *gsn* and *gpn* genes. In the model, WC-1 could act together with VOS-1 in *gsn* rhythmic expression and VOS-1 and CSP-1 in *gpn* rhythmic expression, showing cooperative regulations of three different proteins. Glycogen was quantified in Δ*wc*-1 mutant strain and the rhythmic glycogen accumulation was abolished. Current experiments are underway to determine the WC-1 transcription factor participation in the glycogen metabolism regulation. The interaction or cooperation among these transcription factors is not described yet.

The cell clock machinery consists of several transcriptionl-translational feedback loops, which allow oscillations with a period around 24 hours. The downstream effects are dependent on the core components of the clock, temperature, light and environmental conditions. We focused in the transcriptional regulation of the main glycogenic genes, but it is necessary to emphasize that GSN and GPN enzymes are both regulated by allosterism and phosphorylation. These post-transcriptional events can be clock regulated and could influence the final glycogen accumulation, besides the participation of other glycogenic enzymes. Crosstalk between the circadian rhythm and metabolism is essential for maintaining metabolic homeostasis, and much more studies are necessary to understand the complex regulatory system involving both processes in *N. crassa*.

In addition to the VOS-1 transcription factor, other proteins were also described here in their role in glycogen and/or trehalose metabolism regulation. Initially, we characterized the pH signaling components, consisting of six *pal* genes orthologs to the *A. nidulans pal* genes. Different results were found when compared to other fungi. Interestingly, the expression of tyrosinase, which encodes the limitant enzyme in melanin metabolism, was induced by pH and regulated by PAC-3. PAC-3

undergoes only one proteolytic cleavage under alkaline pH and this cleavage can occur independent of the pH, since the PAC-3 processed form was found in acid to normal pH. Another interesting data was the interaction between PAC-3 NLS and importin-α *in vitro*. New experiments are important to determine the *in vivo* interaction between PAC-3 NLS and importin-α and the participation of PAL proteins in the PAC-3 processing, particularly the PAL-8 (*A. nidulans* PalH – pH sensor) and PAL-2 (*A. nidulans* PalB – signaling protease).

Our previous results showed that glycogen accumulation and *gsn* expression were down-regulated under alkaline pH in *N. crassa* (CUPERTINO et al., 2012). In addition, some genes alkali-regulated were regulated by calcium, showing that calcium-mediated pathway can be fully or partially responsible for the high pH response in yeast. Rim101- and calcineurin-pathway can be involved in the alkaline pH response in *S. cerevisiae* (SERRANO et al., 2002). Besides that, extracellular concentration of calcium stimulates the cellulase production in *Trichoderma reesei* (CHEN et al., 2016), suggesting that signaling pathways downstream of calcineurin can be involved in regulation of cellulose genes and other metabolic genes. Based on these informations, we decided to evaluate the glycogen and trehalose accumulation at alkaline pH, and examine the effects of Ca^{2+} on glycogenic and trehalose genes regulation.

We found that glycogen and trehalose are differently regulated depending on the stress conditions. Both reserve carbohydrates were down accumulated at alkaline pH and over accumulated in the presence of low calcium concentration. PAC-3 influenced the glycogen and trehalose accumulation under both conditions. It is interesting observe that most of glycogenic genes are down regulated under alkaline pH, while the trehalose genes are up regulated. Our results provide insight about reserve carbohydrates metabolism regulation and suggest a likely connection between pH and calcium signaling by PAC-3 transcription factor.

Finally, we characterized CRE-1 transcription factor, ortholog to CreA/Mig1 from *A. nidulans* and *S. cerevisiae*, respectively, together the RCO-1 and RCM-1 corepressors orthologs to *S. cerevisiae* Tup1-Ssn6, respectively. In yeast, Tup-1 and Ssn6, that do not have DNA binding dominan, form a complex that contribute to the repression of many genes in response to different signaling pathways when interact with other proteins. Various transcription factors recruit the Tup1-Ssn6 complex, such as: Crt1 that regulates genes in DNA damage response (HUANG; ZHOU; ELLEDGE,

1998), Rox1 that regulates genes in anaerobiosis response (BALASUBRAMANIAN; LOWRY; ZITOMER, 1993), Mig1 that regulates genes repressed by glucose (NEHLIN; CARLBERG; RONNE, 1991). Here we describe the partipation of these proteins in the glycogen metabolism regulation.

The glycogen accumulation and glycogen synthase activity were regulated by CRE-1, RCO-1 and RCM-1. However, CRE-1 appears act as a repressor of glycogen accumulation under repressing and non-repressing growth conditions. CRE-1 recognizes the same CreA motif *in vivo* and *in vitro*. An interesting data was that CRE-1 was able to bind to *gsn* and *gpn* promoters *in vitro* without partner proteins. In *in vivo* assay, it was not possible to verify the CRE-1, RCO-1 and RCM-1 interaction. The two-hibrid, pulldown and co-immunoprecipitation assays were performed to identify interactions among these proteins, but were unsuccessful experiments.

Other transcription factors, SEB-1 and NIT-2, were also analyzed in our group. SEB-1 is involved in multiple cellular processes under different stress conditions, such as heat shock, pH, osmotic and oxidative stresses. SEB-1 translocates to nucleus under heat shock, osmotic and oxidative stress conditions, and regulates glycogen and trehalose metabolism under heat shock. The recombinant SEB-1 recognizes and binds to the *N. crassa* STRE (stress responsive elements, 5'-CCCCT-3') motif *in vitro* in *gsn* promoter. The expression of glycogenic genes was differently regulated by SEB-1, since the transcription factor bound to all glycogenic genes, especially under heat shock. Our data suggest the interconnection among many biological processes mediated by SEB-1 (Attachment, FREITAS et al., 2016).

The NIT-2 transcription factor, responsible for the global regulation of genes involved in the catabolism of secondary nitrogen sources, was characterized. Many *N. crassa* NIT-2 motifs (5'-GATA-3') were identified in all glycogenic gene promoters and in *cre-1* promoter, suggesting a regulatory connection between nitrogen and carbon metabolism. NIT-2 was able to bind *in vivo* to all glycogenic promoters under different nitrogen sources, the expression of all glycogenic genes was strongly influenced by nitrogen sources, and glycogen accumulation was down regulated. NIT-2 was also able to bind to *cre-1* promoter, suggesting a link between both processes (data not published).

Taken together all results presented here, we observed that many transcription factors are able to regulate glycogen accumulation by regulating the glycogenic genes, especially *gsn* and *gpn*, that encoding the main regulatory

enzymes. Each transcription factor seems to regulate glycogen in different conditions: PAC-3 in pH and calcium stresses, VOS-1 in the circadian clock, SEB-1 in heat shock stress, NIT-2 in different nitrogen sources and CRE-1 in different carbon sources. However, these transcription factors could act together in the same condition, as described to NIT-2-CRE-1 and VOS-1-CSP-1 transcription factors. We identified NIT-2 motifs in *cre-1* promoter, and NIT-2 and CRE-1 motifs in *gsn* promoter. The CRE-1 motif, located at -1578 pb relative to the ATG start codon, is very close to NIT-2 motif (-1561 pb) in *gsn* promoter. We can speculate that NIT-2 could directly regulate *cre-1* expression, and NIT-2 together CRE-1 could regulate *gsn* gene expression in a cooperative action. In the same promoter, SEB-1, PAC-3 and VOS-1 motifs are located at -1507 pb, -1813 pb and -1812 pb, respectively, relative to the ATG start codon. This region in *gsn* promoter seems to be a very regulatory region, recognized by many transcription factors. It is interesting observe that PAC-3 and VOS-1 share the same motif in *gsn* promoter. We may speculate that more than one transcription factor could act together in gene expression, binds to the same promoter region and/or interacts with other proteins.

A schematic representation was proposed based on the data presented in this work (Figure 4). The circadian clock, light and dark conditions, activates the White-Collar Complex (WC-1 and WC-2) that regulates clock controlled genes, such as *vos-1*. VOS-1 transcription factor regulates the rhythmic expression of *gsn* and *gpn* as an activator. Sucrose, a repressor carbon source, activates CRE-1 transcription factor, which represses the expression of *gsn*, *gbn*, *gdn*, and *gnn*. Alkaline pH signal transduction is activated by pH sensor(s) that requires the PAL proteins to mediate the proteolytic cleavage of PAC-3. PAC-3 activates the expression of *tps-1*, *tre-1* and *tre-2* under alkaline pH and represses the *gsn*, *gbn*, *gdn* and *tps-2* expression. The high calcium concentration also induced the expression of *pac-3,* in a direct or indirect manner. Calcium activates calmodulin activating calcineurin, which activates the CRZ-1 transcription factor. It is not possible to know whether additional transcription factors are activated either by high calcium concentration or by calcineurin. We identified two *N. crassa* PAC-3 motifs in the *crz-1* promoter and five *N. crassa* CRZ-1 motifs (5'-RDGGCKNWR-3') (WEIRAUCH et al., 2014) in *pac-3* promoter. Although the CRZ-1 motif is a degenerate consensus sequece, it is possible to speculate that PAC-3 could regulate the expression of *crz-1* and vice versa. Finally, heat shock stress (transfer from 30ºC to 45ºC) induced the expression

of *seb-1* and SEB-1 transcription factor represses the expression of *gnn* and *gsn* under this condition, leading to down regulation of glycogen accumulation using a wild-type strain.

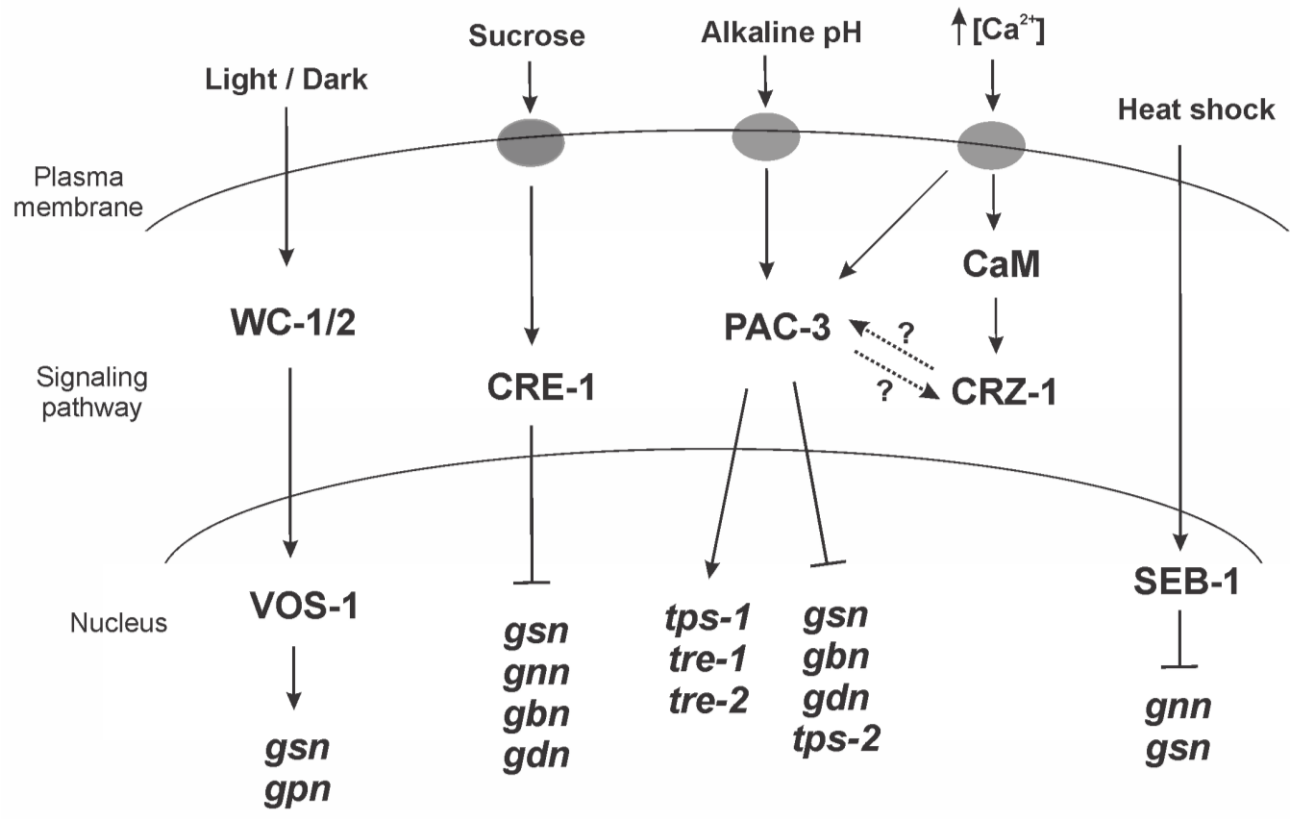

Figure 4- Schematic representation of transcription factors regulating glycogen and trehalose gene expression in *N. crassa* under different conditions: circadian clock (light and dark), sucrose as carbon source, alkaline pH, high concentration of calcium and heat shock. CaM, calmodulin. The question marks and dashed arrows indicate a probably regulation not studied in this work. VOS-1 and PAC-3 are involved in gene expression activation, and CRE-1, PAC-3 and SEB-1 are involved in the gene expression repression.

Our results showed important data about transcription factors in a specific condition, suggesting the existence of a link among them and openning new opportunities for investigating key questions concerning glycogen and trehalose metabolism regulation. Some of these questions are: Would the trehalose accumulation be rhythmic? What transcription factor could participate in this regulation? Could the transcription factors VOS-1, CRE-1 and PAC-3 participate in the carbohydrate metabolism regulation in other conditions? Would form a complex? In conclusion, the regulation of reserve carbohydrates in *N. crassa* involves a complex regulatory system mediates by a transcription factor network, interconnecting glycogen and trehalose metabolism to different cellular processes.

REFERENCES

ADAMS, T. H.; WIESER; J. K.; YU, J. H. Asexual sporulation in *Aspergillus nidulans*. **Microbiol. Mol. Biol. Rev.**, v. 62, n. 1, p. 35-54, 1998.

AHMED, Y. L. et al. The velvet family of fungal regulators contains a DNA-binding domain structurally similar to NF-κB. **PLoS Biol.**, v. 11, n. 12, 2013. doi:10.1371/journal.pbio.1001750.

ALBERTS, B. et al. **Molecular biology of the cell**. 4th ed. New York: Garland Science, 2002. 1463 p.

ALDABBOUS, M. S. et al. The *ham-5*, *rcm-1* and *rco-1* genes regulate hyphal fusion in *Neurospora crassa*. **Microbiology**, v. 156, n. 9, p. 2621-2629, 2010.

ALONSO, M. D. et al. A new look at the biogenesis of glycogen. **FASEB J.**, v. 9, n. 12, p. 1126-1137, 1995.

ARO, N.; PAKULA, T.; PENTTILA, M. Transcriptional regulation of plant cell wall degradation by filamentous fungi. **FEMS Microbiol. Rev.**, v. 29, n. 4, p. 719-739, 2005.

ARPAIA, G. et al. Involvement of protein kinase C in the response of *Neurospora crassa* to blue light. **Mol. Gen. Genet.**, v. 262, n. 2, p. 314-322, 1999.

ARST H. N.; PEÑALVA, M. A. pH regulation in *Aspergillus* and parallels with higher eukaryotic regulatory systems. **Trends Genet.**, v. 19, n. 4, p. 224-231, 2003.

ASHER, G.; SASSONE-CORSI, P. Time for food: the intimate interplay between nutrition, metabolism, and the circadian clock. **Cell**, v. 161, n. 1, p. 84-92, 2015.

BALASUBRAMANIAN, B.; LOWRY, C. V.; ZITOMER, R. S. The Rox1 repressor of the *Saccharomyces cerevisiae* hypoxic genes is a specific DNA-binding protein with a high-mobility-group motif. **Mol. Cell. Biol.**, v. 13, n. 10, p. 6071-6078, 1993.

BALLARIO, P. et al. White collar-1, a central regulator of blue light responses in Neurospora, is a zinc finger protein. **EMBO J.**, v. 15, n. 7, p. 1650-1657, 1996.

BARBOSA, L. C. B. **Caracterização parcial dos sítios de fosforilação da enzima glicogênio sintase de *Neurospora crassa***. 2007. 79 f. Dissertação (Mestrado em Biotecnologia) - Instituto de Química, Universidade Estadual Paulista, Araraquara, 2007.

BELL, W. et al. Composition and functional analysis of the *Saccharomyces cerevisiae* trehalose synthase complex. **J. Biol. Chem.**, v. 273, n. 50, p. 33311-33319, 1998.

BERTOLINI, M. C. et al. Glycogen metabolism regulation in *Neurospora crassa*. In: WITZANY, G. (Ed.). **Biocommunication of fungi**. Dordrecht: Spring Science, 2012. Chap. 2, p. 39-56.

BISTIS, G. N.; PERKINS, D. D.; READ, N. D. Different cell type in *Neurospora crassa*. **Fungal Genet. Newls.**, v. 50, p. 17-19, 2003.

BLACKWELL, M. The fungi: 1, 2, 3 … 5.1 million species. **Am. J. Bot.**, v. 98, n. 3, p. 426-438, 2011.

BONI, A. C. **Caracterização funcional do produto da ORF NCU03043 de *Neurospora crassa* homólogo ao fator de transcrição FlbC de *Aspergillus nidulans***. 2014. 104 f. Dissertação (Mestrado em Biotecnologia) - Instituto de Química, Universidade Estadual Paulista, Araraquara, 2014.

BORKOVICH, K. A. et al. Lessons from the genome sequence of *Neurospora crassa*: tracing the path from genomic blueprint to multicellular organism. **Microbiol. Mol. Biol. Rev.**, v. 1, n. 68, p. 1-108, 2004.

BRODY, S. et al. Circadian rhythms in *Neurospora crassa*: downstream effectors. **Fungal Genet. Biol.**, v. 47, n. 2, p. 159-168, 2010.

CANDIDO, T. S. et al. A protein kinase screen of *Neurospora crassa* mutant strains reveals that the SNF1 protein kinase promotes glycogen synthase phosphorylation. **Biochem. J.**, v. 464, n. 3, p. 323-334, 2014.

CARACUEL, Z. et al. pH response transcription factor PacC controls salt stress tolerance and expression of the P-Type Na^+-ATPase Ena1 in *Fusarium oxysporum*. **Eukaryotic Cell**, v. 2, n. 6, p. 1246-1252, 2003.

CHEN, C. H.; LOROS, J. J. Neurospora sees the light: light signaling components in a model system. **Commun. Integr. Biol.**, v. 2, n. 5, p. 448-451, 2009.

CHEN, C. H.; DUNLAP, J. C.; LOROS, J. J. Neurospora illuminates fungal photoreception. **Fungal Genet. Biol.**, v. 47, n. 11, p. 922-929, 2010.

CHEN, C. H. et al. Genome-wide analysis of light-inducible responses reveals hierarchical light signalling in Neurospora. **EMBO J.**, v. 28, n. 8, p. 1029-1042, 2009.

CHEN, L. et al. Characterization of the Ca^{2+}-responsive signaling pathway in regulating the expression and secretion of cellulases in *Trichoderma reesei* Rut-C30. **Mol. Microbiol.**, v. 100, n. 3, p. 560-575, 2016.

CHENG, C. et al. Requirement of the self-glucosylating initiator proteins Glg1p and Glg2p for glycogen accumulation in *Saccharomyces cerevisiae*. **Mol. Cell. Biol.**, v. 15, n. 12, p. 6632-6640, 1995.

COLLETT, M. A. et al. Light and clock expression of the Neurospora clock gene *frequency* is differentially driven by but dependent on WHITE COLLAR-2. **Genetics**, v. 160, n. 1, p. 149-158, 2002.

COLONNA, W. J.; MAGEE, P. T. Glycogenolytic enzymes in sporulating yeast. **J. Bacteriol.**, v. 134, n. 3, p. 844-853, 1978.

COLOT, H. V. et al. A high throughput gene knockout procedure for Neurospora reveals functions for multiple transcription factors. **Proc. Natl. Acad. Sci. U. S. A.**, v. 103, n. 27, p. 10352-10357, 2006.

COOPER, G. M. **The cell, a molecular approach**. 2nd ed. Washington: ASM Press, 2000. 689 p.

CORNET, M.; GAILLARDIN, C. pH signaling in human fungal pathogens: a new target for antifungal strategies. **Eukaryotic Cell**, v. 13, n. 3, p. 342-352, 2014.

CORREA, A. et al. Multiple oscillators regulate circadian gene expression in Neurospora. **Proc. Natl. Acad. Sci. U. S. A.**, v. 100, n. 23, p. 13597-13602, 2003.

CUPERTINO, F. B. et al. Ambient pH controls glycogen levels by regulating glycogen synthase gene expression in *Neurospora crassa*. New insights into the pH signaling pathway. **PLoS One**, v. 7, n. 8, 2012. doi:10.1371/journal.pone.0044258.

DAVIS, R. H. **Neurospora**: contributions of a model organism. New York: Oxford University Press, 2000. 333 p.

DAVIS, R. H.; PERKINS, D. D. Neurospora: a model of model microbes. **Nature Rev. Genet.**, v. 3, n. 5, p. 397-403, 2002.

DE PAULA, R. et al. Molecular and biochemical characterization of the *Neurospora crassa* glycogen synthase encoded by the *gsn* cDNA. **Mol. Genet. Genomics**, v. 267, n. 2, p. 241-253, 2002.

DE PAULA, R. M. et al. GNN is a self-glucosylation protein involved in the initiation step of glycogen biosynthesis in *Neurospora crassa*. **Arch. Biochem. Biophys.**, v. 435, n. 1, p. 112-124, 2005a.

DE PAULA, R. M. et al. Biochemical characterization of the *Neurospora crassa* glycogenin (GNN), the self-glucosylating initiator of glycogen synthesis. **FEBS Lett.**, v. 579, n. 10, p. 2208-2214, 2005b.

DE PINHO, C. A. et al. Mobilisation of trehalose in mutants of the cyclic AMP signalling pathway, *cr-1* (CRISP-1) and *mcb* (microcycle conidiation), of *Neurospora crassa*. **FEMS Microbiol. Lett.**, v. 199, n. 1, p. 85-89, 2001.

DEGLI-INNOCENTI, F.; POHL, U.; RUSSO, V. E. A. Photoinduction of protoperithecia in *Neurospora crassa* by blue light. **Photochem. Photobiol.**, v. 37, n. 1, p. 49-51, 1983.

DINAMARCO, T. M. et al. Molecular characterization of the putative transcription factor SebA involved in virulence in *Aspergillus fumigatus*. **Eukaryotic Cell**, v. 11, n. 4, p. 518-531, 2012.

DOI, R.; OISHI, K.; ISHIDA, N. CLOCK regulates circadian rhythms of hepatic glycogen synthesis through transcriptional activation of *Gys2*. **J. Biol. Chem.**, v. 285, n. 29, p. 22114-22121, 2010.

DUNLAP, J. C. Molecular bases for circadian clocks. **Cell**, v. 96, n. 2, p. 271-290, 1999.

DUNLAP, J. C.; LOROS, J. J.; DECOURSEY, P. J. **Chronobiology**: biological timekeeping. Massachusetts: Sinauer Associates, 2004. 406 p.

DUNLAP, J. C. et al. Enabling a community to dissect an organism: overview of the Neurospora functional genomics project. **Adv. Genet.**, v. 57, n. 1, p. 49-96, 2007.

ECKEL-MAHAN, K.; SASSONE-CORSI, P. Metabolism and the circadian clock converge. **Physiol. Rev.**, v. 93, n. 1, p. 107-135, 2013.

EDMUNDS, L. N. J. **Cellular and molecular bases of biological clocks**. New York: Springer, 1987. 497 p.

EISENDLE, M. et al. Biosynthesis and uptake of siderophores is controlled by the PacC-mediated ambient-pH Regulatory system in *Aspergillus nidulans*. **Eukaryotic Cell**, v. 3, n. 2, p. 561-563, 2004.

ESPESO, E. A.; PEÑALVA, M. A. Three binding sites for the *Aspergillus nidulans* PacC zinc-finger transcription factor are necessary and sufficient for regulation by ambient pH of the isopenicillin N synthase gene promoter. **J. Biol. Chem.**, v. 271, n. 46, p. 28825-28830, 1996.

ESPESO, E. A. et al. Specific DNA recognition by the *Aspergillus nidulans* three zinc finger transcription factor PacC. **J. Mol. Biol.**, v. 274, n. 4, p. 466-480, 1997.

FARKAS, I. et al. Two glycogen synthase isoforms in *Saccharomyces cerevisiae* are coded by distinct genes that are differentially controlled. **J. Biol. Chem.**, v. 266, n. 24, p. 15602-15607, 1991.

FENG, D.; LAZAR, M. A. Clocks, metabolism, and the epigenome. **Mol. Cell**, v. 47, n. 2, p. 158-167, 2012.

FILLINGER, S. et al.Trehalose is required for the acquisition of tolerance to a variety of stresses in the filamentous fungus *Aspergillus nidulans*. **Microbiology**, v. 147, pt. 7, p. 1851-1862, 2001.

FRANÇOIS, J.; PARROU, J. L. Reserve carbohydrates metabolism in the yeast *Saccharomyces cerevisiae*. **FEMS Microbiol. Rev.**, v. 25, n. 1, p. 125-145, 2001.

FRANÇOIS, J.; VILLANUEVA, M. E.; HERS, H. G. The control of glycogen metabolism in yeast. 1- Interconversion *in vivo* of glycogen synthase and glycogen phosphorylase induced by glucose, a nitrogen source or unconplers. **Eur. J. Biochem.**, v. 174, n. 3, p. 551-559, 1988.

FREITAS, F. Z.; BERTOLINI, M. C. Genomic organization of the *Neurospora crassa gsn* gene: possible involvement of the STRE and HSE elements in the modulation of transcription during heat shock. **Mol. Gen. Genomics**, v. 272, n. 5, p. 550-561, 2004.

FREITAS, F. Z. et al. A systematic approach to identify STRE-binding proteins of the *gsn* glycogen synthase gene promoter in *Neurospora crassa*. **Proteomics**, v. 8, n. 10, p. 2052-2061, 2008.

FREITAS, F. Z. et al. The SEB-1 transcription factor binds to the STRE motif in *Neurospora crassa* and regulates a variety of cellular processes including the stress response and reserve carbohydrate metabolism. **G3**, v. 6, n. 5, p. 1327-1343, 2016.

FROEHLICH, A. C.; LOROS, J. J.; DUNLAP, J. C. Rhythmic binding of a WHITE COLLAR-containing complex to the *frequency* promoter is inhibited by FREQUENCY. **Proc. Natl. Acad. Sci. U. S. A.**, v. 100, n. 10, p. 5914-5919, 2003.

FROEHLICH, A. C. et al. White Collar-1, a circadian blue light photoreceptor, binding to the *frequency* promotor. **Science**, v. 297, n. 5582, p. 815-819, 2002.

FU, Y. H.; MARZLUF, G. A. *nit-2*, the major nitrogen regulatory gene of *Neurospora crassa*, encodes a protein with a putative zinc finger DNA-binding domain. **Mol. Cell Biol.**, v. 10, n. 3, p. 1056-1065, 1990.

GALAGAN, J. E. et al. The genome sequence of the filamentous fungus *Neurospora crassa*. **Nature**, v. 422, n. 6934, p. 859-868, 2003.

GLASS, C. K.; ROSENFELD, M. G. The coregulator exchange in transcriptional functions of nuclear receptors. **Genes Dev.**, v. 14, n. 2, p. 121-141, 2000.

GONÇALVES, R. D. et al. A genome-wide screen for *Neurospora crassa* transcription factors regulating glycogen metabolism. **Mol. Cell. Proteomics**, v. 10, n. 11, 2011. doi:10.1074/mcp.M111.007963.

GRBA, S.; OURA, E.; SUOMALAINEN, H. On the formation of glycogen and trehalose in baker's yeast. **Eur. J. Appl. Microbiol.**, v. 2, n. 1, p. 29-37, 1975.

HAN, K. H.; PRADE, R. A. Osmotic stress-coupled maintenance of polar growth in *Aspergillus nidulans*. **Mol. Microbiol.**, v. 43, n. 5, p. 1065-1078, 2002.

HANKS, D. L.; SUSSMAN, A. S. The relation between growth, conidiation and trehalase activity in *Neurospora crassa*. **Am. J. Bot.**, v. 56, n. 10, p. 1152-1159, 1969.

HARDING, R. W.; TURNER, R. V. Photoregulation of the carotenoid biosynthetic pathway in albino and white collar mutants of *Neurospora crassa*. **Plant Physiol.**, v. 68, n. 3, p. 745-749, 1981.

HARDY, T. A.; ROACH, P. J. Control of yeast glycogen synthase-2 by COOH-terminal phosphorylation. **J. Biol. Chem.**, v. 268, n. 32, p. 23799-23805, 1993.

HARRIS, R. A. Carbohydrate metabolism I: major metabolic pathways and their control. In: DEVLIN, T. M. (Ed.). **Textbook of biochemistry with clinical correlations**. 4th ed. New York: Wiley-Liss, 1997. p. 267-333.

HAWKSWORTH, D. L. The magnitude of fungal diversity: the 1.5 million species estimate revisited. **Mycol. Res.**, v. 105, p. 1422-1432, 2001.

HEINTZEN, C.; LIU, Y. The *Neurospora crassa* circadian clock. **Adv. Genet.**, v. 58, p. 25-66, 2007.

HEINTZEN, C.; LOROS, J. J.; DUNLAP, J. C. The PAS protein VIVID defines a clock-associated feedback loop the represses light input, modulates gating, and regulates clock ressetting. **Cell**, v. 104, n. 3, p. 453-464, 2001.

HERVÁZ-AGUILAR, A. et al. Evidence for the direct involvement of the proteasome in the proteolytic processing of the *Aspergillus nidulans* zinc finger transcription factor PacC. **J. Biol. Chem.**, v. 282, n. 48, p. 34735-34747, 2007.

HUANG, M.; ZHOU, Z.; ELLEDGE, S. J. The DNA replication and damage checkpoint pathways induce transcription by inhibition of the Crt1 repressor. **Cell**, v. 94, n. 5, p. 595-605, 1998.

HURLEY, J. M. et al. Analysis of clock-regulated genes in *Neurospora* reveals widespread posttranscriptional control of metabolic potential. **Proc. Natl. Acad. Sci. U. S. A.**, v. 111, n. 48, p. 16995-17002, 2014.

HYNES, M. J. The *Neurospora crassa* genome opens up the world of filamentous fungi. **Genome Biol.**, v. 4, n. 6, 2003. doi:10.1186/gb-2003-4-6-217.

ISHIKAWA, K.; SHIMAZU, T. Daily rhythms of glycogen synthetase and phosphorylase activities in rat liver: influence of food and light. **Life Sci.**, v. 19, n. 12, p. 1873-1878, 1976.

JOHNSON, L. N. Glycogen phosphorylase: control by phosphorylation and allosteric effectors. **FASEB J.**, v. 6, n. 6, p. 2274-2282, 1992.

JOHNSON, L. N.; BARFORD, D. Glycogen phosphorylase. The structural basis of the allosteric response and comparison with other allosteric proteins. **J. Biol. Chem.**, v. 265, n. 5, p. 2409-2412, 1990.

JOHNSTON, M.; CARLSON, M. Regulation of carbon and phosphate utilization. In: JONES E. W.; PRINGLE, J. R.; BROACH, J. R. (Ed.). **The molecular and cellular biology of the yeast Saccharomyces**. Cold Spring Harbor: Cold Spring Harbor Laboratory Press, 1992. p. 193-281. v. 2. Gene expression.

KANE, S. M.; ROTH, R. Carbohydrate metabolism during ascospore development in yeast. **J. Bacteriol.**, v. 118, n. 1, p. 8-14, 1974.

KELLER, N. P. et al. pH regulation of sterigmatocystin and aflatoxin biosynthesis in *Aspergillus* spp. **Phytopathology**, v. 87, n. 6, p. 643-648, 1997.

KLEMM, E.; NINNEMANN, H. Correlation between absorbance changes and a physiological response induced by blue light in *Neurospora crassa*. **Photochem. Photobiol.**, v. 28, n. 2, p. 227-230, 1978.

KULLAS, A. L.; MARTIN, S. J.; DAVIS, D. Adaptation to environmental pH: integrating the Rim101 and calcineurin signal transduction pathways. **Mol. Microbiol.**, v. 66, n. 4, p. 858-871, 2007.

LAMB, T. M.; MITCHELL, A. P. The transcription factor Rim101p governs ion tolerance and cell differentiation by direct repression of the regulatory genes NRG1 and SMP1 in *Saccharomyces cerevisiae*. **Mol. Cell. Biol.**, v. 23, n. 2, p. 677-686, 2003.

LAUTER, F. R. Molecular genetics on fungal photobiology. **J. Genet.**, v. 75, n. 3, p. 375-386, 1996.

LAUTER, F. R.; YANOFSKY, C. Day/night and circadian rhythm control of *con* gene expression in Neurospora. **Proc. Natl. Acad. Sci. U. S. A.**, v. 90, n. 17, p. 8249-8253, 1993.

LEE, K.; DUNLAP, J. C.; LOROS, J. J. Roles for WHITE COLLAR-1 in circadian and general photoperception in *Neurospora crassa*. **Genetics**, v. 163, n. 1, p. 103-114, 2003.

LELOIR, L. F. Two decades of research on the biosynthesis of saccharides. **Science**, v. 172, n. 990, p. 1299-1303, 1971.

LI, W.; MITCHELL, A. P. Proteolytic activation of Rim1p, a positive regulator of yeast sporulation and invasive growth. **Genetics**, v. 145, n. 1, p. 63-73, 1997.

LILLIE, S. H.; PRINGLE, J. R. Reserve carbohydrate metabolism in *Saccharomyces cerevisiae*: responses to nutrient limitation. **J. Bacteriol.**, v. 143, n. 3, p. 1384-1394, 1980.

LINDEGREN, C. C.; BEANFIELD, V.; BARBER, R. Increasing the fertility of Neurospora by selective inbreeding. **Bot. Gazette**, v. 100, n. 3, p. 592-599, 1939.

LINDEN, H.; MACINO, G. White collar 2, a partner in blue-light signal transduction, controlling expression of light-regulated genes in *Neurospora crassa*. **EMBO J.**, v. 16, n. 1, p. 98-109, 1997.

LINDEN, H.; RODRIGUEZ-FRANCO, M.; MACINO, G. Mutants of *Neurospora crassa* defective in regulation of blue light perception. **Mol. Gen. Genet.**, v. 254, n. 2, p. 111-118, 1997.

LOROS, J. J.; DUNLAP, J. C. Genetic and molecular analysis of circadian rhythms in Neurospora. **Annu. Rev. Physiol.**, v. 63, p. 757-794, 2001.

MacCABE, A. P. et al. Opposite patterns of expression of two *Aspergillus nidulans* xylanase genes with respect to ambient pH. **J. Bacteriol.**, v. 180, n. 5, p. 1331-1333, 1998.

MADSEN, N. B. Glycogen phosphorylase. In: BOYER, P. D.; KREBS, E. G. (Ed.). **The enzymes**. 3rd ed. New York: Academic Press, 1986. p. 366-394. v. 17. Control by phosphorylation, part A.

MAHESHWARI, R. Microconidia of *Neurospora crassa*. **Fungal Genet. Biol.**, v. 26, n. 1, p. 1-18, 1999.

MARCHEVA, B. et al. Disruption of the clock components CLOCK and BMAL1 leads to hypoinsulinaemia and diabetes. **Nature**, v. 466, n. 7306, p. 627-631, 2010.

MARCHEVA, B. et al. Circadian clocks and metabolism. **Handb. Exp. Pharmacol.**, v. 217, p. 127-155, 2013.

METZENBERG, R. L. Implications of some genetic control mechanisms in Neurospora. **Microbiol. Rev.**, v. 43, n. 3, p. 361-383, 1979.

MEYER, V.; STAHL, U. New insights in the regulation of the afp gene encoding the antifungal protein of *Aspergillus giganteus*. **Curr. Genet.**, v. 42, n. 1, p. 36-42, 2002.

MILLER, B. H. et al. Circadian and CLOCK-controlled regulation of the mouse transcriptome and cell proliferation. **Proc. Natl. Acad. Sci. U. S. A.**, v. 104, n. 9, p. 3342-3347, 2007.

MÖLLER, A. **Phycomyceten und Ascomyceten.** Untersuchungen aus brasilien. Jena: Gustav Fischer, 1901. 319 p.

MORENO-MATEOS, M. A. et al. pH and Pac1 control development and antifungal activity in *Trichoderma harzianum*. **Fungal Genet. Biol.**, v. 44, n. 12, p. 1355-1367, 2007.

NEHLIN, J. O.; CARLBERG, M.; RONNE, H. Control of yeast *GAL* genes by Mig1 repressor: a transcriptional cascade in the glucose response. **EMBO J.**, v. 10, n. 11, p. 3373-3377, 1991.

NELSON, D. L.; COX, M. M. Principles of metabolic regulation. In: _____ . **Lehninger principles of biochemistry**. 5th ed. New York: W. H. Freeman, 2008. Cap. 15, p. 594-609.

NEVES, M. J. et al. Effects of heat shock on the level of trehalose and glycogen, and on the induction of thermotolerance in *Neurospora crassa*. **FEBS Lett.**, v. 283, n. 1, p. 19-22, 1991.

NI, H. T.; LAPORTE, D. C. Response of a yeast glycogen synthase gene to stress. **Mol. Microbiol.**, v. 16, n. 6, p. 1197-1205, 1995.

NI, M.; YU, J. H. A novel regulator couples sporogenesis and trehalose biogenesis in *Aspergillus nidulans*. **PLoS One**, v. 2, n. 10, 2007. doi:10.1371/journal.pone.0000970.

NINOMIYA, Y. et al. Highly efficient gene replacements in Neurospora strains deficient for nonhomologous end-joining. **Proc. Natl. Acad. Sci. U. S. A.**, v. 101, n. 33, p. 12248-12253, 2004.

NOVENTA-JORDÃO, M. A. et al. Effects of temperature shifts on the activities of *Neurospora crassa* glycogen synthase, glycogen phosphorylase and trehalose-6-phosphate synthase. **FEBS Lett.**, v. 378, n. 1, p. 32-36, 1996.

NWAKA, S.; HOLZER, H. Molecular biology of trehalose and the trehalases in the yeast *Saccharomyces cerevisiae*. **Prog. Nucleic Acid Res. Mol. Biol.**, v. 58, p. 197-237, 1998.

O'BRIEN, B. L. et al. Fungal community analysis by large-scale sequencing of enviromental samples. **Appl. Environ. Microbiol.**, v. 71, n. 9, p. 5544-5550, 2005.

OLMEDO, M. et al. A role in the regulation of transcription by light for RCO-1 and RCM-1, the Neurospora homologs of the yeast Tup1-Ssn6 repressor. **Fungal Gen. Biol.**, v. 47, n. 11, p. 939-952, 2010.

OLSON, A. L.; PESSIN, J. E. Structure, function and regulation of the mammalian facilitative glucose transporter gene family. **Annu. Rev. Nutr.**, v. 16, p. 235-356, 1996.

PANDA, S. et al. Coordinated transcription of key pathways in the mouse by the circadian clock. **Cell**, v. 109, n. 3, p. 307-320, 2002.

PARK, G. et al. Global analysis of serine-threonine protein kinase genes in *Neurospora crassa*. **Eukaryotic Cell**, v. 10, n. 11, p. 1553-1564, 2011.

PARK, H. S. et al. Characterization of the velvet regulators in *Aspergillus fumigatus*. **Mol. Microbiol.**, v. 86, n. 4, p. 937-953, 2012.

PAYEN, A. Extrait d'un rapport adresseé à M. Le Maréchal Duc de Dalmatie, Ministre de la Guerre, Président du Conseil, sur une altération extraordinaire du pain de munition. **Ann. Chim. Phys.**, v. 9, n. 1, p. 5-21, 1843.

PEÑALVA, M. A.; ARST, H. N. Recent advances in the characterization of ambient pH regulation of gene expression in filamentous fungi and yeasts. **Annu. Rev. Microbiol.**, v. 58, p. 425-451, 2004.

PERKINS, D. D. The first published scientific study of Neurospora, including a description of photoinduction of carotenoids. **Fungal Genet. Newsl.**, v. 38, p. 64-65, 1991.

PERKINS, D. D. Neurospora: the organism behind the molecular revolution. **Genetics**, v. 130, n. 4, p. 687-701, 1992.

PERKINS, D. D.; DAVIS, R. H. Neurospora at the millennium. **Fungal Genet. Biol.**, v. 31, n. 3, p. 153-167, 2000.

PERKINS, D. D.; TURNER, B. C.; BARRY, E. G. Strains of *Neurospora crassa* collected from nature. **Evolution**, v. 30, n. 2, p. 281-313, 1976.

PETERBAUER, C. K.; LITSCHER, D.; KUBICEK, C. P. The *Trichoderma atroviride seb1* (stress response element binding) gene encodes an AGGGG-binding protein which is involved in the response to high osmolarity stress. **Mol. Genet. Genomics**, v. 268, n. 2, p. 223-231, 2002.

PRICE-LLOYD, N.; ELVIN, M.; HEINTZEN, C. Synchronizing the *Neurospora crassa* circadian clock with the rhythmic environment. **Biochem. Soc. Trans.**, v. 33, pt. 5, p. 949-952, 2005.

QUERFURTH, C. et al. Circadian conformational change of the Neurospora clock protein FREQUENCY triggered by clustered hyperphosphorylation of a basic domain. **Mol. Cell**, v. 43, n. 5, p. 713-722, 2011.

RAJU, N. B. Neurospora as a model fungus for studies in cytogenetics and sexual biology at Stanford. **J. Biosci.**, v. 34, n. 1, p. 139-159, 2009.

REISCHL, S.; KRAMER, A. Kinases and phosphatases in the mammalian circadian clock. **FEBS Lett.**, v. 585, n. 10, p. 1393-1399, 2011.

ROACH, P. J. Glycogen and its metabolism. **Curr. Mol. Med.**, v. 2, n. 2, p. 101-120, 2002.

ROACH, P. J. et al. Glycogen and its metabolism: some new developments and old themes. **Biochem. J.**, v. 441, n. 3, p. 763-787, 2012.

ROLLINS, J. A.; DICKMAN, M. B. pH signaling in *Sclerotinia sclerotiorum*: identification of a pacC/RIM1 homolog. **Appl. Environ. Microbiol.**, v. 67, n. 1, p. 75-81, 2001.

ROUNTREE, M. R.; SELKER, E. U. DNA methylation inhibits elongation but not initiation of transcription in *Neurospora crassa*. **Genes Dev.**, v. 11, n. 18, p. 2383-2395, 1997.

RUIJTER, G. J.; VISSER, J. Carbon repression in Aspergilli. **FEMS Microbiol. Lett.**, v. 151, n. 2, p. 103-114, 1997.

SANCAR, G. et al. A global circadian repressor controls antiphasic expression of metabolic genes in Neurospora. **Mol. Cell**, v. 44, n. 5, p. 687-697, 2011.

SCHAFMEIER, T.; DIERNFELLNER, A. C. R. Light input and processing in the circadian clock of Neurospora. **FEBS Lett.**, v. 585, n. 10, p. 1467-1473, 2011.

SCHULTE, U. et al. Large scale analysis of sequences from *Neurospora crassa.* **J. Biotechnol.**, v. 94, n. 1, p. 3-13, 2002.

SCHWERDTFEGER, C.; LINDEN, H. VIVID is a flavoprotein and serves as a fungal blue light photoreceptor for photoadaptation. **EMBO J.**, v. 22, n. 18, p. 4846-4855, 2003.

SELKER, E. Premeiotic instability of repeated sequences in *Neurospora crassa*. **Annu. Rev. Genet.**, v. 24, p. 579-613, 1990.

SERRANO, R. et al. The transcriptional response to alkaline pH in *Saccharomyces cerevisiae*: evidence for calcium-mediated signalling. **Mol. Microbiol.**, v. 46, n. 5, p. 1319-1333, 2002.

SHEAR, C. L.; DODGE, B. O. Life histories and heterothallism of the red bread-mold fungi of the Monilia sitophila group. **J. Agric. Res.**, v. 34, n. 1, p. 1019-1042, 1927.

SHINOHARA, M. L. et al. Neurospora clock-controlled gene 9 (*ccg-9*) encodes trehalose synthase: circadian regulation of stress responses and development. **Eukaryotic Cell**, v. 1, n. 1, p. 33-43, 2002.

SHRODE, L. B. et al. *Vvd* is required for light adaptation of conidiation-specific genes of *Neurospora crassa*, but not circadian condidiation. **Fungal Genet. Biol.**, v. 32, n. 3, p. 169-181, 2001.

SMITH, K. M. et al. Transcription factors in light and circadian clock signaling networks revealed by genome-wide mapping of direct targets for Neurospora white collar complex. **Eukaryotic Cell**, v. 9, n. 10, p. 1549-1556, 2010.

SPRINGER, M. L. Genetic control of fungal differentiation: the three sporulation pathways of *Neurospora crassa.* **Bioessays**, v. 15, n. 6, p. 365-374, 1993.

SPRINGER, M. L.; YANOFSKY, C. A morphological and genetic analysis of conidiophore development in *Neurospora crassa*. **Genes Dev.**, v. 3, n. 4, p. 559-571, 1989.

SQUINA, F. M. et al. Transcription of the *Neurospora crassa* 70-kDa class heat shock protein genes is modulated in response to extracellular pH changes. **Cell Stress Chaperones**, v. 15, n. 2, p. 225-231, 2010.

STRAUSS, J. et al. The function of CreA, the carbon catabolite repressor of *Aspergillus nidulans*, is regulated at the transcriptional and pos-transcriptional level. **Mol. Microbiol.**, v. 32, n. 1, p. 169-178, 1999.

SU, S. S.; MITCHELL, A. P. Identification of functionally related genes that stimulate early meiotic gene expression in yeast. **Genetics**, v. 133, n. 1, p. 67-77, 1993.

SUN, J.; GLASS, N. L. Identification of the CRE-1 cellulolytic regulon in *Neurospora crassa*. **PloS One**, v. 6, n. 9, 2011. doi:10.1371/journal.pone.0025654.

TAYLOR, D. L. et al. Structure and resilience of fungal communities in Alaskan boreal forest soils. **Can. J. For. Res.**, v. 40, p. 1288-1301, 2010.

TÉLLEZ-IÑÓN, M. T.; TORRES, H. N. Interconvertible forms of glycogen phosphorylase in *Neurospora crassa*. **Proc. Natl. Acad. Sci. U. S. A.**, v. 66, n. 2, p. 459-463, 1970.

THEDEI JÚNIOR, G.; DOUBOWETZ, T. H.; ROSSI, A. Effect of carbon source and extracellular pH on the acidification of the culture medium and phosphatase excretion in *Neurospora crassa*. **Braz. J. Med. Biol. Res.**, v. 27, n. 5, p. 1129-1134, 1994.

THEVELEIN, J. M. Regulation of trehalose mobilization in fungi. **Microbiol. Rev.**, v. 48, n. 1, p. 42-59, 1984.

THORENS, B. Glucose transporters in the regulation of intestinal, renal, and liver glucose fluxes. **Am. J. Physiol.**, v. 270, n. 4, pt. 1, p. G541-G553, 1996.

TILBURN, J. et al. The Aspergillus PacC zinc finger transcription factor mediates regulation of both acid- and alkaline-expressed genes by ambient pH. **EMBO J.**, v. 14, n. 4, p. 779-790, 1995.

TURIAN, G.; BIANCHI, D. E. Conidiation in Neurospora. **Bot. Rev.**, v. 38, n. 1, p. 119-154, 1972.

UEDA, H. R. et al. A transcription factor response element for gene expression during circadian night. **Nature**, v. 418, p. 534-539, 2002.

VAN PEIJ, N. N. et al. The transcriptional activator XlnR regulates both xylanolytic and endoglucanase gene expression in *Aspergillus niger*. **Appl. Environ. Microbiol.**, v. 64, n. 10, p. 3615-3619, 1998.

VANKUYK, P. A. et al. *Aspergillus niger* mstA encodes a high-affinity sugar/H+ symporter which is regulated in response to extracellular pH. **Biochem. J.**, v. 379, pt. 2, p. 375-383, 2004.

WALKER, J. R.; CORPINA, R. A.; GOLDBERG, J. Structure of the ku heterodimer bound to DNA and its implications for double-strand break repair. **Nature**, v. 412, n. 6847, p. 607-614, 2001.

WANG, T. Y. et al. A predicted protein-protein interaction network of the filamentous fungus *Neurospora crassa*. **Mol. Biosyst.**, v. 7, p. 2278-2285, 2011.

WEIRAUCH, M. T. et al. Determination and inference of eukaryotic transcription factor sequence specificity. **Cell**, v. 158, n. 6, p. 1431-1443, 2014.

YAMASHIRO, C. T. et al. Characterization of *rco-1* of *Neurospora crassa*, a pleiotropic gene affecting growth and development that encodes a homolog of Tup1 of *Saccharomyces cerevisiae*. **Mol. Cell. Biol.**, v. 16, n. 11, p. 6218-6228, 1996.

ZARRINPAR, A.; CHAIX, A.; PANDA, S. Daily eating patterns and their impact on health and disease. **Trends Endocrinol. Metab.**, v. 27, n. 2, p. 69-83, 2016.

ZOLTOWSKI, B. D.; CRANE, B. R. Light activation of the LOV protein vivid generates a rapidly exchanging dimer. **Biochemistry**, v. 47, n. 27, p. 7012-7019, 2008.

ZOU, C. G. et al. PacC in the nematophagous fungus *Clonostachys rosea* controls virulence to nematodes. **Environ. Microbiol.**, v. 12, n. 7, p. 1868-1977, 2010.

Attachment

G3·Genes | Genomes | Genetics

INVESTIGATION

The SEB-1 Transcription Factor Binds to the STRE Motif in *Neurospora crassa* and Regulates a Variety of Cellular Processes Including the Stress Response and Reserve Carbohydrate Metabolism

Fernanda Zanolli Freitas,* Stela Virgilio,* Fernanda Barbosa Cupertino,* David John Kowbel,† Mariana Fioramonte,‡ Fabio Cesar Gozzo,‡ N. Louise Glass,† and Maria Célia Bertolini*,1

*Departamento de Bioquímica e Tecnologia Química, Instituto de Química, Universidade Estadual Paulista (UNESP), 14800-060, Araraquara, São Paulo, Brazil, †Department of Plant and Microbial Biology, University of California, Berkeley, California, 94720-3102, and ‡Departamento de Química Orgânica, Instituto de Química, Universidade Estadual de Campinas (UNICAMP), 13803-862, Campinas, São Paulo, Brazil

ABSTRACT When exposed to stress conditions, all cells induce mechanisms resulting in an attempt to adapt to stress that involve proteins which, once activated, trigger cell responses by modulating specific signaling pathways. In this work, using a combination of pulldown assays and mass spectrometry analyses, we identified the *Neurospora crassa* SEB-1 transcription factor that binds to the Stress Response Element (STRE) under heat stress. Orthologs of SEB-1 have been functionally characterized in a few filamentous fungi as being involved in stress responses; however, the molecular mechanisms mediated by this transcription factor may not be conserved. Here, we provide evidences for the involvement of *N. crassa* SEB-1 in multiple cellular processes, including response to heat, as well as osmotic and oxidative stress. The Δ*seb-1* strain displayed reduced growth under these conditions, and genes encoding stress-responsive proteins were differentially regulated in the Δ*seb-1* strain grown under the same conditions. In addition, the SEB-1-GFP protein translocated from the cytosol to the nucleus under heat, osmotic, and oxidative stress conditions. SEB-1 also regulates the metabolism of the reserve carbohydrates glycogen and trehalose under heat stress, suggesting an interconnection between metabolism control and this environmental condition. We demonstrated that SEB-1 binds *in vivo* to the promoters of genes encoding glycogen metabolism enzymes and regulates their expression. A genome-wide transcriptional profile of the Δ*seb-1* strain under heat stress was determined by RNA-seq, and a broad range of cellular processes was identified that suggests a role for SEB-1 as a protein interconnecting these mechanisms.

KEYWORDS
SEB-1
stress response
ChIP-qPCR
RNA-seq
Neurospora crassa

All living cells are exposed to a range of environmental conditions, which impact their patterns of gene expression, allowing them to adapt to stress conditions and survive. Heat stress results in the activation of specific proteins, known as heat shock transcription factors (HSFs), which bind to DNA regulatory sequences referred to as Heat Shock Elements (HSE) and activate genes that encode heat shock proteins (HSPs). In this process, gene expression is efficiently either up- or down-regulated, resulting in a global cellular adaptation (Sorger and Pelham 1988; Vihervaara *et al.* 2013). In addition to HSEs, the general stress response also includes a different DNA sequence, known as the Stress Response Element or STRE (CCCCT), which was first reported in *Saccharomyces cerevisiae* (Kobayashi and McEntee 1990, 1993). STRE motifs are present in the promoters of genes that are regulated during stress. A search for proteins able to bind to the STRE sequence showed that the zinc finger transcription factor Msn2p, together with its counterpart Msn4p, are the primary STRE-binding proteins in yeast, acting as inducers of the transcription of stress-induced genes (Schmitt and McEntee 1996; Martínez-Pastor *et al.* 1996). About half of the genes induced by stress

Copyright © 2016 Freitas *et al.*
doi: 10.1534/g3.116.028506
Manuscript received January 8, 2015; accepted for publication March 6, 2016; published Early Online March 16, 2016.
This is an open-access article distributed under the terms of the Creative Commons Attribution 4.0 International License (http://creativecommons.org/licenses/by/4.0/), which permits unrestricted use, distribution, and reproduction in any medium, provided the original work is properly cited.
Supplemental material is available online at www.g3journal.org/lookup/suppl/doi:10.1534/g3.116.028506/-/DC1
[1]Corresponding author: Instituto de Química, UNESP, Departamento de Bioquimica e Tecnologia Química, R. Prof. Francisco Degni, 55, 14,800-060, Araraquara, São Paulo, Brazil. E-mail: mcbertol@iq.unesp.br

belong to the Msn2/4p regulon and include oxidative stress, metabolic, and other cytoprotective genes (Gasch 2007; Causton *et al.* 2001; Morano *et al.* 2012). Under normal growth conditions, these transcription factors are cytoplasmic, but translocate to the nucleus when cells are exposed to stress (Görner *et al.* 1998; Jacquet *et al.* 2003).

In *S. cerevisiae*, a large number of stress-responsive genes have STRE motifs in their promoter regions. Although the presence of these motifs frequently correlates with transcriptional activation under stress, the participation of the STRE motif in transcriptional repression has also been described, which is mediated by the action of different transcriptional repressors (de Groot *et al.* 2000; Vyas *et al.* 2005). In *Neurospora crassa*, the *gsn* gene, which encodes glycogen synthase, the regulatory enzyme in glycogen synthesis, is repressed under heat shock (de Paula *et al.* 2002). This regulation may involve the STRE motif located in its promoter region, since DNA-protein complexes have been observed *in vitro* using the *gsn* STREs and proteins from nuclear extracts after exposure of cells to heat stress (Freitas and Bertolini 2004). However, these elements were unable to induce transcription of a reporter gene in *S. cerevisiae* under heat stress, suggesting a repressor role for this *cis* regulatory element in *N. crassa* (Freitas *et al.* 2010).

Filamentous fungi apparently lack Msn2/4p orthologous proteins, which suggests that the regulation of stress responses may have evolved differently among micro-organisms. However, proteins binding to STRE-like sequences have been functionally characterized in a few filamentous fungi and they show similarity and divergence to the well-characterized Msn2/4 yeast proteins, suggesting the existence of distinct molecular mechanisms regulating stress responses in different fungi. In general, these proteins show very little amino acid sequence conservation to the Msn2/4p, only displaying identity in the zinc finger region. One such protein is Seb1 from *Trichoderma atroviride*, which was reported to be involved in, but not essential for, the osmotic stress response (Peterbauer *et al.* 2002; Han and Prade 2002; Seidl *et al.* 2004). This transcription factor failed to complement the Δ*msn2/4* mutant of *S. cerevisiae*, suggesting that it may not be a direct Msn2/4 ortholog (Peterbauer *et al.* 2002). In *Candida albicans*, a Msn2/4p-like transcription factor was initially reported as not being involved in environmental stress responses (Nicholls *et al.* 2004), whereas the *C. glabrata* CgMsn2 protein complemented the *S. cerevisiae msn2* mutant and was required for full resistance against osmotic stress and the induction of genes involved in trehalose synthesis (Roetzer *et al.* 2008).

In addition to their role in stress responses, some putative Msn2/4 homologs have been described as playing a role in virulence and pathogenicity. The *C. glabrata* CgMsn2 protein was required for virulence in a *Drosophila melanogaster* infection model and, more recently, deletion of *sebA*, an ortholog of *seb1* from *Aspergillus fumigatus*, was demonstrated to have a severe impact on virulence and pathogenicity in a murine model (Dinamarco *et al.* 2012). SebA apparently does not play a role in osmotic stress, but is involved in a broader range of stress responses, including the response to heat shock, oxidative stress, and poor nutrient deprivation adaptation (Dinamarco *et al.* 2012).

In this work, we identified by mass spectrometry a transcription factor that binds a STRE motif present in the promoter region of the *gsn* gene in *Neurospora crassa*. This protein is an ortholog of the *T. atroviride* Seb1 transcription factor and was named here as SEB-1. SEB-1 is involved in environmental stress responses such as exposure to heat shock, acidic, osmotic, and oxidative conditions, as the Δ*seb-1* mutant is more sensitive to these stressors than the wild-type strain. The response to stress was correlated with the localization of SEB-1-GFP in the nucleus. In addition, we showed a new role for SEB-1 in the regulation of the metabolism of the reserve carbohydrates glycogen and trehalose. Finally, we used RNA-seq to determine the *seb-1* regulon under heat stress and showed that, in *N. crassa*, the acquisition of heat tolerance is broadly connected with other stress signaling pathways.

MATERIALS AND METHODS

Fungal strains and growth conditions

The *N. crassa* strains FGSC 2489 (A), FGSC 11345 (Δ*seb-1* a), and FGSC 6103 (*his-3* A) were provided by the Fungal Genetics Stock Center (FGSC) (McCluskey *et al.* 2010). A Δ*seb-1* complemented strain (Δ*seb-1 his-3*::*Pccg-1-seb-1-sfgfp*) was constructed in this work. The strain FGSC 6103 was used as female in crosses with the Δ*seb-1* strain to generate a double-mutant strain (Δ*seb-1 his-3*) to be used in complementation experiments. Media and procedures for growth, maintenance, and crosses were as described by Davis and de Serres (1970). The strains were cultivated either on solid or in liquid Vogel's minimal (VM) medium (Vogel 1956) supplemented, as required, with hygromycin (200 μg/ml) and/or L-histidine chloride (500 μg/ml). Crosses were done by inoculating the opposite mating type strain onto Westergaard's medium (Westergaard and Mitchell 1947). Transformation and other *N. crassa* molecular techniques were performed as previously described (Colot *et al.* 2006) or using the protocols available at the *Neurospora* homepage (http://www.fgsc.net/Neurospora/NeurosporaProtocolGuide.htm).

For heat shock experiments using liquid cultures, conidia (2×10^7/ml) from the wild-type, Δ*seb-1*, and Δ*seb-1* complemented strains were first germinated in 1 L of VM medium containing 2% sucrose at 30° for 24 hr and 250 rpm. After this, the mycelia were harvested by filtration and a sample was removed, frozen in liquid nitrogen, and stored at –80° until use (control sample). The remaining mycelial pads were transferred to 1 L of fresh VM liquid medium containing 0.5% sucrose preheated at 45° and incubated at 250 rpm for 30 min (heat-shocked samples). The heat-shocked mycelia were harvested by filtration, frozen in liquid nitrogen, and stored at –80° to be further used to determine glycogen and trehalose contents and to prepare total RNA for the RT-qPCR experiments.

Phenotypic analyses and stress sensitivity

Macroscopic analysis of the wild-type, Δ*seb-1*, and Δ*seb-1* complemented strains was performed on solid VM medium. A volume of 100 μl of a 2×10^7 conidia/ml cell suspension was inoculated in the center of flasks containing solid VM medium and the strains were incubated at 30° for 3 d. After this, they were maintained in daylight at room temperature for 7 d. The 10-day-old cultures were analyzed macroscopically. The colony morphology and hyphal edges were assessed by inoculating 10 μl of a 2×10^7 conidia/ml cell suspension in the center of VM plates followed by incubation at 30° for 24 hr. The images were captured after 24 hr using an AxioCam ICc3 camera coupled to the Zeiss Discovery V8 stereoscope trinocular at 80× magnification. To evaluate the effect of heat stress, the strains were cultivated on solid VM medium at 45° for 48 hr, followed by 24 hr at 30° to check the conidia viability (heat stress recovery).

Pulldown assay

The pulldown assay was performed to isolate *N. crassa* proteins capable of binding to the STRE motif. The assays used biotinylated oligonucleotides containing the STRE core sequence and NeutrAvidin Plus UltraLink Agarose Resin (Thermo Scientific Pierce Protein Research Products). For this, a nuclear extract was prepared from heat-shocked mycelia (transferred from 30° to 45°) followed by fractionation by affinity chromatography on a Heparin-Sepharose column (GE

HealthCare), according to Freitas *et al.* (2008). Chromatographic fractions were individually analyzed by EMSA for their ability to bind to a DNA fragment from the *gsn* promoter containing the STRE motif (STRE1 probe) (Freitas and Bertolini 2004). The fractions showing DNA-binding activity were pooled and used as the protein source for the pulldown assay. The pulldown assay was done as follows: 200 μl of a 50% slurry NeutrAvidin resin was blocked with 500 μg of BSA and 100 μg of denatured salmon sperm DNA in EMSA binding buffer (25 mM HEPES-KOH, pH 7.9; 20 mM KCl, 10% v/v glycerol; 1 mM DTT; 0.2 mM EDTA; 0.5 mM PMSF; 12.5 mM benzamidine; and 5 μg/ml each of antipain and pepstatin A) under agitation for 2 hr at 4°. After blocking, the resin was washed twice with cold EMSA binding buffer and 450 μg of the dsDNA oligo solution (see below) in EMSA binding buffer was added. The mixture was rocked for 2 hr at 4° to couple the oligonucleotides to the avidin-agarose resin. After coupling, 300 μg (total protein) of the active chromatographic fraction was added and the mixture was incubated under mild agitation for 30 min at room temperature. After incubation, the reactions were rapidly washed in cold EMSA binding buffer followed by the addition of 1× Laemmli buffer (Laemmli 1970), boiled, and fractionated on a 12% SDS-PAGE gel. A mock reaction containing the oligonucleotide-free resin was prepared and used as a control. After electrophoresis, the protein bands present in the reaction, but not present in the mock reaction, were excised from the gel, digested with trypsin, and analyzed by mass spectrometry for protein identification.

Biotinylated DNA oligonucleotides for pulldown assays

Biotinylated double-strand DNA oligonucleotides were prepared as follows and the sequences are shown in Supplemental Material, Table S1. Initially, a pair of complementary oligonucleotides (bioSTRE1-F and STRE1-2R) was designed. The oligonucleotide bioSTRE1-1F was biotinylated and contained two STRE1 core sequences (CCCCT) in tandem with the 5′- and 3′-STRE boundaries, three nucleotides each, acting as a spacer sequence between the two STRE1 motifs. The non-biotinylated oligonucleotide STRE1-2R was complementary to the bioSTRE1-1F oligonucleotide. A second pair of complementary oligonucleotides (bioSTRE1-1R and STRE1-F) was also designed. The oligonucleotide bioSTRE1-1R was biotinylated and contained one STRE1 core sequence and its 5′- and 3′-boundaries, and was complementary to the oligonucleotide STRE1-F. The two pairs of oligonucleotides were prepared as individual solutions by heating and cooling down slowly to form the dsDNA oligonucleotides bioSTRE1-1F/STRE1-2R and bioSTRE1-1R/STRE1-F. The dsDNA oligonucleotides were quantified and their quality was checked on a 15% nondenaturing PAGE (30:2) in TBE buffer. The individual biotinylated dsDNA oligo solutions were mixed and used as bait in pulldown assays.

Mass spectrometry analysis

The protein bands excised from the pulldown gels were subjected to ESI-MS/MS analysis to identify the proteins showing STRE-binding activity. All samples were digested with trypsin (Trypsin Gold, Promega) for 15 hr at 37°. Peptides were extracted from the gel with a 50% acetonitrile (ACN)/5% trifluoroacetic acid (TFA) (v/v) solution. The peptide mixture was separated using a BEH C18 column (100 mm × 100 mm - Acquity Waters) with a gradient of 3–70% acetonitrile/water in 0.1% formic acid, using a nanoAcquity UPLC (Waters Co., Manchester, UK) coupled to a Waters Synapt HDMS mass spectrometer. The instrument was operated using the Data Dependent Analysis (DDA) mode, in which the equipment acquires one spectrum per second. When multi-charged species were detected, the three most intense species were fragmented using CID (collision energy defined by the *m/z* ratio and precursor charge). All mass spectra files were converted to a peak list format using Mascot Distiller (Matrix Science) and searched against the *N. crassa* database (http://www.broad.mit.edu/annotation/genome/neurospora/Home.html) using the MASCOT MS/MS ion search tool (http://www.matrixscience.com). The search parameters were as follows: no restrictions on protein molecular weight, one tryptic missed cleavage allowed, nonfixed modifications of methionine (oxidation), fixed modifications of cysteine (carbamidomethylation), with no other posttranslational modifications taken into account. Peptide mass tolerance in searches was 0.1 Da for MS spectra and 0.1 Da for MS/MS spectra. Peptides were considered as identified when their scoring value exceeded the identity or extensive homology threshold value calculated by MASCOT. The sequences of the proteins identified were examined for the presence of domains at the PFAM (http://pfam.janelia.org/) database.

Cloning and expression of recombinant SEB-1 protein

To clone and express the *seb-1* gene (ORF NCU02671), the 1728 bp full-length *seb-1* cDNA sequence was amplified from the *N. crassa* pYADE5 cDNA plasmid library (Brunelli and Pall 1993) using the primers SEB1-F and SEB1-R (Table S1). The entire ORF was inserted into the pGEX-4T1 expression vector (GE HealthCare) leading to the pGEX-SEB1 construction, which was used to transform *Escherichia coli* Rosetta (DE3) pLysS competent cells (Novagen). Cells expressing the GST-SEB-1 protein were cultured in 1 L of LB medium to an OD_{600nm} = 0.8 and protein expression was induced at 12°, 180 rpm for 16 hr using 0.4 mM IPTG (final concentration). Induced cells were harvested and subjected to 10 sonication pulses of 30 sec ON (50% amplitude, ice bath) and 60 sec OFF in phosphate-buffered saline (PBS), pH 7.4 (100 mM Na_2HPO_4, 2 mM KH_2PO_4, 500 mM NaCl, 2.7 mM KCl, 5% v/v glycerol, 0.5% NP-40 containing 10 mM benzamidine, 0.5 mM EDTA, and 2 mM each of DTT and PMSF) using a Vibra-Cell VCX 750 W cell disrupter (Sonics).

The soluble GST-SEB-1 fusion protein was purified from the crude cellular extract by affinity chromatography (GSTrap HP column, GE HealthCare) on an ÄKTA Purifier purification system, and eluted in 50 mM Tris-HCl (pH 8.0), 20 mM glutathione, 500 mM NaCl, 5% v/v glycerol, and 2 mM DTT. Chromatographic fractions were analyzed by SDS-PAGE on 10% polyacrylamide gels followed by Coomassie Brilliant Blue staining (Laemmli 1970), and the fractions containing the most purified recombinant protein were combined, dialyzed against 10 mM Tris-HCl (pH 7.9), 100 mM KCl, 10% v/v glycerol, 1 mM EDTA, and 0.5 mM DTT, and concentrated. Total protein was determined by the Hartree method (Hartree 1972) using BSA as standard and assayed for DNA-binding activity by EMSA.

Electrophoretic mobility shift assay (EMSA), DNA probes, and competitors

DNA gel shift experiments were performed according to Freitas and Bertolini (2004). The purified GST-SEB-1 recombinant protein was assayed for DNA-binding activity using, as probes, two 150 bp DNA fragments (STRE1 and STRE2) from the *gsn* gene promoter, both of them containing the STRE motif. The purified recombinant protein GST was used as a negative control in the binding reactions. Binding reactions were carried out in 50 μl of EMSA binding buffer containing 2 μg of the nonspecific competitor poly(dI-dC).(dI-dC) (GE HealthCare) and either 2 or 5 μg of either GST-SEB-1 or GST recombinant proteins. The reaction mixtures were incubated with the radiolabeled probes (~10^4 cpm) STRE1 or STRE2, and free probe was separated from DNA-protein complexes on a native 5% polyacrylamide gel. The DNA-protein complexes were detected by autoradiography after

exposing the dried gels to X-ray films. For competition assays, an excess of the specific DNA competitors, STRE1 oligonucleotide and either STRE1 or STRE2 cold probe, was added to the binding reactions 10 min prior to incubation with the respective radiolabeled probes.

To prepare the probes and competitors for EMSA, DNA fragments containing the DNA regulatory motifs STRE1 (158 bp) and STRE2 (146 bp) were prepared by PCR according to Freitas and Bertolini (2004) in the absence and presence of [α-^{32}P]-dATP (3000 Ci/mmol). The unlabeled STRE1 and STRE2 probes were used as specific competitors for their respective labeled probes. An 18 bp DNA oligonucleotide bearing the STRE1 motif and its boundaries was also used as a specific competitor for both the STRE1 and STRE2 probes after annealing the complementary oligonucleotides STRE1-F and STRE1-R (Table S1). A mutated STRE1 probe (mSTRE1), which changes the STRE1 core sequence CCCCT to AAAAG, was used (Freitas and Bertolini 2004). Probes, specific competitors, and the dsDNA oligonucleotide STRE1 were quantified by measuring the absorbance at 260 nm and added to the reaction in 15-fold excess. The oligonucleotides used for EMSA are listened in Table S1.

Construction of a Δseb-1 his-3 double mutant and Δseb-1 rescued strains

To complement the Δ*seb-1* mutant, the strain FGSC 11345 (Δ*seb-1*::*hyg* a) was crossed with a *his-3* strain FGSC#6103 (*his-3* A) to generate the double-mutant strain Δ*seb-1 his-3*. A 2023 bp DNA fragment was amplified by PCR with the primer pair sfGFPseb1-F and sfGFPseb1-R (Table S1) using genomic DNA from the wild-type strain as the template. PCR was performed using the Phusion High-Fidelity PCR kit (Finzymes) and DNA fragments were purified with the QIAquick gel extraction kit (Qiagen, CA), according to the manufacturer's instructions. The purified DNA fragment was cloned into *Xba*I/*Pac*I sites of the plasmid pTSL91-A, resulting in the pTSL91A-*seb-1* construction. The plasmid pTSL91-A allows constitutive expression of *seb-1-sfgfp* from the *ccg-1* promoter. The pTSL91-A-*seb-1* construction was used to transform the Δ*seb-1 his-3* strain, by selection for His+ prototrophy. The transformants (*his-3*::*Pccg-1-seb1-sfgfp*) were selected on VM medium containing hygromicin and/or histidine. The homokaryons were isolated after microconidiation induction (Ebbole and Sachs 1990), followed by filtration using a Millex SV 5 μm (Millipore), and confirmed by PCR using the same primer pair sfGFPseb1-F and sfGFPseb1-R (Table S1).

Quantification of glycogen and trehalose

Glycogen and trehalose were determined in mycelial pads from the wild-type strain, Δ*seb-1*, and Δ*seb-1* complemented strains submitted or not to heat stress. Briefly, glycogen was precipitated with cold ethanol and digested with α-amylase and amyloglucosidase. Free glucose was quantified with a glucose oxidase kit (Labtest) and the glycogen concentration was normalized to the total protein concentration (Freitas *et al.* 2010). Trehalose content was determined in the same samples according to Neves *et al.* (1991). Briefly, trehalose was digested with a partially purified trehalase from *Humicola grisea* (Zimmermann *et al.* 1990), and the trehalose content was determined by quantifying free glucose using a glucose oxidase kit and normalized to the total protein concentration. Total protein was quantified by the Hartree method (Hartree 1972) using BSA as standard.

RNA extraction and RT-qPCR analysis

For the RT-qPCR analysis, total RNA from the wild-type strain, Δ*seb-1*, and Δ*seb-1* complemented strains was prepared using mycelial samples subjected or not to heat shock, according to Sokolovsky *et al.* (1990). Expression of the genes *gnn* (glycogenin, NCU06698), *gsn* (glycogen synthase, NCU06687), *gbn* (glycogen branching enzyme, NCU05429), *gpn* (glycogen phosphorylase, NCU07027), *gdn* (glycogen debranching enzyme, NCU00743) related to glycogen metabolism, and the *seb-1* gene was determined by RT-qPCR, using specific oligonucleotides (Table S1). For this, total RNA samples (20 μg) were first treated with RQ1 RNAse-free DNAse (Promega) and subjected to cDNA synthesis using the SuperScript III First Strand Synthesis kit (Invitrogen) and oligo (dT) primer, according to manufacturer's instructions. The cDNA libraries were subjected to RT-qPCR on a StepOnePlus Real Time PCR system (Applied Biosystems) using the Power SYBR Green PCR Master Mix (Applied Biosystems) and specific primers for each gene amplicon (Table S1). Data analysis was done with the StepOne software (Applied Biosystems) using the comparative CT (ΔΔCT) method (Livak and Schmittgen 2001). Six biological replicates, with three experimental replicates per sample, were performed. The fluorescent dye ROX was used as the passive reference to normalize the SYBR green reporter dye fluorescent signal. The PCR products were subjected to melting curves analysis to verify the presence of single amplicons. All reaction efficiencies varied from 94 to 100%. The actin gene (*act* gene, NCU04173) was used as the reference gene.

Subcellular localization of SEB-1-sfGFP protein

To determine the subcellular localization of the fluorescent SEB-1-sfGFP protein under heat stress, 200 μl of a conidial suspension (2×10^6 conidia/ml) from the Δ*seb-1* complemented strain were inoculated onto coverslips, covered with VM liquid plus 1% sucrose, and incubated at 30° for 10 hr. After incubation, the coverslips were transferred to fresh VM media containing 0.5% sucrose preheated to 45° and incubated at the same temperature for up to 2 hr. For osmotic stress, the coverslips were shifted to fresh VM media containing 0.5% sucrose, and either 1.5 M sorbitol or 1.5 M NaCl, and incubated at 30° for up to 4 hr. To analyze oxidative stress, the coverslips were shifted to fresh VM liquid media containing 0.5% sucrose and either 500 μM paraquat, 100 μM menadione, or 25 mM hydrogen peroxide, and incubated at 30° for up to 2 hr. For nuclei analysis, mycelia were fixed [3.7% formaldehyde, 50 mM NaH_2PO_4 (pH 7.0), 0.2% (v/v) Tween 80], washed twice with PBS and stained with 100 μl DAPI (4',6-diamidino-2-phenylindole, 0.5 mg/ml) for 5 min. Fluorescence was visualized using a fluorescence microscope with excitation and emission wavelengths of 359 nm and 461 nm, respectively. The images were captured using an AXIO Imager.A2 Zeiss microscope coupled to an AxioCam MRm camera and processed using AxioVision software, version 4.8.2.

cDNA libraries preparation and RNA-seq

Total RNA was extracted from wild-type and Δ*seb-1* heat-shocked mycelial pads as previously described (Sokolovsky *et al.* 1990), quantified in a NanoDrop ND1000 spectrophotometer (Thermo Scientific), and checked for integrity of rRNA by electrophoresis on a 1.2% formaldehyde agarose gel. The mRNA from biological triplicates was isolated from total RNA samples using Dynabeads Oligo(dT)25 (Invitrogen) and fragmented by the RNA Fragmentation Reagents kit (Ambion). The mRNA fragments were precipitated with 0.1 vol of 3 M sodium acetate and 2 vol of cold 100% ethanol, and washed with 70% ethanol. The precipitate was resuspended in Tris-EDTA buffer. The first cDNA strand was prepared using the SuperScript III First Strand Synthesis kit (Invitrogen) and [d(N_6)] random primers (Invitrogen), and the second cDNA strand was prepared using the Second Strand Buffer (Invitrogen), according to the manufacturer's instructions.

For the RNA-seq experiments, the double-stranded cDNAs were end-labeled with different adaptors using the TruSeq DNA LT sample prep kit (Illumina), according to the manufacturer's instructions. The end-labeled cDNAs of about 200 bp were purified by electrophoresis on a 2.5% low-melting point agarose gel (Qiagen, CA). The gel-purified cDNA libraries were amplified by PCR (TruSeq v2 LT sample prep kit PCR, Illumina), quantified, and checked for quality on an Agilent 2100 Bioanalyzer, and sequenced as single-end 50 bp reads on an Illumina Genome Analyzer GX platform.

RNA-seq data analysis

The short reads were aligned to the published genome of *N. crassa* (http://www.broadinstitute.org/annotation/genome/neurospora/MultiDownloads.html) using TopHat v2.04 software (Trapnell *et al.* 2009). Cufflinks v2.02 software (Trapnell *et al.* 2010) was used to normalize the reads as fragments per kb or exon model per million mapped fragments (FPKM) for each gene identified. The statistical significance of differences in FPKM among the samples was determined using the CuffDiff component of the Cufflinks package. Only adjusted *P*-values below 0.05 were used to identify significant differences in gene expression before and after heat stress. DEseq v1.14 was utilized for clustering the whole RNA-seq data sets by a Euclidean distance matrix using a variance-stabilizing transformation (Anders and Huber 2010). The retrieved ORFs were functionally annotated and analyzed using the web tool Blast2GO version 2.7.2 (http://www.blast2go.com/start-blast2go) (Conesa *et al.* 2005).

ChIP-qPCR analysis

Chromatin immunoprecipitation (ChIP) assays were performed on mycelial samples from the Δ*seb-1* complemented strain according to Tamaru *et al.* (2003), with modifications described in Cupertino *et al.* (2015). Briefly, chromatin from mycelia submitted or not to heat shock was fixed with formaldehyde and suspended in ChIP lysis buffer (50 mM HEPES, pH 7.9; 90 mM NaCl; 1 mM EDTA, pH 8.0; 1% Triton X-100; 0.1% sodium deoxycholate; 1 mM PMSF; 0.1 mM TCLK; 1 mM benzamidine; and 1 μg/ml each of pepstatin and antipain). The chromatin was sheared to an average size of 0.3–0.8 kb using Vibra Cell Sonics (10 cycles: 1 min, 40% amplitude, 8.0 sec ON, 9.9 sec OFF). Sonicated chromatin was precleared with Dynabeads Protein A (Novex) preblocked with 0.5% BSA in PBS, and then immunoprecipitated with anti-GFP antibody (Sigma) and Dynabeads Protein A. The DNA concentration was quantified and 25 ng of input DNA (positive control), no Ab, and IPs (immunoprecipitated DNAs from anti-GFP) was analyzed by qPCR on the StepOnePlus Real-Time PCR system (Applied Biosystems) using the Power SYBR Green PCR Master Mix (Applied Biosystems). Oligonucleotides for the *gsn* (emsaSTRE1-F/emsaSTRE1-R and STRE2i-F/STRE2i-R), *gpn* (pGPNNit-F2/pGPNNit-R2), *gnn* (GNNp-F2/GNNp-R3), *gbn* (BRANCH-FP3/BRANCH-RP1), and *gdn* (DEBp-F2/DEBp-R2) promoters are described in Table S1. A ubiquitin gene fragment (NCU05995), which does not have the SEB-1 motif, was amplified with the primers qUbi-F/qUbi-R and used as a negative control of binding. The amplifications were carried out in triplicates in a 96-well plate. All PCR products had melting curves indicating the presence of a single amplicon. For each promoter region analyzed, at least five independent standard curves were run and the mean cycle threshold value at each 10-fold dilution of three independent runs was used for the final standard curve.

Data availability

Strains and plasmids can be provided upon request. File S1 contains detailed descriptions of all supplemental files.

RESULTS

Identification of SEB-1 as a transcription factor that binds to STRE in N. crassa

In *S. cerevisiae*, STRE is a motif present in the promoters of stress-regulated genes and is recognized by the transcription factors Msn2p/4p (Martínez-Pastor *et al.* 1996). The *GSY2* gene in *S. cerevisiae*, which encodes an isoform of glycogen synthase, has STRE in its promoter and is activated under heat stress (Ni and LaPorte 1995). However, the gene encoding the same enzyme (*gsn*) in *N. crassa* is down-regulated under heat stress (de Paula *et al.* 2002), although it has STRE motifs in its 5′-flanking region (Freitas and Bertolini 2004), suggesting that the stress response mediated by STRE may differ between yeast and *N. crassa*. A search for Msn2p/4p orthologs in the *N. crassa* genome retrieved no significant results, suggesting that *N. crassa* may lack orthologs of these transcription factors. We used pulldown assays with biotinylated primers and cellular extracts from heat-shocked cells to isolate proteins able to bind STRE, and to identify the proteins by mass spectrometry. Oligonucleotides containing tandem repeats of the STRE core sequence and genomic nucleotide sequences as spacer regions (Table S1) were coupled to streptavidin beads, and a chromatographic fraction showing DNA-binding activity was used as the protein source. The proteins were eluted from the resin and separated on a SDS-PAGE gel, revealing the presence of two regions in the gel containing protein bands that were not present in the mock reaction (Figure 1A, compare the mock lane with pulldown lanes). These regions were excised from a SDS gel, trypsin digested, and submitted to mass spectrometry analysis for protein identification. Of the proteins identified in the pulldown assays (Figure 1B), one protein had a double C_2H_2-type zinc finger DNA-binding domain at its C-terminus – the protein encoded by the ORF NCU02671. This ORF is annotated in the *N. crassa* database as encoding a cutinase G-box binding protein, containing 575 amino acid residues with theoretical molecular mass and pI values of 62.7 kDa and 5.2, respectively. The two zinc finger motifs extend from amino acid residues 448–497 (Figure 1C). A Delta-BLAST analysis showed that the protein was a homolog of the Seb1 from *T. atroviride* (40% identity) (Peterbauer *et al.* 2002), MsnA from *A. nidulans* (34% identity) (Han and Prade 2002), and SebA from *A. fumigatus* (31% identity) (Dinamarco *et al.* 2012) proteins. The identities are mainly localized in the C-terminus, where the two zinc finger motifs are located (Figure 1C). According to PSORT II (http://psort.hgc.jp/form2.html), the protein has three monopartite nuclear localization signals at amino acid positions 363 (PSKRARH), 432 (PTNRRGR), and 568 (KKKR). The Seb-1, MnsA, and SebA proteins are transcription factors that are responsive to stress conditions in filamentous fungi. In addition, the *T. atroviride* Seb1 transcription factor binds *in vitro* to the *S. cerevisiae* STRE core sequence 5′-AGGGG-3′ (Peterbauer *et al.* 2002). Therefore, we named NCU02671 as *seb-1* and predicted that SEB-1 protein may be a transcription factor that binds to the STRE motif in *N. crassa*.

The seb-1 deletion causes morphological defects and sensitivity to stress

To assess the effects of the loss of SEB-1 function, we examined the morphology of the Δ*seb-1* strain during vegetative growth. Flasks of 10-day-old cultures of the Δ*seb-1* strain exhibited a cauliflower-like growth aspect, as compared to the wild-type strain (Figure 2A). The radial growth of the Δ*seb-1* mutant showed the presence of growth bands with different regions of pigmentation (Figure 2A). Analysis of the hyphal edges of the Δ*seb-1* mutant revealed numerous short hyphae, most likely resulting from a hyper-branching phenotype (Figure 2A). To confirm that the morphological changes were due to the *seb-1*

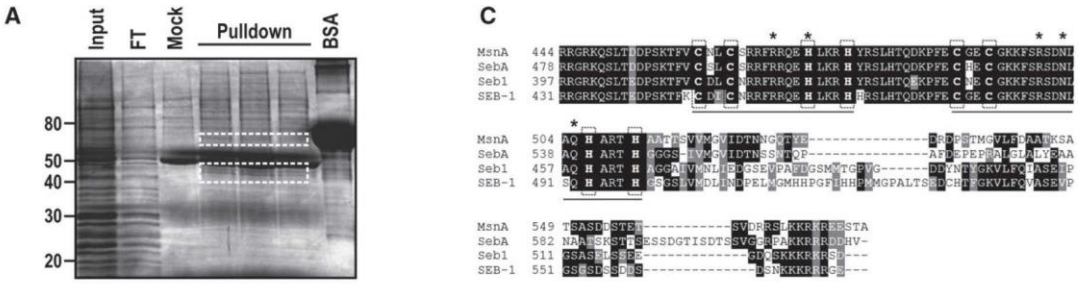

B

Putative protein binding to the STRE motif of the *gsn* promoter [a)]

Gene n° [b)]	Protein ID [b)]	Pfam	Protein score	Sequence coverage (%)	n° of matched peptides	Theoretical pI / MM (kDa)
NCU00497	Hypothetical protein	WD-40 repeats	25	1	1	5.36 / 56.6
NCU02671	Cutinase-G box binding protein	C_2H_2-zinc finger	30	2	2	5.20 / 62.7
NCU04164	Hypothetical protein	RNA recognition motif (a.k.a. RRM, RBD, or RNP domain)	88	7	7	8.72 / 37.7
NCU06479	Hypothetical protein	Six-bladed beta-propeller, TolB-like	21	1	1	4.75 / 40.9
NCU08638	Hypothetical protein	Bipartite NLS	32	2	3	8.31 / 33.7

[a)] Proteins were analyzed using ESI-MS/MS and the isotopic peaks were searched against the *N. crassa* database using MASCOT tool, with peptide and MS/MS tolerances of 0.1 Da each and allowing up to 1 missed trypsin cleavage site.

[b)] BROAD Institute (http://www.broadinstitute.org/annotation/genome/neurospora/MultiHome.html).

Figure 1 Pulldown assay identified SEB-1 as the transcription factor that binds to the STRE motif in *N. crassa*. (A) Biotin-streptavidin pulldown assay. Biotinylated dsDNA oligonucleotides containing the *N. crassa* STRE consensus sequence in tandem were used as bait in a pulldown reaction with nuclear extract prepared from heat-shocked mycelia as a protein source. Protein bands not present in the mock reaction were removed from the gel, trypsin digested and submitted to mass spectrometry (white rectangles). Input: protein fraction showing DNA-binding activity; Mock: pulldown reaction without dsDNA coupled to the resin; FT: flow-through chromatographic sample. (B) The putative proteins identified by mass spectrometry. Proteins were analyzed by ESI (electrospray ionization)-MS/MS. Monoisotopic peaks were searched against the *N. crassa* database with a maximum of one missed trypsin cleavage and a mass tolerance of 0.1 Da for precursor ions and 0.1 Da for MS/MS spectra. Database was searched by using MASCOT. (C) Sequence alignment of different Msn2p/4p orthologs present in filamentous fungi. Alignment was done using Delta-BLAST (BLASTP 2.2.29+) in a nonredundant database. MsnA: *A. nidulans* ortholog (XP659256.1); SebA: *A. fumigatus* ortholog (XP751917.1); Seb-1: *T. atroviride* ortholog (AAM73769.1); SEB-1: *N. crassa* ortholog (EAA36208.2). The bars indicate the Zinc finger domains, and the cysteine and histidine residues are highlighted in vertical rectangles (dotted lines). The putative amino acid residues interacting with the STRE motif are indicated by asterisks. BSA, bovine serum albumin; STRE, stress response element.

knockout, we constructed the Δ*seb-1* complemented strain by inserting the *seb-1* gene from the wild-type strain into the *his-3* locus (Δ*seb-1 his-3*::*seb-1*). When cultured under the same conditions as the mutant and wild-type strains, the rescued strain (Δ*seb-1 his-3*::*seb-1*) restored the wild-type growth phenotype, confirming that the morphological aspects observed in the mutant strain were indeed due to the *seb-1* deletion (Figure 2A).

To investigate the function of the SEB-1 protein in stress responses, we evaluated the sensitivity of the Δ*seb-1* and Δ*seb-1* complemented strains to heat and pH changes and to a variety of chemical stresses, such as exposure to high concentrations of sorbitol, NaCl, paraquat, menadione, and hydrogen peroxide, and compared the results with those of the wild-type strain. We first analyzed the radial growth of the mutant strain after 24 and 48 hr of incubation at 45°. Radial growth at 30° for 24 hr was lower than those observed in the wild-type and complemented strains. Compared to the wild-type strain, Δ*seb-1* showed defective growth after 48 hr of heat stress (Figure 2B). The response to heat shock mediated by SEB-1 was confirmed by analyzing the Δ*seb-1* complemented strain under the same condition; the rescued strain showed similar growth to the wild-type strain (Figure 2B). The viability of the heat-shocked cells was evaluated by shifting the 48 hr cultures back to 30° for 24 hr. All of the strains recovered their normal morphological aspects, confirming that the growth response to high temperature was due to viable cells (Figure 2B).

The pH stress response was analyzed by comparing the growth of the strains under acidic (4.2) and alkaline (7.8) pH with growth under pH 5.8 (normal pH) for 24 and 48 hr. The Δ*seb-1* strain was sensitive to both pH, exhibiting lower radial growth than the wild-type and rescued strains, and high sensitivity at pH 7.8 (Figure S1). The Δ*seb-1* strain exhibited a dense growth halo under pH 4.2 after 48 hr, which consisted of thin, highly vacuolated hyphae, suggesting that this halo corresponded to a zone of cellular death (results not shown).

Oxidative stress in the Δ*seb-1 vs.* wild-type and rescued strains was evaluated by cultivating the strains in liquid and solid VM medium in the presence of increasing concentrations of the ROS-forming agents paraquat, menadione, and hydrogen peroxide. These oxidant agents orchestrate different responses that converge to a same final product, *i.e.*, the generation/accumulation of ROS within the living cells. Paraquat is a viologen herbicide that interferes with the respiratory chain, accepting electrons from a donor such as NADPH and transferring them to molecular oxygen, thereby producing high amounts of the ROS superoxide anion (O_2^-). On the other hand, menadione (or

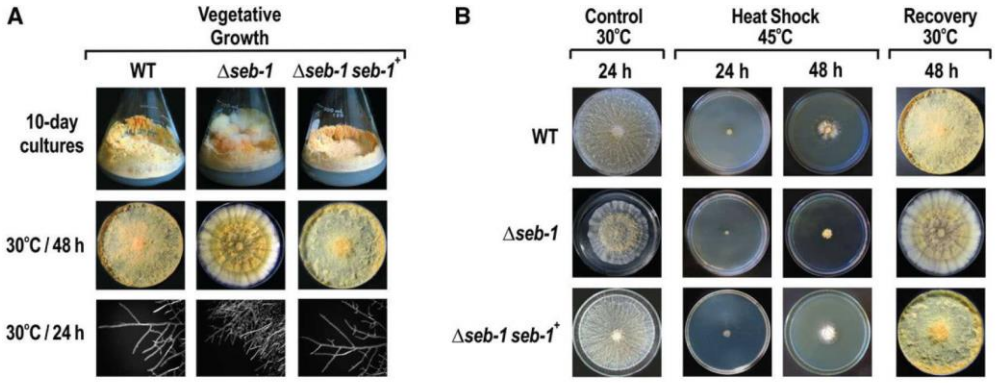

Figure 2 Functional characterization of the mutant strain Δ*seb-1*. (A) 10-day-old conidia of the Δ*seb-1* strain were cultivated in Erlenmeyer flasks and on plates containing solid VM medium. The images of the hyphae tips were captured after 24 hr using an AxioCam ICc3 camera coupled to a trinocular Discovery V8 stereoscope (Zeiss) at 80× magnification. (B) Heat stress assay. The Δ*seb-1* strain was cultivated at 45° for 2 d and then brought back to 30° for 24 hr to evaluate cellular viability. Cultures at 30° for 24 hr are shown as control. The Δ*seb-1 seb-1*$^{+}$ strain is the Δ*seb-1* complemented strain (Δ*seb-1 his-3*::*Pccg-1-seb1-sfgfp*). VM, Vogel's minimal; WT, wild-type.

vitamin K3) is a synthetic naphthoquinone derivative that is reduced to its hydroquinone form in a NADPH-dependent way. An excess of menadione causes NADPH depletion and glucose-6-phosphate dehydrogenase (G6PD) deficiency. As a consequence of NADPH decay, there is no supply of reduced glutathione, which leads to increased levels of intracellular hydrogen peroxide. The Δ*seb-1* strain showed high sensitivity to all oxidative stress agents, both in liquid and solid cultures (Figure S2, compare A and B), mainly at the lower concentrations used in this assay (see right panel in Figure S2A).

The tolerance to osmotic stress was analyzed by growing the strains in the presence of increased concentrations of sodium chloride and sorbitol in solid and liquid VM medium. The Δ*seb-1* strain was highly sensitive to both high salt and high carbohydrate concentrations (Figure S3, A and B). The sensitivity of the mutant strain was also higher under lower concentrations of sodium chloride and sorbitol (see right panel in Figure S3A). The rescued strain exhibited a phenotype similar to the wild-type strain in all stress conditions analyzed here, confirming that the increased sensitivity to stress was indeed caused by the lack of the SEB-1 transcription factor.

SEB-1 cellular localization under different environmental conditions

The functionality of SEB-1 was also evaluated by determining its subcellular localization under different stress conditions. To assess this, we used the Δ*seb-1* complemented strain, in which SEB-1 is produced as a C-terminus GFP-tagged fusion protein. We first evaluated the SEB-1 cellular localization under heat stress by germinating conidia at 30° for 10 hr and then transferring to medium at 45°. The SEB-1-GFP protein was found to be predominantly in the cytoplasm after 30 min of heat stress, but was translocated to the nucleus after 2 hr of exposure to 45° (Figure 3). These data are consistent with its role in regulating the heat stress response in *N. crassa*. The cellular localization of SEB-1-GFP was also analyzed under osmotic and oxidative stress. For osmotic stress, *N. crassa* conidia were germinated in glucose VM medium for 10 hr and then transferred to VM medium containing either NaCl or sorbitol. In both conditions, SEB-1-GFP was mainly detected in the nucleus, but some cytoplasmic localization was observed even 4 hr after transfer (Figure 4). The cellular location of SEB-1-GFP was also evaluated under oxidative stress induced by paraquat, menadione, or H_2O_2. All chemicals caused translocation of SEB-1-GFP to the nucleus, although the protein was also observed in the cytoplasm (Figure 4). Therefore, the *N. crassa* SEB-1 transcription factor cycles between the cytoplasm and the nucleus under environmental situations that promote stress.

The SEB-1 transcription factor binds to STRE in vitro

As previously described, SEB-1 was identified using an approach to isolate a transcription factor capable of binding to the STRE motif present in the promoter of the gene encoding glycogen synthase (*gsn*), the rate-limiting enzyme in glycogen synthesis. This gene has two STRE motifs in its 5′-flanking region (Figure 5A), the first one located within the promoter region upstream of the putative TATA-box (STRE1), and the other one within the intron located in the 5′-UTR (STRE2) (Freitas and Bertolini 2004). To confirm that SEB-1 binds to STRE in *N. crassa*, the GST-tagged recombinant protein was produced in *E. coli* and used as a protein source for EMSA using two DNA fragments of the 5′-flanking region, one bearing STRE1 (probe STRE1) and the other one bearing STRE2 (probe STRE2). The gel shift assay showed that the GST-SEB-1 fusion protein bound to both motifs *in vitro* (Figure 5B, lanes 2, 3, 8, and 9). The binding specificity was confirmed for both DNA probes since the specific competitors (the cold probes STRE1 and STRE2), strongly decreased the shifted bands when 5 μg of the recombinant protein was used (Figure 5B, lanes 4 and 10). The specificity of binding was also confirmed by using an 18 bp dsDNA oligonucleotide bearing the STRE1 motif and its boundary genomic sequences (Table S1) and a DNA probe containing the mutated motif STRE1 (Freitas and Bertolini 2004). The competitor dsDNA oligonucleotide abolished the DNA band shifts observed with the probes STRE1 and STRE2 (Figure 5B, lanes 5 and 11). In addition, the DNA-protein complex was not observed when using the mutated probe STRE1 (Figure 5B, lanes 14 and 15), thus confirming the specificity of the GST-SEB-1 binding to STRE1.

The accumulation of reserve carbohydrates is regulated by SEB-1

We described above that SEB-1 binds *in vitro* to the STRE motifs present in the *gsn* promoter and that the Δ*seb-1* strain was sensitive to heat, pH, oxidative, and osmotic stress. In order to correlate both results,

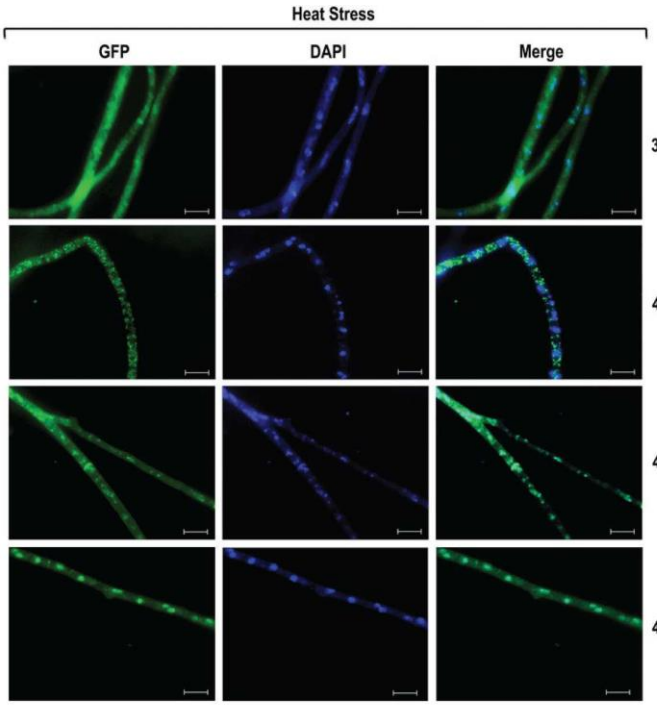

Figure 3 SEB-1 protein translocates to the nucleus during heat stress. Conidia from the Δ*seb-1* complemented strain (Δ*seb-1 his-3*::*Pccg-1-seb1-sfgfp*) were grown on coverslips in liquid VM medium containing 1% sucrose at 30° for 10 hr. After this period, mycelia were transferred to VM medium preheated at 45° (heat stress) for 30 min, 1 hr, and 2 hr. Heat-shocked mycelia were fixed in PBS with formaldehyde, the nuclei were stained with DAPI (0.5 mg/ml), and the fluorescence was examined. Mycelium cultured in liquid VM medium at 30° for 10 hr was used as a control. Images were taken after 30 min, 1 hr and 2 hr after transferring to 45°. Fluorescence was evaluated using the AXIO Imager.A2 microscope (Zeiss) at a magnification of 100×. The images are representative of at least two independent experiments. Scale bar: 10 μm. DAPI, 4′,6-diamino-2-phenylindole; GFP, green fluorescent protein; PBS, phosphate-buffered saline; VM, Vogel's minimal.

we quantified the glycogen accumulated by the wild-type strain and the Δ*seb-1* and Δ*seb-1* complemented strains under normal growth temperature (30°) and after exposure to heat stress (transferring from 30° to 45°). In *N. crassa*, glycogen is accumulated at the end of the exponential growth phase and is degraded after heat shock (de Paula *et al.* 2002; Freitas and Bertolini 2004). The Δ*seb-1* strain exhibited the same profile of glycogen accumulation as compared to the wild-type strain, *i.e.*, lower levels after heat stress (Figure 6A). However, the mutant strain accumulated much higher glycogen levels than the wild-type strain under normal growth temperature, *i.e.*, before heat shock, indicating that SEB-1 affects glycogen accumulation under normal growth temperature (Figure 6A). SEB-1 also controls glycogen accumulation under heat stress, however, the major control seems to be at 30°.

We also quantified trehalose, another reserve carbohydrate. Trehalose is a nonreducing disaccharide found at high levels in fungi, which accumulates preferentially in spores to be used as a carbon and energy source for conidial germination (Hanks and Sussman 1969; Fillinger *et al.* 2001). In *N. crassa* conidia, trehalose corresponds to 10% of the dry-weight, and its levels decrease upon germination and remain at low levels during vegetative growth. Trehalose levels rise again at the end of the growth and accumulate in conidia (Hanks and Sussman 1969). A temperature-shift (from 30° to 45°) results in an accumulation of trehalose concomitant with a decrease in glycogen levels (Neves *et al.* 1991). These effects may depend on the activities of glycogen synthase, glycogen phosphorylase, and trehalose-phosphate synthase, the regulatory enzymes in glycogen and trehalose metabolism, respectively (Noventa-Jordão *et al.* 1996). SEB-1 affects trehalose levels under normal growth temperature and under heat stress. The levels were significantly reduced in the Δ*seb-1* under heat stress, while the levels under normal growth temperature showed a slight but significant increase (Figure 6B). The rescued strain showed similar glycogen and trehalose levels to the wild-type strain. All together, these findings suggest that SEB-1 influences the metabolism of both reserve carbohydrates in *N. crassa*.

SEB-1 modulates the expression of all glycogenic genes and binds in vivo to their promoters

To investigate whether SEB-1 controls glycogen accumulation by regulating the genes encoding the glycogenic enzymes, we performed RT-qPCR on genes encoding enzymes of glycogen synthesis (*gnn*, *gsn*, and *gbn*) and glycogen degradation (*gpn* and *gdn*) in samples taken before (30°) and after heat shock (45°). An *in silico* analysis of the gene promoters revealed the existence of the STRE motif in all promoters, either adjacent to each other or separate (Figure 7A). A STRE motif was also identified in the *seb-1* promoter itself. All genes were overexpressed in the *seb-1* strain at normal growth temperature (30°, $P < 0.001$), indicating that SEB-1 acts as a repressor of the glycogenic genes under this condition (Figure 7B). It is important to note that the genes encoding enzymes for glycogen synthesis and degradation were highly expressed at 30°, which means that both processes would be similarly repressed by the transcription factor in the wild-type strain. However, the glycogen levels were higher in the *seb-1* strain under the same growth condition (see Figure 6A). Considering these results, we suggest that glycogen accumulation likely results from gene expression regulation and the balance between the enzyme activities of synthesis and degradation. It is important to emphasize that glycogen synthase and glycogen phosphorylase are enzymes regulated by phosphorylation. We also observed that the *gnn* and *gsn* genes (encoding enzymes of glycogen synthesis) were significantly overexpressed at 45° in the *seb-1* strain ($P < 0.001$, Figure 7B), which may explain the glycogen accumulated by the *seb-1* strain under this condition (see Figure 6A). Heat stress also induced the expression of the *seb-1* gene (Figure 7B) in the wild-type strain, a finding that is consistent with the involvement of this transcription factor in heat stress response. In this case, heat stress

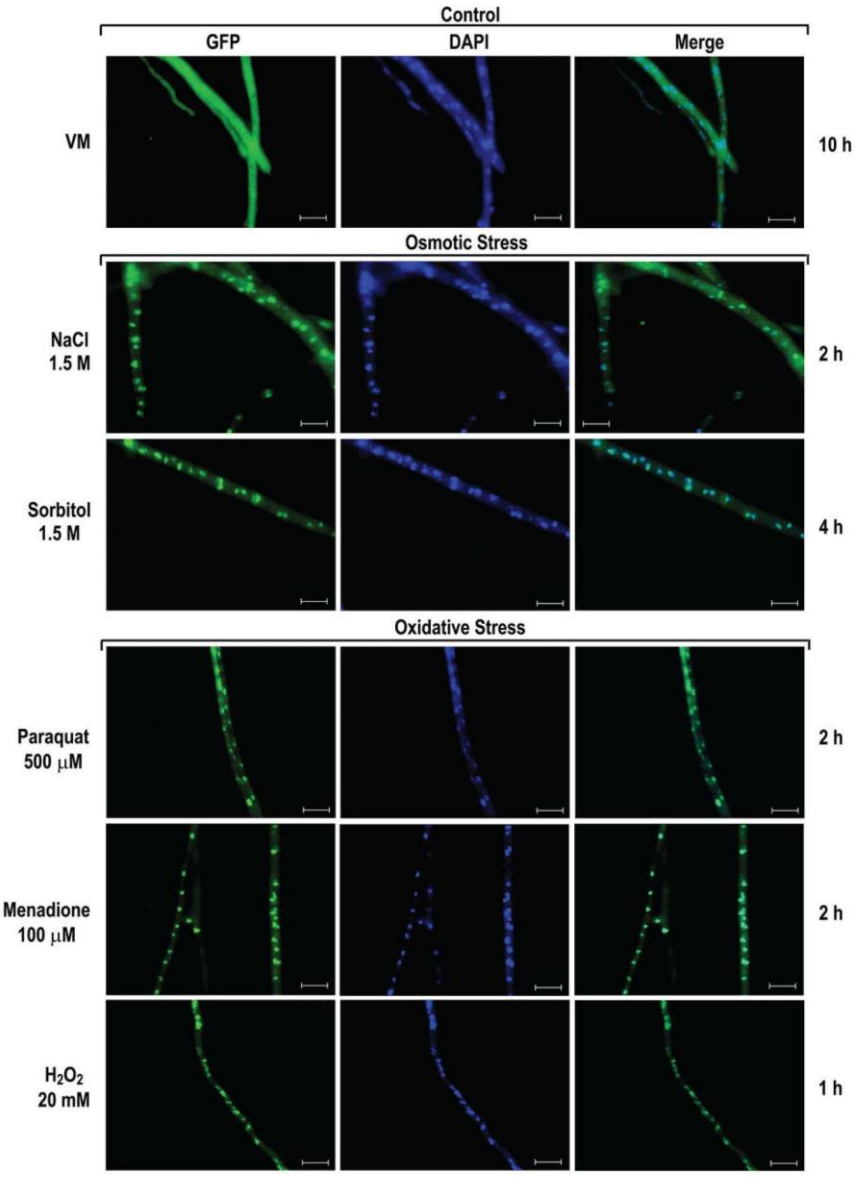

Figure 4 SEB-1 protein translocates to the nucleus under osmotic and oxidative stress conditions. Conidia from the Δ*seb-1* complemented strain (Δ*seb-1 his-3*::*Pccg-1-seb1-sfgfp*) were grown on coverslips in liquid VM medium containing 1% sucrose at 30° for 10 hr. After this period, mycelia were subjected to osmotic and oxidative stresses for 1 hr, 2 hr, or 4 hr. Stressed mycelia were fixed in PBS with formaldehyde, the nuclei were stained with DAPI, and the fluorescence were visualized. Mycelia from liquid VM medium cultured for 10 hr at 30° was used as control. Fluorescence was evaluated using the AXIO Imager.A2 microscope (Zeiss) at a magnification of 100×. The images are representative of at least two independent experiments. Scale bar: 10 μm. DAPI, 4′,6-diamino-2-phenylindole; GFP, green fluorescent protein; PBS, phosphate-buffered saline; VM, Vogel's minimal.

induced *seb-1* expression, whose product is required for the expression regulation of genes under stress.

ChIP-qPCR assays were performed to confirm the regulation of all the genes by SEB-1. All genes involved in glycogen metabolism have STRE motifs in their 5′-flanking regions and some of them were analyzed for *in vivo* binding (the gray boxes in Figure 7A). In these experiments, we used the Δ*seb-1* complemented strain (*his-3*::*Pccg-1-seb-1-sfgfp*) and anti-GFP antibody. Chromatin was collected from mycelia before (sample zero) and after heat stress (sample HS) and binding of SEB-1 was quantified in the *gsn*, *gpn*, *gdn*, *gnn*, and *gbn* promoters. The input DNA was used as a positive control and a fragment of the ubiquitin gene lacking the motif was used as a negative control for binding. SEB-1 bound to all motifs analyzed both before and after heat stress; however, binding was significantly increased under heat stress (Figure 8). It is noteworthy to observe the high amplification of the *gsn* gene when using the STRE2 probe, which may suggest a major role for this motif in the regulation of *gsn* expression by SEB-1 (compare with the amplification of the STRE1 probe). Together, these results indicated that SEB-1 recognized and bound to all glycogenic gene promoters *in vivo*, before and after heat shock; such binding would control the glycogen levels under both conditions through the regulation of gene expression.

Determining the SEB-1 regulon

In *S. cerevisiae*, the *cis* regulatory motif STRE is involved in the response to different stress conditions such as heat shock, osmotic stress, and oxidative stress, and requires the Msn2/4p proteins as transactivators (Martínez-Pastor *et al.* 1996). In *T. atroviride*, the transcription factor

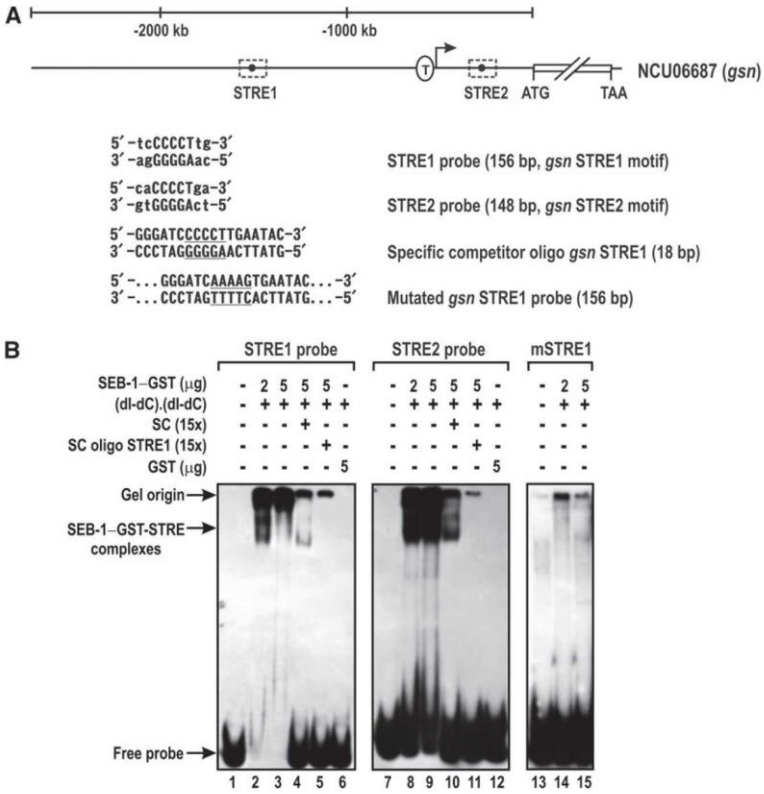

Figure 5 Recombinant SEB-1 binds specifically to the *N. crassa* STRE motif *in vitro*. (A) Schematic representation of the *gsn* gene and the STRE positions in the promoter region. The sequences of the STRE1 and STRE2 DNA elements are represented. The STRE1 DNA oligonucleotide containing the motif sequence (underlined) and the STRE1 probe with mutations in the STRE core sequence (underlined) are also represented. T: transcription start site (Freitas and Bertolini 2004). (B) DNA probes containing both STRE motifs present at the 5′-flanking region of the gene *gsn* (STRE1 and STRE2) were assayed for DNA-binding activity using the GST-tagged recombinant SEB-1 as a protein source. The specificity of the DNA shifts was demonstrated by the prior addition of specific competitors: the cold probes STRE1 and STRE2, the dsDNA oligonucleotide STRE1, and the dsDNA fragment containing the mutated STRE1 motif. SC: specific competitor (unlabeled probes STRE1 and STRE2); SC oligo STRE1: specific competitor corresponding to a short dsDNA oligonucleotide (18 bp) containing the STRE1 motif; mSRE1: probe STRE1 containing the mutated STRE1 motif. dsDNA, double-stranded; GFP, green fluorescent protein; STRE, stress response element.

Seb1 was also described as binding to STRE in response to osmotic stress (Seidl *et al.* 2004) and the *A. fumigatus* SebA protein is involved in the responses to heat and oxidative stress, nutrient starvation, and pathogenesis (Dinamarco *et al.* 2012). In this work, we showed that the *N. crassa* Seb-1/SebA ortholog is the SEB-1 protein, a transcription factor involved in the response to a variety of stresses, as demonstrated above. We characterized the SEB-1 regulon by RNA-seq by analyzing the genome-wide transcriptional profile of the Δ*seb-1* strain during vegetative growth (30°) and after shifting it to a high temperature (45°). As a control, we performed the same analysis with the wild-type strain grown at both temperatures. When we compared the Δ*seb-1* strain before and after heat stress, the number of transcripts identified after heat stress was high. A total of 2683 ORFs (28.4% of the annotated genome) showed an expression profile that was significantly affected by the *seb-1* deletion (adjusted to $P < 0.05$). Of these, 1117 ORFs were significantly dependent on the functional SEB-1 transcription factor (Figure 9A), indicating that these were genes likely regulated directly or indirectly by SEB-1 under heat stress. Of the genes regulated by SEB-1 under heat stress, 62.1% (693 ORFs) encode proteins annotated in public databases, 33.9% (379 ORFs) encode proteins classified as hypothetical proteins, and 4% (45 ORFs) encode sequences not yet annotated (Figure 9B and Table S2). The overall similarity among each of the samples was calculated using the Euclidean distance and transcript abundance values for all genes and data sets were clustered (Figure 9C). These analyses indicated that the data sets generated from mycelia exposed to heat stress were significantly different from those of mycelia not exposed to heat stress. Additionally, the samples from the *seb-1* strain exposed to heat stress (j, k, and l) formed a separate clade from those of the wild-type strain under the same condition (d and e). This event was also observed before heat shock, *i.e.*, there were separate clades between the wild-type and *seb-1* strains during vegetative growth (30°), indicating that under this condition there were genes whose expression was modulated by SEB-1.

An analysis of the 1117-gene set identified as differentially regulated in the Δ*seb-1 vs.* wild-type strains (Table S2) was used to predict the function of each gene based on the Gene Ontology (GO) categories using Blast2GO (Conesa *et al.* 2005). The most represented GO categories within the differentially expressed genes under heat stress were identified using Fisher's exact test, with an adjusted $P < 0.05$ (Table S3 and Table S4). The 1117 genes and their respective GO terms are represented in Figure 9D. Among the highly enriched biological processes, genes related to general stress responses that include cellular response to osmotic stress, starvation, autophagy, lipid modifications, response to oxidative stress, and response to chemical stimulus were identified (Table S3). Many GO terms enriched only in the *seb-1* strain data set as compared with the wild-type strain, such as cellular component biogenesis, single-organism developmental processes, and methylation, while other categories, such as those belonging to metabolic processes, were highly represented in the Δ*seb-1* strain compared to the wild-type strain (Figure 9D).

Many of the 1117 genes that comprise the *seb-1* regulon have an annotated function within the stress response category. For the oxidative stress response pathway, four cytochrome c oxidases (*cox-7c*, NCU03340; *cox-4*, NCU05689; *cox-6*, NCU06695; and *cox-6b*, NCU06741), a cytochrome c peroxidase (*cpe-1*, NCU03297), a NADPH-oxidase (*nox-2*, NCU10775), a FAD-dependent sulfhydryl oxidase (*fad-1*, NCU09291), four superoxide dismutases (*sod-2*, NCU01213; *sod-1*, NCU02133; *sod-1c*, NCU07851; and *sod*, NCU09560), two

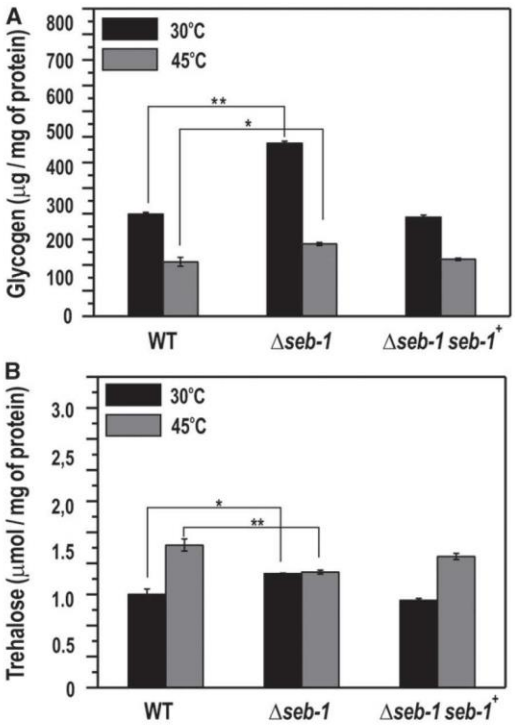

Figure 6 The Δ*seb-1* strain exhibits impaired accumulation of reserve carbohydrates during heat stress. Liquid cultures of the WT, Δ*seb-1*, and Δ*seb-1* complemented strains were exposed to a temperature shift from 30° to 45° for 30 min. After this, the heat-shocked mycelia were used to prepare a cellular extract used for glycogen and trehalose quantification, as described in the *Materials and Methods*. (A) Glycogen content. (B) Trehalose content. WT: wild-type strain; Δ*seb-1*: strain mutated in the ORF NCU02671; Δ*seb-1 seb-1*$^{+}$: Δ*seb-1* complemented strain (Δ*seb-1 his-3*::*Pccg-1-seb1-sfgfp*). The error bars represent the standard deviation. Values of three biological replicates were used for statistical analysis and the significances (*$P < 0.05$, **$P < 0.01$) between the strains were estimated by the Tukey-Kramer multiple comparison test.

catalases (*cat-4*, NCU05169 and *cat-2*, NCU05770), and four glutathione transferases (*gst-1o*, NCU00549; *gst-3*, NCU01320; *gst*, NCU04676; and *gst-1*, NCU05780) were identified (Figure 10A, see oxidative and pH stress panel). Heat stress also regulated the expression of many genes previously described as genes belonging to the pH-stress response pathway, such as the pH-responsive *pacC* gene (NCU00090) (Cupertino *et al.* 2012) and the *A. nidulans palH* orthologous gene (termed *pal-8*, NCU00007) (Figure 10A, see oxidative and pH stress panel). For the osmotic stress pathway, heat stress induced *sln-1* (osmolarity two-component system protein, NCU04615) and repressed *os-2* (osmotic sensitive-2, NCU07024), *sdh-1* (sorbitol dehydrogenase 1, NCU01905), and *sou-2* (sorbitol utilization protein 2, NCU03803) genes (Figure 10A, see osmotic stress panel). As expected, all genes identified by RNA-seq ($P < 0.05$) within heat stress response, such as those encoding heat shock proteins (*hsp98*, NCU00104; *hspSTI1*, NCU00714; *hsp60*, NCU01589; *hsp90a*, NCU01792; *hsp78*, NCU02630; *hsp80*, NCU04142; *hsp88*, NCU05269; *hsp30*, NCU07232; *hsp70*, NCU08693; and *hsps*, NCU09602) and a hypothetical protein (NCU01788), were induced after shifting the mycelia from 30° to 45° (Figure 10A, see heat stress panel). Expression of the *hsp90a* gene and the gene encoding a hypothetical protein was SEB-1-dependent.

All of the genes encoding glycogen metabolism enzymes, *i.e.*, glycogenin (*gnn*, NCU06698), glycogen synthase (*gsn*, NCU06687), glycogen branching enzyme (*gbn*, NCU05429), glycogen phosphorylase (*gpn*, NCU07027), and glycogen debranching enzyme (*gdn*, NCU00743) were repressed by heat stress (Figure 10B, see FPKM graphs), consistent with the results shown in Figure 7B. The effect of the *seb-1* deletion was clearly demonstrated for these genes before heat stress, since all of them showed expression levels significantly higher than those observed in the wild-type strain during vegetative growth (30°). These results suggest a repressor role for SEB-1 on the expression of these genes under this environmental condition. In addition, these results also suggested that the main targets of regulation are genes involved in glycogen synthesis (Figure 10C, *gnn*, *gsn*, and *gbn*, FPKM panels). This finding is very important since it is consistent with the higher glycogen levels observed in the Δ*seb-1* strain compared to the wild-type strain (see Figure 6A). On the other hand, the gene encoding trehalose phosphate synthase (*tps*, NCU00793), the rate-limiting enzyme in trehalose synthesis, was induced after heat stress in both strains (Figure 10C, see *tsp* FPKM graph). However, the expression of this gene was lower in the mutant strain under heat stress. These results were consistent with the trehalose levels in the wild-type strain and could explain the levels observed in the Δ*seb-1* strain under heat stress (see Figure 6B). The results presented here support our hypothesis that the SEB-1 transcription factor plays a role as an activator and/or a repressor for different genes, depending on the environmental condition.

DISCUSSION

All living cells have the ability to respond and adapt to environmental changes by using cellular mechanisms that integrate environmental sensing and signal transduction pathways, which lead to the induction or repression of gene expression. The availability of whole genome sequences allows comparison of the global responses to diverse environmental stresses in different organisms. Comparative studies have revealed the existence of conserved mechanisms in addition to specific responses that highlight unique defense systems (Gasch *et al.* 2000; Swan and Sistonen 2015). Genetic and cell biological studies using different organisms have led to the discovery of global stress regulators and mechanisms conferring resistance to adverse environmental conditions. As a result, knowledge of the molecular mechanisms of adaptation to stress conditions in fungi is extensive (Estruch 2000; Gasch *et al.* 2000; Duran *et al.* 2010; Berry *et al.* 2011; Kroll *et al.* 2014; Brown *et al.* 2014; and others). In this work, we developed an approach that included capturing proteins using streptavidin-conjugated beads/biotinylated STRE oligonucleotides followed by mass spectrometry to identify *N. crassa* protein(s) able to bind to STRE, a DNA element present in the upstream regions of stress responsive genes in *S. cerevisiae*. Among the candidate proteins identified was SEB-1. Although orthologs of this protein have been reported to be involved in stress responses in a few filamentous fungi (Peterbauer *et al.* 2002; Dinamarco *et al.* 2012), its requirement for resistance to different stress responses may vary among organisms. Whereas the *T. atroviride* Seb1 transcription factor is only involved in osmotic stress (Peterbauer *et al.* 2002), the *A. fumigatus* SebA appears to play no role in osmotic stress, and instead is required for the response to heat and oxidative stresses and poor nutrient conditions (Dinamarco *et al.* 2012). Our data indicates that the *N. crassa* SEB-1 transcription factor is involved in the response to heat, pH, osmotic, and oxidative stresses. These data suggest that SEB-1 orthologs in different fungi may function by targeting different

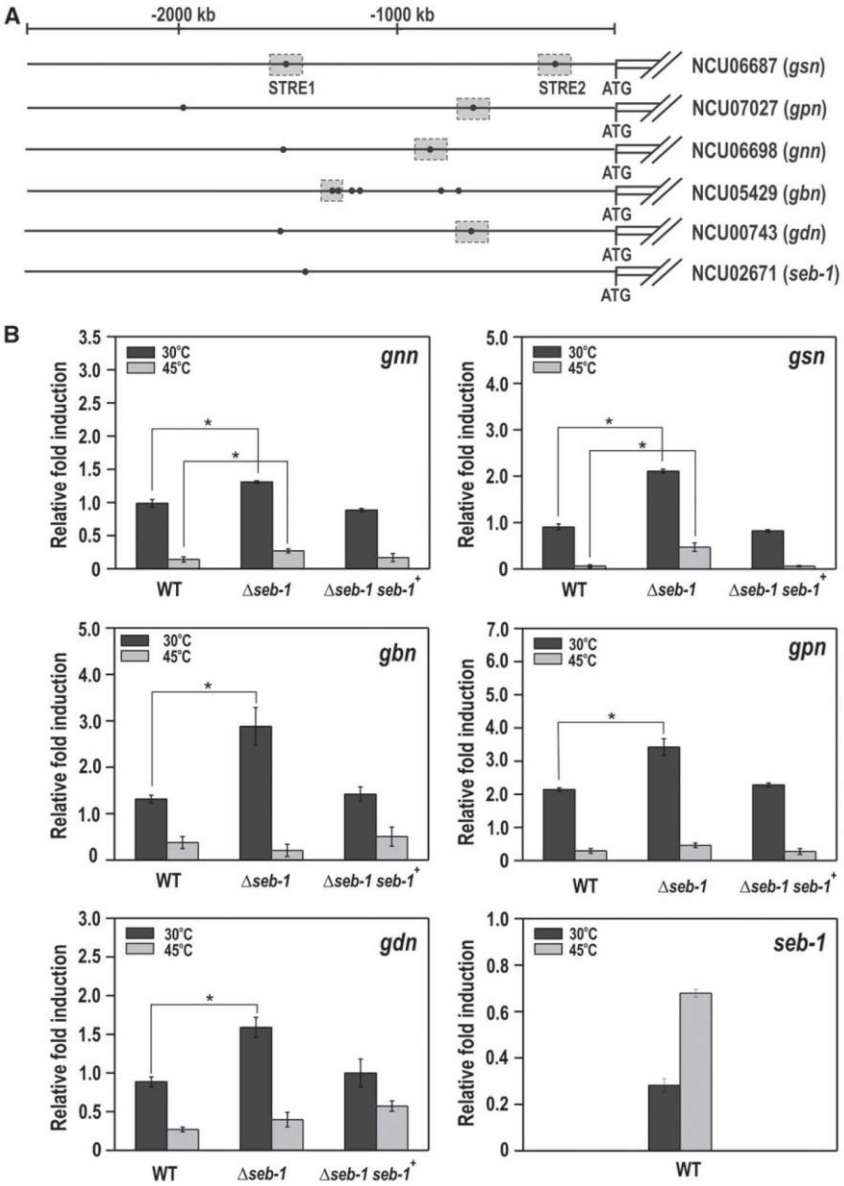

Figure 7 The expression of glycogenic genes is regulated by SEB-1. To analyze gene expression, mycelia were grown at 30° for 24 hr in VM (Vogel's minimal) medium containing 2% sucrose, collected, and subjected to RNA extraction and cDNA synthesis. (A) Schematic representation of the genes including their 5′-flanking regions with the putative STRE motifs (filled black circles). Gray rectangles indicate the STRE motifs analyzed by ChIP-qPCR. (B) Gene expression analysis of the genes encoding glycogenic enzymes – glycogen synthase *gsn* (NCU06687), glycogen phosphorylase *gpn* (NCU07027), glycogenin *gnn* (NCU06698), glycogen branching enzyme *gbn* (NCU05429), glycogen debranching enzyme *gdn* (NCU00743) genes, and the *seb-1* gene (NCU02671). WT: wild-type strain; *seb-1*: strain mutated in the ORF NCU02671; Δ*seb-1 seb-1*$^{+}$: Δ*seb-1* complemented strain (Δ*seb-1 his-3*::*Pccg-1-seb1-sfgfp*). Expression of the *act* gene (NCU04173) was used as the reference, and the wild-type samples at 30° and 45° were used as references samples at 30° and 45°, respectively. The error bars represent the standard deviation for each condition. Values of six replicates were used for statistical analysis and the significance (*$P < 0.001$) between strains was estimated by the Tukey-Kramer multiple comparison test. STRE, stress response element.

signaling pathways, resulting in differences in cellular responses to stress that are dependent upon SEB-1 orthologs.

We identified SEB-1 as the *N. crassa* transcription factor capable of binding to the STRE sequence (AGGGG), which is the nucleotide sequence recognized by the Msn2/4p transcription factors in *S. cerevisiae*. The ability of SEB-1 to bind to the STRE sequence was further confirmed by showing that SEB-1 binds *in vitro* to STRE sequences present in the promoter of the gene encoding an enzyme of glycogen metabolism (*gsn*). SEB-1 regulates the expression of all glycogenic genes (see Figure 7 and Figure 10B) and the *tps* gene, which encodes trehalose phosphate synthase, the enzyme that catalyzes the first step in trehalose synthesis, consistent with a role for SEB-1 in glycogen and trehalose metabolism. However, gene expression was either up- or down-regulated in the Δ*seb-1* strain (see Figure 10B). This double regulatory function of SEB-1 was also observed for the expression of genes involved in oxidative, pH, heat, and osmotic stress. Since all glycogenic genes have STRE in their promoter regions and, in yeast, STRE mediates the activation of stress-responsive gene, these data suggest that either STRE is not required for the gene expression regulation by SEB-1 or that SEB-1 requires interaction with additional transcription factors and/or proteins in *N. crassa*. The *A. fumigatus* SebA transcription factor has also been described as regulating gene expression by activating or repressing genes involved in the heat stress response (Dinamarco *et al.* 2012). All these data reinforce the hypothesis that the transcription factors of the SEB family are not the real yeast Msn2/4p functional homologs; rather, they are proteins that regulate stress responses likely involving an alternative mechanism of action.

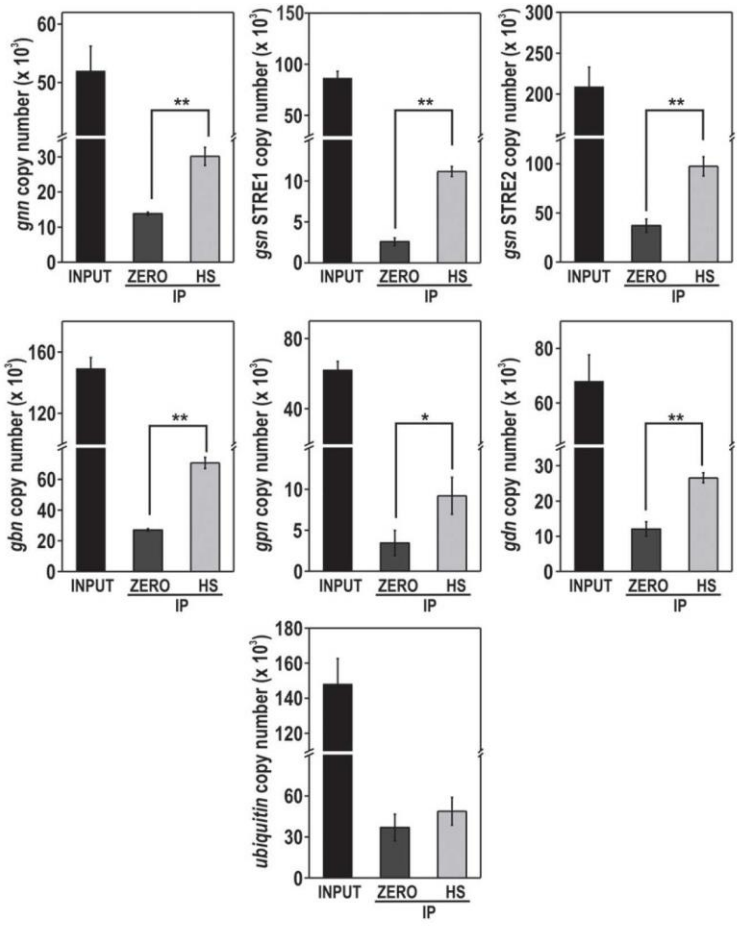

Figure 8 The transcription factor SEB-1 binds *in vivo* to the promoters of glycogenic genes. Genomic DNA from the Δ*seb-1* complemented strain (Δ*seb-1 his-3*::*Pccg-1-seb1-sfgfp*) subjected or not to heat stress was immunoprecipitated with anti-GFP antibody and the immunoprecipitates (IPs) were used to analyze the binding of SEB-1 to the target genes *gnn*, *gsn*, *gbn*, *gpn*, and *gdn* by ChIP-qPCR. A region inside the coding sequence of the ubiquitin gene was used as a negative control for binding. Values of three replicates were used for statistical analysis (*$P < 0.05$, **$P < 0.01$, estimated by the Tukey-Kramer multiple comparison test) and the error bars represent the standard deviation for each condition. INPUT: genomic DNA before IP; ZERO: mycelium from a culture at 30° for 24 hr, HS: mycelium from a culture submitted to heat stress (45°) for 30 min; IP: genomic DNA after anti-GFP immunoprecipitation.

In yeast, trehalose-6-P synthase (Tps1), but not trehalose, is indispensable for withstanding high temperature and oxidative stresses. It was suggested that Tps1 is a sensing/signaling intermediate with regulatory function(s), at least regarding energy homeostasis (Petitjean *et al.* 2015; Gibney *et al.* 2015). As shown here, SEB-1 regulated the expression of genes related to reserve carbohydrate metabolism and also genes often induced by stress, which includes the *hsp*, *cat*, and *sod* genes, among others. In the latter case, the majority of genes were up-regulated by SEB-1 (see Figure 8A). Whether the genes involved in reserve carbohydrate metabolism are regulated by SEB-1 in the same manner as stress-responsive genes, or whether the regulation of such genes is required for stress survival (as shown here), deserves further investigation. In *S. cerevisiae*, some genes involved in central carbon metabolism, such as *PYC1* (pyruvate carboxylase), *PFK1* (phosphofructokinase), and *CIT2* (citrate synthase), were described as having a fundamental role in heat-shock resistance. In addition, genes involved in cellular signaling and chromatin regulation were also related to confer hypersensitivity to heat, suggesting a connection between heat shock and these processes (Gibney *et al.* 2013).

We used RNA-seq to determine the expression profile of the Δ*seb-1* strain under heat stress (by transferring from 30° to 45°). Using this approach, we demonstrated that SEB-1 might connect the heat stress response to a broad range of cellular mechanisms, including chromatin architecture, as would be expected under this environmental condition. We observed a high number of genes implicated in this process as a putative target of regulation by SEB-1. All genes encoding histone proteins were differently expressed in the Δ*seb-1* strain, being down-regulated under heat stress. In addition, genes encoding proteins involved in histone modifications, such as the histone deacetylases HAD-2 and HAD-3 (Smith *et al.* 2010) and the histone acetyltransferase HAT-4 (Borkovich *et al.* 2004), were overexpressed in the Δ*seb-1* strain. Interestingly, we also identified the ORFs NCU03482 and NCU06679 as genes differently regulated by SEB-1 under heat stress; the proteins encoded by these genes were previously described in *N. crassa* as STRE-binding proteins (Freitas *et al.* 2008). The NCU06679 gene, previously annotated as *cac-3* (chromatin assembly complex 3, Borkovich *et al.* 2004), was recently named as *npf*, a component of a multimeric complex involved in histone methylation in *Neurospora* (Jamieson *et al.* 2013), whereas NCU03482 is a DNA helicase homologous to the mammalian RuvBL1 protein. This latter protein, together with RuvBL2, belongs to the AAA+ (ATPases associated with various cellular activities) protein family and is highly conserved in eukaryotes. They are known by multiple names, depending on the organism, and are components of several multiprotein complexes involved in a wide range of cellular processes, including chromatin remodeling and transcriptional regulation (Nano and Houry 2013).

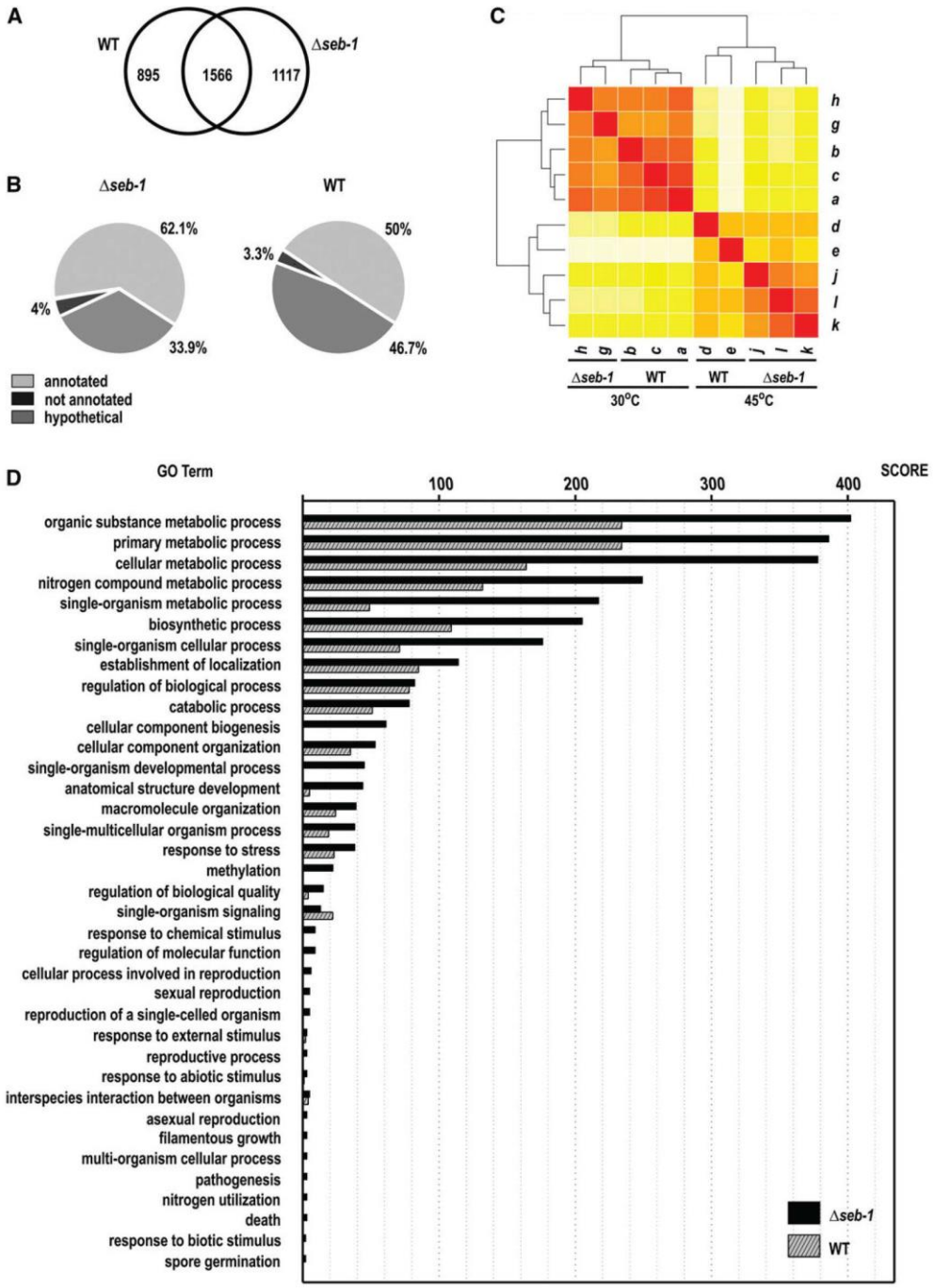

Figure 9 The *seb-1* regulon. (A) Venn diagram showing the overlap between the differentially expressed genes exhibiting a statistically significant profile during heat shock in the wild-type and Δ*seb-1* strains ($P < 0.05$). (B) Distribution of the ORFs (open reading frames) identified by RNA-seq. (C) Heat map showing Euclidean distances between wild-type (WT) and Δ*seb-1* strains under heat shock. The darker the color, the closer are the two datasets. a, b, and c, RNA-seq libraries from the wild-type strain at 30°; d and e, RNA-seq libraries from the wild-type strain at 45°; g and h, RNA-seq libraries from the Δ*seb-1* strain at 30°; j, k, and l, RNA-seq libraries from the Δ*seb-1* strain at 45°. (D) Distribution of differentially expressed genes showing a statistically significant profile in the response to shock in the wild-type and Δ*seb-1* strains, according to functional categories (GO terms). The scores represent the number of ORFs identified as differentially expressed. GO terms are listed on the left and the Blast2GO score of molecular function is shown on top. Gene Ontology (GO) analyses were performed using the Blast2GO web tool, as described in *Material and Methods*.

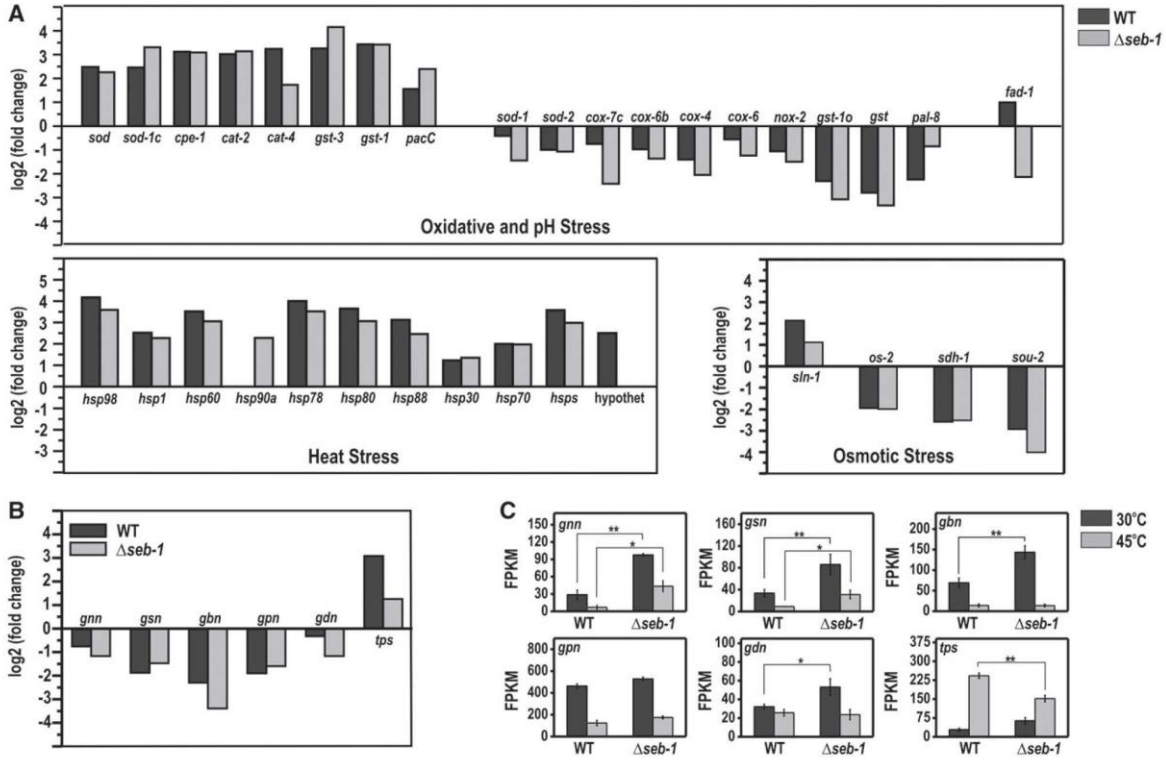

Figure 10 SEB-1 controls the expression of genes involved in glycogen and trehalose metabolism and some stress responsive genes under heat stress. The expression levels were indicated as fold change (log2) and FPKMs (fragments per kb of transcript per million mapped reads). (A) Genes involved in oxidative, pH, heat, and osmotic stress responses in wild-type (WT) and Δ*seb-1* strains exposed to heat stress (45°). (B) Genes involved in glycogen and trehalose metabolism in WT and Δ*seb-1* strains exposed to heat stress (45°). (C) Genes involved in glycogen and trehalose metabolism in the WT and Δ*seb-1* strains exposed or not exposed to heat stress (45°). *gnn*, glycogenin (NCU06698); *gsn*, glycogen synthase gene (NCU06687); *gbn*, glycogen branching enzyme gene (NCU05429); *gpn*, glycogen phosphorylase gene (NCU07027); *gdn*, glycogen debranching enzyme gene (NCU00743); *sod*, superoxide dismutase variant gene (NCU09560); *sod-1*, superoxide dismutase-1 gene (NCU02133); *sod-2*, superoxide dismutase-2 gene (NCU01213); *cat-2*, catalase-2 gene (NCU05770); *cat-4*, catalase-4 gene (NCU05169); *os-2*, osmotic sensitive-2 gene (NCU07024); *pacC*, pH-response transcription factor pacC/RIM101 gene (NCU00090). The error bars represent the standard deviation for each condition, with triplicate measurements. Values of three replicates were used for statistical analysis and the significances (*$P < 0.01$ and **$P < 0.001$) between strains were estimated by the Tukey-Kramer multiple comparison test.

The transcriptomic results also provided evidence that SEB-1 controls the expression of genes encoding protein components of the circadian clock in *N. crassa*. Genes encoding the proteins WC-1 (white collar-1), VIVID, and the Frequency-Interacting RNA Helicase protein (FRH) were clearly up-regulated in the Δ*seb-1* strain under heat stress, suggesting that the clock mechanism may be impaired in the mutant strain under such conditions. The clock-controlled gene-8 (*ccg-8*) was also identified as regulated by SEB-1. Since the mutant strain also exhibited impairment in the accumulation of the reserve carbohydrate glycogen and trehalose under heat stress, it is tempting to suggest that SEB-1 could play a role in coordinating the carbohydrate metabolism controlled by the clock in *N. crassa*. The connection between the circadian clock and metabolism has been under investigation in recent years (Asher and Sassone-Corsi 2015). Many genes involved in metabolism have recently been identified as clock-controlled genes in a *N. crassa* transcriptomic assay, including some genes involved in trehalose metabolism (Hurley *et al.* 2014). The results of this analysis revealed that much of metabolism is clock-controlled; daytime favors catabolism and nighttime favors the biosynthesis of cellular components. Regarding the clock-control of glycogen metabolism, Doi *et al.* (2010) have shown that the mouse CLOCK transcription factor regulates the circadian rhythms of hepatic glycogen synthesis through transcriptional activation of Gys2, the gene encoding glycogen synthase. In *N. crassa*, the *gsn* and *gpn* genes, which encode glycogen synthase and the glycogen phosphorylase enzymes, respectively, have been reported to be light-regulated genes (Wu *et al.* 2014).

Autophagy is another cellular process that may be regulated by SEB-1, since the *ATG8* gene is a target of regulation under heat stress. A number of genes have been implicated in this process and the Atg8 protein was described as a key component of the autophagosome in yeast (Xie *et al.* 2008). Interestingly, Wang *et al.* (2001) reported a connection between glycogen metabolism and autophagy mediated by the action of the protein kinases Snf1p and Pho85p. We also identified the SNF-1 protein kinase as a target of regulation by SEB-1. A high number of proteins implicated in a variety of additional cellular processes were also identified as targets of regulation by SEB-1, including membrane transporters, proteins involved in carbohydrate, nitrogen, and calcium metabolism, and light-responsive proteins. However, the regulation of these processes by SEB-1 and the conditions in which the processes are regulated in *N. crassa* require further investigation.

Taken together, all our data suggest that SEB-1 acts as a regulatory hub in a network linking different cellular processes.

ACKNOWLEDGMENTS

We thank Dr. Gustavo Henrique Goldman (Faculdade de Ciências Farmacêuticas, Universidade de São Paulo, Ribeirão Preto, São Paulo, Brazil) for reviewing the manuscript and for comments, and Dr. Trevor Lee Starr (University of California at Berkeley, Laboratory of Plant and Microbial Biology, Berkeley, California) for the pTSL91-A plasmid. We also thank the Fungal Genetics Stock Center, Manhattan, Kansas, for the *N. crassa* strains. We would like to thank the Fundação de Amparo à Pesquisa do Estado de São Paulo (FAPESP) and Conselho Nacional de Desenvolvimento Científico e Tecnológico (CNPq) for providing research grants to M.C.B. and fellowships to F.Z.F., S.V., F.B.C., and M.C.B.

LITERATURE CITED

Anders, S., and W. Huber, 2010 Differential expression analysis for sequence count data. Genome Biol. 11: R106.

Asher, G., and P. Sassone-Corsi, 2015 Time for food: the intimate interplay between nutrition, metabolism, and the circadian clock. Cell 161: 84–92.

Berry, D. B., Q. Guan, J. Hose, S. Haroon, M. Gebbia *et al.*, 2011 Multiple means to the same end: the genetic basis of acquired stress resistance in yeast. PLoS Genet. 7: e1002353.

Borkovich, K. A., L. A. Alex, O. Yarden, M. Freitag, G. E. Turner *et al.*, 2004 Lessons from the genome sequence of *Neurospora crassa*: tracing the path from genomic blueprint to multicellular organism. Microbiol. Mol. Biol. Rev. 68: 1–108.

Brown, A. J., S. Budge, D. Kaloriti, A. Tillmann, M. D. Jacobsen *et al.*, 2014 Stress adaptation in a pathogenic fungus. J. Exp. Biol. 217: 144–155.

Brunelli, J. P., and M. L. Pall, 1993 A series of yeast/*Escherichia coli* lambda expression vectors designed for directional cloning of cDNAs and *cre/lox*-mediated plasmid excision. Yeast 9: 1309–1318.

Causton, H. C., B. Ren, S. S. Koh, C. T. Harbison, E. Kanin *et al.*, 2001 Remodeling of yeast genome expression in response to environmental changes. Mol. Biol. Cell 12: 323–337.

Colot, H. V., G. Park, G. E. Turner, C. Ringelberg, C. M. Crew *et al.*, 2006 A high throughput gene knockout procedure for *Neurospora* reveals functions for multiple transcription factors. Proc. Natl. Acad. Sci. USA 103: 10352–10357.

Conesa, S., J. M. Götz, J. M. Garcia-Gómez, J. Terol, M. Talón *et al.*, 2005 Blast2GO: a universal tool for annotation, visualization and analysis in functional genomics research. Bioinformatics 21: 3674–3676.

Cupertino, F. B., F. Z. Freitas, R. M. de Paula, and M. C. Bertolini, 2012 Ambient pH controls glycogen levels by regulating glycogen synthase gene expression in *Neurospora crassa*. New insights into the pH signaling pathway. PLoS One 7: e44258.

Cupertino, F. B., S. Virgilio, F. Z. Freitas, T. S. Candido, and M. C. Bertolini, 2015 Regulation of glycogen metabolism by the CRE-1, RCO-1 and RCM-1 proteins in *Neurospora crassa*. The role of CRE-1 as the central transcriptional regulator. Fungal Genet. Biol. 77: 82–94.

Davis, R. H., and F. J. de Serres, 1970 Genetic and microbial research techniques for *Neurospora crassa*. Methods Enzymol. 17: 79–143.

de Groot, E., J. P. Bebelman, W. H. Mager, and R. J. Planta, 2000 Very low amounts of glucose cause repression of the stress-responsive gene *HSP12* in *Saccharomyces cerevisiae*. Microbiology 146: 367–375.

de Paula, R., C. A. de Pinho, H. F. Terenzi, and M. C. Bertolini, 2002 Cloning and molecular characterization of the *gsn* cDNA encoding glycogen synthase in *Neurospora crassa*. Mol. Genet. Genomics 267: 241–253.

Dinamarco, T. M., R. S. Almeida, P. A. de Castro, N. A. Brown, T. F. dos Reis *et al.*, 2012 Molecular characterization of the putative transcription factor SebA involved in virulence in *Aspergillus fumigatus*. Eukaryot. Cell 11: 518–531.

Doi, R., K. Oishi, and N. Ishida, 2010 CLOCK regulates circadian rhythms of hepatic glycogen synthesis through transcriptional activation of *Gys2*. J. Biol. Chem. 285: 22114–22121.

Duran, R., J. W. Cary, and A. M. Calvo, 2010 Role of the osmotic stress regulatory pathway in morphogenesis and secondary metabolism in filamentous fungi. Toxins (Basel) 2: 367–381.

Ebbole, D., and M. S. Sachs, 1990 A rapid and simple method for isolation of *Neurospora crassa* homokaryons using microconidia. Fung. Genet. Newsl. 37: 17–18.

Estruch, F., 2000 Stress-controlled transcriptions factors, stress-induced genes and stress tolerance in budding yeast. FEMS Microbiol. Rev. 24: 469–486.

Fillinger, S., M. K. Chaveroche, P. van Dijck, R. de Vries, G. Ruijter *et al.*, 2001 Trehalose is required for the acquisition of tolerance to a variety of stresses in the filamentous fungus *Aspergillus nidulans*. Microbiology 147: 1851–1862.

Freitas, F. Z., and M. C. Bertolini, 2004 Genomic organization of the *Neurospora crassa gsn* gene: possible involvement of the STRE and HSE elements in the modulation of transcription during heat shock. Mol. Genet. Genomics 272: 550–561.

Freitas, F. Z., A. Chapeaurouge, J. Perales, and M. C. Bertolini, 2008 A systematic approach to identify STRE-binding proteins of the *gsn* glycogen synthase gene promoter in *Neurospora crassa*. Proteomics 8: 2052–2061.

Freitas, F. Z., R. M. de Paula, L. C. B. Barbosa, H. F. Terenzi, and M. C. Bertolini, 2010 cAMP signaling pathway controls glycogen metabolism in *Neurospora crassa* by regulating the glycogen synthase gene expression and phosphorylation. Fungal Genet. Biol. 47: 43–52.

Gasch, A. P., 2007 Comparative genomics of the environmental stress response in ascomycete fungi. Yeast 24: 961–976.

Gasch, A. P., P. T. Spellman, C. M. Kao, O. Carmel-Haul, M. B. Eisen *et al.*, 2000 Genomic expression programs in the response of yeast cells to environmental changes. Mol. Biol. Cell 11: 4241–4257.

Gibney, P. A., C. Lu, A. A. Caudy, D. C. Hess, and D. Botstein, 2013 Yeast metabolic and signaling genes are required for heat-shock survival and have little overlap with the heat-induced genes. Proc. Natl. Acad. Sci. USA 110: E4393–E4402.

Gibney, P. A., A. Schieler, J. C. Chen, J. D. Rabinowitz, and D. Botstein, 2015 Characterizing the in vivo role of trehalose in *Saccharomyces cerevisiae* using the AGT1 transporter. Proc. Natl. Acad. Sci. USA 112: 6116–6121.

Görner, W., E. Durchschlag, M. T. Martinez-Pastor, F. Estruch, G. Ammerer *et al.*, 1998 Nuclear localization of the C2H2 zinc finger protein Msn2p is regulated by stress and protein kinase A activity. Genes Dev. 12: 586–597.

Han, K. H., and R. A. Prade, 2002 Osmotic stress-coupled maintenance of polar growth in *Aspergillus nidulans*. Mol. Microbiol. 43: 1065–1078.

Hanks, D. L., and A. S. Sussman, 1969 The relation between growth, conidiation and trehalase activity in *Neurospora crassa*. Am. J. Bot. 56: 1152–1159.

Hartree, E. F., 1972 Determination of protein: A modification of the Lowry method that gives a linear photometric response. Anal. Biochem. 48: 422–427.

Hurley, J. M., A. Dasgupta, J. M. Emerson, X. Zhou, C. S. Ringelberg *et al.*, 2014 Analysis of clock-regulated genes in *Neurospora* reveals widespread posttranscriptional control of metabolic potential. Proc. Natl. Acad. Sci. USA 111: 16995–17002.

Jacquet, M., G. Renault, S. Lallet, J. D. Mey, and A. Goldbeter, 2003 Oscillatory nucleocytoplasmic shuttling of the general stress response transcriptional activators Msn2 and Msn4 in *Saccharomyces cerevisiae*. J. Cell Biol. 161: 497–505.

Jamieson, K., M. R. Rountree, Z. A. Lewis, J. E. Stajich, and E. U. Selker, 2013 Regional control of histone H3 lysine 27 methylation in *Neurospora*. Proc. Natl. Acad. Sci. USA 110: 6027–6032.

Kobayashi, N., and K. McEntee, 1990 Evidence for a heat shock transcription factor-independent mechanism for heat shock induction of transcript in *Saccharomyces cerevisiae*. Proc. Natl. Acad. Sci. USA 87: 6550–6554.

Kobayashi, N., and K. McEntee, 1993 Identification of *cis* and *trans* components of a novel heat shock stress regulation pathway in *Saccharomyces cerevisiae*. Mol. Cell. Biol. 13: 248–256.

Kroll, K., V. Pahtz, and O. Kniemeyer, 2014 Elucidating the fungal stress response by proteomics. J. Proteomics 97: 151–163.

Laemmli, U. K., 1970 Cleavage of structural protein during the assembly of the head of bacteriophage T4. Nature 227: 680–685.

Livak, K. J., and T. D. Schmittgen, 2001 Analysis of relative gene expression data using real-time quantitative PCR and the $2^{-\Delta\Delta CT}$ method. Methods 25: 402–408.

Martínez-Pastor, M. T., G. Marchler, C. Schüller, A. Marchler-Bauer, H. Ruis *et al.*, 1996 The *Saccharomyces cerevisiae* zinc finger proteins Msn2p and Msn4p are required for transcriptional induction through the stress response element (STRE). EMBO J. 15: 2227–2235.

McCluskey, K., A. Wiest, and M. Plamann, 2010 The Fungal Genetics Stock Center: a repository for 50 years of fungal genetics research. J. Biosci. 35: 119–126.

Morano, K. A., and C. M. Grant, and W. S. Moye-Rowley, 2012 The response to heat shock and oxidative stress in *Saccharomyces cerevisiae*. Genetics 190: 1157–1195.

Nano, N., and W. A. Houry, 2013 Chaperone-like activity of the AAA+ proteins Rvb1 and Rvb2 in the assembly of various complexes. Phil. Trans. R. Soc. B 368: 20110399.

Neves, M. J., J. A. Jorge, J. M. François, and H. F. Terenzi, 1991 Effects of heat shock on the level of trehalose and glycogen, and on the induction of thermotolerance in *Neurospora crassa*. FEBS Lett. 283: 19–22.

Ni, H. T., and D. C. LaPorte, 1995 Response of a yeast glycogen synthase gene to stress. Mol. Microbiol. 16: 1197–1205.

Nicholls, S., M. Straffon, B. Enjalbert, A. Nantel, S. Macaskill *et al.*, 2004 Msn2- and Msn4-like transcription factors play no obvious roles in the stress responses of the fungal pathogen *Candida albicans*. Eukaryot. Cell 3: 1111–1123.

Noventa-Jordão, M. A., M. L. T. M. Polizeli, B. M. Bonini, J. A. Jorge, and H. F. Terenzi, 1996 Effects of temperature shifts on the activities of *Neurospora crassa* glycogen synthase, glycogen phosphorylase and trehalose-6-phosphate synthase. FEBS Lett. 378: 32–36.

Peterbauer, C. K., D. Litscher, and C. P. Kubicek, 2002 The *Trichoderma atroviride* seb1 (stress response element binding) gene encodes an AGGGG-binding protein which is involved in the response to high osmolarity stress. Mol. Genet. Genomics 268: 223–231.

Petitjean, M., M. A. Teste, J. M. François, and J. L. Parrou, 2015 Yeast tolerance to various stresses relies on the trehalose-6P synthase (Tps1) protein, not on trehalose. J. Biol. Chem. 290: 16177–16190.

Roetzer, A., C. Gregori, A. M. Jennings, J. Quintin, D. Ferrandon *et al.*, 2008 *Candida glabrata* environmental stress response involves *Saccharomyces cerevisiae* Msn2/4 orthologous transcription factors. Mol. Microbiol. 69: 603–620.

Schmitt, A. P., and K. McEntee, 1996 Msn2p, a zinc finger DNA-binding protein, is the transcriptional activator of the multistress response in *Saccharomyces cerevisiae*. Proc. Natl. Acad. Sci. USA 93: 5777–5783.

Seidl, V., B. Seiboth, L. Karaffa, and C. P. Kubicek, 2004 The fungal STRE-element-binding protein Seb1 is involved but not essential for glycerol dehydrogenase (gld1) gene expression and glycerol accumulation in *Trichoderma atroviride* during osmotic stress. Fungal Genet. Biol. 41: 1132–1140.

Smith, K. M., J. R. Dobosy, J. E. Reifsnyder, M. R. Rountree, D. C. Anderson *et al.*, 2010 H2B- and H3-specific histone deacetylases are required for DNA methylation in *Neurospora crassa*. Genetics 186: 1207–1216.

Sokolovsky, V., R. Kaldenhoff, M. Ricci, and V. E. A. Russo, 1990 Fast and reliable mini-prep RNA extraction from *Neurospora crassa*. Fung. Genet. Newsl. 37: 39–40.

Sorger, P. K., and H. R. B. Pelham, 1988 Yeast heat shock factor is an essential DNA-binding protein that exhibits temperature-dependent phosphorylation. Cell 54: 855–864.

Swan, C. L., and L. Sistonen, 2015 Cellular stress response cross talk maintains protein and energy homeostasis. EMBO J. 34: 267–269.

Tamaru, H., X. Zhang, D. McMillen, P. B. Singh, J. Nakayama *et al.*, 2003 Trimethylated lysine 9 of histone H3 is a mark for DNA methylation in *Neurospora crassa*. Nat. Genet. 34: 75–79.

Trapnell, C., L. Patchter, and S. L. Salzberg, 2009 TopHat: discovering splice junctions with RNA-seq. Bioinformatics 25: 1105–1111.

Trapnell, C., B. A. Williams, G. Pertea, A. Mortazavi, G. Kwan *et al.*, 2010 Transcript assembly and quantification by RNA-seq reveals unannotated transcripts and isoform switching during cell differentiation. Nat. Biotechnol. 18: 511–515.

Vihervaara, A., C. Sergelius, J. Vasara, M. A. Blom, A. N. Elsing *et al.*, 2013 Transcriptional response to stress in the dynamic chromatin environment of cycling and mitotic cells. Proc. Natl. Acad. Sci. USA 110: E3388–E3397.

Vogel, H. J., 1956 A convenient growth medium for *Neurospora crassa* (medium N). Microbiol. Genet. Bull. 13: 42–43.

Vyas, V. K., C. D. Berkey, T. Miyao, and M. Carlson, 2005 Repressors Nrg1 and Nrg2 regulate a set of stress-responsive genes in *Saccharomyces cerevisiae*. Eukaryot. Cell 4: 1882–1891.

Wang, Z., W. A. Wilson, M. A. Fujino, and P. J. Roach, 2001 Antagonistic controls of autophagy and glycogen accumulation by Snf1p, the yeast homolog of AMP-activated protein kinase, and the cyclin-dependent kinase Pho85p. Mol. Cell. Biol. 21: 5742–5752.

Westergaard, M., and H. K. Mitchell, 1947 *Neurospora*. V. A synthetic medium favoring sexual reproduction. Am. J. Bot. 34: 573–577.

Wu, C., F. Yang, K. M. Smith, M. Peterson, R. Dekhang *et al.*, 2014 Genome-wide characterization of light-regulated genes in *Neurospora crassa*. G3 (Bethesda) 4: 1731–1745.

Xie, Z., U. Nair, and D. J. Klionsky, 2008 Atg8 controls phagophore expansion during autophagosome formation. Mol. Biol. Cell 19: 3290–3298.

Zimmermann, A. L., H. F. Terenzi, and J. A. Jorge, 1990 Purification and properties of an extracellular conidial trehalase from *Humicola grisea* var. *thermoidea*. Biochim. Biophys. Acta 1036: 41–46.

Communicating editor: B. J. Andrews

Appendix

unesp UNIVERSIDADE ESTADUAL PAULISTA
"JÚLIO DE MESQUITA FILHO"
Campus de Araraquara

Instituto de Química

PROGRAMA DE PÓS-GRADUAÇÃO EM BIOTECNOLOGIA

NORMAS INTERNAS PARA A DEFESA DA DISSERTAÇÃO DE MESTRADO OU DA TESE DE DOUTORADO, APROVADAS PELO CONSELHO EM REUNIÃO 23/11/2001.

Alterações nas Normas aprovada pelo Conselho em reunião de 08/11/2010
Aprovada pela Congregação em reunião de: 16/12/2010.

(Adequação e complementação das disposições Regimentais da UNESP e do INSTITUTO DE QUÍMICA).

1) O conteúdo do trabalho de Dissertação ou Tese deverá ser aquele do projeto de pesquisa previamente aprovado pelo Conselho de Programa de Pós-Graduação em Biotecnologia do Instituto.

2) O requerimento para apresentação da Dissertação ou Tese somente poderá ser encaminhado após o candidato ter sido aprovado no Exame Geral de Qualificação.

3) O aluno de Doutorado deverá comprovar a aceitação de um artigo referente ao seu projeto, em revista científica indexada com fator de impacto dentro do Qualis periódicos da área de Biotecnologia (A1 a B4), Caso o trabalho resultar em patente o artigo poderá ser substituído pelo protocolo de depósito da patente quando da solicitação da defesa da tese.

4) Para o aluno de Mestrado é altamente recomendado que até a defesa da Dissertação, tenha submetido um artigo referente ao seu projeto, em revista científica indexada com o corpo editorial permanente.

5) Opcionalmente para os candidatos ao Doutorado, a Tese poderá ser redigida na forma de discussão de "Artigos Científicos" de autoria do candidato, desde que tenha no mínimo um artigo aceito e outro submetido a periódicos com fator de impacto dentro do Qualis da área de Biotecnologia (A1 a B4). Estes artigos deverão estar relacionados ao projeto de Tese. A tese deverá conter:

1. Capa
2. Folha de rosto
3. Dedicatórias e agradecimentos
4. Índice
5. Resumo {apresentação concisa dos pontos relevantes do conteúdo e das conclusões do trabalho. Não deve ultrapassar 1 página. Incluir, no final, até 6 palavras chave}.
6. Abstract
7. Introdução contendo revisão bibliográfica e justificativa do problema
8. Trabalhos completos publicados ou aceitos para publicação (Capítulos II, III,....) dos resultados da Tese. Na versão impressa os artigos deverão estar incluídos em "anexos". Na versão "on line" estes artigos deverão ser apenas citados.
9. Conclusões
10. Referências bibliográficas

6) Para efeito de escolha da banca de defesa da Dissertação ou Tese o candidato deverá preparar somente o número de cópias necessárias para distribuição aos membros da banca, num total de 5 (cinco) para o Mestrado e 8 (oito) para o Doutorado. Os exemplares deverão ser todos encadernados. Deverão constar dos exemplares os dados curriculares do aluno e nos exemplares definitivos (após a defesa), além dos dados, deverá constar a Comissão Examinadora.

Instituto de Química
Rua Prof. Francisco Degni, s/nº- Bairro Quitandinha - CEP 14800-900 - Araraquara - S.P. - Brasil
Tel. 16 3301-6600 - fax 16 3301-6692 - http://www.iq.unesp.br

unesp UNIVERSIDADE ESTADUAL PAULISTA
"JÚLIO DE MESQUITA FILHO"
Campus de Araraquara

Instituto de Química

7) Após a defesa pública o candidato deverá protocolar na Seção Técnica de Comunicações, com aval do orientador, **04 exemplares, sendo obrigatóriamente 01 impresso e 03 opcionalmente impressos ou CDs na versão PDF** da Dissertação, ou **06 exemplares, sendo obrigatóriamente 01 impresso e 05 opcionalmente impressos ou CDs na versão PDF** da Tese em forma definitiva. Esta versão deverá atender às sugestões e comentários propostos pela banca examinadora. O prazo máximo será de 30 dias a partir da data da defesa. O orientador ficará responsável por zelar para que as sugestões apresentadas pela banca examinadora estejam contempladas na versão definitiva da Dissertação ou Tese.

8) A liberação de qualquer documentação relativa à defesa da Dissertação ou Tese pela Seção de Pós-Graduação, fica condicionada a entrega dos números pré-fixados de exemplares definitivos.

9) A Dissertação ou Tese será examinada em sessão pública exceto nos casos em que o trabalho demande proteção de propriedade intelectual, por uma Comissão Examinadora composta respectivamente, de três e cinco membros propostos pelo Conselho do Programa, ouvido o Orientador e aprovados pela Congregação. O Orientador é membro nato e presidente da Comissão. Os membros das Comissões Examinadoras deverão possuir, no mínimo, o título de Doutor, salvo os casos especificados no § 2º do art. 8º do Regimento Geral da Pós-Graduação da UNESP (RGPG).

10) Nas Comissões Examinadoras para o Mestrado, pelo menos um membro titular e um membro suplente não deverão pertencer ao corpo docente e de orientadores do Programa bem como da Unidade.

11) Nas Comissões Examinadoras para o Doutorado, pelo menos dois membros titulares e dois membros suplentes não deverão pertencer ao corpo docente e de orientadores do Programa bem como da Unidade sendo, pelo menos um membro titular e suplente não pertencentes à UNESP.

12) No início da sessão pública da defesa da Dissertação ou Tese o candidato deverá realizar uma exposição oral sobre o seu trabalho, utilizando para isso um tempo médio de 30 (trinta) minutos.

13) No julgamento da Dissertação ou Tese serão atribuídos os conceitos de "aprovado" ou "reprovado", prevalecendo, no mínimo, a avaliação de dois examinadores, no caso de Mestrado e de três examinadores, no caso de Doutorado.

14) Ao aluno que cumprir todas as exigências regulamentares previstas para o Mestrado ou Doutorado será conferido o título de Mestre ou de Doutor, respectivamente.

Despacho nº 197/2010-CoPGr IQ/CAr
de 07/12/2010
Aprovado pelo Conselho do Programa de
Pós-Graduação em Biotecnologia
em reunião de 08/11/2010

EDUARDO MAFFUD CILLI
Coordenador do Programa de
Pós-graduação em Biotecnologia

12/11/2010

Instituto de Química
Rua Prof. Francisco Degni, s/nº- Bairro Quitandinha - CEP 14800-900 - Araraquara - S.P. - Brasil
Tel. 16 3301-6600 - fax 16 3301-6692 - http://www.iq.unesp.br